

University of St Andrews



Full metadata for this thesis is available in
St Andrews Research Repository
at:

<http://research-repository.st-andrews.ac.uk/>

This thesis is protected by original copyright

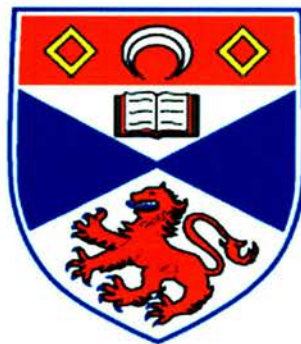
Flow-dependent restructuring of the intermediate filament cytoskeleton and activation of NF- κ B in cultured endothelial cells.

Catherine Beers

A thesis submitted in partial fulfillment of the requirements for the degree of Doctor of Philosophy at the University of St Andrews.

School of Biology

March 2002



- (i) I, Catherine Beers, hereby certify that this thesis, which is approximately 51,000 words in length, has been written by me, that it is the record of work carried out by me and that it has not been submitted in any previous application for a higher degree.

Date.. 28th MARCH 2002..... Signature of Candidate... ..

- (ii) I was admitted as a research student in September 1997 and as a candidate for the degree of Doctor of Philosophy in Biology: the higher study for which this is a record was carried out in the University of St Andrews between 1997 and 2002.

Date.. 28th MARCH 2002... Signature of Candidate.... ..

- (iii) I hereby certify that the candidate has fulfilled the conditions of the Resolution and Regulations appropriate for the degree of Doctor of Philosophy in the University of St Andrews and that the candidate is qualified to submit this thesis in application for that degree.

Date..... 28/03/02..... Signature of Supervisor.....

In submitting this thesis to the University of St Andrews I understand that I am giving permission for it to be made available for use in accordance with the regulations of the University Library for the time being in force, subject to any copyright vested in the work not being affected thereby. I also understand that the title and abstract will be published, and that a copy of the work may be made and supplied to any bona fide library of research worker.

Date... 23rd MARCH 2002 ...

Signature of Candidate.....

.....

ACKNOWLEDGEMENTS

I would like to express my thanks to the following people whose help and support have been invaluable throughout the course of my PhD:

‘Dr E’ for his help, advice and support through the trials and tribulations of this project.

Vicky for her friendship and help in the lab, putting up with my anally-retentive obsessions about most things (especially dish-washing) and not least for all those ‘stress’ relief, bargain hunts.

Dr Dave Hay for his collaboration on this project and enthusiasm about NFκB.

Jean Melville, my second mum, for all her help during her time here – not to mention her continued support and ‘mummy chats’ since leaving the lab.

The photographic boys Dave, Sean and Jim for always being willing to help, no matter how last minute the work got to them, and for their help in producing the ‘final version’.

Murray Coutts – the ‘virus slayer’ for his help, patience and optimism when viruses attack!

‘Auntie’ Tina, for her willingness to help out at all times and for her story telling – I look forward to reading the book one day.

Julie for her support and friendship over the last few months.

Alice for all those nights and weekends of study in the lab – not sure that I would have got through it all without your help (not to mention Peter’s baked potatoes).

Ian for his never ending patience, support and hugs.

My family for their constant support and encouragement throughout this and indeed all my years of studying.

Finally, my friends (if you are reading this you must be) who have put up with my moods swings and whinging for what must seem like an eternity.

ABSTRACT

Endothelial cells are profoundly influenced by shear stresses associated with blood flow. A parallel plate chamber was used to study the effects of flow on (i) the morphology of the intermediate filament cytoskeleton; and (ii) the activation of an inducible nuclear transcription factor, NF- κ B/Rel, in cultured human and bovine endothelial cells.

The experiments described in Part One show that the distribution of intermediate filaments in static cultures is dramatically altered when cells become confluent. Immunostaining with antibody to vimentin showed that the diffuse meshwork of fine intermediate filaments characteristic of sub-confluent cells is reconfigured, forming a network dominated by a prominent 'ring' of intermediate filaments that surrounds the nucleus. The transition between the two states is triggered by the formation of cell-cell contacts. Immunoblots of whole cell lysates showed a time-dependent increase in vimentin expression and a simultaneous down-regulation of both actin and tubulin. The effect of exposing confluent and sub-confluent cultures to flow was therefore quite different. However, in both circumstances, some cells were seen to respond more rapidly than others and were affected to a much greater extent. This heterogeneity is attributed to spatial gradients of shear stress caused by irregularities in cell surface topography. The distribution of the intermediate filament-associated protein (IFAP) plectin was also investigated. Immunostaining using a monoclonal antibody (417D) to plectin showed that the protein is associated with the intermediate filament network. However, the staining was not uniform and the intensity was greatest on the basal cell surface, in the form of discrete 'streaks', a pattern very similar to that seen using antibodies to focal adhesion proteins. Studies have since shown that the tips of actin stress fibres and vimentin co-localise with plectin 'streaks', and with staining for the $\alpha_v\beta_3$ integrin and the α_4 sub unit of laminin. These so-called vimentin-associated matrix adhesions (VMA) serve to anchor both actin stress fibres and vimentin to the extracellular matrix, with plectin possibly acting as a cytoskeletal 'linker' protein.

Part Two describes the results of experiments on the activation of NF- κ B by flow. Cells were grown on cover slips or on glass microscope slides and then subjected to steady laminar flow. Indirect immunofluorescence was used to monitor nuclear translocation of the p65 sub-unit in endothelial cells over-expressing either wild type or catalytically inactive mutant forms of putative 'upstream' kinases (including IKK1, IKK2 and NIK). Endogenous IKK1 and IKK2 activities were determined by measuring ^{32}P incorporation into a GST-I κ B α fusion protein substrate. Transcriptional activity of NF- κ B was quantified by means of a Con A Luciferase reporter gene, driven by a 3 κ B enhancer element. A 19-fold increase in reporter activity confirmed that NF- κ B induced by flow is transcriptionally active. Immunoblots of whole cell extracts were used to investigate the time course of the degradation of NF- κ B inhibitor proteins (I κ B α , I κ B β_1 , and p105). The results show that flow rapidly activates IKK1 and IKK2 and transiently degrades I κ B α and I κ B β_1 , but not p105. Nuclear translocation of p65 is induced by flow in wild type cells, and also in cells over-expressing wild type IKK1, IKK2 and NIK but it is prevented in cells transfected with kinase-inactive mutants. These results show that IKK1, IKK2 and NIK are essential components of the signalling pathway activated by flow.

CONTENTS

Declarations		i
Acknowledgements		iii
Abstract		iv
Contents		v
Figure Index		xi
Abbreviations		xv
Chapter 1	Introduction Part I	1
1.1	The endothelium	2
1.1.1	The endothelium and blood flow	3
1.1.2	Arterial fluid shear stress	5
1.1.3	Atherosclerosis	6
1.2	The cytoskeleton	7
1.2.1	Actin stress fibres	9
1.2.2	Intermediate filaments	10
1.2.2.1	Dynamic properties of intermediate filaments	14
1.2.2.2	Regulation of intermediate filament assembly and disassembly	17
1.2.2.3	Intermediate filament networks in endothelial cells	22
1.2.2.4	Intermediate filament-associated proteins (IFAP)	24
1.3	Focal adhesions	27

1.3.1	Focal adhesion components	28
1.3.2	Focal adhesion assembly	30
1.3.3	Focal adhesions as mechanosensors and force transducers	32
1.4	Effects of fluid shear stress on endothelial cell morphology	34
1.5	Systems to study the effects of fluid shear stress on endothelial cells	39
Chapter 2	Materials and Methods Part I	42
2.1	Cell culture techniques	43
2.1.1	Bovine aortic endothelial cells	43
2.1.1.2	Trypsinisation procedure for BAEC	44
2.1.2	Human coronary artery endothelial cells	44
2.1.2.1	Trypsinisation procedure for HCAEC	44
2.1.3	Growing cells on coverslips or microscope slides	45
2.2	Indirect Immunofluorescence	45
2.2.1	Immunofluorescence of BAEC and HCAEC	46
2.2.2	Microscopy	47
2.2.3	Image analysis	47
2.3	Shearing experiments	48
2.3.1	Introduction	48
2.3.2	Chamber design	48
2.3.3	Perfusion system	51
2.3.4	Experimental protocol	51
2.4	Western blotting	52
2.4.1	Preparation of cell extracts	52

2.4.2	Protein estimation	53
2.4.3	Protein separation and western blotting	54
Chapter 3	Results Part 1	55
	Morphology of intermediate filament networks in sub-confluent and confluent cells and related changes in cytoskeletal protein expression.	
3.1	Introduction	56
3.2	Cell growth and shape in static cultures	56
3.3	Remodelling of the intermediate filament network in static culture: Formation of perinuclear bundles of intermediate filaments and related changes to the actin cytoskeleton.	57
3.4	The time course of perinuclear ring formation	59
3.5	Morphometric analysis of perinuclear ring structure	59
3.6	Changes in the distribution of plectin, an intermediate filament-associated protein, with time in culture	60
3.7	Changes in cytoskeletal protein expression with time in culture	61
3.8	Discussion	63
Chapter 4	Results Part I	68
	Flow-induced cytoskeletal remodelling and protein expression	
4.1	Introduction	69
4.2	Changes in sub-cellular distribution of vimentin intermediate filaments and actin stress fibres in response to flow	69
4.2.1	Effects of flow on confluent cells with well developed perinuclear rings	69
4.2.2	Effects of flow on the distribution of intermediate filaments in sub-confluent or newly-confluent cells	71
4.3	Effects of flow on the sub-cellular distribution of plectin	72
4.4	Effects of flow on cytoskeletal protein expression	73
4.5	Discussion	74

Chapter 5	Results Part I	79
	Vimentin-associated matrix adhesions and flow-dependent endothelial gene transcription: an overview.	
5.1	Introduction	80
5.2	Flow-induced activation of NF- κ B	80
5.3	Flow-induced activation of NF- κ B involves the $\alpha_v\beta_3$ integrin	81
5.4	Vimentin-associated matrix adhesions (VMA)	81
Chapter 6	Introduction Part II	84
	The Nuclear factor-κB (NF-κB) activation pathway.	
6.1.	Introduction	85
6.1.1	Rel/NF- κ B transcription proteins	86
6.1.2	Binding of NF- κ B to DNA	87
6.1.3	Inhibitory κ B proteins – ‘The I κ Bs’	88
6.1.4	I κ B structure – Ankyrin repeat domains (ARD) and PEST regions	89
6.1.5	NF- κ B activation	91
6.1.5.1	Phosphorylation of I κ B	91
6.1.5.2	Ubiquitination of phospho-I κ B	92
6.1.5.3	I κ B degradation, NF- κ B nuclear translocation and I κ B feedback mechanism	94
6.1.6	The I κ B kinase (IKK) and the IKK complex	95
6.1.6.1	Regulation of I κ B-kinase (IKK) activity	98
6.2	Fluid shear stress and NF- κ B activation	100
6.2.1	Role of the cytoskeleton in gene regulation by flow	101
6.2.2	Fluid shear stress, gene expression and implications for cardiovascular disease	103

Chapter 7	Materials and Methods Part II – NF-κB.	107
7.1	Cell culture	108
7.1.1	DNA plasmids and transient transfection- NIK, IKK1 and IKK2	108
7.2	Drug treatment of HUVEC	109
7.3	Immunostaining and fluorescence microscopy	109
7.4	Immunoblotting	110
7.5	Luciferase assay	111
7.6	IKK immunocomplex kinase activity assay	111
Chapter 8	Results Part II	113
	The effects of flow on IκB proteolysis in bovine and human endothelial cells.	
8.1	Introduction	114
8.2	Fluid shear stress enhances NF- κ B dependent gene transcription	114
8.3	Fluid shear stress-induced degradation of I κ B isoforms in BAEC	114
8.4	Fluid shear stress-induced degradation of I κ B isoforms in HUVEC	115
8.5	Time course of I κ B degradation in response to TNF α stimulation	116
8.6	Discussion	117
Chapter 9	Results Part II	119
	Role of IKK1, IKK2 and NIK in flow-induced NF-κB activation.	
9.1	Introduction	120
9.2	Fluid shear stress induces IKK activation in cultured endothelial cells	120

9.3	Immunofluorescence analysis of flow-induced NF- κ B activation in cultured HUVEC	121
9.4	Catalytically inactive mutants of IKK1 and IKK2 inhibit NF- κ B nuclear translocation	122
9.5	The catalytically inactive mutant of NIK inhibits NF- κ B nuclear translocation	123
9.6	Activation of NF- κ B by flow is not dependent upon protein kinase C	123
9.7	Discussion	125
Chapter 10	Overall discussion and scope for further research.	128
References		136
Appendices		
Appendix 1	Cell culture materials	174
Appendix 2	Indirect immunofluorescence materials	177
Appendix 3	Lysate preparation and Western blotting materials	183
Appendix 4	Flow chamber characterisation	193
Appendix 5	Perinuclear ring formation and cytoskeletal protein distribution and expression in static culture and upon exposure to flow.	204
Appendix 6	NF- κ B materials, I κ B expression and IKK transfection studies	212
Appendix 7	Key to micrograph images	215

FIGURES

Chapter 1

Introduction Part I

- 1.1 Diagram of blood vessel transverse section.
- 1.2 Schematic representation of effects of blood pressure and shear stress on endothelial cells.
- 1.3 Comparison of the effects on the endothelium of steady laminar flow versus low shear stress or turbulent flow.
- 1.4 Classes and structure of intermediate filaments.
- 1.5 Diagrammatic representation of focal adhesion components and structure.
- 1.6 Representation of endothelial force transmission and force transduction processes.

Chapter 2

Materials and Methods Part I

- 2.1 Photograph of parallel plate flow chamber.
- 2.2 Schematic representation of flow chamber dimensions.
- 2.3 Schematic diagram of experimental set-up.

Chapter 3

Results Part I

Morphology of intermediate filament networks in sub-confluent and confluent cells and related changes in cytoskeletal protein expression.

- 3.1 Changes in cell density with time in culture.
- 3.2 Changes in mean cell area and shape index with time in culture.
- 3.3 Micrographs of vimentin perinuclear ring development.
- 3.4 Micrographs depicting enclosure of both the Golgi apparatus and the MTOC by vimentin perinuclear rings.
- 3.5 Micrographs illustrating that in contrast to actin, the vimentin network does not extend completely to the cell periphery.

-
- 3.6 Micrographs suggesting collapse of the developing vimentin ring towards the nucleus.
 - 3.7 Sequence of low power micrographs depicting perinuclear ring development with time in culture.
 - 3.8 Graphical representation of changes in cell density and percentage of cells exhibiting vimentin perinuclear rings with time in culture.
 - 3.9 Changes in mean perinuclear ring area and shape index with time in culture.
 - 3.10 Micrographs of plectin and focal adhesion protein distribution in sub-confluent and confluent endothelial cells.
 - 3.11 Micrographs comparing plectin and PY20 distribution in sub-confluent and confluent endothelial cells.
 - 3.12 Possible co-localisation of plectin with the G58K Golgi-associated protein.
 - 3.13 ECL™ scans illustrating vimentin, actin and tubulin expression with time in culture.
 - 3.14 Overall comparison of changes in actin, vimentin and tubulin expression with time in culture.
 - 3.15 Changes in individual cytoskeletal protein expression as a function of time in culture.
 - 3.16 Changes in the ratio of vimentin:actin and vimentin:tubulin as a function of time in static culture.

Chapter 4 Results Part I

Flow-induced cytoskeletal remodelling and protein expression.

- 4.1 Effects of flow on the vimentin cytoskeleton of confluent monolayers of cells containing perinuclear rings.
- 4.2 Actin cell-cell contacts remain after 4 hours exposure to shear stress.
- 4.3 Exposure to flow reveals structural connections between vimentin intermediate filaments and the nuclear envelope.
- 4.4 Actin stress fibre re-alignment in response to flow occurs from the luminal to basal surface of the cell.

- 4.5 Effects of flow on the vimentin network in newly confluent monolayers.
- 4.6 Effects of flow on plectin distribution in newly confluent monolayers.
- 4.7 ECL scans illustrating vimentin, actin and tubulin expression with increased exposure to flow.
- 4.8 Exposure to flow produces no significant difference in expression of vimentin, actin and tubulin.

Chapter 5 Results Part I

Vimentin-associated matrix adhesions and flow-dependent endothelial gene transcription: an overview.

- 5.1 Comparison of vimentin and actin cytoskeletal networks with the distribution of the focal adhesion proteins talin and vinculin in static culture.
- 5.2 Comparison of actin and vimentin cytoskeletal networks with plectin distribution in static culture.
- 5.3 Comparison of vimentin and actin cytoskeletal networks with β_3 distribution in static culture.
- 5.4 Comparison of the distribution of plectin and vinculin with β_3 integrin.
- 5.5 Schematic representation of proposed VMA components.

Chapter 6 Introduction Part II

The nuclear factor- κ B (NF- κ B) activation pathway.

- 6.1 Schematic representation of the mammalian Rel/NF- κ B family of proteins.
- 6.2 Schematic diagram of the I κ B family of proteins.
- 6.3 Table listing examples of NF- κ B activated genes.
- 6.4 Summary of NF- κ B activation.
- 6.5 Summary of the ubiquitination process.
- 6.6 Schematic representation of the domain structures of IKK1 (IKK α) and IKK2 (IKK β).

- 6.7 Suggested signal transduction pathways which lead to NF- κ B activation.
- 6.8 Table of fluid shear stress activated genes.

Chapter 7 Materials and Methods PartII

- 7.1 Structure of Con A Luc and 3enh Con A Luc plasmids.

Chapter 8 Results Part II

The effects of flow on I κ B proteolysis in bovine and human endothelial cells.

- 8.1 Fluid shear stress activates NF- κ B dependent transcriptional activity.
- 8.2 Fluid shear stress induces degradation of I κ B α , I κ B β and I κ B ϵ in BAEC.
- 8.3 Fluid shear stress induces I κ B α and I κ B β degradation but not p105 degradation in HUVEC.

Chapter 9 Results Part II

Role of IKK1, IKK2 and NIK in flow-induced NF- κ B activation.

- 9.1 Fluid shear stress induces IKK activity in HUVEC.
- 9.2 Fluid shear stress induces NF- κ B nuclear translocation. Effects of pre-treatment with MG132 and LMB.
- 9.3 Transfection of HUVEC with IKK1 and IKK1mut and effects on shear-induced NF- κ B nuclear translocation.
- 9.4 Transfection of HUVEC with IKK2 and IKK2mut and effects on shear-induced NF- κ B nuclear translocation.
- 9.5 Transfection of HUVEC with NIK and NIKmut and effects on shear-induced NF- κ B nuclear translocation.
- 9.6 Flow-induced NF- κ B activation is not dependent on PKC.

ABBREVIATIONS

ρ	Density of medium (g.cm ⁻³)
τ^*	Theoretical FSS
τ	Measured FSS
A	Area (cm ²)
a	Channel half height
AP-1	Activator protein-1
APS	Ammonium persulphate
ARD	Ankyrin repeat domain
ARG	Arginine
ASP	Aspartic acid
β TRCP	β -transducin repeat containing protein
BAEC	Bovine aortic endothelial cells
BCE	Bovine corneal EC
BHK	Baby hamster kidney cells
Bisin	Bisindolylmaleimide-1
BP	Blood pressure
BP230	Bullous pemphigoid antigen
BPAG1	Bullous pemphigoid antigen 1
BPAGe	Epidermal bullous pemphigoid antigen
BSA	Bovine serum albumin
CaMKII	Calmodulin-dependent protein kinase II
CKII	Casein kinase II
Con A Luc	Con A Luciferase reporter
CVS	Cardiovascular system
DAG	Diacylglycerol
DCS	Donor calf serum
DMEM	Dulbeccos modification of Eagle's medium
DMSO	Dimethyl sulphoxide
E	Glutamic acid

E1	Ubiquitin activating enzyme
E2	Ubiquitin carrier enzyme
E3	Ubiquitin protein ligase
EB	Electrophoresis buffer
EBS	Epidermolysis bullosa simplex
EBS - DM	EBS-Dowling-Meara
EBS - K	EBS-Kobner
EBS-WC	EBS-Weber-Cockayne
ECL	Enhanced chemiluminescence
ECM	Extracellular matrix
EGF	Epidermal growth factor
ERK	Extracellular signal related kinase
ET-1	Endothelin-1
FAK	Focal adhesion kinase
FBHE	Foetal (bovine) heart EC
FCS	Foetal calf serum
FR	Flow rate (ml/s) through chamber
FRAP	Fluorescence recovery after photobleaching
FSS	Fluid shear stress
<i>g</i>	Acceleration due to gravity (cm.s^{-2})
G58K	58kDa Golgi protein
GFAP	Glial fibrillary acidic protein
GFP	Green fluorescent protein
GRR	Glycine rich region
<i>h</i>	Pressure difference across flow chamber
HAEC	Human aortic endothelial cells
HBSS	Hepes buffered saline solution
HCAEC	Human coronary artery endothelial cells
hEGF	Human recombinant epidermal growth factor
hFGF	Human fibroblast growth factor
HIV	Human immunodeficiency virus

HLH	Helix –loop-helix
hnRNP	Heterogeneous nuclear ribonuclear protein
HRP	Horseradish peroxidase
HUVEC	Human umbilical vein endothelial cells
I κ B	Inhibitory κ B protein
IFAP	Intermediate filament associated protein
IKAP	IKK complex associated protein
IKK	I κ B kinase
IKKAP-1	I κ B kinase associated protein 1
IL-1	Interleukin-1
IL-1R	Interleukin-1 receptor
IP3	Inositol triphosphate
<i>l</i>	Distance between 2 pressure points of chamber
LMB	Leptomycin B
LPS	Lipopolysaccharide
LZ	Leucine zipper
MAP	Microtubule associated proteins
MAP3K/ MAPKKK	Mitogen-activated protein kinase-kinase-kinase
MEKK-1	Mitogen activated protein kinase/ERK kinase kinase-1
MD	Muscular dystrophy
MG132	MG132 protease inhibitor
MTOC	Microtubule organising centre
MW	Molecular weight
NEMO	NF- κ B essential modulating factor (also IKK γ)
NES	Nuclear export sequence
NF- κ B	Nuclear factor κ B
NIK	NF- κ B inducing kinase
NLS	Nuclear localising signal
NO	Nitric Oxide
NOS	Nitric oxide synthase

NP40	Nonidet P40 detergent
NPC	Nuclear pore complex
p	perimeter (cm)
P	Proline
PBS	Phosphate buffered saline
PBST	PBS/0.05% Tween 20
PD	Pressure difference across flow chamber
PDGF	Platelet derived growth factor
PDGF-B	Platelet derived growth factor B
PEST region	Region rich in proline (P), glutamic acid (E), serine (S) and threonine (T) residues
PIP2	Phosphoinositol 4,5-bisphosphate
PKA	Protein kinase A
PKC	Protein kinase C
PMA	Phorbol 12-myristate 13 acetate
PNR	Perinuclear ring (of vimentin)
PY-20	Phosphotyrosine 20
Q	Flow rate (ml.s^{-1})
RHD	Rel homology domain
Rho-kinase	Rho-associated kinase
RT	Room temperature
S	Serine
SDS	Sodium dodecylsulphate
SDS-PAGE	Sodium dodecyl sulphate-polyacrylamide gel electrophoresis
SI	Shape Index
SSRE	Shear stress response element
T	Threonine
TB	Transfer buffer
TEMED	N'N'N'N'-tetramethylethylenediamine
TK	Tyrosine kinase
TNF α	Tumour necrosis factor α

TNFR	Tumour necrosis factor receptor
TNS	Trypsin neutralising solution
TPL2	Tumour progression locus 2 kinase
TRAF	Tumour necrosis factor associated factors
Ub	Ubiquitin
ν	Viscosity of medium (poise)
VEGF	Vascular endothelial growth factor
VMA	Vimentin-associated matrix adhesion
w	Channel width (cm)

CHAPTER ONE

INTRODUCTION PART 1.

1.1 *The endothelium*

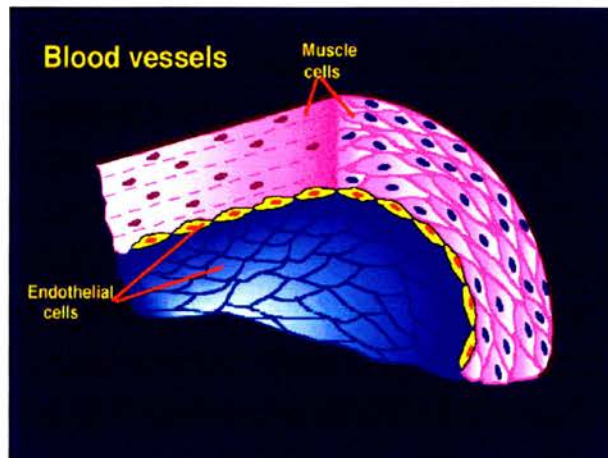
The endothelium is composed of a single layer of endothelial cells located at the blood - vessel wall interface (Figure 1.1) forming a continuous lining throughout the entire cardiovascular system (CVS). For many years the endothelium was thought of as an inert 'protective barrier' with the sole function of allowing the exchange of water and small molecules with the surrounding tissue, while keeping large molecules and 'blood' confined within the vessel lumen (Berne & Levy, 1993; Noll, 1997). However, as a result of much research over the last two decades, it has become apparent that the endothelium is in fact a highly active and dynamic layer of cells with multiple physiological functions. At the blood-tissue interface, endothelial cells are exposed to both biochemical and biomechanical stimuli, which can induce cellular activation. Cytokines and bacterial products have been identified as important biochemical stimuli while endothelial cells are also responsive to haemodynamic forces associated with flow (Gimbrone *et al*, 1997).

Endothelial functions include the control of vascular tone and vascular permeability, regulation of haemostasis via the maintenance of anti-coagulant properties, mediation of inflammatory responses, regulation of cell growth and repair and stimulation of angiogenesis (Berne & Levy, 1993; Alberts *et al*, 1994; Davies, 1995; Kirkpatrick, 1997).

The endothelium regulates blood vessel tone in response to altered flow. Endothelial cells produce both vasodilator agents, such as prostacyclin and endothelium derived relaxing factor (EDRF), now known to be nitric oxide (NO) (Palmer & Moncada, 1987), as well as several vasoconstrictors such as endothelin -1 (ET-1) (Kirkpatrick, 1997). It seems that impaired NO release from the endothelium is a forerunner to endothelial dysfunction and disease states.

Endothelial cells also play an essential role in haemostasis and blood coagulation (Davies, 1995; Kirkpatrick, 1997). Under normal physiological conditions, the endothelium is a potent anti-thrombogenic surface which has anticoagulants such as heparan sulphate and other plasma inhibitors of thrombin present (Berne & Levy,

(a)



(b)

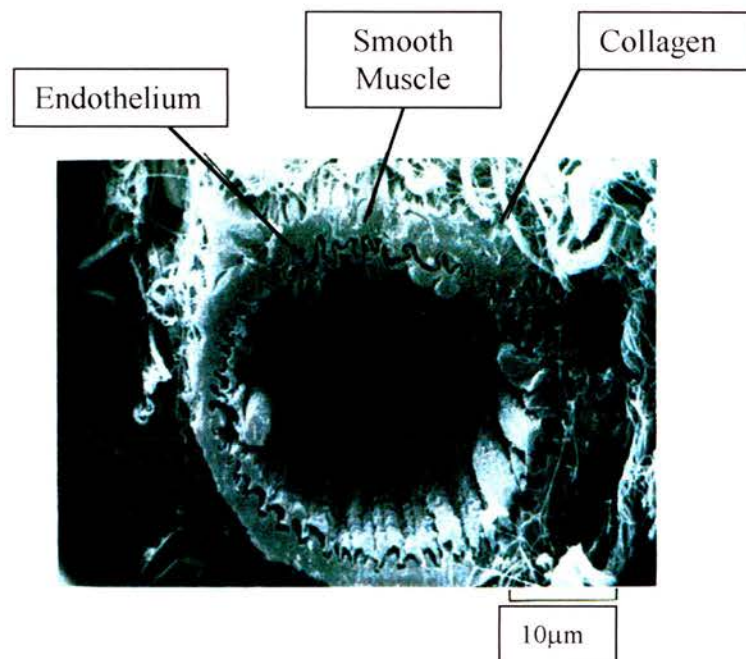


Figure 1.1. (a)&(b) show diagrammatic and photographic representations of a blood vessel transverse section. A single layer of endothelial cells can be seen on the luminal surface of the vessels, surrounded by a layer of smooth muscle cells which are involved in vessel contraction and dilation. (Illustrations courtesy of Dr. R. Pritchard).

1993; Kirkpatrick, 1997). However, disruption of this state, for example by endotoxins in septic shock, results in the release of ‘procoagulants’ that induce the clotting response.

The endothelium is essential for tissue growth during development and for repair following injury. In the embryo, arteries and veins develop from small vessels composed entirely of endothelial cells. In the adult, endothelial cells retain their ability to proliferate and migrate towards sites of damage, forming new vessels (neovasculature), by a process known as angiogenesis.

1.1.1 The endothelium and blood flow

Most cells in the body are exposed to some sort of mechanical force and need to be able to do more than simply tolerate it; they must be able to sense, measure and respond to it (McNeil, 1993; Wang *et al*, 1993). Research has shown that endothelial cells can alter their metabolism, gene expression and cytoskeletal architecture in response to altered blood flow (McNeil, 1993; Girard & Nerem, 1995; Davies, 1995; Topper & Gimbrone, 1999).

Blood ‘fluid dynamics’ are complex. Poiseuille’s Law of fluid dynamics applies to non-pulsatile flow in a rigid tube of even cross sectional area. However, arterial vessels are compliant tubes, with uneven cross sectional area and side branches, and are exposed to pulsatile flow. Much research in this area, using *in vitro* models based on *in vivo* scenarios, as well as fixed vessels has resulted in what are believed to be fairly accurate blood flow characteristics allowing estimations of haemodynamic forces to be made (Davies, 1995).

‘Stress’ is a term frequently associated with blood flow dynamics, with regard to forces it exerts on the vessel wall. By definition, stress is force per unit area and has two components; a normal component, blood pressure (BP), which produces tension and compression and a parallel component known as fluid shear stress which exerts a frictional force. A schematic diagram of these forces can be seen in Figure 1.2.

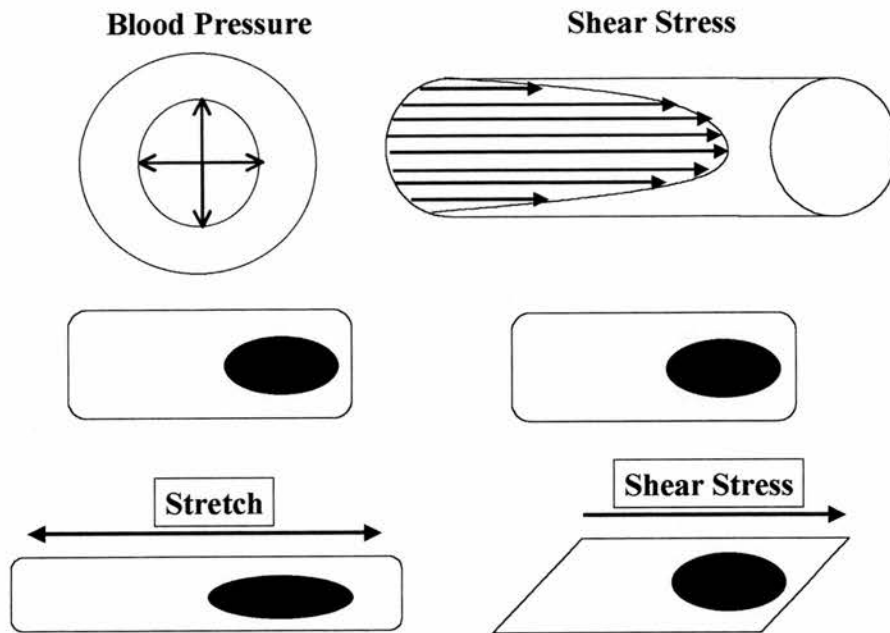


Figure 1.2. Schematic representation of the effects of blood pressure and shear stress respectively on the morphology endothelial cells. Blood pressure can be seen to act perpendicularly while shear stress acts parallel to the vessel wall. (Adapted from Ballerman et al, 1998).

BP acts perpendicularly to the vessel wall. The pulsatile nature of flow in the vasculature means that this component continually oscillates, creating transmural pressure that exerts 'stretch' or cyclical strain on the endothelium and vessel wall.

In contrast, fluid shear stress is a frictional force that acts parallel to the direction of flow. It exerts force tangentially to the endothelial cell apical surface and is responsible for the induction of many cellular responses (Davies, 1995). The magnitude of shear forces experienced by endothelial cells is very small in relation to the forces associated with BP changes, however fluid shear stress has proved to be extremely important in regulating both endothelial cell structure and function. Masuda & Fujiwara (1993a) determined that shear stress and not shear-rate was responsible for endothelial stimulation and that endothelial cells can sense both the magnitude and direction of the force.

Overall, blood flow in the vascular system is unidirectional and laminar, with turbulence only occurring in areas of branching or curving. Turbulence results in the breakdown of direction, magnitude and frequency of forces acting on the endothelium (Davies, 1989). Despite shear forces being significantly smaller than those due to pressure, much more attention has been focused on shear responses as it has been shown that these greatly influence vascular biology (Dewey *et al*, 1981; Levesque & Nerem, 1985; Ives *et al*, 1986). It is important to note that changes in blood flow cannot occur without changes in pressure, however, the effects of shear stress can be dissociated from those produced as a consequence of pressure changes (Bevan, 1997). Different regions of the vasculature experience varying flow conditions which influence endothelial cells individually, which often results in dramatic cellular differences (Nerem *et al*, 1998). In contrast to BP which is absorbed to a large extent by the smooth muscle components of the vessel wall, the full force of fluid shear stress acts directly on the endothelium (Davies, 1989).

In order to sense and then respond to changes in blood flow, the endothelium acts as a mechanically sensitive signal transduction interface (Davies & Tripathi, 1993; Davies, 1995). Much work has been carried out in this field and it has been found that endothelial shear stress-induced responses occur in a time dependent manner (Davies, 1995; Topper & Gimbrone, 1999). 'Acute' responses can occur within

seconds of commencing flow, and include potassium (K^+) channel activation, elevated intracellular calcium (Ca^{2+}), hyperpolarisation of the cell membrane, increased phosphoinositide turnover and the release of potent vasoactive agents that serve to regulate vessel tone, such as NO and prostacyclin. On a longer time scale (minutes – hours), shear stress causes activation of protein kinase cascades and of downstream nuclear transcription factors that regulate gene expression. Exposing endothelial cells to fluid shear stress for longer time periods (i.e. several hours to days) leads to ‘chronic’ responses. These include focal adhesion and cytoskeletal remodelling, leading to cell elongation and realignment in direction of flow. Other responses include cell flattening, to minimise the effects of shear stress, increased adhesion to the substrate, stimulation of nitric oxide synthase (NOS) activity, altered mRNA (for protein synthesis) and inhibition of cell growth and division (Levesque & Nerem, 1985; Davies, 1995; Ballerman, 1998).

Over the years, there has been increasing evidence of the importance of blood flow and its associated shear stress in the regulation of endothelial biology at the blood-endothelial cells (vessel wall) interface. Based on evidence demonstrating that endothelial cell deformation as a result of shear forces is dependent on the mechanical and structural properties of the cells, this study focused on the effects of fluid shear stress on the cytoskeleton of bovine aortic endothelial cells (BAEC). Haemodynamic forces are known to be involved in changes in cell morphology, metabolism and gene expression along with the release of vasoactive substances (Davies, 1995; Traub & Berk, 1998), although exactly how cells sense these forces remains unsolved.

1.1.2 Arterial Fluid Shear Stress

The mean fluid shear stress in the arterial system under normal physiological conditions is in the range of 2-40 dynes.cm⁻², which can increase up to around 200 dynes.cm⁻² in branching regions of the aorta (Dewey *et al*, 1981; Levesque & Nerem, 1985). In major arteries, fluid shear stress is generally in the range 2-20 dynes.cm⁻² but can increase locally from 30-100 dynes.cm⁻² near branch points (White *et al*, 1983). Work by Fry in 1973 (cited Davies, 1995) showed that forces of up to 400

dynes.cm⁻² and in some cases up to 1000 dynes.cm⁻², (Levesque & Nerem, 1985) were required to detach the endothelium in arteries. The pulsatile flow present in the arterial system produces a velocity profile along the length of the vessel which results in varying shear gradients and hence fluid shear stress. Non-geometric regions of the arteries e.g. artery branches, exhibit lumen narrowing and curvature resulting in disruption of laminar flow to varying degrees, which can in turn lead to blood vortices and turbulent flow, especially at bifurcations. Areas of turbulent flow have been identified as potential initiation sites for endothelial cell dysfunction, with areas of laminar flow being relatively protected (Traub & Berk, 1998). Some cellular responses to laminar and turbulent flow can be seen in figure 1.3. Early studies in this field (Davies *et al*, 1986) highlighted an increased turnover of endothelial cells in areas exposed to turbulent shear stress which suggested disturbance of endothelial integrity, while others (Dimmeler *et al*, 1996) showed that low shear stress led to apoptosis of endothelial cells. It has also been reported that steady shear stress is required for wound healing and integrity of the endothelium (Traub & Berk, 1998). All this points towards shear stress functioning as a ‘survival’ determinant of endothelial cells, maintaining their normal function.

1.1.3 Atherosclerosis

In the 19th century Rokitansky & Virchow (cited Davies, 1995) noted non uniform distributions of atherosclerotic lesions in blood vessels. They suggested that variations in haemodynamic forces operating in the arteries may be responsible. Atherosclerosis is now recognised as a progressive disease of the vasculature, characterised by a spectrum of changes within the vessel wall reflecting a chronic response-to-injury process. It can lead to partial or in some cases complete occlusion of the vessel lumen, resulting in ischaemia of tissues downstream of the lesion and, in severe cases, to cerebrovascular accident (stroke) or myocardial infarction. Atherosclerosis is the primary cause of heart attack, stroke and gangrene of the extremities and is ultimately responsible for more than 50% of mortalities in Europe, USA and Japan (Ross, 1993).

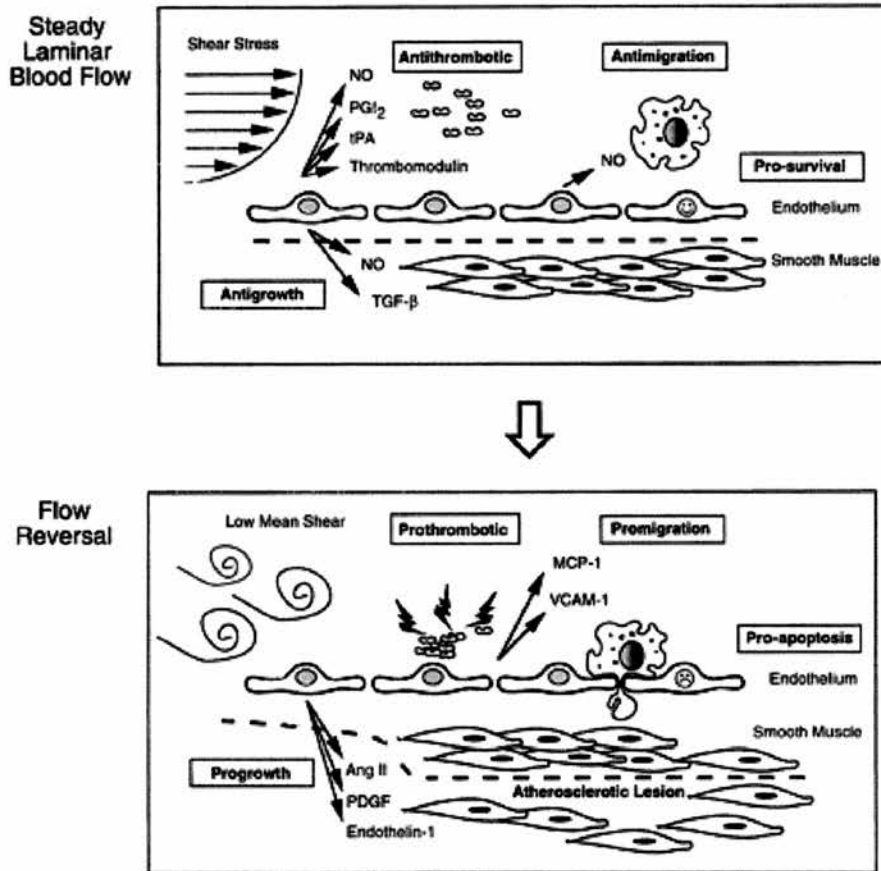


Figure 1.3. Comparison of the effects of steady laminar flow and low shear stress or turbulent flow on the endothelium. Steady laminar shear stress induces the release of factors from endothelial cells which promote endothelial cell survival by inhibiting coagulation, leukocyte migration and smooth muscle proliferation. In contrast low shear stress or flow reversal resulting from turbulent flow produce the opposite effects. This shift in profile has been found to contribute to the development of atherosclerotic lesions. Abbreviations: AngII, angiotensin II; PGI₂, prostacyclin; PDGF, platelet derived growth factor; TGF- β , transforming growth factor β ; tPA, tissue plasminogen activator. (Diagram taken from Traub et al, 1998).

The trigger for atherogenesis is thought to be injury to the endothelium, specifically in regions of the vasculature that experience disturbed patterns of blood flow. Typically, these areas are found where blood vessels branch, bifurcate, or are sharply curved. Certain vessels have been found to be more susceptible than others. Interestingly, it has been shown that atherosclerotic lesions are more likely to form in areas of low-mean wall fluid shear stress, coupled with disturbed flow, rather than in those experiencing exceptionally high unidirectional laminar fluid shear stress (Davies, 1995). General wear and tear of the endothelium has been implicated as a result of low or high shears rates, resulting in modification of the plasma membrane and hence endothelial cell function *in vitro* (McNeil, 1993).

Traub & Berk (1998) suggest that laminar shear stress stimulates endothelium responses which are atheroprotective, whereas disturbed flow patterns tend to be pro-atherogenic. Dimmeler (1998) comments that laminar shear stress protects endothelial cells from apoptotic cell death, a cellular process that would otherwise cause denudation of areas of blood vessel and initiate atherogenesis. Therefore responses to flow can be beneficial or harmful, depending on the type of shear force exerted on the cells. This has led to the view that the endothelium is in a state of dynamic equilibrium, where opposing functions are strictly controlled under normal physiological conditions but which can result in pathological changes if the balance is perturbed (Kirkpatrick, 1997).

The work of this thesis is concerned with the effects of shear stress on, (a) cytoskeletal remodelling of BAEC, in particular, on the intermediate filament component, and (b) the signalling pathway associated with activation of the inducible nuclear transcription factor, NF- κ B. Endothelial cells provide an ideal model as they have been shown to maintain their *in vivo* characteristics in culture (Blöse & Chacko, 1976) and exhibit contact inhibition once a confluent monolayer is obtained.

1.2 *The Cytoskeleton*

The cytoskeleton is a complex array of protein filaments that provides an internal structural support system in all eukaryotic cells. This cell ‘scaffolding’ is involved in

a diverse array of cell functions, including: cell migration, muscle contraction, shape changes in the developing embryo, chromosome segregation in mitosis, intracellular movement and organelle transport. It is composed primarily of three types of protein filament, along with numerous ‘associated’ proteins. All three components can assemble and disassemble in response to environmental changes. Together these filamentous proteins form complex, interconnected networks that function in an integrated fashion. Hence, disruption of one element necessarily influences the others.

The three main cytoskeletal components are microtubules, microfilaments and intermediate filaments. Microtubules have a diameter of ~25nm and are composed of tubulin subunits. They are highly conserved between different cell types and are thought to be the primary organisers of the cytoskeleton. Microtubules can be arranged individually, in parallel bundles or in extended networks. They are often modified by microtubule associated proteins (MAP) that are involved in microtubule assembly and disassembly, as well as by their interactions with other elements of the cytoskeleton. The microtubule network arises from a microtubule organising centre (MTOC), or centrosome, and extends out towards the cell periphery in a wavy pattern. These elements are involved in the trafficking of vesicles, organelles and proteins throughout the cell as well as in spindle-chromosome alignment and segregation during mitosis (Fuchs & Yang, 1999).

Microfilaments are 7nm in diameter, made up of polymerised globular actin (G-actin) subunits arranged in a double helical array. They are highly conserved in eukaryotic cells with a primary role in cell movement and contractility. When G-actin polymerises to form filaments it becomes known as filamentous, or F-, actin. Microfilaments can be found in various arrangements. These can take the form of bands of actin around the cell periphery, known as dense peripheral bands, or parallel bundles within the cell interior, called stress fibres. Alternatively, actin also exists as a cortical meshwork (cortical actin) anchored to the plasma membrane which is thought to contribute to the mechanical properties of the cell surface. It is thought that microfilaments evolved for cell polarity, contractility and migratory purposes (Fuchs & Yang, 1999).

The third component, intermediate filaments, have a diameter between microtubules and microfilaments. These 10nm filaments, in contrast to the other components, belong to one of six tissue or cell-specific classes (Figure 1.4). Intermediate filaments are thought to play a structural role in the cell providing mechanical strength. They can be found singly or in bundles within the cell, forming a loose wavy network, radiating outwards from the nucleus towards the plasma membrane (section 1.2.2). Intermediate filaments are thought to have appeared later in evolution than both microfilaments and microtubules as exoskeletons gradually gave way to endoskeletons and higher eukaryotes developed the need for mechanical integration in the cytoskeleton (Fuchs & Yang, 1999).

1.2.1 *Actin stress fibres*

Much research has shown that cells exposed to fluid forces *in vivo* contain prominent stress fibres, frequently orientated in the direction of blood flow (Gabbiani *et al*, 1983). Stress fibres are also present in sub-confluent cultures of endothelial cells. Stress fibres are thick bundles of actin microfilaments that extend in straight paths throughout the cytoplasm, making contact with the cell membrane at focal adhesion sites where they connect with the extracellular matrix (ECM). These sites were first reported by Lewis and Lewis (1924) in cultured vascular endothelial cells. During growth and spreading of cultured endothelial cells, stress fibres are present in random arrays. However, once a confluent monolayer is achieved and cells contact-inhibit, stress fibres are replaced with dense peripheral bands (Gabbiani *et al*, 1983; Wong & Pollard, 1983).

Exposure to steady flow is known to alter endothelial cell shape and orientation, from polygonal to ellipsoid, as the cells progressively elongate and then later become aligned in the direction of flow. It has been suggested that the cytoskeleton dictates this change (Gabbiani *et al*, 1983; Wong *et al*, 1983), with *in vitro* models supporting *in vivo* experiments. White *et al* (1983), working on perfusion fixed aortas from hyper and normo-tensive rats, reported that the prevalence of stress fibres varied between regions in the same vessel, and that their distribution was also influenced by sex and haemodynamic forces. Comparisons between aortas and other vessels

(a)

TYPE OF IF	COMPONENT	LOCATION
I & II	Keratins (40-70kDa)	Epithelial cells, hair and nails.
III	Vimentin (55kDa), Desmin (54kDa), Glial fibrillary acidic protein (45kDa)	Mesenchymal cells e.g. EC & fibroblasts Muscle cells Glial cells, astrocytes & some Schwann cells
IV	Neurofilaments (68, 150, 200 kDa)	Neurones
V	Nuclear lamins (63-68 kDa)	Nuclear membrane
VI	Nestin (200 kDa)	Primarily embryonic cells

(b)

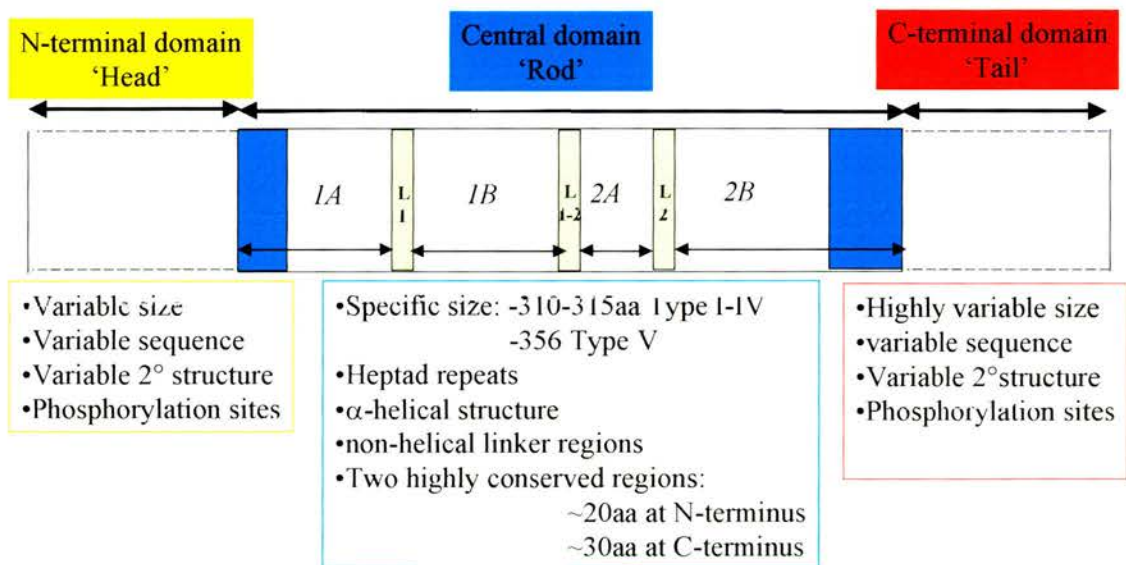


Figure 1.4. Figure 1.4a shows the various classes of intermediate filaments along with the cell type in which they are found. Figure 1.4b is a schematic diagram of general intermediate structural organisation. In types I-IV, 3 non-helical linker (L) regions (green shaded areas) interrupt the rod domain. The solid blue sections represent conserved sequences, common to all intermediate filament proteins which are similar but not identical in each intermediate filament type. (Adapted from Skalli et al, 1992).

highlighted differences in cytoskeletal organisation, with stress fibres being most abundant in aortas, suggesting local, as opposed to systemic, modifying factors (Wong & Pollard, 1983). Experiments using *en face* endothelial preparations (Gabbiani *et al*, 1983) concluded that stress fibres are present *in vivo* and that they re-organise during the adaptation of endothelial cells to unfavourable or pathological conditions (e.g. endothelium regeneration). White and Fujiwara (1986) propose that stress fibres play a role in increased cell adhesion and become upregulated when there is an appropriate demand. They also suggest that stress fibres on the luminal cell surface, which cannot be involved in cell adhesion, serve to strengthen cells when faced with increased mechanical stress. It has been postulated that luminal stress fibres also transmit forces from the cell surface to focal attachment sites located on the abluminal surface (Wong & Pollard, 1983).

Further work has shown that *in vivo*, parallel stress fibres form from dense peripheral bands in response to shear stress, but not blood pressure. This results in increased cell adhesion, achieved by the formation of new focal adhesions, and improved structural integrity of the endothelium, characterised by the alignment of stress fibres in the direction of flow (White & Fujiwara, 1986; Davies, 1993). The distribution of focal adhesions is also altered by flow, which suggests a possible cytoskeletal interaction, generating cell morphology appropriate to the prevailing flow pattern (Levesque & Nerem, 1985). Experiments have shown that actin plays a major role in force transmission throughout cells as microfilament disrupting drugs were found to prevent cell re-alignment and focal adhesion remodelling (Malek & Izumo, 1996).

1.2.2 *Intermediate filaments*

Intermediate filaments are expressed in cell-type specific patterns following various pathways throughout embryonic development and cell differentiation. In contrast to actin and tubulin, which are highly conserved globular proteins, intermediate filaments are fibrous proteins with no enzymatic activity (Hermann & Aebi, 2000). Intermediate filaments are also more complex than either microfilaments or microtubules and are formed from a heterogeneous, multigene family of proteins that can be distinguished both biochemically and immunologically (Steinert & Roop,

1988). In fact, over 50 types of intermediate filament proteins have been identified, forming morphologically similar filaments in different cell types. These can be classified into 6 different types (Figure 1.4). All intermediate filament proteins possess a tripartite structure (Figure 1.4), composed of N-terminal head and C-terminal tail domains on either side of a protease-resistant α -helical rod with heptad, hydrophobic amino acid repeats (Ho *et al*, 1998).

Intermediate filaments form networks which resemble those of microtubules, but are quite distinct from the stress fibres and dense peripheral band arrangements of actin microfilaments. Intermediate filaments emerge from a perinuclear region, forming a 'cage-like' structure that surrounds and 'positions' the nucleus (Skalli & Goldman, 1991), and extend outwards to form a meshwork that permeates the cytoplasm. Intermediate filaments make contact with the nuclear envelope via a 6.6kDa sequence in the C terminus tail of vimentin, resulting in the formation of 10nm filaments in a concentration dependent manner (Georgatos & Blobel, 1987a). The nuclear envelope attachment site was identified as lamin B (Georgatos & Blobel, 1987b). Georgatos & Marchesi (1985) had previously used human red blood cells as a model system for intermediate filament-membrane interactions. Georgatos & Blobel (1987a) later identified specific vimentin attachment sites in the plasma membrane. In contrast to those in the nuclear envelope, they recognise the amino-terminal of the head domain and interact with vimentin in a non co-operative, saturable manner, which does not lead to the formation of extensive intermediate filament arrays *in vitro*. However, interaction of vimentin at both sites does result in a continuous network connecting the plasma membrane and the karyoskeleton with intermediate filament assembly beginning around the nuclear envelope region and emanating outwards

Intermediate filaments form transcellular networks in epithelial cells, through cell-cell contacts called desmosomes, and they make contact with the extracellular matrix through structures called hemidesmosomes (Jones & Green, 1991; Green & Jones, 1996). Hemidesmosomes are lacking in endothelial cells, but vimentin-associated matrix adhesions that resemble both hemidesmosomes and focal adhesions are found on the basal surface (Flitney *et al*, 1996; Gonzales *et al*, 2001).

Over the years much research has been carried out on microfilaments and microtubules, including their interactions with one other, but with much less emphasis being given to intermediate filaments. Intermediate filaments were originally thought to be disaggregation products of microtubules since they collapse to form a diffuse, perinuclear cap when exposed to colcemid and nocodazole, agents that selectively depolymerise microtubules. However, they were later found to be a distinct but integrated part of the cytoskeleton with an important role to play in normal cell functioning (Lazarides, 1980). Since then much more work has focused on intermediate filaments coupled with their association with other cytoskeletal proteins. Green *et al* (1986) showed intermediate filament-microfilament interactions in chick embryo fibroblasts. Immunofluorescence studies not only showed intermediate filaments running alongside actin stress fibres, but also highlighted phalloidin binding ‘nodules’ that appeared to act as foci, from where bundles of intermediate filaments diverged and/or converged in spreading cells. Later studies concluded that the tail domain of vimentin, which is not required for the assembly of intermediate filament bundles, binds to actin microfilaments (Cary *et al* 1994).

In contrast to both microtubules and microfilaments, intermediate filaments have been shown to increase their rigidity when exposed to increased strain, suggesting that intermediate filaments are the cytoskeletal element most responsible for maintaining cell integrity (Janmey *et al*, 1991, Goldman *et al*, 1996). This visco-elastic property of intermediate filaments is mediated by the C terminal domain (Janmey *et al*, 1991). It has been suggested that as intermediate filaments appeared in evolutionary terms after microtubules, microfilaments and some cell-cell adhesions that they took advantage of some pre-existing cell constituents to develop an organisation which suited their function (Coulombe *et al*, 2000). Coulombe *et al* (2000) discussed two different influences on intermediate filament organisation referred to as ‘ins’ and ‘outs’. ‘Ins’ are described as sequence determinants with intermediate filaments themselves which influence both the distribution and intermediate filament-intermediate filament interaction within the cytoplasm while ‘outs’ are associated with non-intermediate filament proteins which tether intermediate filaments to other cellular elements influencing intermediate filament spatial arrangement in the cytoplasm.

In endothelial cells, intermediate filaments are composed entirely of vimentin, a type III intermediate filament protein, arranged into bundles of 10 nm filaments forming an extensive 3-D network. Studies have shown that mammalian, avian and amphibian vimentin antibodies cross-react, illustrating its conservation throughout evolution (Lazarides, 1982). Unlike microtubules and microfilaments, intermediate filaments have no known force generating system directly associated with them. In fibroblasts, drug induced aggregation of intermediate filaments has been found to be an active event requiring ATP coupled with the actin cytoskeleton (Tint *et al*, 1991). The involvement of the acto-myosin network was supported by the fact that intermediate filament aggregation was blocked in the presence of cytochalasin D.

For some time, intermediate filaments have been viewed as the structural ‘back bone’ of the cytoskeleton based on their viscoelastic properties (Janmey *et al*, 1991; Goldman *et al*, 1996; Chou & Goldman, 2000). Their subcellular organisation and physical properties suggest that intermediate filaments play a major role in the mechanical integrity of cells and tissues. While lower eukaryotes may survive in the absence of intermediate filaments, mutations in human (and mouse) intermediate filaments can result in the development of degenerative diseases. For example epidermal fragility syndromes where the ability of the intermediate filament network to resist stress is compromised. An example of this type of condition is epidermolysis bullosa simplex (EBS) where keratinocytes rupture when exposed to physical trauma such as scratching or rubbing (Fuchs & Weber, 1994; Lane, 1994; McLean & Lane, 1995). Three forms of this condition are recognised. EBS-Dowling-Meara (EBS-DM) is the most severe form, where clusters of fluid filled blisters can form on any part of the body. Less severe are EBS-Kobner (EBS-K) which forms non-clustered blisters and EBS – Weber-Cockayne (EBS-WC), the mildest condition, where blisters are less frequent and generally restricted to thickened skin on palms of hands and soles of feet. The mutations responsible for different forms of this condition are found on 2 primary keratins, synthesised from undifferentiated keratinocytes of the basal epidermal layer (K5 and K14), and are clustered at various sites along the protein (Lane, 1994; McLean & Lane, 1996). Estimated levels of the occurrence of EBS range from 1:20,000 to 1:50,000 of the

population, although exact figures are difficult to ascertain as EBS-WC can go undetected (Lane, 1994; McLean & Lane, 1995).

Deficiency of the IFAP plectin has also been linked with EBS. Research has shown that a mutation in the plectin gene is responsible for the development of autosomal recessive muscular dystrophy (MD) associated with EBS (EBS-MD), where plectin was found to simultaneously account for structural complications in muscle and skin (Smith *et al*, 1996; McLean *et al*, 1996). EBS-MD shows epidermal blistering at the level of the hemidesmosome (McLean *et al*, 1996) which mediates adhesion of the keratinocytes to the basal membrane (Jones & Green, 1991). In EBS-MD patients approximately two thirds of keratinocyte hemidesmosomes lacked an inner plaque with which plectin associates (Smith *et al*, 1996). McLean *et al* (1996), suggest that plectin may perform a similar role in muscle, but it is not clear whether it is the intermediate filament-membrane or actin-membrane connections which lead to muscle fragility in EBS-MD.

1.2.2.1 *Dynamic properties of intermediate filaments*

Until quite recently, relatively little was known of their dynamic properties. Indeed, intermediate filaments were widely thought of as being very stable, inert, mechanical elements which were uninteresting compared to microtubules and microfilaments (Steinert & Leim, 1990). However, research has shown that intermediate filaments exhibit a range of complex, dynamic properties (Steinert & Roop, 1988; Vikstrom *et al*, 1989; Vikstrom *et al*, 1992; Prahlad *et al*, 1998; Yoon *et al*, 1998). Research on baby hamster kidney cells (BHK) has shown that exogenous rhodamine-labeled vimentin is rapidly incorporated into the endogenous network of intermediate filaments. The process begins in the perinuclear region and progresses outwards towards the cell membrane (Vikstrom *et al*, 1989; Vikstrom *et al*, 1992). The existence of a dynamic equilibrium between a pool of unpolymerised vimentin subunits and fully-formed intermediate filaments was confirmed using the fluorescence recovery after photobleaching (FRAP) technique (Vikstrom *et al*, 1992). Various

techniques have been developed over the past decade which have given a better insight into intermediate filament dynamics. Microinjections of fluorescent tagged intermediate filaments and FRAP were somewhat limited due to bleaching of the fluorochrome. However, the introduction of green fluorescent protein (GFP) fusion proteins has allowed structural studies to be made on living cells, including studies of cell growth, gene expression, protein-protein interactions, cell movement and cytoskeletal dynamics (Chalfie *et al* 1994; Yang *et al*, 1996; Ludin & Matus, 1998). One obvious advantage of this technique is the elimination of artefacts which fixation can sometimes produce. To date GFP fusion proteins have been successfully expressed in bacteria, yeast, plant, *Drosophila* and mammalian cells (Yang *et al*, 1996).

The development of GFP fusion proteins has provided greater insights into intermediate filament dynamics in living cells. Studies with GFP-vimentin have revealed that intermediate filaments are constantly moving and altering their shape within the cytoplasm (Prahlad *et al*, 1998; Yoon *et al*, 1998; Ho *et al*, 1998). Prahlad *et al* (1998) monitored the reorganisation of GFP-vimentin networks following trypsinisation and replating. They describe the formation of vimentin ‘dots’ at the cell periphery, which are neither membrane bound or filamentous in nature. However, with time these ‘dots’ lengthen and develop into longer fibrils, or ‘squiggles,’ which subsequently become incorporated into the ‘classic’ filamentous network observed in fully spread cells (This can be viewed in video #1 <http://www.jcb.org/cgi/content/full/150/3/f101/dc1>;) (Chou & Goldman, 2000). ‘Dots’ and ‘squiggles’ were found to move at different speeds suggesting increased control of both spatial and temporal intermediate filament assembly. Chou *et al* (2001) suggest the most obvious benefit of being able to move these intermediate filament precursors around the cell is that it provides an efficient mechanism to ‘shuttle’ intermediate filament ‘building blocks’ to the region of the cytoplasm where mechanical stability is required.

The movement of ‘dots’ and ‘squiggles’ is sensitive to treatment with nocodazole, a microtubule depolymerising drug. Microinjections of kinesin antibodies prevents the assembly of an extended intermediate filament network and causes pre-existing networks to collapse, suggesting some level of involvement of kinesin in cross-

linking microtubules with intermediate filaments (Gyoeva & Gelfand, 1991; Prahlad *et al*, 1998; Liao & Gundersen, 1998). Blose *et al* (1976 & 1984) had previously implied a microtubule-intermediate filament association as they showed that microtubule depolymerisation and injection of tubulin antibodies caused intermediate filaments to retract from the cell periphery within 2 hours but had no effect on protein synthesis or deleterious effect on cell metabolism. Interestingly, by the time intermediate filament collapse was complete the microtubule network appeared intact (Blose *et al*, 1984). It appeared that intermediate filament disruption occurred through some form of direct interaction with either α or β tubulin subunits at specific sites, which in turn disturbed microtubule-intermediate filament interactions. The ‘collapse’ of complex intermediate filament networks from the cell periphery to a juxtannuclear region in response physiological stimuli, as well as treatment of cells with microtubule and microfilament inhibitors, is the least well understood aspect of intermediate filament dynamics. This reinforces the view that cytoskeletal proteins do not function independently of each other.

Fully formed intermediate filament networks in fibroblasts and endothelial cells constantly change their arrangement, without altering overall cell shape (Ho *et al*, 1998, Helmke *et al*, 2000). Changes in ‘long fibril’ distribution occur when cells are treated with metabolic inhibitors but not with microtubule or microfilament inhibitors, suggesting the involvement of a currently unidentified mechanism (Yoon *et al*, 1998). Goldman *et al* (1996) used mimetic peptides from the amino acid sequence of the helix initiation 1A domain of intermediate filament proteins to disassemble the intermediate filament network. This 1A peptide is the most highly conserved domain of intermediate filament structure and targets intermediate filaments specifically (Goldman *et al*, 1996). Results showed a reversible disassembly of intermediate filaments from oligomers to monomers within 30 minutes, accompanied by dramatic alteration of cell shape, de-stabilisation of the microtubule and microfilament networks and loss of cell-adhesion contacts. These were all re-established when cells re-spread. This was suggested to be due to the involvement of intermediate filament associated proteins (IFAP) which form bridges between intermediate filaments and other cytoskeletal elements (Goldman *et al*, 1998).

1.2.2.2 Regulation of intermediate filament assembly and disassembly

Intermediate filaments are controlled by unique and complex molecular pathways, the details of which are as yet not completely identified. Over the last decade, phosphorylation has been shown to modify intermediate filaments in a cell-type specific manner with the degree of phosphorylation correlating with changes in intermediate filament arrangement (Steinert & Liem, 1990, Skalli & Goldman, 1991). Research has shown phosphorylation to be both spatially and temporally regulated during cellular events with each type of intermediate filament under the control of a distinct set of kinases (Inagaki *et al*, 1996). Intermediate filament phosphorylation is also site-specific and highly regulated with the ability to produce local alterations of filament properties and sequences which regulate the interaction of intermediate filaments with each other as well as with other proteins (Coulombe *et al*, 2000). Phosphorylation of intermediate filaments may also modify their mechanical properties as well as their interaction with other cytoskeletal components (Skalli *et al*, 1992).

Mitosis is a stage of the cell cycle when dramatic changes in cytoplasmic and nuclear architecture occur. In some cells, intermediate filaments depolymerise and move towards the perinuclear area, while in others the intermediate filament network disappears completely and reassembles once mitosis is complete (Yang *et al*, 1985; Chou *et al*, 1989; Steinert & Liem, 1990). However, not all cells disassemble their intermediate filament networks to a perinuclear region during mitosis. Skalli *et al* (1992) proposed that several protein kinases used intermediate filaments as substrates but that not every filament acted as a substrate to every kinase. They suggested that this concept might explain differences in the extent of cell-type specific mitotic re-organisation of intermediate filaments.

In mouse epidermal keratinocytes the intermediate filament network retracts towards the nucleus during mitosis and later re-assembles in the cytoplasm of the daughter cells (Jones & Goldman, 1985). Endothelial cells are another cell type in which intermediate filaments do not ‘collapse’ to a perinuclear region (Blöse, 1979), a characteristic discussed in the next section. These cell-type specific alterations in

intermediate filament networks during mitosis suggest the involvement of cell cycle and regional regulatory mechanisms controlling intermediate filament assembly and disassembly, with phosphorylation mediated modulation as the likely mechanism (Fuchs & Weber, 1994). Nishizawa *et al*, 1991 commented that not only does phosphorylation increase during mitosis, but different sites are phosphorylated during interphase and mitosis. They showed that in the case of glial fibrillary acidic protein (GFAP) that site specific phosphorylation was not only found to induce intermediate filament mitotic configuration changes but it was also found to be highly concentrated in the constricted area of the cell before the final separation during cytokinesis. Research on mitotic BHK cells (Chou *et al*, 1996) demonstrated that site specific phosphorylation of the N-terminal but not the C-terminal domain of vimentin plays an important role in determining the state of intermediate filament polymerisation and supramolecular organisation in mitotic cells. Thus both the site and extent of phosphorylation are crucial factors in mediating structural changes of vimentin.

Earlier studies had shown that increased vimentin phosphorylation was found to accompany cell division, with up to a 6-fold increase in phosphate incorporation in dividing BHK cells as compared to interphase cells (Chou *et al*, 1989). It is now known that the non α -helical head domain of vimentin can be phosphorylated on numerous serine (S) residues located in the N terminus. Much research has mapped the residues phosphorylated by different protein kinases. It has been shown that protein kinase A (PKA) phosphorylates serine (S) 6, S24, S38, S46, S50 and S65, which are located close to the carboxyl-terminal side of arginine (ARG) residues (Ando *et al*, 1989). Protein kinase C (PKC) phosphorylates S6, S8, S9, S20, S24, S25, S33, S38, S41, S50 and S65 which are located on the amino-terminal side of ARG residues (Ando *et al*, 1989). For both these kinases, as well as Cam kinase II, only phosphoserine residues were detected. It has also been demonstrated that calmodulin-dependent protein kinase II (CaM II) phosphorylates S38 and S82 (Ando *et al*, 1991) and aspartic acid (ASP) 84 residues play an essential role in determining phosphorylation of S82. p34^{cdc2} kinase phosphorylates vimentin on S55 (Chou *et al*, 1990; Chou *et al*, 1991) and S41 (Ando *et al*, 1993), while rho-kinase is now known to phosphorylate vimentin on S38 and S71 (Goto *et al*, 1998). It is interesting to note that several serine residues can be phosphorylated by more than one kinase,

implicating the involvement of various signalling pathways. The pattern of phosphate incorporation differs in other intermediate filament proteins. For example, while nuclear lamins are phosphorylated by p34^{cdc2} (Chou *et al*, 1990), keratin intermediate filaments are not (Goldman *et al*, 1991). Work by Inagaki *et al* (1996) showed that while p34^{cdc2} directly phosphorylates vimentin in mitotic cells, CaM II phosphorylates vimentin when activated by cell signalling and PKC vimentin phosphorylation occurs concomitantly with intracellular membrane reorganisation.

The development of 4A4 antibody allowed researchers to recognise S55 phosphorylated vimentin (Tsujimura *et al*, 1994). Phosphorylation, accompanied by varying degrees of vimentin assembly, was found to occur at the metaphase stage of the cell cycle, with dephosphorylation occurring during cytokinesis. This pattern was observed in a variety of cell-types. Phosphorylation activity was found to be zero in cells during interphase.

Ogawara *et al* (1995) showed that hydrolysis of inositol phospholipids resulted in the activation of two signalling pathways. The production of diacylglycerol (DAG) and inositol triphosphate (IP3) targets protein kinases PKC and CaMII respectively. These in turn phosphorylate vimentin S33 and S82 respectively. The development of the phospho-specific antibodies, YT33 and MO82, have proved useful in the identification of vimentin site-specific phosphorylation. Studies have shown that PKC and CaMII target vimentin via separate pathways and different physiological conditions (Ogawara *et al*, 1995). In contrast to endogenous expression of CaMII which produced little phosphorylation-induced vimentin reorganisation, ectopic expression of constitutively active PKC or CaMII caused the vimentin network to alter dramatically. These results suggested that under normal conditions, receptor mediated cell signalling induced a sub-maximal level of vimentin phosphorylation which produces a small co-ordinated change in the vimentin network, rather than a dramatic one. Tsujimura *et al* (1994) used the 4A4 antibody that recognises phosphorylated S55 to show the pattern and time scale of p34cdc2-induced vimentin phosphorylation. Takai *et al* (1996) identified mitosis-specific PKC phosphorylation of S33 using the YT33 antibody. Phosphorylation begins in metaphase and is maintained throughout anaphase. No phosphorylation was detected during

interphase even in the presence of a PKC activator, implying that PKC may activate a group of proteins specifically during mitosis (Takai *et al*, 1996).

Inagaki *et al* (1997) studied the effects of calcium (Ca^{2+}) on signalling by CaMII. Using antibodies GK38 and MO82, they showed that elevated levels of Ca^{2+} produced increased phosphorylation of serine³⁸ and serine⁸² respectively. Reorganisation of the vimentin network due to phosphorylation of these 2 serine residues was illustrated using immunogold labelling. Gold labeled GK38 and MO82, showed a much greater percentage of gold particles on aggregates of disassembled vimentin filaments ($11.7.\mu\text{m}^{-1}$) relative to complete filaments ($2.9.\mu\text{m}^{-1}$), reinforcing previous findings showing phosphorylation as the cause of intermediate filament network disassembly.

Goto *et al* (1998) recently showed that vimentin acts as a substrate for Rho-associated kinase (Rho-kinase), which is generally associated with actin containing cell components (Sin *et al*, 1998; Wiche, 1998). Vimentin phosphorylated in this way also lost its ability to form filaments *in vitro*. Further investigations determined that vimentin was specifically phosphorylated at S38 and S71, with S71 being identified as the preferential phosphorylation site. *In vitro* and *in vivo* analysis of vimentin phosphorylation was determined by the development of phospho-specific polyclonal (GK71) (Goto *et al*, 1998) and monoclonal antibodies (Kosako *et al*, 1999) which specifically identified phosphorylated S71. The patterns observed *in vitro* matched those *in vivo* which showed that S71 phosphorylation only occurred at the cleavage furrow of late mitotic cells but not during interphase or early mitosis. Levels of phosphorylated vimentin S71 increased at onset of anaphase, remaining elevated throughout telophase and decreasing at the end of mitosis (Goto *et al*, 1998). Rho-kinase has also been found to phosphorylate the desmin intermediate filaments at the cleavage furrow of NIH3T3 cells (Inada *et al*, 1999). These findings suggest a role for Rho-kinase in the regulation of vimentin re-organisation in the cleavage furrow of cells undergoing cytokinesis via a common molecular mechanism, ensuring that intermediate filaments are segregated effectively into daughter cells.

In contrast to extensive research concerning protein kinases, relatively little has focussed on the role of protein phosphatases. Investigations by Eriksson *et al* (1992)

using three phosphatase inhibitors; calyculin A, okadaic acid and dinophysistoxin, showed that cytoskeletal structural changes occurred within minutes of the inhibitors being administered. Nano-molar concentrations of each chemical resulted in the disruption of intermediate filament networks followed by the loss of microtubule arrangements. These effects were found to be reversible 2-6 hours after removal of the inhibitors. These findings showed that protein phosphatases are essential for the maintenance of cytoskeletal integrity during the interphase. Thus the activation/deactivation of kinases and phosphatases account for the dynamic properties of intermediate filaments during different phases of the cell cycle. Inada *et al* (1999) highlighted a balance between rho-kinase and a type 1 phosphatase in the phosphorylation of vimentin and desmin intermediate filaments. They suggested that rho-kinase is active during interphase as well as mitosis but that the level of phosphorylation is reduced to a non-detectable level as a result of the constitutive action of type 1 phosphatase. It is likely that the equilibrium between these two enzymes may alter the continuous exchange of intermediate filament subunits between the cytoplasmic soluble pool and polymerised filaments.

It is evident that phosphorylation and dephosphorylation regulate intermediate filament dynamics *in vivo*. Serine/threonine phosphorylation results in the major rearrangement of the intermediate filament network in various cell types, a redistribution which may involve peptide motifs associated with intermediate filament assembly or interaction with other cellular proteins. Phosphorylation appears to create a soluble pool of intermediate filament subunits which are ready for intermediate filament polymerisation following dephosphorylation. It seems feasible that phosphorylation may also play a role in the structural dynamics of intermediate filaments, especially since intermediate filament proteins are now known to act as substrates for several protein kinases which are involved in signal transduction pathways. Phosphorylation and dephosphorylation cycles may be involved in subunit exchange between soluble intermediate filament proteins and intact intermediate filaments described by Yoon *et al* (1998). Chou & Goldman (2000) suggest that phosphorylation may also be involved in the selective disassembly of some intermediate filaments into smaller units for transportation to other parts of the network. They speculate that this regional and temporal control of intermediate filament phosphorylation could provide a biochemical mechanism for enhancing

intermediate filament network dynamics in areas of the cytoplasm where rapid reorganisation of cytoskeletal elements is required, for example, during cell spreading.

1.2.2.3 *Intermediate filament networks in endothelial cells*

The ‘classic’ vimentin arrangement in various cell types consists of a ‘wavy’ network of intermediate filament bundles emanating from the nucleus and radiating outwards towards the periphery. The juxtannuclear intermediate filaments extend above and below the nucleus creating a cage-like structure. However, confluent monolayers of contact-inhibited endothelial cells contain a unique arrangement of intermediate filaments. In order for cells to be fully contact inhibited they should meet three criteria. Morphologically, cells should be closely apposed to each other and exhibit a highly flattened appearance, DNA synthesis should be almost completely inhibited and there should be a 10-20-fold decrease in the rate of protein synthesis (Savion *et al*, 1982).

Blose & Chacko (1976) working on confluent monolayers of guinea pig aortic endothelial cells discovered that the majority of cells contain a prominent, phase lucent ring of intermediate filaments, encircling the nucleus. Perinuclear rings of intermediate filaments were found to be orientated in a plane parallel to the substratum with smaller bundles of filaments emerging from the ring and forming a network extending throughout the cytoplasm. Interestingly, during mitosis, perinuclear rings were reported to remain intact until the daughter cells were pulled apart during cytokinesis (Blose & Chacko, 1976). Later studies shed more light on how the ring structure changes during division. During prophase and metaphase, as the cell rounds up to divide, the perinuclear ring first becomes distorted (‘wavy’) but remains intact. Then, as the cell progresses into anaphase, the rings elongate, finally being ‘cleaved’ into 2 crescents during late telophase and cytokinesis (Blose, 1979; Lazarides, 1982). The crescent in each daughter cell gradually closes off to form a complete ring as the cell develops. This lack of intermediate filament disassembly and re-assembly contrasts with other cytoskeletal elements, as well as intermediate

filaments in other cell types, suggesting a flexible scaffolding role of intermediate filaments during mitosis in endothelial cells (Blose, 1979). Experiments to investigate the percentage of perinuclear rings present in confluent endothelial cells have found that at least 70% of cells in intact aortas contain a perinuclear ring and around 60-80% in confluent cultured cells, with vimentin accounting for approximately 11% of the total cell protein (Blose & Meltzer, 1981).

Further studies on bovine aortic (BAE), corneal (BCE) and foetal heart (FBHE) endothelial cells showed that perinuclear rings only formed in BAEC monolayers. This was accompanied by a 50-fold decrease in DNA synthesis, a 14-fold decrease in protein synthesis and a 15-fold increase in the relative synthesis of vimentin in confluent monolayers, while the levels of other proteins decreased (Savion *et al*, 1982). These changes were not observed in BCE or FBHE. Because endothelial cells form an interface between the vessel wall and blood flowing under high pressure, it has been suggested that perinuclear rings may have a specialised cardiovascular function (Blose & Meltzer, 1981; Savion *et al*, 1982).

Intermediate filaments are prominent in cells exposed to mechanical stress, for example in epithelial and endothelial cells, although until fairly recently the effects of fluid shear stress on intermediate filaments had been ignored. Studies on the response of endothelial cells to fluid shear stress suggested that a common link exists between intermediate filaments and microfilaments (Flitney *et al*, 1995). Davies (1995) showed alignment of the two cytoskeletal components when exposed to fluid shear stress but it remains unclear how intermediate filament movements are mediated i.e. whether due to passive association with actin or, alternatively, whether intermediate filaments actively disassemble and re-assemble quite independently of actin (Flitney *et al*, 1996). One of the principal aims of this study was to shed some light on the nature of the mechanism of cytoskeletal remodelling in response to fluid shear stress.

1.2.2.4 *Intermediate filament-associated proteins (IFAP)*

Like microtubules and microfilaments, intermediate filaments have proteins associated with them in the cytoplasm (Starger *et al*, 1978). These are generally high molecular weight, tissue-specific proteins, known as intermediate filament-associated proteins (IFAP). IFAP are involved in crosslinking intermediate filaments and regulating their interactions with other cell components (Yang *et al*, 1985). By definition, IFAP are morphologically and functionally related to intermediate filaments but are unable to form filaments themselves (Goldman *et al*, 1986; Goldman & Steinert, 1990). One of the first IFAP to be described was a 300kDa protein isolated from BHK cells (Starger *et al*, 1978; Yang *et al* 1985; Lieska *et al*, 1985), called IFAP300. Many more proteins that have a close association with intermediate filaments have been identified and characterised including, filaggrin, plectin, synemin, paranemin, epinemin (Yang *et al*, 1985; Goldman & Steinert, 1990). Very few IFAP (cross-bridgers) are specific to intermediate filaments, as they tend to link intermediate filaments to other proteins or cellular structures. Various proteins, associated with other cellular elements, are also known to interact with intermediate filaments. These include desmoplakins and desmosome-associated proteins in the cell-cell adhesion junctions desmosomes (Jones & Goldman, 1985), as well as bullous pemphigoid antigen 1 (BPAG1) in hemidesmosomes, cell-matrix adhesion sites which contain actin microfilaments and intermediate filaments (Yang *et al*, 1996b). As mentioned previously, mutations or loss of IFAP can cause functional diseases. Lack of BPAGe (epidermal) can cause the skin blistering disease EBS while plectin deficiency in humans results in EBS-MD (Smith *et al*, 1996; Mc Lean *et al*, 1996).

Double immunofluorescence studies showed that IFAP300 co-localised with vimentin intermediate filaments in interphase cells, as well as during mitosis. Experiments by Lieska *et al* (1985) demonstrated that it co-sedimented with vimentin, but not with actin, and did not affect filament structure when added to polymerising or pre-formed intermediate filaments. These findings suggested that IFAP300 interacted specifically with intermediate filaments and was localised on the surface of intermediate filaments, rather than forming an integral filament component

(Lieska *et al* 1985). Immunogold labelling techniques showed non-uniform clusters of the antibody along intermediate filaments at regions of close contact between filaments. Some gold particles appeared to associate with microtubules or microfilaments but intermediate filaments were always present as well (Yang *et al*, 1985, Leiska *et al*, 1985).

The related IFAP plectin, exhibits a similar staining pattern (Yang *et al*, 1985; Lieska *et al*, 1985) and much debate has revolved around whether or not these proteins are one and the same. Polyclonal but not monoclonal antibodies against IFAP300 were found to recognise rat plectin, while monoclonal antibodies to rat plectin failed to recognise hamster IFAP300 (Skalli *et al*, 1994). Clubb *et al* (2000) recently cloned hamster plectin cDNA and confirmed that plectin is found in BHK cells and that its sequence is highly conserved between species. Their study showed that monoclonal antibody 417D raised against IFAP300 actually recognises an epitope located in the central α -helical rod domain of plectin, confirming that the two proteins are identical.

Plectin (507-527kDa) is a member of the plakin family, a group of cross-linking proteins characterised by huge genes (MW 200-700kDa) which encode many isoforms each with unique functions, tailored to suit tissue specific needs for cytoskeletal dynamics. Due to their large size, this group of proteins which also include desmoplakin and BPAG1, are referred to as the ‘Goliaths’ of the connector protein world (Fuch & Karakesisoglou, 2001). These proteins associate with intermediate filaments via their C-terminal segments (Fuchs & Yang, 1999). Plectin is the most versatile linker protein identified to date and is especially prominent in cells which are located at the interface of tissues and fluid-filled cavities, including endothelial cells (Wiche, 1998). Research has led to the suggestion that IFAP may crosslink intermediate filaments to microfilaments and microtubules. Plectin can associate with vimentin, actin, tubulin, vinculin, adhesion plaques, hemidesmosomes and desmosomes (Seifert *et al*, 1992; Svitkina *et al*, 1998; Fuchs & Karakesisoglou, 2001) and is a phospho-protein, providing a substrate for various protein kinases, including PKA, PKC and p34^{cdc2} (Wiche, 1998). Immunogold labelling of vimentin intermediate filaments revealed 2-3nm long ‘sidearms’ of plectin that attach to microtubules and microfilaments (Svitkina *et al*, 1998) and double

immunofluorescence has shown that plectin is located at focal adhesions (Flitney *et al*, 1996; Gonzales *et al*, 2001). The tripartite structure of plectin is conducive to multiple interactions. The long central α -helical domain mediates coiled coil formation, whilst the non α -helical amino domain contains actin and tubulin binding sites and the carboxy terminus harbours intermediate filament binding sites (Hermann & Aebi, 2000). It has been suggested that plectin can stabilise the actin cytoskeleton via scaffolding to intermediate filaments and may also activate stress fibres and focal adhesion formation (Fuchs & Yang, 1999). The discovery of microfilament-microtubule connections and plakins in lower eukaryotes lacking intermediate filaments suggest that the formation of newly recognised cellular pathways have ancient origins (Fuchs & Yang, 1999).

Transgenic studies using mice showed that plectin is involved in the cellular dynamics of the actin cytoskeleton (Andra *et al*, 1998; Wiche, 1998; Allen & Shah, 1999). In plectin-deficient mice, the actin cytoskeleton and numbers of focal adhesions were significantly upregulated. In these cells, actin stress fibres were found to be resistant to the effects of Rho, which is known to regulate their formation. These cells also exhibited increased adhesion to the substratum when exposed to a defined fluid shear stress (Wiche, 1998). Since the formation of both stress fibres and focal adhesions are Rho dependent processes, actin may modulate signalling pathways of the Rho family of GTP-ases (Allen & Shah, 1999). These findings imply that plectin has a role in regulating cell processes e.g. actin filament dynamics, a theory which goes beyond that previously discussed regarding scaffolding and mechanical stabilisation. From the above findings it appears that plectin may act as a ‘docking site’ for cytoplasmic proteins, providing a platform for protein interactions, regulatory factors and signalling cascades (Wiche, 1998).

IFAP have been shown to interact with proteins associated with cell-cell contacts. Previous research using bovine tongue epithelial cells (Skalli *et al*, 1994) showed IFAP300/plectin concentrated in the peripheral cytoplasm of keratinocytes. Further investigations (Skalli *et al*, 1994) led to the discovery of IFAP300 /plectin at sites where intermediate filaments insert into desmosomes (cell-cell adhesions) and hemidesmosomes (cell-substrate adhesions). Previously, no protein had been shown to be common to both these structures. Furthermore, IFAP300/plectin staining

extended further into the cytoplasm than that of BP230 (bullous pemphigoid antigen), a hemidesmosome component, and desmoplakin, indicating that it may also be functioning to stabilise or crosslink intermediate filaments before they insert into the membrane plaques. Based on its involvement in fibroblasts, keratinocytes and endothelial cells, IFAP300/plectin has been labelled as a multifunctional protein (Skalli *et al*, 1994).

Recent studies (Gonzales *et al*, 2001) using endothelial cells have identified a new type of cell-ECM junction, known as a vimentin-associated matrix adhesion (VMA). This connects to the ECM via the $\alpha_v\beta_3$ integrin and the α_4 sub-unit of laminin 5. This site resembles a hemidesmosome due to its association with the intermediate filament cytoskeleton. However, it is enriched with vinculin and also serves to anchor actin stress fibres, both of which are features of classic focal adhesions (Burrige *et al*, 1997). Plectin has been localised in VMAs where it appears to mediate the attachment of vimentin to the cytoplasmic face at these sites.

Steinert *et al* (1999) have implicated the high molecular weight protein nestin as an intermediate filament linker protein in BHK-21 cells. Nestin, which is primarily expressed in embryonic cells, was found to co-assemble with type III (vimentin and desmin) and type IV (α -internexin) but not type I /II (keratins) intermediate filaments. This study identified nestin as an IFAP, since it lacks the ability to form intermediate filaments on its own, but can co-assemble with vimentin in a ratio of 1:4, an association that is maintained throughout the cell cycle. It has also been suggested that protrusions from nestin may act as bridging elements, or spacers, between intermediate filaments, participating in the interaction of intermediate filaments with microfilaments and microtubules.

1.3 Focal adhesions

Cultured cells growing on an artificial surface need to adhere to the underlying substrate. Focal adhesions, also referred to as focal contacts or adhesion plaques are discrete areas of the cell surface where cells are anchored to the extracellular matrix (ECM) via transmembrane proteins known as integrins. These in turn are linked to

actin stress fibres through a complex arrangement of proteins (BurrIDGE *et al*, 1988; BurrIDGE & FATH, 1989). The functions of these adhesion sites include regulation of cell morphology, growth and differentiation in response to environmental changes, as well as cell anchorage and signal transduction from ECM to the cell interior. Focal adhesions are highly dynamic structures, typically found in cells with low motility e.g. fibroblasts, epithelial cells and endothelial cells (BurrIDGE & FATH, 1989). They were first identified by Abercrombie *et al* in 1971. EM studies showed that some regions of the ‘ventral’ cell surface were very close to ECM. Cytoplasmic stress fibres were shown to be associated with what appeared to be ‘dense plaques’, typically 2-10um long and 0.25-0.5um wide, in the plasma membrane region (BurrIDGE *et al*, 1988). Further work, including immunological studies, identified several other proteins present at these sites, which are discussed below. Although focal adhesions are most prominent in static cell cultures, many characteristics suggest that they are similar in both structure and function to cell-matrix attachments *in vivo* (Beckerle, 1990). Focal adhesions provide a suitable model for studying structural links between the ECM and the cytoskeleton, as well as bi-directional signal transduction (BurrIDGE *et al*, 1997).

1.3.1 Focal adhesion components

The extracellular matrix (ECM), composed of either fibronectin or vitronectin can influence cell behaviour, including effects on both growth and adhesion. Cells grown in the absence of serum and thus ECM express poorly developed focal adhesions (BurrIDGE *et al*, 1988; BurrIDGE & FATH, 1989). Mammalian cell lines can have different ECM receptors depending on the matrix laid down (Lampugnani *et al*, 1991). Certain fibroblasts have been found to express both vitronectin and fibronectin receptors with different distributions throughout the cell. Research on endothelial cells has shown that only vitronectin receptors are expressed when cells are seeded on vitronectin-coated plates and vice versa for fibronectin. However, with time, vitronectin receptors predominate at focal adhesions in both conditions (BurrIDGE & FATH, 1989). Stress fibre development requires substrate attachment. Thus, deletion of fibronectin, vitronectin and vinculin receptors in the endothelium results in the absence of stress fibres (Girard & Nerem, 1995).

Integrins are a family of glycoproteins composed of non-covalently linked α and β sub-units which have been identified as ECM receptors throughout the animal kingdom, from nematodes and arthropods to birds and mammals (Burrige *et al*, 1988). They function as transmembrane linkers, or ‘integrators’, allowing cells to attach to the ECM. They are also involved in cell-cell adhesion (Hynes, 1992). The ECM-intracellular communication that they allow is bi-directional. Thus they act as ‘adapters’ allowing cells and matrices to orientate within a tissue. They have also been identified as mechanoreceptors which transmit mechanical signals to the cytoskeleton (Wang *et al*, 1993) and are known to be involved in the activation of intracellular signalling cascades (Bhullar *et al*, 1998). Wang *et al* (1993) used integrin-covered beads in an attempt to establish how the stress fibre–multiprotein complex - membrane link was formed. β -integrin was found to link fibronectin to the intracellular complex, allowing force transmission across the cell surface (Wang *et al*, 1993; Davies, 1995). Selective integrin expression by individual cells has been found to modify their adhesion to the ECM along with their binding properties to other proteins (Hynes, 1992).

Vinculin was the first protein component of focal adhesions to be identified and this discovery (Geiger *et al*, 1979) allowed focal adhesions to be easily recognised in cells. Since then, much work has been carried out to identify other proteins present at these sites and establish how they interact to form an ECM - plasma membrane - intracellular link. It is now known that α -actinin, talin, vinculin, paxillin and focal adhesion kinase (FAK) associate with integrins in the focal adhesion -cytoskeletal complex, although the exact arrangement of these proteins remains unclear. Vinculin is widely distributed in actin-containing cell junctions, and soluble pools of vinculin are found in the cytoplasm, which act as a precursor for focal adhesion assembly. As vinculin was the first protein associated with adhesion sites, it was suggested that it might link actin directly with the cell membrane. This was found not to be the case. However, vinculin does bind with moderate affinity to talin and α -actinin, which is an actin cross-linking protein (Otto, 1990). Vinculin is phosphorylated on serine, threonine and tyrosine residues by PKC, which is also localised at focal adhesions.

Talin, another focal adhesion protein has been found to enhance vinculin phosphorylation by PKC by altering access to vinculin phosphorylation sites (Otto, 1990). Talin, like vinculin, has soluble cytoplasmic pools and is associated with adherens- type junctions in various cell types. However in endothelial cells, talin has been found at focal adhesions but not at inter-cellular contacts (Lampugnani *et al*, 1991). In cultured cells it has been found predominantly at focal adhesions where it interacts with the β -integrin subunit (Beckerle, 1990) and vinculin (Otto, 1990). Other research has shown that the binding of talin to integrin does not affect its ability to bind to vinculin or integrin binding with the ECM. PKC phosphorylation of talin involves the same residues (serine/threonine) as vinculin. However, in contrast to vinculin, talin phosphorylation is associated with a dramatic loss of focal adhesion integrity and stress fibre arrangement in BS-C1 cells (Beckerle, 1990). Vinculin and talin bind each other with high affinity while α -actinin directly binds actin as well as vinculin. The accepted model for interaction between the cytoplasm and ECM for some time has been an actin – α -actinin – vinculin – talin – integrin – ECM protein (Burrige *et al*, 1988), with other protein components located at various points (Figure.1.5).

Paxillin is another focal adhesion protein present in small amounts and known to bind to vinculin but not talin, α -actinin or actin, suggesting a regulatory, rather than a structural, role in focal adhesions (Turner *et al*, 1990).

Cytoskeletal associated molecules, including α -actinin, talin and vinculin, require integrin clustering and ligand occupancy in order to accumulate in adhesion complexes such as focal adhesions. One advantage of this may be to ensure formation of long term cytoskeletal stabilisation adhesion complexes only in the presence of a stable integrin-ligand attachment (Yamada & Geiger, 1997).

1.3.2 Focal Adhesion Assembly

More recent work on the assembly of focal adhesions has investigated the roles of tyrosine kinases (TK), phosphatases, arachadonic acid and Rho GTP-ases. GTP-ases

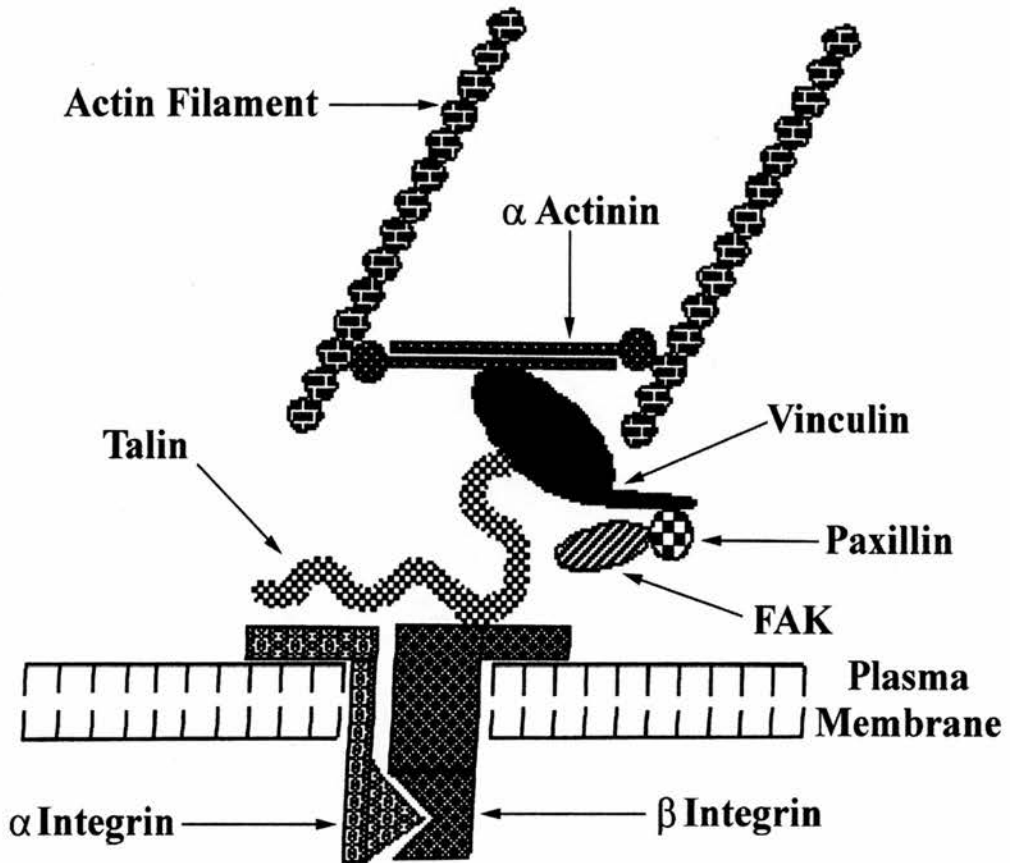


Figure 1.5 Schematic diagram of a basic model of a classic focal adhesion.

are active and inactive when bound to GTP and GDP respectively, thus acting as molecular on/off switches, often in the regulation of actin binding proteins (Craig & Johnson, 1996). Platelet derived growth factor (PDGF) and epidermal growth factor (EGF) stimulate focal adhesion assembly through the activation of RhoA. RhoA leads to synthesis of PIP2 (phosphoinositol 4,5-bisphosphate) which modulates α -actinin, thus affecting actin stress fibres, although the reason for this is unknown.

Focal adhesions in many cultured cells have been found to be the most concentrated sites of tyrosine phosphorylation. Two tyrosine kinases, c-Src and p125^{FAK} (FAK), appear to regulate signals involved in integrin mediated cell adhesion. FAK is autophosphorylated and moved to focal adhesions in response to ligand binding at receptors, or in response to integrin clustering in the absence of ligand binding sites. Phosphorylated FAK activates paxillin, at its p125^{FAK} binding site, as well as tensin which is thought to bind vinculin and integrin (Figure 1.5). Research has suggested that FAK has the potential to integrate extracellular signals for cell growth and development with those of dynamic cytoskeletal-membrane associations, though it may not be essential for assembly or maintenance of focal adhesions (Craig & Johnson, 1996). TK inhibition results in a decrease in FAK and paxillin phosphorylation coupled with a decrease in stress fibres and focal adhesion assembly. It was not known whether FAK phosphorylation was upstream or downstream of focal adhesion assembly. However recent evidence (BurrIDGE *et al*, 1997) concluded that crucial tyrosine kinases lie upstream of focal adhesion assembly but FAK does not play a part, although it is involved in the assembly of signalling components associated with focal adhesions. BurrIDGE *et al* (1997) suggest that the GTP-binding protein Rho is involved in focal adhesion assembly. Rho is part of the Ras superfamily of GTP-binding proteins, which also includes Rac and cdc42, involved with actin filaments in lamellipodia and filopodia formation respectively. Work on quiescent cells has led to rapid progress in the understanding of focal adhesion assembly, with the involvement of Rho in focal adhesions and stress fibre formation being a major breakthrough. These three G-proteins are also involved in transcription and other signalling pathways within the cells. Exposure to serum in quiescent, serum starved, cells results in rapid focal adhesion assembly as a consequence of Rho activation (BurrIDGE *et al* 1997). Rho (ROCK/ROK) is also essential for focal contact formation (Riveline, 2001). Focal contacts are the mature,

elongated forms of focal adhesion complexes. Inhibition of ROCK by chemical inhibitors prevents focal contact but not focal complex formation.

The most recent model for focal adhesion assembly is that when quiescent cells adhere, integrins are not clustered into focal adhesions, although they do interact ‘loosely’ with the ECM and cytoskeletal elements. Rho activation in the presence of serum results in a greater tension being produced and clustering of the integrins and the initiation of signalling pathways. Thus focal adhesion assembly is driven from within the cell but cell attachment with sustained tension is required to maintain focal adhesions. As a result they are rarely seen in tissues (BurrIDGE *et al*, 1997).

1.3.3 Focal adhesions as mechanosensors and force transducers.

Focal contacts contain high levels of tyrosine phospho-proteins which is characteristic of signalling molecules, including tyrosine kinases, phosphatases and adaptor proteins. Thus focal contacts function as both adhesion and signal transduction organelles relaying information regarding the ECM. Integrin containing focal complexes behave as individual mechanosensors, which exhibit directional assembly in response to local force. These sites are also involved in adhesion-dependent signalling (Riveline, 2001). Application of mechanical force via micropipettes to ‘dot-like’ adhesions (focal contacts) showed that stress is not sensed at the point of contact but rather via transmission of forces through the cytoskeleton to the cells basal surface and focal adhesions (Riveline, 2001). The response of focal contacts and complexes to tension is of vital importance in the reaction of cells to their microenvironment and particularly to flow in the case of endothelial cells.

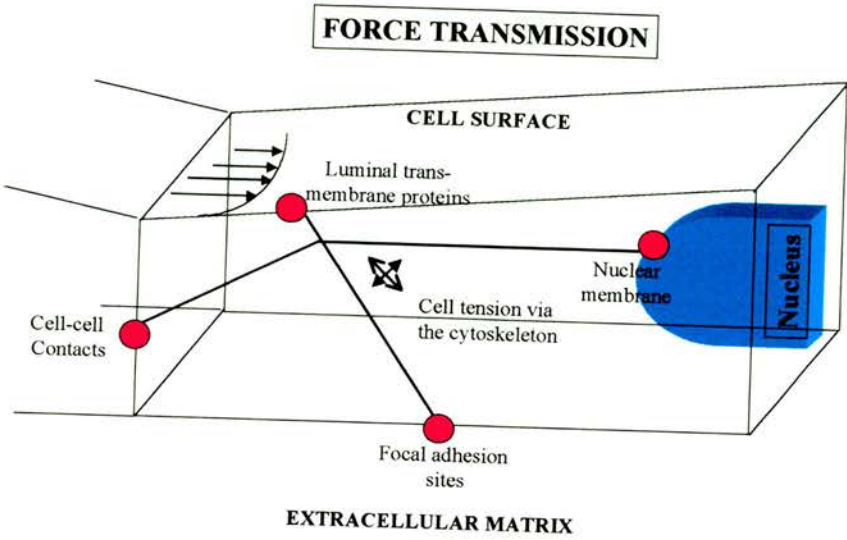
In quiescent cells, focal adhesions re-model in a random fashion. However, just like cytoskeletal elements, focal adhesion components become re-aligned upon exposure to flow, accompanied by little change in the overall contact area (Girard & Nerem, 1995; Davies, 1995). The rate of re-modelling as well as cell adhesion is altered upon exposure to different ECM components, probably as a consequence of different integrin binding (Davies, 1995). Stress at the luminal surface of HUVEC and BAEC results in directional remodelling at the abluminal surface, providing evidence of

connections between actin stress fibres and the plasma membrane (Davies & Tripathi, 1993; Davies, 1995; Girard & Nerem, 1995). Fluid shear stress results in increased paxillin phosphorylation in endothelial cells suggesting a role in the mechanotransduction of blood flow (Davies, 1995). Results suggest that focal adhesion proteins may play a specific role in stress fibre re-alignment in response to fluid shear stress. It is also possible that other mechanisms are involved in the re-alignment process and that once they become positioned, focal adhesions re-distribution is promoted (Girard & Nerem, 1995). Recent experiments using latrunculin highlighted that actin filament assembly is necessary for focal contact formation (Riveline, 2001).

There is some evidence to suggest that intermediate filaments and microtubules may terminate at focal adhesions, suggesting intermediate filament association may increase stability (Burrige *et al*, 1988). Correia *et al* (1999) working on macrophages, reported a novel adhesion-dependent interaction between microfilaments and intermediate filament cytoskeletons. They propose that the actin cross-linking protein fimbrin may interact with vimentin to aid in the direct assembly of the intermediate filament network at cell adhesion sites and associate with actin stress fibre bundles. More recently, Flitney *et al* (1995) and Gonzales *et al* (2001) have demonstrated the co-localisation of intermediate filaments and plectin with focal adhesions in BAEC at the tips of actin stress fibres. The streaks of plectin co-localise not only with stress fibres but also with vinculin and talin, suggesting that plectin is an integral part of focal adhesions, establishing a structural link between intermediate filaments and microfilaments in endothelial cells.

Endothelial cells are anchorage dependent cells, which *in vivo* exist in a state of cell tension in order to maintain cell shape. This tension is generated by interaction of the cytoskeleton with the nucleus and focal adhesions, implicating the cytoskeleton in transmission of flow induced forces across the cell. The detection and transmission of fluid shear stress must involve a combination of mechanisms including; sensor displacement at the cell surface, cytoskeletal aided transmission throughout the cell and mechanotransduction at sites remote from detection point (Davies, 1995), a model of which can be seen in figure 1.6. The re-organisation of focal adhesion sites during flow is most likely due to the transfer of stress from

(a)



(b)

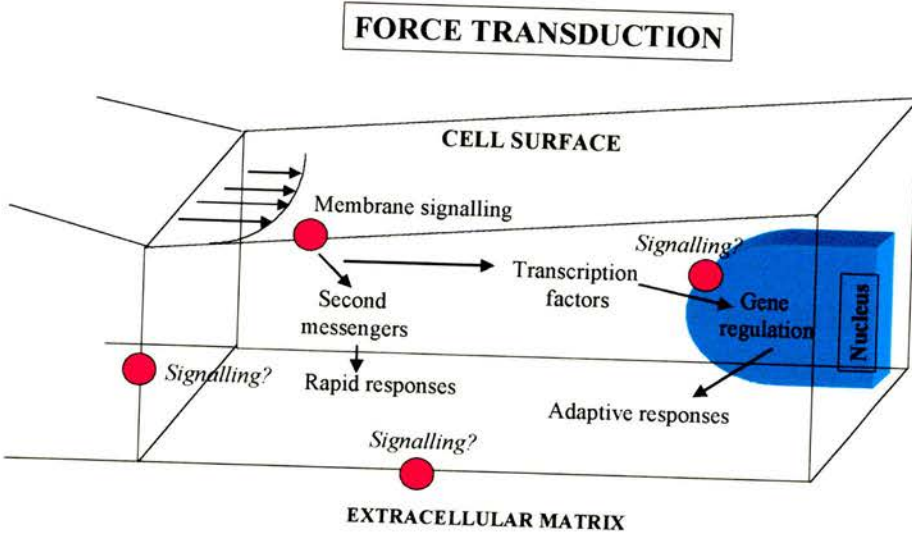


Figure 1.6. Schematic representation of (a) force transmission and (b) force transduction processes in endothelial cells. 3-dimensional surface topography of the cell influences force distribution from the cell surface throughout the cell. The cytoskeleton is involved in transmission of stress (a) to different regions of the cell from where mechanotransduction may occur (Adapted from Davies, 1995).

luminal to abluminal surfaces across the cell, accompanied with cytoskeletal involvement at every level (Davies *et al*, 1997). Flow instigates other effects that result in morphological and functional changes.

1.4 *Effects Of Fluid Shear Stress on Endothelial Cell Morphology*

Regulation and / or reorganisation of pre-existing structures occurs in response to acute changes in flow. These involve enzyme-substrate rate limiting steps and result in the stimulation of stress-activated signalling cascades involving transcription factors. Chronic flow-induced responses involve de-novo protein synthesis which ultimately regulate gene expression as well as structural responses and changes in cell cycle kinetics. At the level of gene expression, endothelial cells sense and respond to varying fluid shear stress. Exposure to laminar fluid shear stress can regulate certain genes upon which turbulent flow would have no effect (Topper & Gimbrone, 1999).

As a result of the complexity and diversity of stimuli to which the endothelium is exposed, the effects of any one stimulus must be considered in the context of the diversity of signals it may produce and their effects on the endothelium.

Shear forces *in vivo* are known to alter the morphology of endothelial cells (Silkworth & Stehbens, 1975). As well as this, fluid shear stress produces dozens of cellular responses via its effects on the endothelium, comprehensively reviewed by Davies (1995). It is now accepted that shear stress mediates its effects through the endothelium to regulate acute vessel tone and chronic restructuring in blood vessels.

This study focuses on the effects of fluid shear stress on the cytoskeleton of BAEC, in particular on vimentin perinuclear rings. The cytoskeleton physically connects with many cell components to generate tension and determine cell shape. Throughout the last few decades, much research has been carried out on the cytoskeleton, concentrating predominantly on actin, since the discovery that it plays a major role in cellular response to haemodynamic forces. Less work has concentrated on intermediate filaments due to the fact that for a long time they were thought of as the ‘inert’ component of the cytoskeleton.

In vivo studies (Nerem *et al*, 1981) illustrated that both the morphology and alignment of endothelial cells are indicative of blood flow. From this it was speculated that alterations in endothelial cell geometry, involving elongation and narrowing of the cells, might occur in response to shear stress. Further studies exposed confluent cultured BAEC to different levels of shear stress for varying lengths of time using a parallel plate flow chamber (Levesque & Nerem, 1985). Results showed that cell alignment, elongation and shape change occurred in a time dependent fashion with cell alignment requiring longer exposure to fluid shear stress than elongation and higher shear stresses producing a greater degree of elongation. The transition from ‘cobble-stone’ to elongated shaped cells was found to be reversible and specific to endothelial cells, as it was not evident in muscle or fibroblasts (cited Malek & Izumo, 1996). Realignment of cellular cytoarchitecture was found to involve some protein synthesis but not cell division (Davies & Tripathi, 1993).

Work by Viggers *et al* (1986) exposed confluent BAEC to shear stresses of 60 and 128 dynes.cm⁻², which correspond to moderate and high physiological forces respectively. The cells were exposed to fluid shear stress for 6, 12 and 24 hours. In cells exposed to shear stresses of 60 dynes.cm⁻², elongation was evident after 6 hours, with almost complete elongation and alignment at both 12 and 24 hours. In contrast, cells exposed to 128 dynes.cm⁻² exhibited scattered cell detachment, which was inconsistent between coverslips. Alignment was perpendicular to the direction of flow at 6 hours but by 12 and 24 hours it was highly variable with patches of similarly orientated cells clustered together. They suggested that re-alignment in cells exposed to the higher fluid shear stress took longer because increased adhesion to the substratum was required before structural responses could begin. Masuda & Fujiwara (1993) exposed cells to smaller shear forces of 6-10 dynes.cm⁻². Again, cells became elongated and re-aligned but the process took 36 hours, providing further evidence that morphological responses to fluid shear stress depend on both the magnitude of force applied and exposure time. Thoumine *et al* (1995) investigated elongation of confluent BAEC in culture. They suggested that the specific and directional elongation patterns exhibited by the cells in response to flow were influenced by force transduction via the cytoskeleton. This theory was

supported by the preferential alignment of actin, vimentin and vinculin with the major cell axis occurring concomitantly with BAEC elongation. The realignment of vinculin suggests a mechanical link between the external and internal environments via focal adhesion sites. In contrast, dermal microvascular endothelial cells were found to arrange perpendicular to flow, suggesting that the cytoskeleton organises in a cell-type specific way in response to external forces.

The dramatic changes in actin stress fibre organisation, from their random orientation in static culture to alignment with flow, led to speculation that fluid shear stress-induced cellular re-organisation was the result of cytoskeletal remodelling (Wong *et al*, 1984; Franke *et al*, 1984; Levesque & Nerem, 1985; White & Fujiwara, 1986; Masuda & Fujiwara, 1993; Girard & Nerem, 1995; Satcher *et al*, 1997; Fujiwara *et al*, 1998; Kataoka *et al*, 1998). *In vivo* studies (White *et al*, 1983) showed that the aorta contained greater numbers of stress fibres than the vena cava. This is likely to be due to the differential shear forces exerted in these regions of the vasculature. Girard & Nerem (1995) determined that fibronectin, vitronectin and vinculin receptors were absent from focal adhesions if stress fibres were not formed in response to shear stress. They suggested that focal adhesion proteins may play a role in flow induced actin cytoskeleton rearrangement and that stress fibres may act as flow sensors. Recent work found that changes in actin distribution can occur within minutes of being subjected to flow. While there was still no macroscopic shape change even after an hour at 20 dynes.cm⁻², this was significantly altered by 3 hours (Katoaka, 1998).

Coan *et al* (1993) studied the effects of fluid shear stress on the localisation of the MTOC and the Golgi apparatus in bovine carotid artery endothelial cells. Results showed a temporary redistribution of the Golgi apparatus and MTOC by 2 hours at 22 dynes.cm⁻² and 8 hours at 88 dynes.cm⁻². This effect was lost by 24 hours with no significant difference existing between sheared and non-flow control samples, suggesting that Golgi apparatus and MTOC positioning are not completely dependent on flow direction. Earlier research had suggested that the positioning of the Golgi apparatus was dependent on microtubules (Ho *et al*, 1989). Coan *et al* hypothesise that Golgi apparatus/MTOC colocalisation form a functional unit where Golgi apparatus secretory vesicles are directed along microtubules which extend into

the cytoplasm. Other research has shown MTOC orientation which is towards the heart *in vivo* is lost once the cells are cultured *in vitro*.

Non-confluent cells were found to align more rapidly than cells in confluent monolayers (Levesque & Nerem, 1985). This is because the structural re-organisation of each cell in a confluent monolayer being dependent on its neighbours. Confluent monolayers appear to remain contact inhibited despite exposure to fluid shear stress (Davies, 1989). Cells exposed to fluid shear stress make contact with an average of 4 other cells, while those in static culture associate with up to 6 (Levesque & Nerem, 1985). These findings suggest that the response of cells to fluid shear stress is influenced not only by substrate adhesion but also by association with neighbouring cells. Further experiments have shown that an intact monolayer is required to sense and transduce signals which ultimately result in changes in structure and function of the entire layer (Topper & Gimbrone, 1999). More recent research involving bovine carotid artery endothelial cells (Masuda & Fujiwara, 1993 a) found that single endothelial cells showed no alignment with flow even when exposed to 10 dynes.cm^{-2} for up to 100 hours. However, changing from 1 dyne.cm^{-2} to more than 6 dynes.cm^{-2} stimulated cells to migrate downstream. These cells exhibited well-developed lamellipodia which appeared within 10 minutes of exposure to fluid shear stress, a response which was found to be reversible (Masuda & Fujiwara, 1993b). This was accompanied by MTOC transition from an anterior to a posterior position relative to the nucleus, which is consistent with *in vivo* observations.

Until relatively recently, most research has concentrated on individual cytoskeletal elements, with little attention being focused on the interactions between them and other cellular structures. Olivier *et al* (1999) investigated the effects of varying shear forces of 20 minutes on the adhesion sites of sub-confluent endothelial cells. Results suggested that fluid forces were transmitted to the abluminal surface focal adhesion sites at the onset of flow, by a rapid increase in contact, movement and signal transmission via the cytoskeleton. However they did not investigate the responses of confluent cells, as they are contact inhibited and focal adhesion responses are sensitive to actin re-organisation and local stress distribution.

Microtubules were found to be the first cytoskeletal element in fibroblasts to re-orientate and align upon exposure to fluid shear stress (Oakley & Brunette, 1993). They have also been shown to associate with the plasma membrane and are implicated in resisting shear induced torque exerted on integrins along with intermediate filaments (Wang *et al* 1993). Malek & Izumo (1996) found that an intact microtubule network was essential for stress fibre formation. Using nocodazole and taxol, to disrupt and stabilise microtubules respectively, they found that in the absence of an intact microtubule network, endothelial cells did not re-align or initiate stress fibre formation, although the role of microtubule re-distribution in response to shear induced shape remained unclear. Arteriole microtubule disruption by nocodazole or colchicine inhibits flow-dependent dilation of the vessels (Sun *et al*, 2001). Thus cytoskeletal integrity is essential for fluid shear stress signal transduction pathways which result in the release of factors necessary for dilation in response to increased blood flow.

Malek & Izumo, (1996) also found that acrylamide-induced disruption of the vimentin network did not significantly interfere with stress fibre arrangement, despite the importance of intermediate filaments in cell anchorage, stabilisation and mechanical functions. Studies by Flitney *et al* (1995) showed that flow induced changes to the vimentin network in BAEC. Within two hours, the network showed a decrease in intermediate filament continuity throughout the cell, coupled with the formation of ‘whorls’ of intermediate filaments. These developed into short continuous bands, with time resulting in a less dense network aligned with the cell axis. This change in the intermediate filament network was accompanied by a decrease in dense peripheral bands of actin accompanied by an increase in parallel stress fibres aligned in the direction of flow. Immunological studies determined that intermediate filaments were associated with focal adhesions and vimentin re-arrangement was accompanied by rapid re-distribution of plectin. Further investigations (Flitney *et al*, unpublished) suggested a co-association of plectin, actin and vimentin at focal adhesion sites. This led to speculation of a intermediate filament-plectin-stress fibre link in endothelial cells, which could play an important role not only in cytoskeletal reorganisation in response to fluid shear stress, but in cytoskeletal re-organisation during mitosis and cell communication.

Schnittler *et al* (1998) found that vessels that are exposed to high levels of shear forces (e.g. aorta) expressed 2-3 fold more vimentin than those exposed to lower shear forces (e.g. vena cava). Within the aorta itself, there was a 1.5 increase in vimentin from proximal to distal regions, making up 2-3.5% of total cell protein. They postulated that if vimentin is involved in mechanical functions within the cell, the amount of vimentin should correlate with the degree of fluid shear stress. Helmke *et al* (2000) investigated the response of the intermediate filament network in living cells to a 3 minute step up in fluid shear stress using GFP-transfected BAEC. Shear stress was found to significantly increase 3-dimensional directional intermediate filament movement within the cells but did not result in acute polymerisation or depolymerisation responses. The filament redistribution was greatest in intermediate filaments located 'higher' in the cell. Thus fluid shear stress acting on the luminal surface of endothelial cells for short period of time result in the deformation of stable intermediate filament networks throughout the cell, decreasing in magnitude from luminal to basal surfaces. Research on intact mesenteric arteries of vimentin knockout mice showed that although arterial diameter was unchanged, flow-induced vasodilation was significantly decreased, an effect which was exaggerated by blocking NO release. This reinforces the theory that vimentin intermediate filaments are involved in mechanotransduction (Henrion *et al*, 1997).

1.5 Systems used to study the effects of Fluid Shear Stress on endothelial cells.

The frictional force acting on the apical surface of the endothelium is determined by the mean flow rate, the viscosity of the blood and physical dimensions of the vessel. Laminar flow occurs when a fluid flows with a uniform velocity gradient i.e. a series of layers (laminae) which pass each other with increasing velocity towards the centre of the vessel (Figure 1.2). In Newtonian fluids i.e. those in which flow velocity does not alter viscosity, fluid shear stress can be derived from Poiseuille's law (Ballerman, 1998) with shear stress being proportional to flow rate and viscosity and inversely proportional to the vessel radius. In general blood is regarded as a non-Newtonian fluid as viscosity decreases with increasing velocity and vessels are non-rigid as well as non-uniform in their composition. However, laminar flow is assumed in larger vessels, where the diameter exceeds 0.5mm (Ballerman *et al*, 1998). This permits

blood to be approximated to a Newtonian fluid, allowing shear stress to be related to viscosity, shear rate and velocity gradient (Nerem *et al*, 1998).

Cone-plate viscometers (Dewey *et al*, 1981; Dewey, 1984) and parallel plate (Levesque & Nerem, 1985) flow chambers have been employed in numerous studies to analyse the effects of varying magnitudes of fluid shear stress on endothelial cell monolayers (Dewey, 1981; 1984; Levesque & Nerem 1985; Viggers *et al* 1986; Masuda & Fujiwara 1993; Flitney *et al*, 1995). Cone-plate viscometers have a well-defined flow field with no pressure gradients and it is relatively easy to induce turbulent flow for comparison to laminar flow. However, they are awkward to assemble in conjunction with a microscope making continuous observation difficult.

Parallel plate chambers provide a well-defined mechanical environment allowing the operator to expose the cells to a specific magnitude of fluid shear stress (Levesque & Nerem, 1985). Cells are cultured to confluence on a glass substrate that may or may not be coated with an ECM protein and exposed to known laminar shear stress. In the present study, the chamber design is based on that used by Viggers *et al* (1986), the details of which will be discussed in the chapter 2. The chamber is inserted in a perfusion loop between two reservoirs containing culture medium. A roller pump drives the system and fluid shear stress is measured using a formula which incorporates flow rate, pressure difference across the chamber, medium viscosity and chamber dimensions (see Appendix 4). The advantages of this type of chamber include easy assembly in conjunction with light microscopes, which allows constant monitoring of the cells. Problems such as cell detachment or contamination can also be detected more easily.

The focus of this study is primarily on changes in the intermediate filament cytoskeleton, in particular perinuclear rings of vimentin, in response to shear stress. Based on findings which concentrated on vimentin networks in the absence of rings, this study aimed to monitor the development of perinuclear rings with respect to other cytoskeletal elements. A flow-chamber based on a similar model used by Viggers *et al* (1986) was designed to investigate the effects of fluid shear stress on cytoskeletal remodelling, especially of perinuclear rings in an attempt to identify a shear stress-induced cytoskeletal response mechanism which to date remains elusive.

Endothelial cells provide an ideal model as they have been shown to maintain their *in vivo* characteristics in culture (Blose & Chacko, 1976) and exhibit contact inhibition once a confluent monolayer is obtained. The second section of the thesis deals with the signalling pathway associated with activation of the inducible transcription factor, nuclear factor-kappa B (NF- κ B) which is introduced in Chapter 6.

CHAPTER 2

MATERIALS AND METHODS.

PART I

2.1 Cell culture techniques

Experiments were performed on cultured endothelial cells from both human and bovine sources. All culture procedures were carried out under sterile conditions in a Class II flow hood (Microflow Ltd., M51424/2, Somerset). Details of materials can be found in appendix 1.

2.1.1. Bovine Aortic Endothelial Cells

Bovine aortic endothelial cells (BAEC) were obtained from the European Collection of Animal Cell Cultures (ECACC, Centre for Applied Microbiology and Research, Salisbury, Wiltshire) and cultured in high glucose Dulbeccos modification of Eagle's medium DMEM (Gibco BrL). Medium was supplemented with 10% foetal calf serum (FCS) (Globepharm, Surrey) or 10% donor calf serum (DCS) (TCS Biologicals, Buckingham) and 2mM glutamine, together with 50iu.ml⁻¹ penicillin/50ug.ml⁻¹ streptomycin (Sigma). The growth medium was changed on alternate days.

BAEC were passaged as follows. After rederiving cells from liquid nitrogen, each vial (approximately 1x10⁶ cells) was seeded into a 25cm² flask and 10ml of medium was added dropwise. The medium was changed once the cell had adhered to the flask in order to remove any residual dimethyl sulphoxide (DMSO) used in the freezing process. At confluence cells were trypsinised (see below) and counted using a Coulter counter[®] Z1™ series particle Counter (Beckman Coulter Ltd, Bucks), then seeded into the appropriate number of 75cm² flasks, at a density of ~2 x 10⁴ cells.cm⁻². Cells were cultured in a non-humidified incubator (LTE scientific, Oldham) at 37°C and gassed with 95% O₂ - 5% CO₂ every 2 days.

2.1.1.2 Trypsinisation procedure for BAEC

Growth medium was removed and the cells were rinsed with 3ml of 0.05% Trypsin/0.01% EDTA solution to remove any residual medium. A further 3ml of the trypsin solution was added and the flask was placed in the incubator for either 2 minutes or until the cells had rounded up. 4ml of culture medium were then added to the flask to inhibit the trypsin. The cell suspension was pipetted up and down a few times, to break up any cells clumps, before being counted and then added to fresh medium.

2.1.2 Human Coronary Artery Endothelial Cells

Human coronary artery endothelial cells (HCAEC) were obtained from Clonetics[®] and cultured in Clonetics[®] basal medium supplemented with 5% foetal calf serum (FCS), human recombinant epidermal growth factor (hEGF), human fibroblast growth factor (hFGF), vascular endothelial growth factor (VEGF), ascorbic acid, hydrocortisone, long R3-IGF-1, heparin and gentamicin/amphotericin.

On derivation from liquid nitrogen, the cells were resuspended in 1ml of warmed medium and seeded into a T-25 flask. Medium was changed the following day, to remove residual DMSO, and thereafter on alternate days. The amount of medium added to the cells was dependent on the degree of confluency: either 1ml, 1.5ml or 2ml per 5cm² was added, corresponding with <25%, 25-45% or >45% confluent cells.

2.1.2.1 Trypsinisation procedure for HCAEC

Cells were trypsinised at 70-90% confluency to prevent irreversible contact inhibition occurring. Each T-75 flask was split using 9ml Clonetics[®] HEPES buffered saline solution (HBSS) followed by 9ml Clonetics[®] 0.025% trypsin/0.01%EDTA solution and finally 9ml of Clonetics[®] trypsin neutralising solution (TNS). The cell suspension was

centrifuged for 10 minutes at 100rpm (Chillspin) then resuspended in 4-5ml of medium. Cells were counted before seeding at $2.4 \times 10^4 \text{.cm}^{-2}$ and grown in a non-humidified incubator at 37°C, gassed with 95%O₂ /5%CO₂ every 2 days.

2.1.3. Growing cells on coverslips or glass microscope slides

Cells were grown on uncoated cover slips, for immunofluorescence studies, or on glass microscope slides, for biochemical studies. Both were sterilised prior to use by autoclaving. Cells were seeded on to 22mm² (N^o.1 thickness) borosilicate glass coverslips (BDH) at a density of $2 \times 10^4 \text{.cm}^{-2}$ for immunocytochemical studies and placed in a 30mm non-tissue culture Petri dish (Bibby Sterilin, Staffordshire). For biochemical studies, cells were seeded onto 76mm x 26mm plain microscope slides (BDH, Leicestershire) at a density of $2 \times 10^4 \text{ cells.cm}^{-2}$ and placed in a 90mm Petri dish (Bibby Sterilin). When plating out the cells, 1ml and 2ml of cell suspension was added to the coverslips and microscope slides respectively, followed by a further 1ml and 23ml once they became attached. The medium was changed every 2 days: cells growing on coverslips were given a complete change on alternate days, while those growing on microscope slides had 10ml replaced with fresh medium. The cells were maintained in culture for varying periods of time, up to 21 days, and their development monitored by immunofluorescence or by immunoblotting whole cell extracts.

2.2 Indirect Immunofluorescence

The technique of double indirect immunofluorescence was used to study the distribution of cytoskeletal elements (Chapters 3-4) and components of the NF-κB pathway (Chapters 8-9), before or after exposing cells to controlled fluid shear stresses.

2.2.1 Immunofluorescence of BAEC and HCAEC

Cells grown on coverslips were removed from culture medium and rinsed (x2) for 3 minutes in phosphate buffered saline (PBSc) (Gibco) at room temperature (RT) in a Columbia jar. They were then fixed for 10 minutes in 1% EM grade formaldehyde (TAAB Lab Ltd.) in PBSc before being rinsed (x2) again in PBSc. The fixed cells were permeabilised with 0.1% Nonidet P40 detergent (NP40; Sigma) for 20 minutes followed by further washings (x2) in PBSc. A 15 minute 'blocking' step, using 5% goat serum (Diagnostics Scotland, Carluke) in PBSc, was used to inhibit non-specific binding of the primary antibody. Alternatively, non specific binding was prevented by treating cells with 0.1% bovine serum albumin ((BSA); BDH) in PBSc for 15 minutes. Each coverslip was then removed from the coplin jar, lightly blotted on filter paper to remove any excess fluid and placed on two cocktail sticks in a moist chamber. 100µl of primary antibody in 5% goat serum (or 1% BSA) solution was added to the appropriate coverslip. The lid was replaced and the cells were incubated for 30 minutes at 37°C. After incubation of cells in primary antibody, the coverslips were returned to the Columbia jars and rinsed (x2) for 10 minutes in 5% goat serum. They were then returned to the Petri dish where 100µl of the appropriate secondary antibody, with or without fluorescent phalloidin to stain filamentous (F)-actin, was added. The cells were incubated for a further 30 minutes at 37°C, then given a final (x2) rinse in PBSc, before mounting the cover slip on a microscope slide with a drop of Gelvatol (Airvol 205) containing an anti-fade agent DABCO ((1,4-Diazabicyclo [2,2,2] Octane; 100mg.ml⁻¹; Sigma). Slides were then left for at least 30 minutes to set and thereafter examined microscopically (see below) or stored at 4°C for viewing later. Some preparations were mounted using Hydromount (BDH) which set in 15 minutes and did not require additional anti-fade agent.

2.2.2 *Microscopy*

Cells were viewed and photographed using a Zeiss Axioplan 2 Universal epifluorescence microscope (Carl Zeiss Inc), equipped with x40 (NA 0.75), x63 (NA 1.4 oil immersion) and x100 (NA 1.3 oil immersion) objectives. Specimens were illuminated using a 50W mercury lamp (HBO 50 Osram). The excitation-emission filter combinations were 490nm and 525nm (fluorescein) and 540-560nm and 580nm (rhodamine) respectively. Monochrome photographs were taken on Kodak T-max100 (TMX) film run at ASA 800. Colour photographs were recorded on Kodak Ektachrome slide film (ASA 1600). The scale bar superimposed on the micrographs represented 25µm and 10µm at x40 and x100 magnification respectively.

2.2.3 *Image analysis*

Low power photographs from a range of cell development stages were studied using a Videoplan Image Analyser (Carl Zeiss Inc., Germany). Measurements of area, length and shape index were made for whole cells and for perinuclear rings of vimentin. The shape index (SI) is defined as

$$\frac{4\pi A}{P^2}$$

where A is the area (cm²) and P is the perimeter (cm) (Levesque & Nerem, 1985).

A perfect circle would have a SI of 1 and a straight line would have a SI of 0.

Measurements were obtained by drawing around either the entire cell or the perinuclear ring with a digitising pen for a sample of cells for each of the days studied. Mean values and standard errors of the mean (mean +/- SEM) were calculated for each of the above parameters and the values were plotted as a function of time in culture (see chapter 3.5).

2.3 Shearing Experiments

2.3.1. Introduction

Modified cone and plate viscometers (Dewey *et al*, 1981; Levesque & Nerem, 1985) and rectangular parallel plate (Levesque & Nerem, 1985; Viggers *et al*, 1986) chambers have been widely used to generate laminar flow to investigate the effects of uniform shear stress on cultured endothelial cells. The chambers used in the present study were of the 'parallel plate' type, described by Viggers *et al* (1986). This design provides a well-defined mechanical environment in which to study the responses of endothelial cells to flow. Two types of chamber were constructed, one of which accommodated cells grown on microscope slides, while the other was used for cells mounted on coverslips, allowing biochemical and structural analyses respectively.

2.3.2 Chamber design

The requirement was to generate uniform, laminar flow between two parallel surfaces forming the flow channel. Laminar flow is characterised by a parabolic velocity profile: liquid in direct contact with each surface is motionless, while the velocity of flow is greatest along the central axis of the channel. An important design consideration is that the width of the channel must be uniform and much greater than its height in order to generate *two-dimensional* (laminar) flow and maintain it along the length of the chamber.

Both types of chamber referred to above were constructed from Perspex (Plexiglass) in the School workshop. Each consisted of an upper and lower section held together by screws (Figure 2.1). When assembled, the cover slip or microscope slide was located in a recess in the lower section, so that the surface of the cell monolayer was flush with the

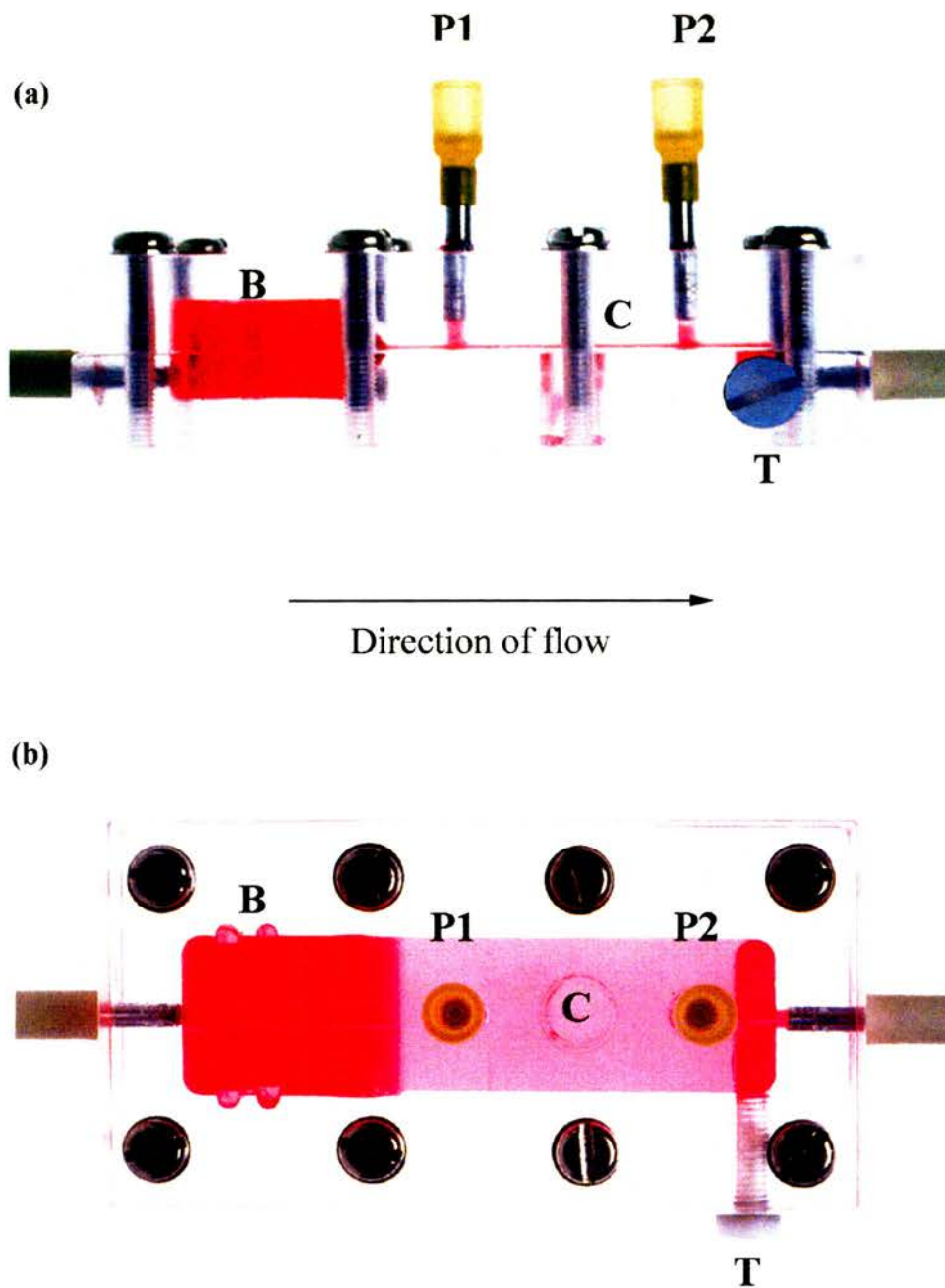


Figure 2.1

Figure 2.1 (a)&(b) illustrate the side-on and aerial views of one of the parallel plate flow chambers. Medium enters the chamber from the left into the entrance bell. This contains 2 baffles (B) which ensure uniform velocity of the medium as it enters the flow channel containing the cells on either coverslips (C) or microscope slides. Pressure points (P1 & P2) are located at opposite ends of the flow channel and were used to determine the pressure gradient across the cells. The temperature of the medium was measured by inserting a temperature probe attached to a screw (T).

Perspex surround. A rectangular section was milled out of the upper half of the chamber to form the flow channel. Culture medium first entered the chamber through a wedge-shaped entrance 'bell' where it was made to pass through two vertical baffles. The baffles were located *ca* 2 mm apart and each was perforated by 75 small holes approximately 1mm in diameter. This arrangement ensured that the velocity of flow was uniform when the liquid entered the flow channel. Two holes were drilled in the upper section of the chamber, at each end of the channel. These were used to measure the pressure gradient along the channel at different flow rates. Shear stress is related to the pressure gradient (see below) and this information was required for calibration purposes. The shear stresses (dynes.cm^{-2}) developed for a range of different flow rates were measured for each chamber and the results obtained were compared to those expected on theoretical grounds, based on the channel dimensions.

The measured shear stress (τ) is given by:

$$\tau = (\rho g h a) / l \quad (1)$$

where ρ = medium density (g.cm^{-3})
 g = acceleration due to gravity (cm.s^{-2})
 h = pressure difference across chamber (cm water)
 a = 1/2 channel height (cm)
 l = distance between pressure points (cm)

The density of the culture medium was determined at 37°C using a density bottle. Acceleration due to gravity was taken to be 980cm.s^{-2} . The pressure difference (cm H₂O) across the chamber was measured using two vertical glass tubes (*ca* 50cm long, with 4mm internal diameter) connected to each of the pressure points and to each other by rubber tubing. The difference in height of the water meniscus was recorded at each flow rate. The centre-to-centre distance between the pressure points was measured directly with a ruler. The channel height was measured directly using a microscope. In

order to do this, the microscope was first focussed on the Perspex surround and then on the base of the channel. The procedure was repeated several times along the length of the channel and mean (+/- SEM) channel height calculated from the results. A schematic diagram of chamber dimensions can be seen in Figure 2.2.

Theoretical shear stress (τ^*) was calculated for different flow rates from the relation:

$$\tau^* = 3Qv/2a^2w \quad (2)$$

where Q = flow rate (ml.s^{-1})
 v = viscosity (poise)
 a = 1/2 channel height (cm)
 w = channel width (cm)

Flow rate was measured directly by collecting the volume of liquid delivered by the pump per unit time (ml.sec^{-1}) at each pump setting. Viscosity at 37°C was determined using a Cannon-Fenske viscometer (BDH). The channel width was measured directly using a ruler. Details of the experimental procedures used in calibrating the chambers and the data obtained are given in Appendix 4.

Several parallel plate chambers were constructed and their characteristics carefully assessed in this way. Two were rejected because they did not generate uniform laminar flow, as shown by a significant discrepancy between the measured performance and that expected on theoretical grounds. Three chambers were eventually selected and used for the following purposes:

Chamber 2	for use with microscope slides
Chambers 3 and 4	for use with cover slips

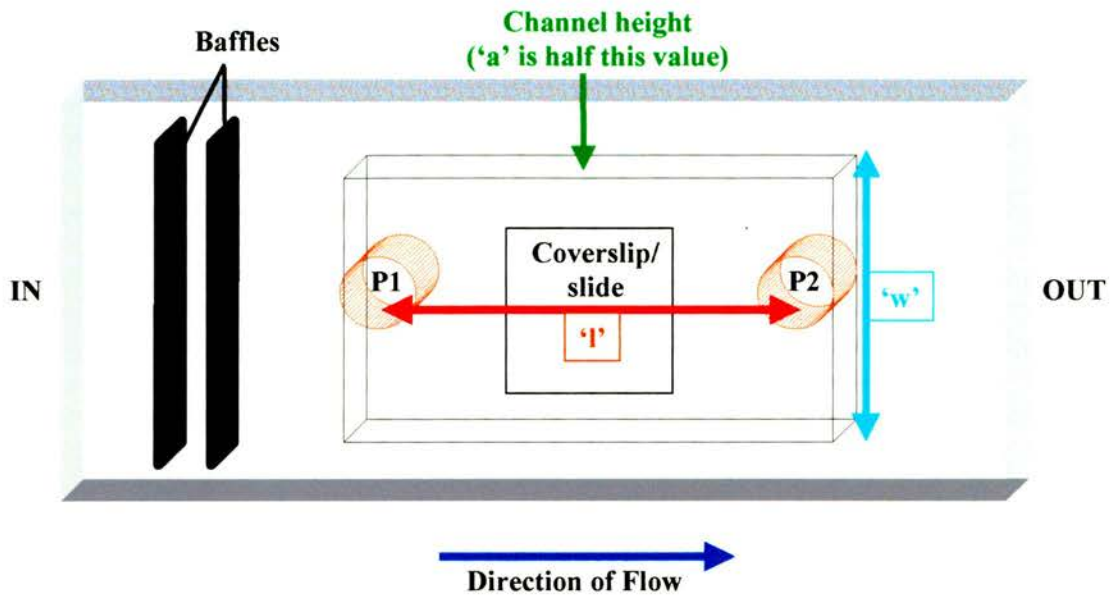


Figure 2.2. Schematic representation of chamber dimensions. In order to calculate the measured and theoretical magnitudes of FSS generated within the chamber (equations 1&2 section 2.3.2.), various dimensions were required. ' l ' is the distance (cm) between the two pressure points (P1 & P2). ' w ' is the width of the flow channel (cm). ' a ' is the half height (cm) of the channel.

Chamber 4 was designed so that its performance closely matched that of chamber 2. This meant that both chambers could be connected in series and perfused simultaneously, generating the same shear stresses. Biochemical measurements (chamber 2) could therefore be correlated directly with morphological changes (chamber 4) obtained under identical experimental conditions.

2.3.3. Perfusion system

The experimental arrangement is shown diagrammatically in Figure 2.3. Shearing experiments were performed in a class I flow hood in a hot room maintained at 37°C. The appropriate chamber was incorporated into a closed loop perfusion system driven by a peristaltic pump (Cole-Parmer, Hertfordshire model #7521-47). The chamber was located between two 500ml bottles containing culture medium. These acted as reservoirs for the re-circulating medium and served to absorb pulsations created by the pump and to trap any bubbles in the system. Medium was delivered to the chamber through Masterflex™ tubing (PharMed®; L/S® 16, 3.1 mm internal diameter). The output of the pump was adjusted for each chamber so that cells were exposed to shear forces of either 15 or 50 dynes.cm⁻² (see Appendix 4). These values were chosen since they fall within the physiological range and because they have been used extensively by previous authors. Medium was pumped into the chamber from reservoir 1. On leaving the chamber, the medium entered reservoir 2 from where it passed through the pump to reservoir 1 and finally back into the chamber.

2.3.4. Experimental protocol

The apparatus was assembled as shown in Figure 2.3, but without connecting the inlet and outlet tubes to the flow chamber. The pump was then switched on to ensure that all air bubbles were removed from the system. The free ends of the tubes were then

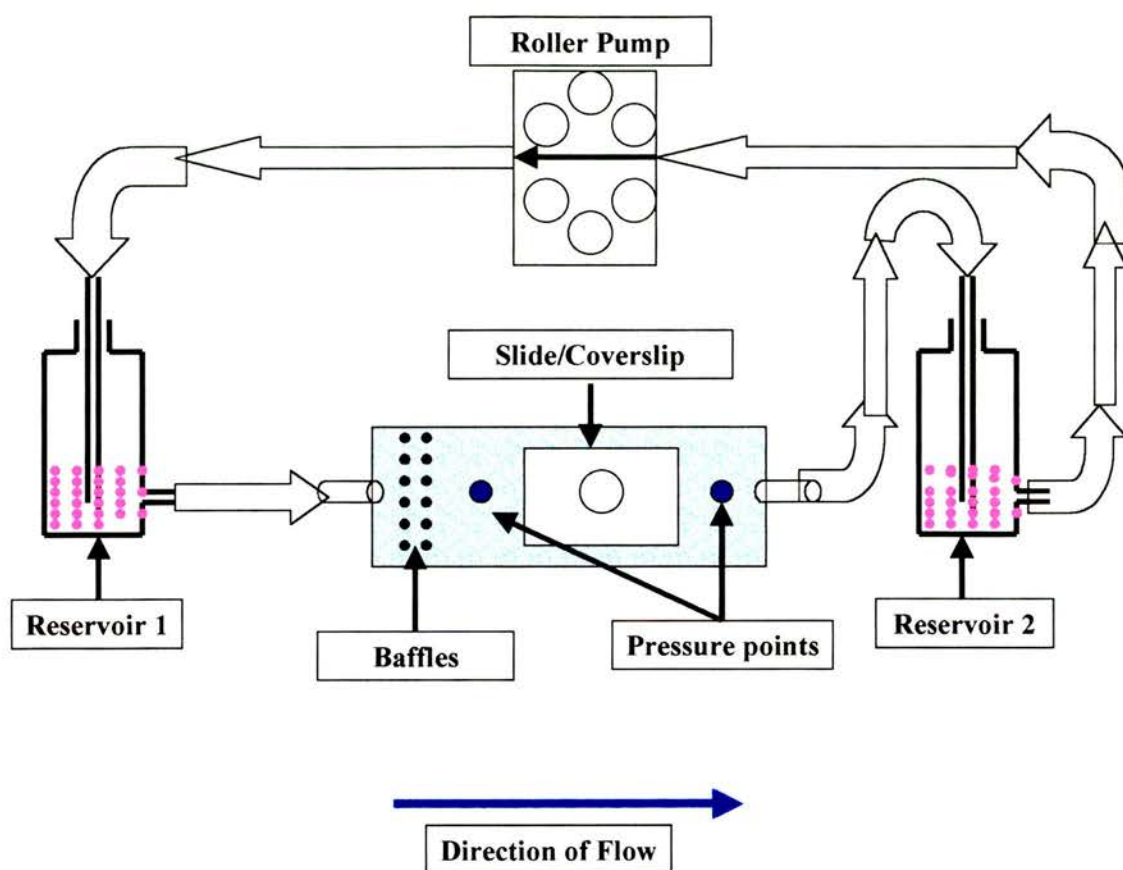


Figure 2.3. Schematic representation of experimental set-up based on a design by Viggers et al, 1986. All experiments were carried out in a 37°C maintained room. The parallel plate chamber was incorporated in a closed perfusion loop. Medium was circulated by means of a peristaltic pump. Medium entered the chamber from reservoir 1 and on leaving entered reservoir 2. From here it was pumped back to reservoir 1 and the circuit was repeated.

clamped off. A coverslip or slide bearing cells was removed from its Petri dish with the aid of forceps, taking great care to avoid damaging the monolayer. The coverslip/microscope slide was then placed in the recess of the chamber where a very thin layer of high vacuum grease (Borer Chemie, France #CH4528) had previously been applied to the surface to create a water-tight seal. A little medium was placed on the cells to prevent them drying out while the screws for holding the two halves of the chamber were gently tightened. The chamber containing the cells was then connected to the perfusion system and the clamps were released. The pump was switched on, initially at a low setting that was gradually increased over a one-minute period until the appropriate flow rate was reached. The chamber was then checked for leaks, before being left in the dark for the relevant time (5, 10, 30, 60, 120, 240, 480 or 960 minutes).

Once a run was complete, the coverslip was removed by gently pressing on the underside with a cotton bud. Before processing for immunofluorescence, a small piece of one corner of the cover slip was snapped off to facilitate orientation with respect to the flow direction. Microscope slides were removed from the chamber using a glass rod. The surface was wiped clean of grease before cell lysates were made.

2.4 *Western Blotting*

Cytoskeletal protein expression was monitored in whole cell extracts by gel electrophoresis followed by Western blotting. Extracts were made from cells that were grown in culture for different times, or from cells that had been exposed to shear stress.

2.4.1 *Preparation of cell extracts*

Cells were grown on microscope slides and extracted using a hot lysis method. Medium was drained from the slide and the grease layer on the underside was wiped clean. The

slide was then rinsed with 1-2ml of warm PBSa and excess fluid drained onto tissue. The slide was placed on a warm, flat surface and 750 μ l of boiling Laemmli buffer (see Appendix 3) was pipetted onto the surface. The cells were then removed by rubbing a syringe plunger over the slide in an ordered fashion. The 'sticky' solution that resulted was transferred to an Eppendorf tube and syringed 3 times through a 25G (orange) needle. The lysate was then boiled for 5 minutes in a water bath and centrifuged for 5 minutes at 12,000 RPM. Finally the supernatant was transferred to a clean tube and stored at -20°C .

2.4.2 Protein estimation

Total protein present in each sample was measured using a protein estimation kit (Bio-Rad 500-0112) that was compatible with the lysis buffer. The kit contained an aliquot of BSA and this was diluted to give standard concentrations of 0.2, 0.4, 0.8 and 1.2mg.ml⁻¹ respectively. Once the appropriate solutions from the kit had been added, the absorbances of the blanks and standards, followed by the lysate samples were read in a dual-beam spectrophotometer (Cecil, Cambridge #CE594) operating at a wavelength (λ) of 720nm. A standard calibration curve allowed the protein concentrations of the lysates to be determined and from this the relevant dilutions were made using single strength Laemmli solution. At this point, 1 μ l bromophenol blue and 3 μ l β -mecaptoethanol were added per 100 μ l lysate. The lysates were then boiled for 5 minutes in a fume hood and stored ready for use at -20°C .

For some biochemical analysis, cold lysates were prepared. Cells were extracted using 1ml of ice cold PBSa, centrifuged and the supernatant removed before being 'snap frozen' in liquid nitrogen. The cell extracts were resuspended in the appropriate lysis buffer for biochemical investigation.

2.4.3 Protein separation and Western blotting

Proteins were separated by sodium dodecyl sulphate-polyacrylamide gel electrophoresis (SDS-PAGE) and transferred from the gel onto nitrocellulose membranes for immunoblotting. Detailed methodology is given in Appendix 3. Membranes were probed with antibodies to various cytoskeletal proteins (vimentin, actin & tubulin) afterwards treated with appropriate secondary antibodies labeled with horseradish peroxidase. The secondary antibodies were detected by the enhanced chemiluminescence technique (ECL™), (Amersham, Buckinghamshire). Quantitative analysis of proteins was performed by densitometry against known quantities of authentic protein (recombinant human vimentin, bovine brain tubulin and chicken gizzard actin). Alternatively, band densities for sheared cell extracts were compared to unsheared controls.

CHAPTER 3

RESULTS PART I

MORPHOLOGY OF INTERMEDIATE FILAMENT NETWORKS IN SUB-CONFLUENT AND CONFLUENT CELLS AND RELATED CHANGES IN CYTOSKELETAL PROTEIN EXPRESSION.

3.1 Introduction

Preliminary experiments showed that the morphology of vimentin intermediate filament networks was strikingly different in growth phase (sub-confluent) cells compared to cells that were fully confluent. This led to the experiments now to be described, the purpose of which was to document changes in the sub-cellular distribution and levels of expression of cytoskeletal proteins, primarily of vimentin intermediate filaments, as a function of time in culture. This information was needed to provide a morphological 'baseline' for later studies concerned with the effects of flow (Chapter 4).

BAEC from passage 20-25 were studied initially. These experiments revealed that the rate of growth diminished significantly in higher passage numbers, therefore cells of passage number 20-22 only were used in later experiments. Double indirect immunofluorescence was used to study the sub-cellular distribution of the proteins concerned. Cells were grown on cover slips and maintained in static culture for periods of 2, 5, 7, 10, 14, 17 or 21 days. They were then fixed and stained using appropriate combinations of antibodies to vimentin, actin, plectin (IFAP-300), vinculin, phosphotyrosine (PY20) and a 58kDa protein of the Golgi complex. Stained cells were viewed and photographed using a fluorescence microscope. The levels of expression of cytoskeletal proteins (vimentin, actin and tubulin) were determined by immunoblotting whole cell extracts. Known amounts of authentic protein samples (recombinant human vimentin, non-muscle actin and α tubulin) were run on the gels alongside cell lysates to provide calibration curves. The quantity of protein expressed ($\mu\text{g} \cdot \text{mg}^{-1}$ total protein) was then determined by densitometry.

3.2 Cell growth and shape in static cultures

During the logarithmic phase of growth cells were highly polymorphic, but as their density increased they became smaller and more uniformly shaped. The confluent monolayer that ultimately formed took on the 'cobblestone' appearance characteristic of

endothelial cells in culture (Booyse *et al*, 1975; Gimbrone, 1976). Mean cell densities (cells.cm⁻²) (Figure 3.1) were determined from photographic enlargements of micrographs taken on the days specified above (Figure 3.7). The scale bar (x 40 lens) on each image represents 25µm (Appendix 5). Cell density increased from 2 x 10⁴.cm⁻² (seeding density) to around 1.8 x 10⁵.cm⁻² by day 7, then declined to a steady-state value of around 1.4 x 10⁵.cm⁻² (Figure 3.1). Maximum cell density (day 7) was reached after approximately 3 population doublings, equivalent to a cell cycle time of ~2.3 days.

Image analysis was used to quantify changes in cell area and shape index. Cells became smaller and more uniformly-shaped as they progressed towards confluence. The mean cell area decreased *ca* 2.7 fold between days 2 and 5, from 828 +/- 45 µm² to 312 +/- 9.6 µm² (Figure 3.2a). The shape index, derived from measurements of the mean cell area and perimeter (Levesque & Nerem, 1985), increased from around 0.69 to 0.87 by day 10, indicative of a tendency for the profile to become more circular (Figure 3.2b).

3.3 Remodelling of the intermediate filament network in static culture: formation of perinuclear bundles of intermediate filaments and related changes to the actin cytoskeleton

The above changes in cell density and shape were accompanied by a dramatic redistribution of intermediate filament networks. Sub-confluent cells contained a dense meshwork of slender intermediate filaments emanating from an amorphous, juxtannuclear 'cap' and extending out towards the cell periphery (Figure 3.3a). This pattern was replaced in fully-confluent cells by one dominated by the presence of an unusually thick bundle of intermediate filaments, forming a prominent ring or torus that completely encircled the nucleus (Figure 3.3c & d). The nucleus was invariably positioned eccentrically within the perinuclear ring of intermediate filaments (Figure 3.3d). The inner surface of a portion of the perinuclear ring contacted part of the nuclear envelope (adherent segment) while the remainder extended out to enclose a region of cytoplasm (non-adherent segment). Double indirect immunofluorescence of cells stained for

3.1

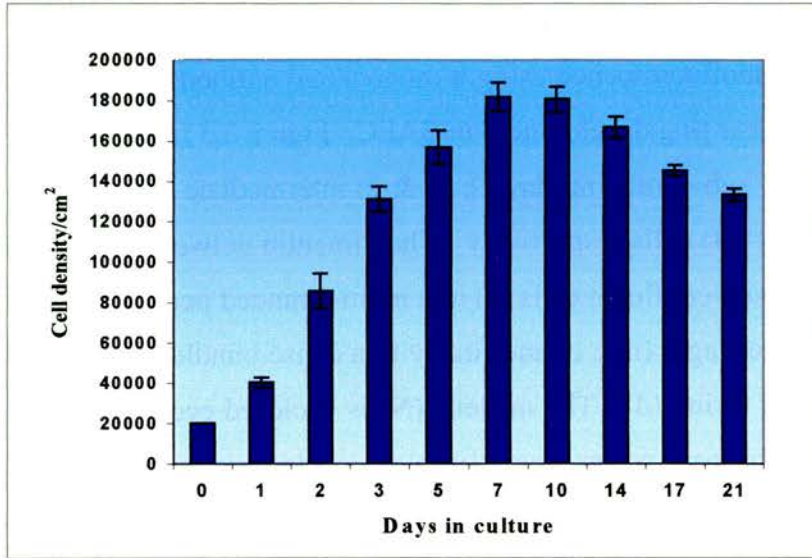
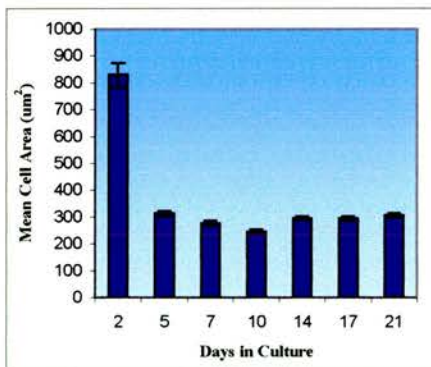


Figure 3.1. Changes in mean (\pm SEM; $n=5-23$) cell density (cells.cm⁻²) in BAEC grown in culture over a 21 day period. Cells were counted from enlarged micrographs of known area (see appendix 5) which allowed the density to be calculated. The mean cell density increased from the seeding density (2×10^4 .cm⁻²) to a maximum between days 7-10 ($\sim 1.8 \times 10^5$.cm⁻²) before tailing off a little between days 10-21.

3.2 (a)



3.2 (b)

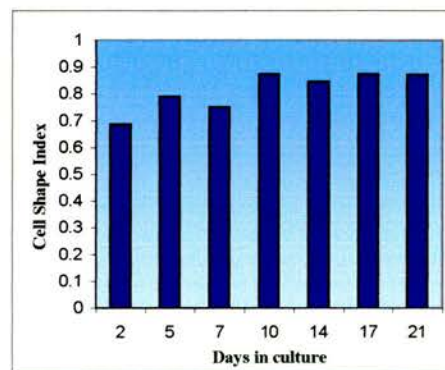


Figure 3.2 a & b. Changes with time of mean (\pm SEM; $n=364-825$) cell area (μm^2) and shape index respectively. Figure 3.2a shows a dramatic change in the mean cell area between days 2-5 but from then onwards maintaining a plateau. The smallest mean cell area was observed around day 10. Figure 3.2b represents changes in the cell shape index (SI) with time in culture. A shape index of one represents a perfect circle. Corresponding with the smallest mean cell area, SI reached a maximum around day 10. Measurements of both of these values were recorded using a Zeiss image analyser.

Figure 3.3 (a-d) Vimentin perinuclear ring development with time in culture.

Indirect immunofluorescence using a monoclonal antibody to vimentin was used to study perinuclear ring development in BAEC. Figure 3.3 (a-d) illustrate the vimentin network in (a) sub-confluent (day 2), (b & c) intermediate (day 7 & 10) and (d) fully confluent (day 14) cells respectively. The vimentin network changes from a diffuse meshwork in sub-confluent cells (a) to a multi-stranded perinuclear ring arrangement in intermediate stages (b & c) and finally to a dense bundle of intermediate filaments in the form of a ring (d). The nucleus (**N**) is enclosed eccentrically within the ring. One area of the perinuclear ring is in close contact with the nuclear membrane (**i**) while the other extends outwards to enclose a region of cytoplasm (**ii**). An example of a dividing cell in late cytokinesis can be seen in day 2 cells (indicated by *). Micrographs were taken at x100 and the scale bar represents 10 μ m.

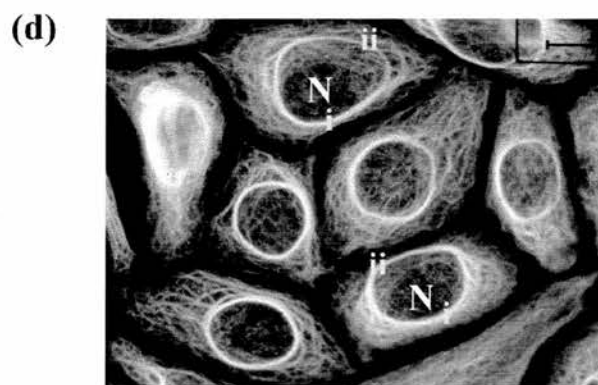
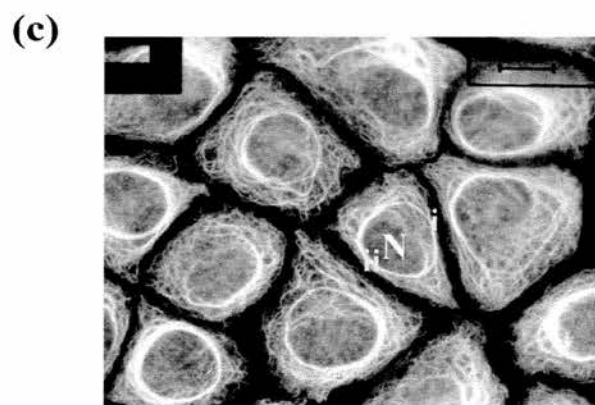
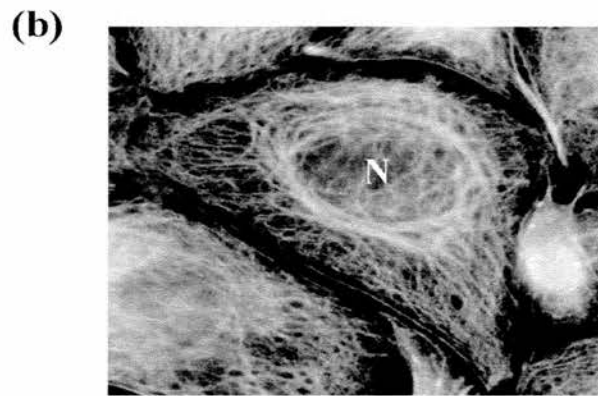
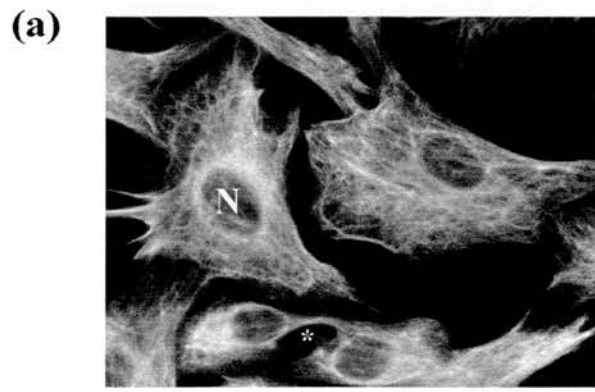


Figure 3.3

vimentin and *either* monoclonal antibody to a 58kDa Golgi protein (G58K) *or* antibody to α -tubulin revealed that the area of cytoplasm delimited by the non-adherent segment invariably contained both the Golgi apparatus (Figure 3.4b) and the centrosomes (or MTOC) (Figure 3.4d). The remainder of the intermediate filament network consisted of bundles of intermediate filaments that radiated outwards from the perinuclear ring, reaching towards the cell surface. A comparison of phase contrast and fluorescence images showed that these radially-oriented bundles of intermediate filaments actually terminate short of the cell periphery (compare Figure 3.4a with 3.4c). This can be seen most clearly in high power micrographs of fully-confluent monolayers stained for vimentin and actin, as revealed by the dark areas between neighbouring cells (Figure 3.5c-d). Finally, fine bundles of intermediate filaments emerged from the inner aspect of the perinuclear ring to form a cage-like meshwork tightly apposed to the nuclear envelope.

The transition between the intermediate filament network typical of sub-confluent cells and that found in confluent cells was studied in cultures as they *approached* confluence. In some cells, multi-stranded ‘cables’ of intermediate filaments were observed near the cell periphery. Other cells within the same population contained similar, circular bundles of intermediate filaments, but these were located at varying distances between the periphery and the nucleus. This suggests that the formation of a perinuclear ring could involve the progressive collapse of circumferential cables of intermediate filaments towards the nucleus. Figure 3.6 (a-c) shows a sequence of images illustrating this hypothesis.

The sub-cellular distribution of actin also changes markedly with time in culture. This was studied using fluorescent-labelled phalloidin, a fungal toxin that binds selectively to polymerised (F-) actin. Sub-confluent cells that are well spread and firmly attached to the cover slip contain numerous prominent actin stress fibres distributed over the basal cell surface, often in near parallel arrays (Figure 3.10). Each stress fibre terminates in a focal adhesion, as revealed by double staining with phalloidin and antibody to vinculin, talin or PY20 (Figures 3.10 (e-f) & 3.11(c-f)), known components of focal adhesions.

Figure 3.4. (a-f) Non adherent portion of the perinuclear ring encloses both the Golgi apparatus and the microtubule organising centre (MTOC).

Double indirect immunofluorescence using monoclonal and polyclonal vimentin (a & f), monoclonal 58kDa Golgi protein (b) and monoclonal α -tubulin (e) reveals that the non-adherent portion of the vimentin perinuclear ring (R) encloses both the Golgi apparatus (G) and MTOC (M). The enclosure of the nucleus and the Golgi and MTOC containing region of the cells was illustrated using phase contrast (c). The observations were confirmed by EM micrographs (Courtesy of Dr F.W.Flitney) (d) which clearly show the perinuclear ring enclosing the nucleus (N), MTOC and Golgi. All micrographs (excluding 3.4d) were taken at x100 magnification and the scale bar represents 10 μ m.

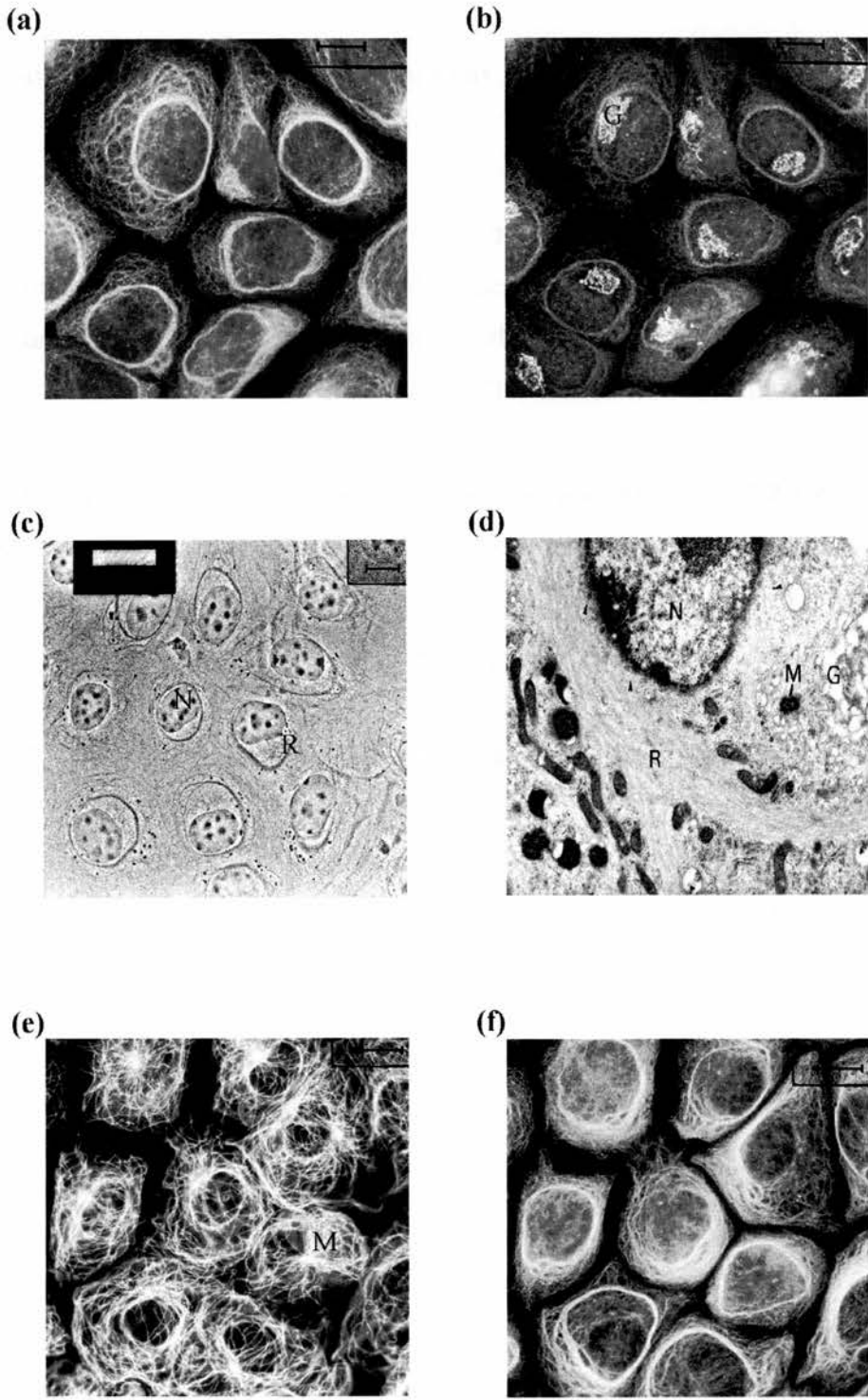


Figure 3.4

Figure 3.5 In contrast to actin, the vimentin network does not extend to the cell periphery.

Double indirect immunofluorescence using polyclonal vimentin and monoclonal plectin antibodies as well as fluorescent labelled phalloidin was used to highlight differences in the distribution of the vimentin (a & c), plectin (b) and actin (d) networks in confluent endothelial cells.

Figures 3.5 a & b show vimentin and plectin staining for the same region of cells. As plectin associates with vimentin, the two staining patterns are similar. However the plectin network extends further towards the periphery than vimentin network (\rightarrow), often terminating in intensely staining streaks (see figure 3.10).

In contrast to vimentin and plectin, actin extends to the cell periphery. Micrographs of the vimentin network alone (a & c) suggest no cell-cell contact (denoted by \rightarrow and *). However phalloidin staining of the actin network (d) confirms that the cells are confluent (*) as cell-cell contact is observed.

Micrographs were taken using x100 magnification. Scalebar represents 10 μ m.

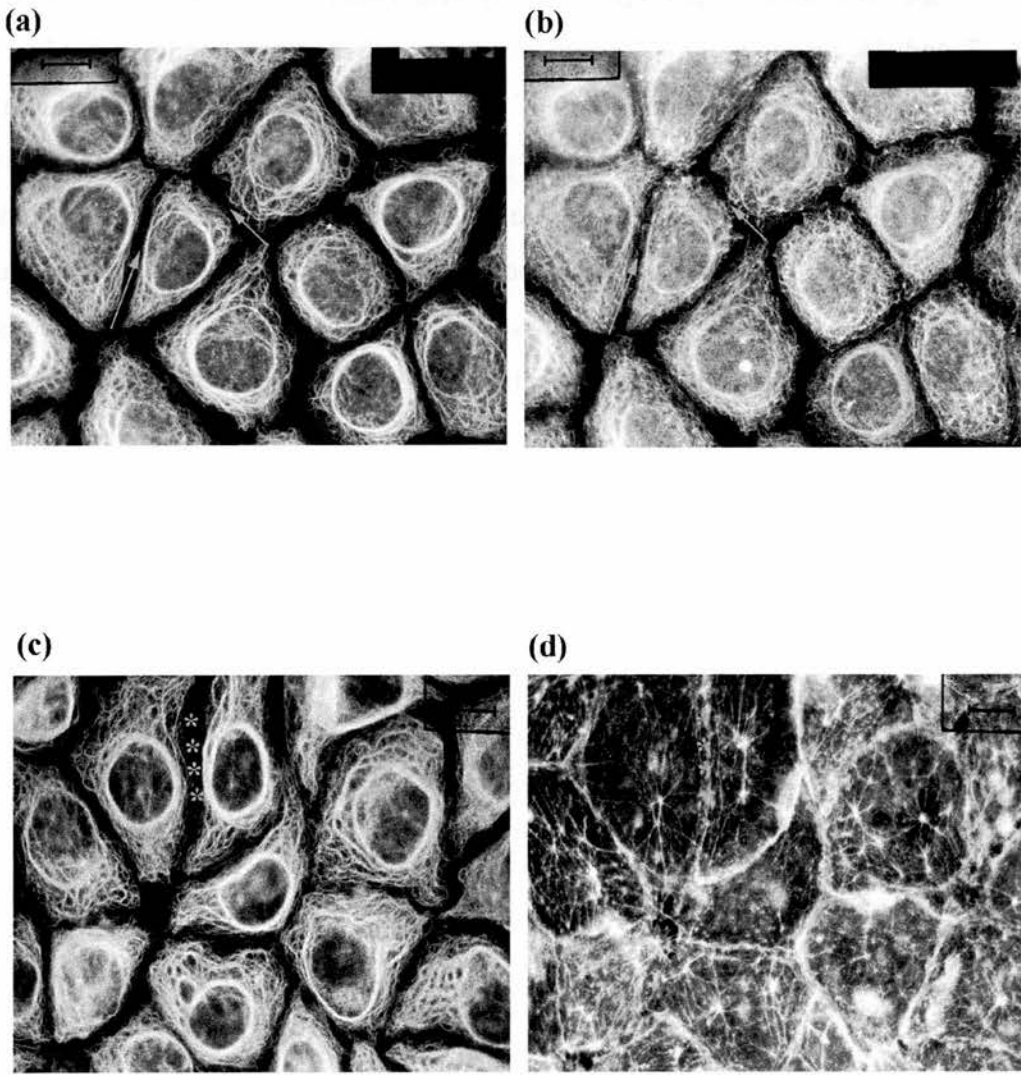
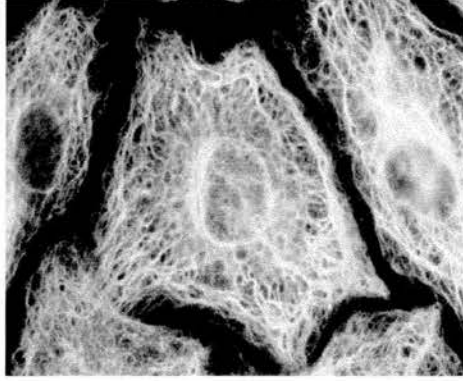


Figure 3.5

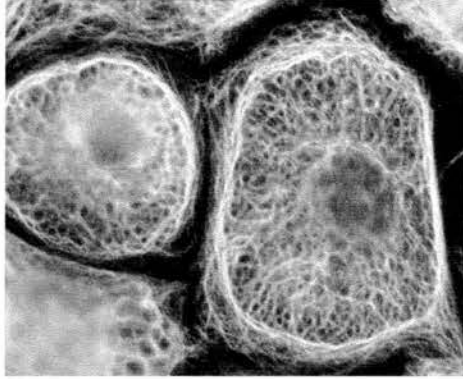
Figure 3.6. Collapse of the developing vimentin ring towards the nucleus.

Figure 3.6 (a-c) illustrates alterations in the typical vimentin network in BAEC on days 2, 7 and 15 respectively. Immunostaining with a monoclonal antibody to vimentin showed multi-stranded bundles of vimentin were initially observed at the periphery of sub-confluent cells (3.6 a & b). As cells became confluent (c), vimentin bundles were present at varying distances between the periphery and the perinuclear region. These observations suggest that vimentin PNR development may involve the progressive collapse of the circumferential strands of vimentin towards the nucleus. Images were recorded using x100 magnification; the scale bar represents 10 μ m.

(a)



(b)



(c)

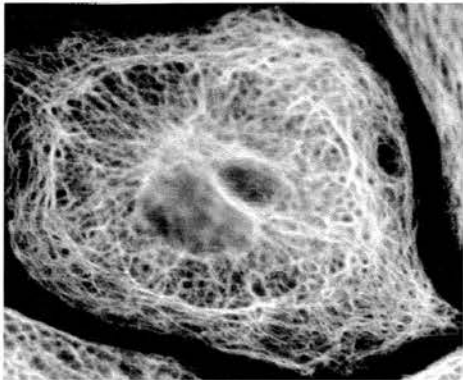


Figure 3.6

This pattern gradually changed with time in culture. In confluent monolayers, stress fibres are either absent or very sparse and F-actin becomes redistributed around the periphery of the cell, forming so-called dense peripheral bands. The presence of large amounts of F-actin near the periphery effectively blocks the incursion of vimentin intermediate filaments into this region, referred to earlier. This creates a false impression when monolayers are stained with the vimentin antibody alone, that the cells are not in contact with one another. However, if cells are also stained for F-actin, a single 'line' marks the boundary between adjacent cells (Figure 3.5 c-d). This implies a very close association between the actin in one cell and that in its immediate neighbour. Indeed, actin based cell-cell contacts are seen in cells after they have been subjected to flow (Figure 4.2).

3.4 The time course of perinuclear ring formation

Figure 3.7 shows a series of low power micrographs recorded on different days. Images like these were used to determine the number of cells containing a perinuclear ring. The proportion was very low (< 10%) in young, sub-confluent cultures (< day 5) but by day 5 it increased rapidly, rising to over 90% by day 10 (Figure 3.8a). The increase in the frequency of cells containing a perinuclear ring coincided with the time at which cell density reached its maximum. The growth curve presented earlier (Figure 3.1) is re-plotted here (Figure 3.8b) in order to emphasise this point.

3.5 Morphometric analysis of perinuclear ring structure

A sample of 1305 fully-formed perinuclear rings (7-21 days) was analysed morphometrically, using a Zeiss Image Analyser. The area of cytoplasm (mean +/- SEM) encircled by the perinuclear ring was found to be $130 \pm 4.2 \mu\text{m}^2$ (Figure 3.9a) and the ring perimeter was $42 \pm 0.8 \mu\text{m}$. perinuclear rings ranged in thickness

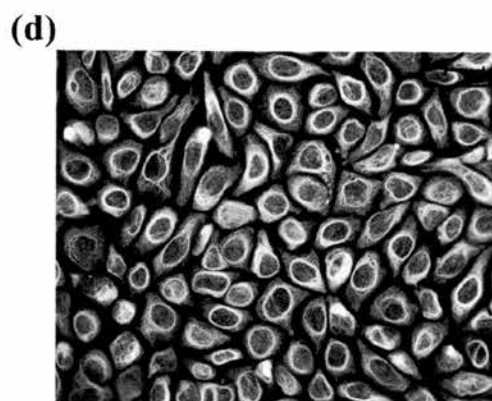
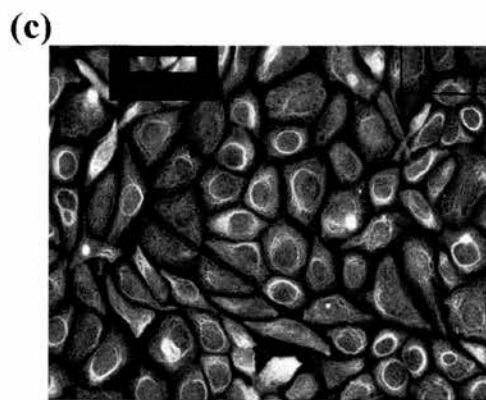
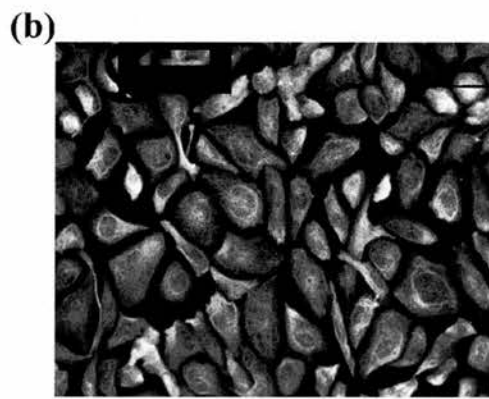
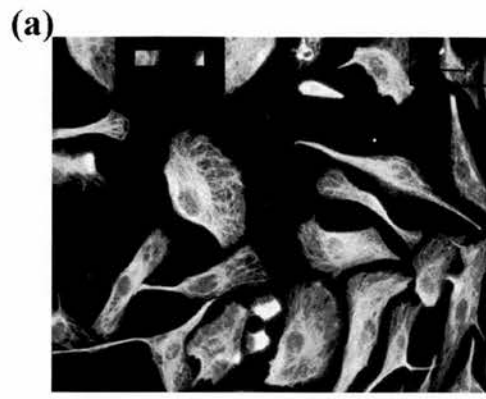
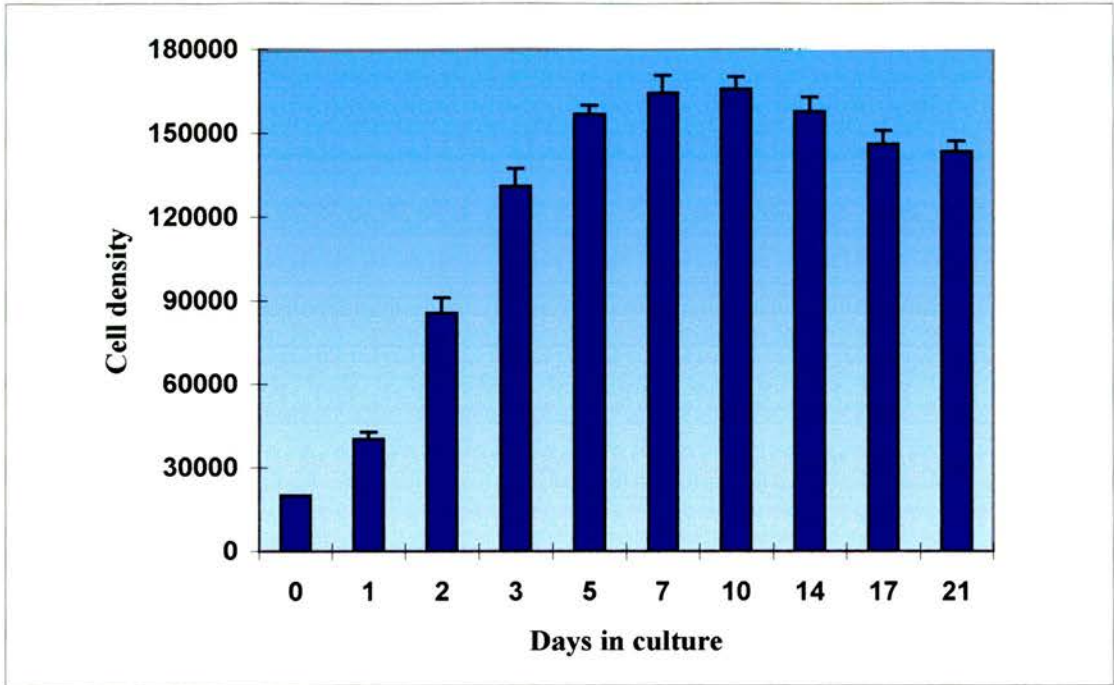


Figure 3.7

(a)



(b)

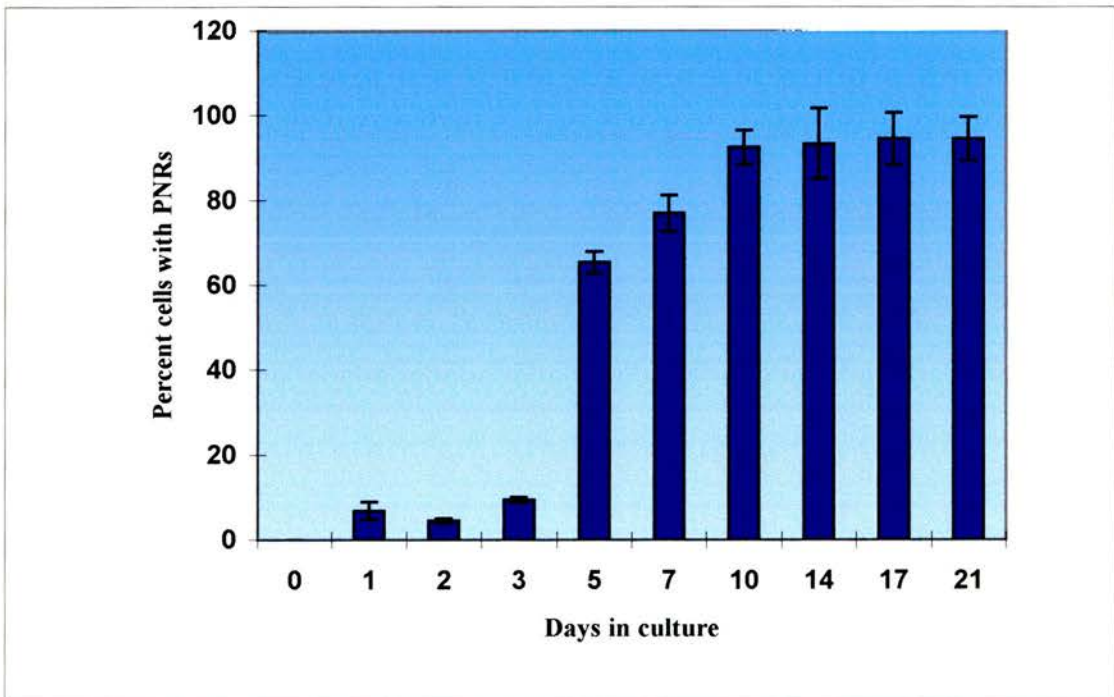
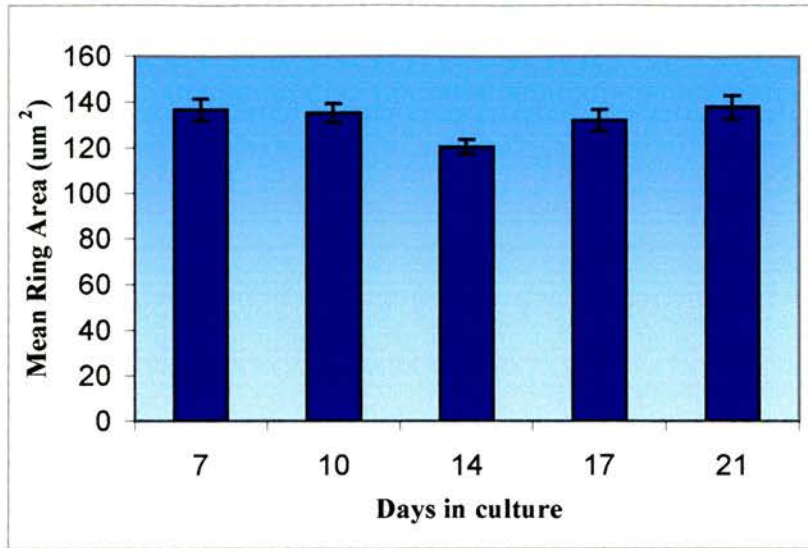


Figure 3.8 a & b. Changes with time in culture of mean cell density and vimentin PNR development respectively. Figure 3.8a shows mean (\pm SEM; $n=5-23$) cell density increasing with time in culture, reaching a maximum around days 7-10. Figure 3.8b follows the time course of PNR development in BAEC and represents the mean number of cells (\pm SEM; $n=140-2384$) possessing PNR. The occurrence of PNR in young cells is very low ($<10\%$) but increases rapidly between days 3-10 to around 95%. It should be noted that the steep increase in the number of cells exhibiting PNR coincided with the same time period as maximum cell density. Details of this data can be seen in appendix 5.

(a)



(b)

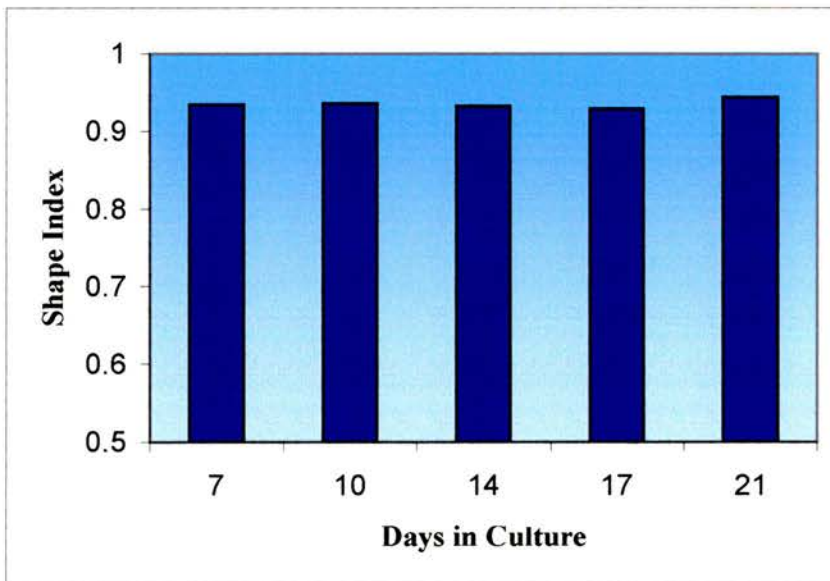


Figure 3.9 a & b. Two graphs illustrating changes in the mean (\pm SEM; $n=100-405$) ring area (μm^2) and shape index (SI) of the vimentin PNR with time in culture. Figure 3.9a. shows that once PNR form (from around day 7) they maintain a more or less constant area. Figure 3.9b illustrates that the values obtained for SI of the PNR were almost constant with a mean value of 0.93. These data were obtained using a Zeiss image analyser (details in appendix 5).

(diameter) from ~1-4 μm , with a mean value of 1.85 +/- 0.18 μm . The shape index was 0.93 (Figure 3.9b), indicating a near circular profile.

3.6 Changes in the distribution of plectin, an intermediate filament-associated protein, with time in culture

Intermediate filament bundling and the maintenance of intermediate filament networks in general are regulated by molecular interactions with a family of proteins called intermediate filament-associated proteins (or IFAP). Endothelial cells express plectin, a 580kDa IFAP that has been shown to cross-link vimentin intermediate filaments (Wiche, 1998; Allen & Shah, 1999). The distribution of plectin was studied by immunofluorescence using a monoclonal antibody (# 417D) that recognises the central rod domain (Clubb *et al*, 2000), kindly provided by Dr Robert Goldman.

As anticipated the distribution of plectin, like that of vimentin, changed dramatically with time in culture. However, immunoreactivity to plectin was not distributed uniformly throughout the intermediate filament network. In sub-confluent cells, plectin staining was moderately intense in a region that corresponded with the vimentin-containing juxtannuclear body and also in intermediate filaments located in the vicinity of the nucleus (Figures 3.10a & 3.10c). The staining co-localised with individual bundles of intermediate filaments, but it was particulate, rather than uniform, giving a beaded appearance to the filament bundles. The intensity diminished gradually towards the cell periphery. The most intense staining for plectin presented as discrete 'streaks', randomly scattered over the basal cell surface (Figures 3.10a & 3.10c). This pattern is strikingly similar to that seen after staining cells with antibodies to known focal adhesion proteins, such as vinculin or paxillin (Figures 3.10 e & f). Staining for actin, using rhodamine-tagged phalloidin, together with plectin confirmed that the streaks were located close to the tips of most stress fibres (Figures 3.10e & 3.10f).

Figure 3.10 Plectin and focal adhesion protein distribution in sub-confluent endothelial cells.

Figures a & b show cells labelled with monoclonal plectin and polyclonal vimentin antibodies respectively. Although the overall pattern of plectin staining is similar to that of vimentin it appears particulate with most intense staining present as 'streaks' over the basal surface (*). Counter staining with rhoadamine- labelled phalloidin (d) show these plectin 'streaks' (c) to co-localise with the tips of actin stress fibres. This staining pattern is similar to that seen with the focal adhesion proteins using monoclonal vinculin (e) and monoclonal talin (f). Double exposed micrographs of actin (red) and vinculin (green) (e), and actin and paxillin (green) (f) respectively illustrate that focal adhesion proteins co-localise with the tips of actin stress fibres. Micrographs were taken using x100 magnification and the scale bar represents 10 μ m.

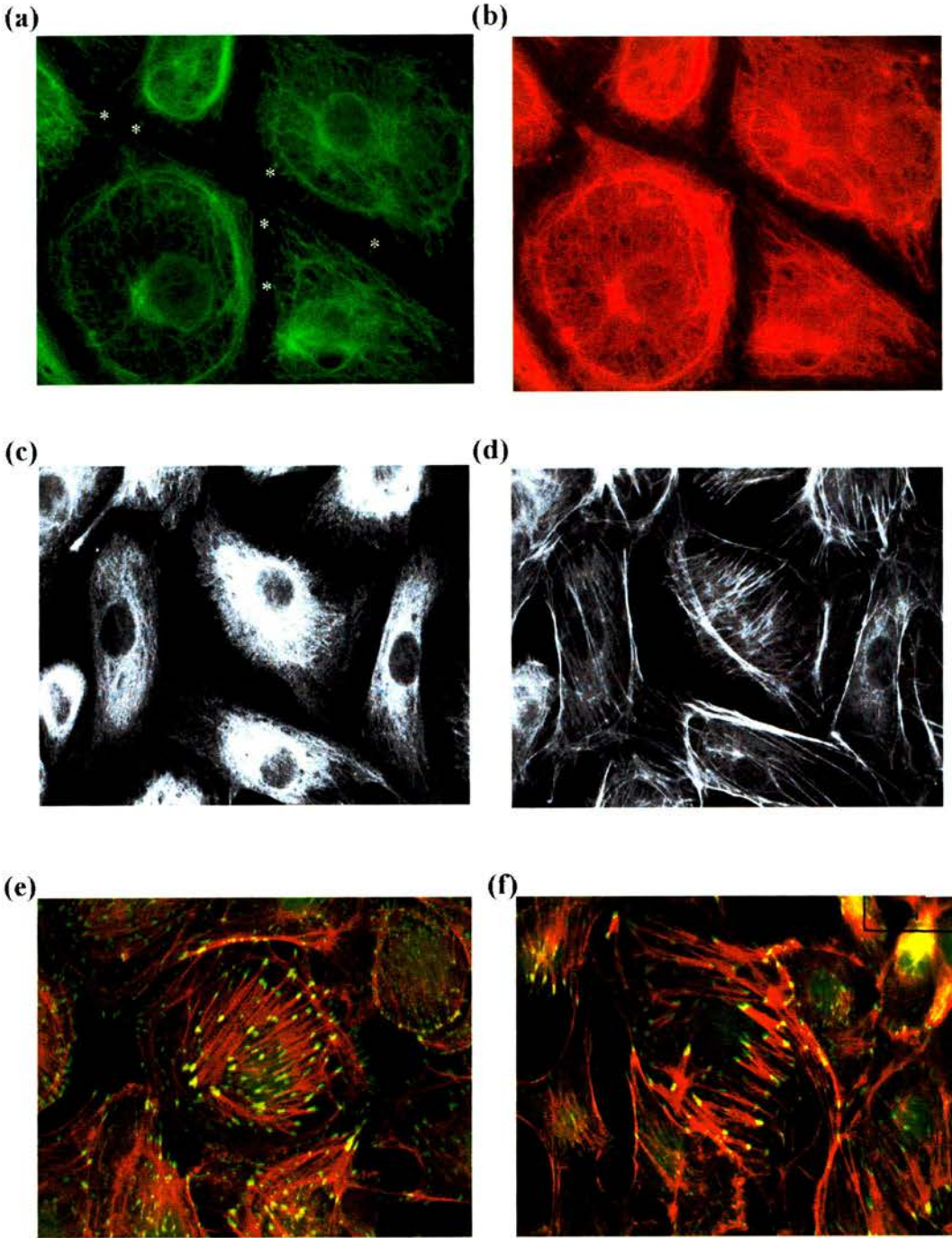


Figure 3.10

Double indirect immunofluorescence showed that plectin staining in fully-confluent cells coincided with perinuclear rings of vimentin (Figure 3.11b). ‘Streaks’ of plectin staining were also seen on the basal cell surface, but these were now preferentially distributed near the cell periphery, rather than scattered over the entire basal surface, as in sub-confluent cells (Figure 3.11a). This pattern was strikingly similar to that obtained when cells were stained using monoclonal antibodies to either vinculin or phosphotyrosine (PY20). PY20 immunoreactivity corresponded with the position of actin stress fibres in sub confluent cells (Figure 3.11 c & d) and also with the actin dense peripheral bands that form around the circumference of confluent cells (Figure 3.11 e & f). This similarity suggests that plectin-rich sites coincide with focal attachments. This was confirmed in a study by Flitney *et al* (1996) using BAEC and more recently by Gonzales *et al* (2001) using several different types of human endothelial cells.

There was also evidence of intense immunoreactivity to plectin in the form of a juxtannuclear reticular body (Figure 3.12 b, d, e & f) that clearly resembled the Golgi complex (Figure 3.12h). This pattern of staining was present when cells were double stained with plectin and vimentin (Figure 3.12 a & b) or with plectin and actin (Figure 3.12 c & d). However, attempts to precisely co-localise plectin with the 58kDa Golgi-associated protein, using a polyclonal plectin antibody and a monoclonal antibody to G58K protein, failed to provide convincing evidence due to a high degree of non-specific staining seen with the plectin antibody.

3.7 Changes in cytoskeletal protein expression with time in culture

Analysis of whole cell lysates by semi-quantitative Western blotting revealed time-dependent changes in the expression of all three cytoskeletal proteins. Sample immunoblots showing changes in vimentin, actin and tubulin expression in cells grown in static culture for up to 21 days are shown in Figure 3.13. Scans of similar gels (n = 7-14 for each protein) were obtained and the results (mean +/- SEM) are shown graphically in Figure 3.14. The amount of each protein was estimated by comparing gel band densities with known standards for vimentin, actin and α -tubulin. The quantities

Figure 3.11 Comparison of plectin and phosphotyrosine distribution in confluent cells

Figures 3.11 a & b represent the same area of confluent (day 14) cells labelled with monoclonal plectin and polyclonal vimentin antibodies respectively. Cells 1 & 2 show contrasting plectin and vimentin staining patterns, more generally seen in sub-confluent (1) and confluent (2) cell monolayers respectively. In cell 1, plectin forms a diffuse network similar to that of vimentin but exhibits plectin 'streaks' (depicted by arrows) across the cell resembling focal adhesion staining previously shown in Figure 3.10.

The presence of a vimentin perinuclear ring (2) is accompanied by a change in the plectin network. Immunostaining shows 'streaks' predominantly confined to the periphery of the cell (arrows) with denser band around the region of the vimentin perinuclear ring. This ring pattern of plectin staining was also observed when plectin was double stained with actin (not shown) which rules out the possibility of vimentin staining 'bleed-through'.

Figures 3.11 c & d represent sub-confluent cells (day 3) labelled with a monoclonal phosphotyrosine-20 (PY-20) antibody and actin respectively. PY-20 staining co-localises with the ends of actin stress fibres (depicted by arrows), similar to the staining pattern of vinculin and talin (Figure 3.10 e & g). In contrast, figures 3.11 e & f illustrate the PY-20 and actin staining patterns in confluent (day 21) cells. The large numbers of stress fibres present in figure 3.11d are replaced by dense peripheral bands of actin (D) and PY-20 staining (3.11c) now occurs mainly at the cell periphery (arrows).

Micrographs were taken using x100 magnification. Scalebar represents 10 μ m.

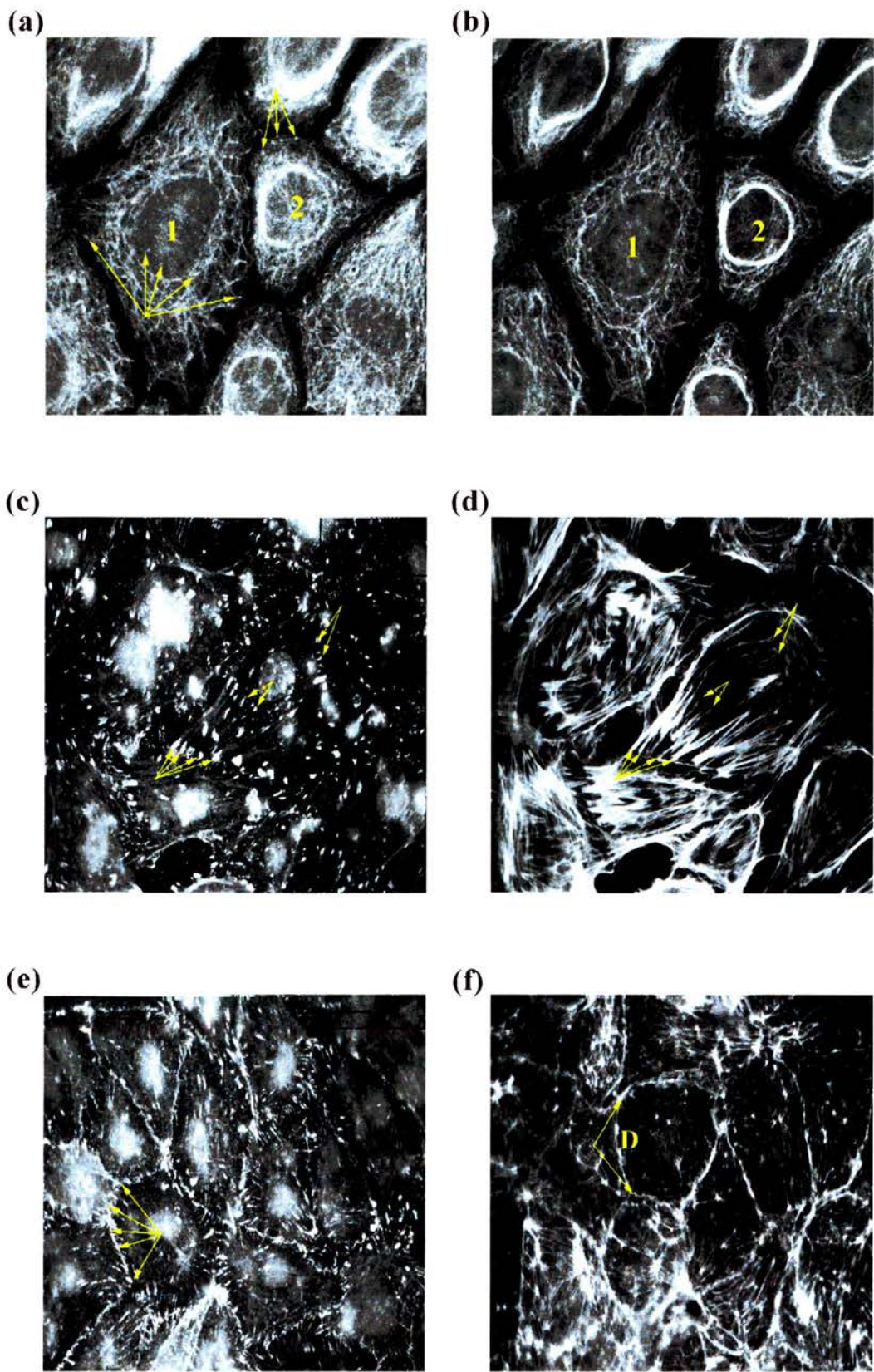


Figure 3.11

Figure 3.12 Possible co-localisation of plectin with the G58K Golgi-associated protein.

Double indirect immunofluorescence with monoclonal plectin (3.12 b, d, e &f), polyclonal vimentin (3.12 a & e), and rhodamine labelled phalloidin (3.12c) highlighted a concentrated reticular, juxta-nuclear body of plectin (depicted by arrows) similar to the staining pattern obtained using the G58K- Golgi-associated protein (3.12 h). Micrographs were taken using x100 magnification and the scalebar represents 10 μ m.

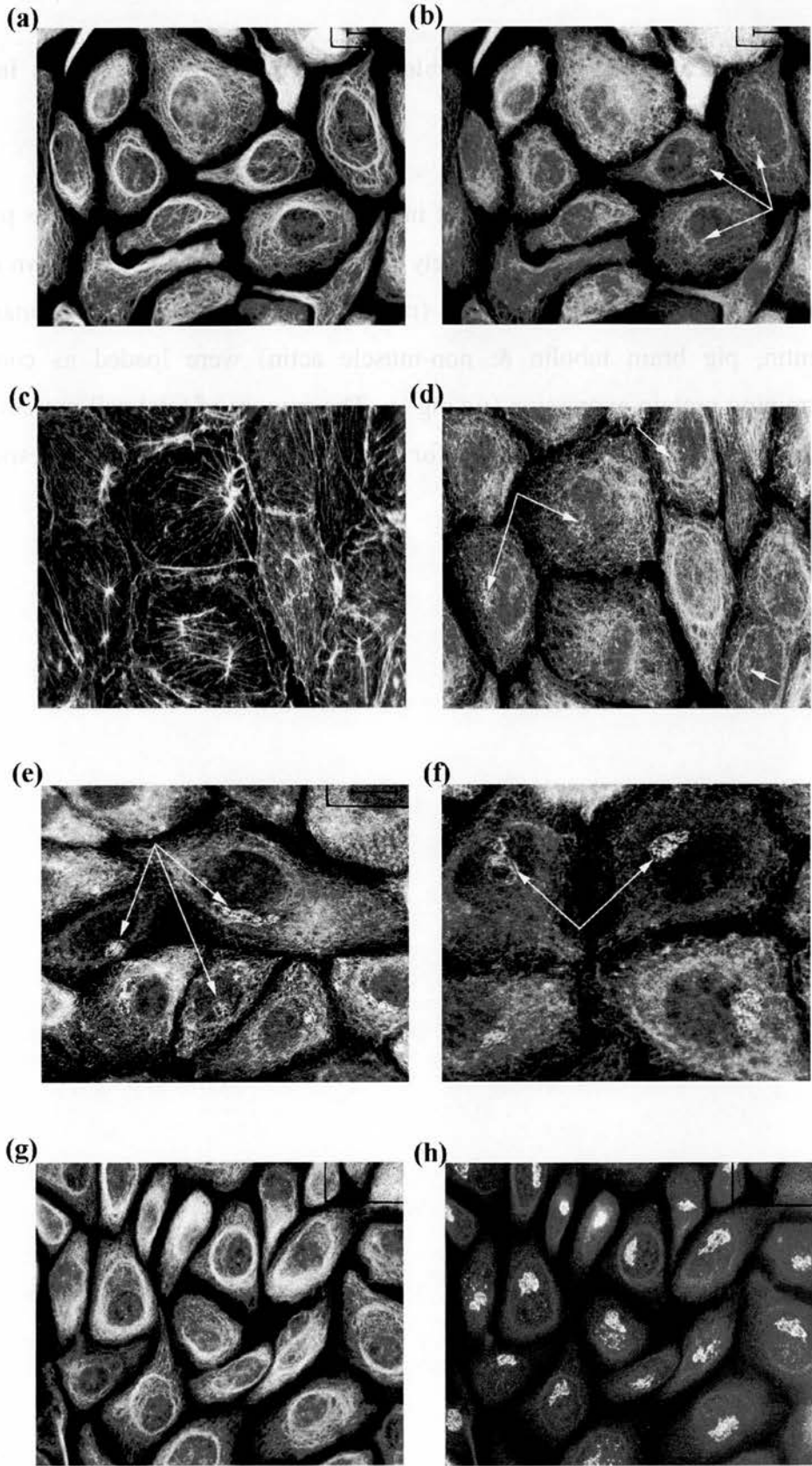


Figure 3.12

Figure 3.13 Examples of immunoblots used to determine changes in protein expression with time in culture.

Figure 3.13 (a-c) shows examples of immunoblots of whole cell lysates probed for vimentin, actin and tubulin respectively using cells which had been grown in culture for up to 21 days. Varying amounts (ng) of protein standards (recombinant human vimentin, pig brain tubulin & non-muscle actin) were loaded as controls for determining protein expression ($\mu\text{g}\cdot\text{mg}^{-1}$). The amount of total cell protein added to each gel well was $1\mu\text{g}$, $2\mu\text{g}$ and $3\mu\text{g}$ for the vimentin, actin and tubulin respectively.

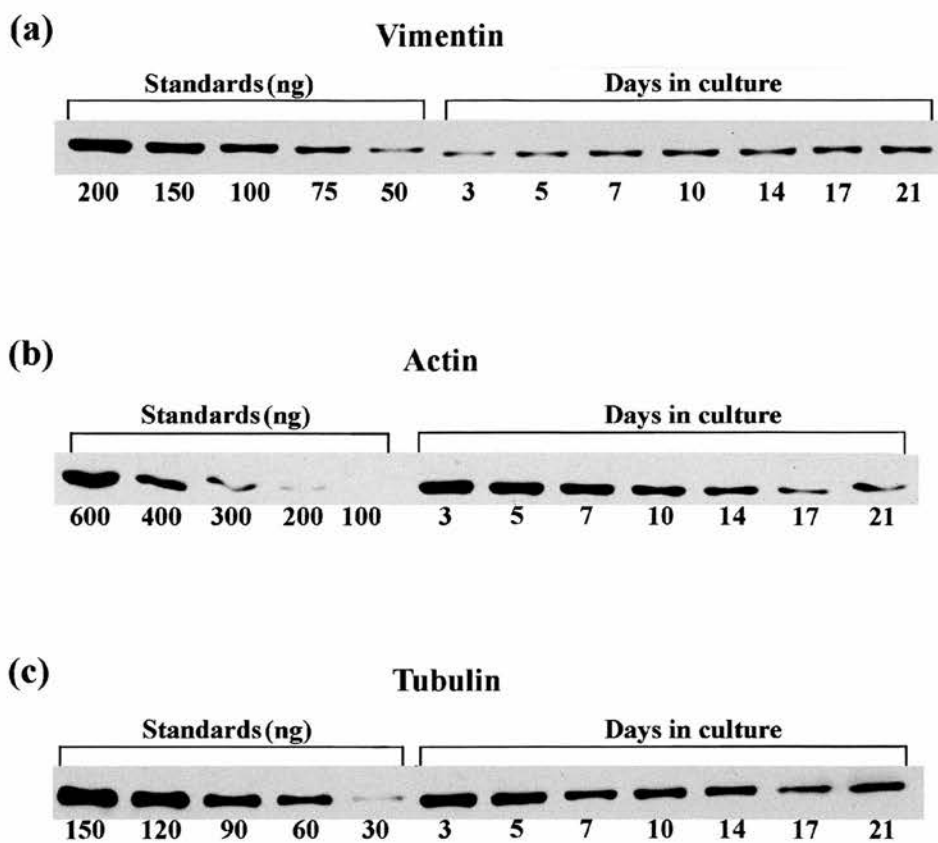
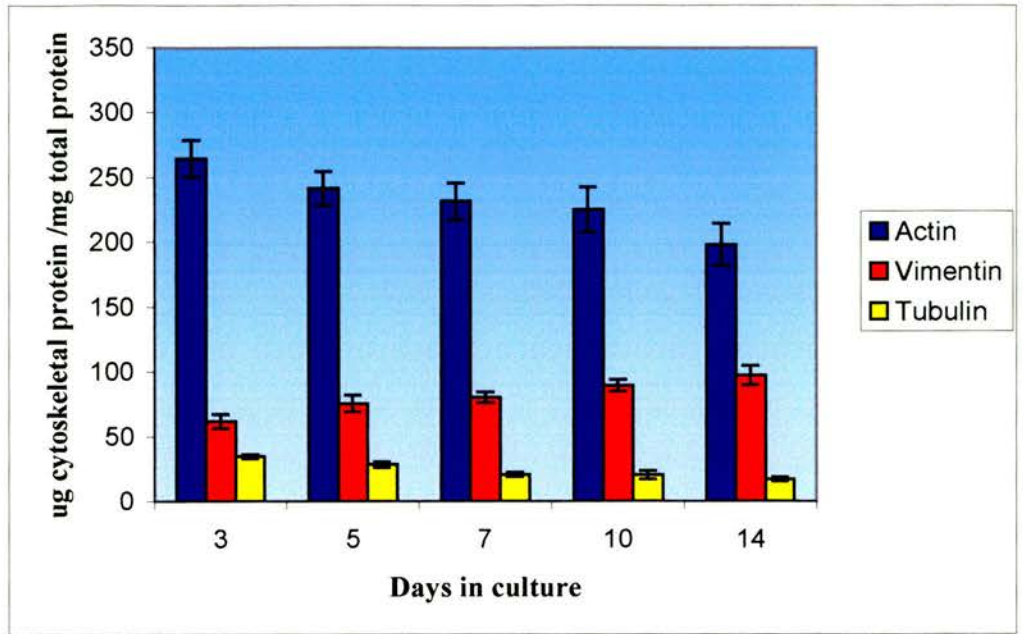


Figure 3.13

(a)



(b)

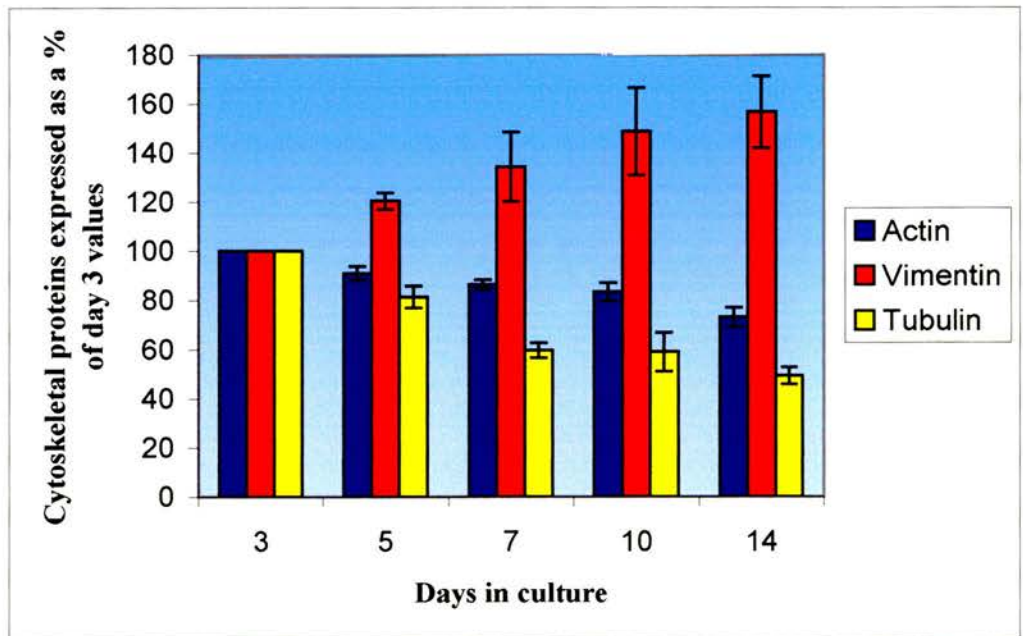
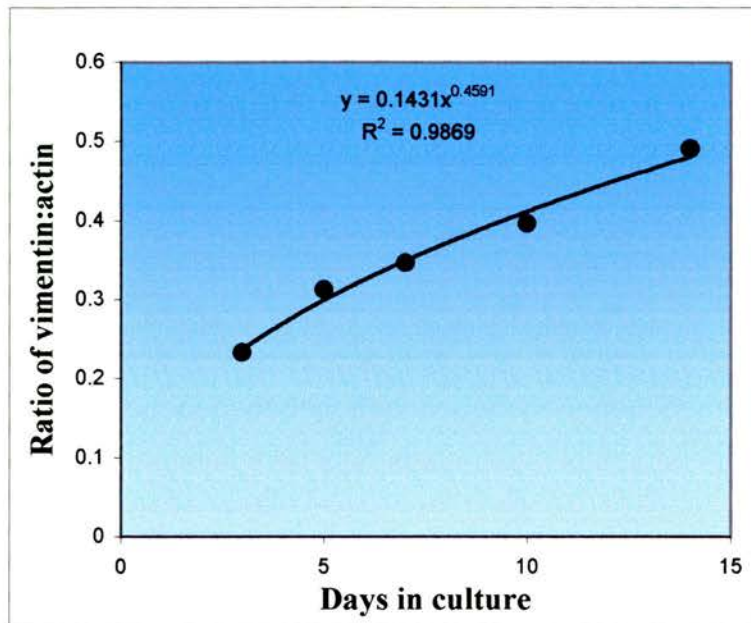


Figure 3.14 a & b. Changes in cytoskeletal proteins (actin, vimentin and tubulin) with time in culture. Figure (a) represents mean (\pm SEM; $n=14, 9$ & 7 respectively) changes in individual cytoskeletal protein concentrations, expressed as $\mu\text{g}/\text{mg}$ of total cell protein while figure (b) illustrates mean changes (\pm SEM) in actin, vimentin and tubulin expressed as a percentage of day 3 values. Actin and tubulin levels were seen to decrease while vimentin expression increased. These trends are most evident in figure 3.14b.

Chapter 3 – Morphology of intermediate filament networks in sub-confluent and confluent cells and related changes in cytoskeletal protein expression.

of vimentin, actin and tubulin ($\mu\text{g}\cdot\text{mg}^{-1}$ total cell protein \pm SEM) present in sub-confluent cultures (day 3) were estimated to be 61.67 \pm 5.32; 264.5 \pm 14.2 and 34.71 \pm 1.6 respectively (Figure 3.15 a, c & e). Overall, the amount of cytoskeletal protein expressed in relation to total cell protein decreased with time in culture, from 33.4% on day 3 to 24.1% between days 17-21 (not shown). This was due to significant down-regulation of both actin (Figure 3.15 d) and tubulin (Figure 3.15 f), while the expression of vimentin showed a modest increase (Figure 3.15 b). As a result of these changes, the *ratio* of vimentin *relative* to that of both actin and tubulin increased significantly (Figure 3.16 a & b), by 2.1 and 3.2 times respectively, after 14 days in culture.

(a)



(b)

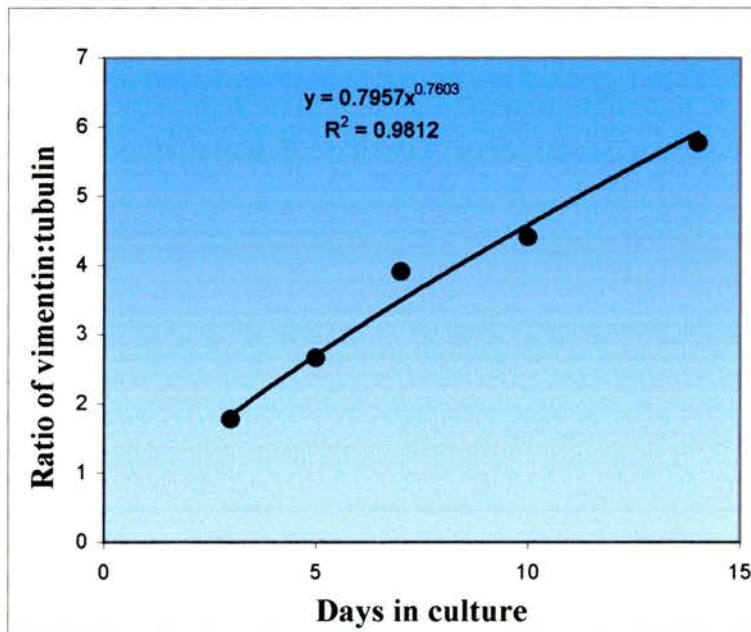


Figure 3.16 a&b Changes in the ratio of (a) vimentin: actin and (b) vimentin: tubulin with time in culture. Ratios were determined using the mean values (μg cytoskeletal protein. mg^{-1} total protein) for each time point. The vimentin:actin ratio (a) increased from 0.23 at day 3 to 0.49 at day 14. The ratio of vimentin:tubulin (b) increased from 1.78 to 5.77 between days 3 and 14.

3.8 Discussion

The results of this study show that the cellular distribution of intermediate filaments and the expression of vimentin both change with time in culture. In the growth phase, both the size and the shape of cells are highly variable: some are rounded up, either in preparation for mitosis or immediately afterwards, while others are actively migrating and/or spreading and forming attachments to the substrate. Confluent cells are generally much smaller and more uniformly shaped, giving rise to the ‘cobblestone’ appearance characteristic of well-established monolayers.

Sub-confluent cells contain a dense meshwork of unusually fine bundles of intermediate filaments, distributed more or less uniformly throughout the cytoplasm. This contrasts with the pattern in fully-confluent cells, where the network is dominated by a distinctive, thick band of intermediate filaments that completely surrounds the nucleus and also encloses both the Golgi body and MTOC. This perinuclear ring configuration was first described by Blose and his colleagues in a series of papers referred to earlier (Introduction 1.2.2.3). Phase lucent perinuclear rings that were strongly birefringent when viewed in polarised light and that stained positively for vimentin were first reported in primary cultures of guinea pig aorta and portal vein endothelial cells (Blose & Chacko, 1976). The rings were seen only in ‘older’ cultures (*ca* 10-14 days) and they were located in a plane parallel to the substratum. Perinuclear rings were also found in endothelial cells of fixed and sectioned guinea pig aorta and portal vein, confirming that they are a normal cytoskeletal component *in vivo* (Blose & Chacko, 1976). In a later study, Blose & Meltzer (1981) showed that over 70% of cells lining the thoracic aorta contained vimentin-positive rings and a similar proportion, between 60-80%, was found in primary cultures of guinea pig endothelial cells. Similar results were obtained in this study with more than 90% of BAEC exhibiting signs of a perinuclear ring after 10 days in culture.

Interestingly, the perinuclear ring does not disassemble prior to cell division, unlike microtubules and actin stress fibres, both of which undergo extensive disassembly and

reassembly during mitosis. Instead it persists throughout most of the cell cycle, only dividing into two, crescent-shaped halves in late telophase, during cytokinesis (Blose, 1979). During anaphase, the ring becomes somewhat elongated and encircles both the spindle apparatus and chromosomes. Treating dividing cells with cytochalasin B, to prevent cytokinesis, leaves the perinuclear ring intact, surrounding both daughter nuclei.

The results of the present study also suggest that the perinuclear ring is a relatively stable configuration. The coefficients of variation (SEM/mean x 100) of measurements of the area enclosed by the ring and the ring perimeter made over a 7 day period (day 14-21) are remarkably small (3.2% and 1.9%, respectively). This implies that the morphology of perinuclear ring changes little with time once it is fully-formed. The somewhat larger coefficient of variation in the measurement of perinuclear ring thickness (9.7%) may be due to the progressive addition of intermediate filaments to the ring with time.

The results presented here show that the increase in the frequency of occurrence of perinuclear rings is not directly related to the age of the culture. Instead, the number of cells containing a perinuclear ring only begins to increase at around the time the cell density reaches a maximum (*ca* day 5). Prior to this, cells with a fully differentiated perinuclear rings are encountered only sporadically. In other words, ring formation is cell density- rather than time-dependent. This suggests that activation of the signal pathway that is responsible for initiating the rearrangement of intermediate filaments probably depends upon establishing cell-cell contact.

Vimentin is a major protein component of endothelial cells. Immunoblots of cell extracts revealed a modest (*ca* 1.7 fold) up-regulation of vimentin expression with time in culture, within the range *ca* 6% (day 3) to *ca* 10% (day 14). These values are comparable to that obtained by Blose & Meltzer (1981), who estimate that vimentin accounts for *ca* 11% of total cell protein in cultured guinea pig endothelial cells. However, they contrast markedly with those of Savion *et al* (1982), who reported a 15-fold increase in the relative amount of vimentin expression in BAEC as cells reached

confluence. Schnittler *et al* (1998) reported that freshly isolated endothelial cells contained around 3-5 times less vimentin than cultured endothelial cells. The vimentin gene is known to be growth regulated and is transcriptionally activated by serum and by platelet derived growth factor (Ferrari *et al* 1986). Since the cells used in this study were grown in culture medium supplemented with 10% foetal calf serum, vimentin expression is likely to be higher under these conditions.

In contrast to vimentin, the quantities of actin and tubulin were found to decrease over the same time period, so that the relative amounts of vimentin:actin and vimentin:tubulin rose substantially (2-3 fold). Thus it appears likely that vimentin intermediate filaments play an increasingly important role in confluent monolayers of endothelial cells. This conclusion raises the question: *what might this role be?*

Although the perinuclear ring is a unique feature of endothelial cells, it is not found in all types of endothelial cells. Savion *et al* (1982) reported perinuclear rings in BAEC but not in foetal bovine heart endothelial cells. Human coronary and dermal microvascular cells were cultured for up to 21 days in the present study, but they did not form prominent perinuclear rings either. On the other hand, it has been reported that endothelial cells in the large vessels of several mammalian species contain a perinuclear ring. These include guinea pig aorta (Blose & Chacko, 1976; Blose & Meltzer, 1981), rat abdominal vein (Franke *et al*, 1978), human umbilical vein (Franke *et al*, 1979; Franke *et al*, 1979b), monkey aorta (Chalmley-Campbell *et al*, 1979), rabbit aorta (Campbell *et al*, 1979; Blose & Meltzer, 1981) and aortae of mouse and hamster (Blose & Melzter, 1981). These comparative studies could hold a clue as to the possible function of the perinuclear ring. Perinuclear rings are generally found in the endothelial cells of large vessels, ones that are exposed to relatively large, uniform wall shear stresses, but not in small vessels. This suggests that intermediate filaments might be involved in the response of cells to haemodynamic factors. There is evidence that transmural pressure and/or wall shear stress could play a role in regulating vimentin expression *in situ*. Schnittler *et al* (1998) showed that the vimentin content of arterial endothelial cells is 2-3 times higher than in endothelial cells of the inferior vena cava. Fluid shear stress and pressure are known to modify the structure and function of

cultured endothelial cells, and both parameters are significantly greater in arteries than veins. Schnittler *et al* (1998) also found that the vimentin content of endothelial cells increased 1.5 fold in a proximal to distal direction in pig aorta, from 2% in thoracic aorta to 3.5% in the abdominal aorta. Here again, one would expect shear stress to increase as the internal diameter of the aorta decreases.

The rearrangement of the vimentin network in confluent monolayers was accompanied by redistribution of the IFAP plectin. Plectin staining in sub-confluent cells appeared as a diffuse network emanating from a juxtannuclear body, accompanied by intensely staining 'streaks' distributed over the basal surface. The streaks of plectin co-localised with the tips of actin stress fibres and resembled the staining pattern obtained using antibodies to focal adhesion proteins. The association suggested that plectin may interact with focal attachment sites. A recent study by Gonzales *et al*, (2001) has shown this to be the case in human endothelial cells (see Chapter 5).

In contrast to the above pattern, rings of plectin were seen to co-localise with the vimentin perinuclear ring in confluent monolayers. A reticular body of intense plectin immunoreactivity was observed in the region of the Golgi apparatus. Unfortunately, this study failed to provide convincing evidence that plectin and the G58k Golgi protein were co-localised due to non-specific antibody binding. Recent work by Gao & Sztul (2001) has shown interaction of the Golgi complex with the vimentin intermediate filament network via the Golgi protein formiminotransferase cyclodeaminase (FTCD) which is now known to be identical to the 58K Golgi protein. FTCD associates with Golgi membranes and directly interacts with vimentin intermediate filaments, acting as a Golgi-intermediate filament linker protein and a potential new IFAP. Based on the staining pattern of plectin observed in this study, it would be interesting to determine whether plectin associates with FTCD and vimentin at these sites.

These observations provide circumstantial evidence to support the idea that vimentin intermediate filaments and their associated proteins provide structural support to

Chapter 3 – Morphology of intermediate filament networks in sub-confluent and confluent cells and related changes in cytoskeletal protein expression.

endothelial cells and enable them to resist the physical forces associated with flowing blood. It is conceivable that they might also play a role in the mechanotransduction of shear stress, perhaps functioning as sensors, responding to altered shear stress either by tilting or becoming deformed under flow. It was therefore decided to study the effects of laminar shear stress on the morphology of intermediate filament networks in both confluent and sub-confluent cells and these experiments are described in the next chapter.

CHAPTER 4

RESULTS PART II

FLOW INDUCED CYTOSKELETAL REMODELLING AND PROTEIN EXPRESSION.

4.1 Introduction

The perinuclear ring configuration of intermediate filaments that develops when cells form a well-packed monolayer appears to be unique to endothelial cells. Interestingly, the perinuclear ring is oriented in a plane that lies close to and parallel with the substrate, with bundles of intermediate filaments radiating out towards the cell surface and in towards the nuclear envelope. This configuration suggests that perinuclear rings could perhaps function as flow sensors, responding to altered shear forces either by tilting or becoming deformed in some way. The experiments described here were undertaken to monitor changes in the sub-cellular distribution of intermediate filaments and of actin stress fibres in cells that were grown under static conditions and then exposed to flow. Most of the experiments were performed on confluent monolayers in which the intermediate filaments were organised into a clearly-defined perinuclear ring. For comparative purposes, some experiments were also carried out on sub-confluent cells that lacked a perinuclear ring, or *newly* confluent cells that had not had sufficient time to develop a perinuclear ring. The design of the flow chambers and the experimental procedures used were described earlier (2.3.1 - 2.3.2.).

4.2 Changes in sub-cellular distribution of vimentin intermediate filaments and actin stress fibres in response to flow

BAEC were exposed to laminar shear stress of 15 dynes.cm⁻² for times ranging from 5 minutes – 16 hours. Cells were then fixed and immunostained (sections 2.2.1 - 2.2.2) using monoclonal antibodies to vimentin and fluorescent-labelled phalloidin.

4.2.1 Effects of flow on confluent cells with well-developed perinuclear ring

The response to flow of cells containing a well-developed perinuclear ring was found to be highly variable. Changes were visible in some cells within 30 minutes of

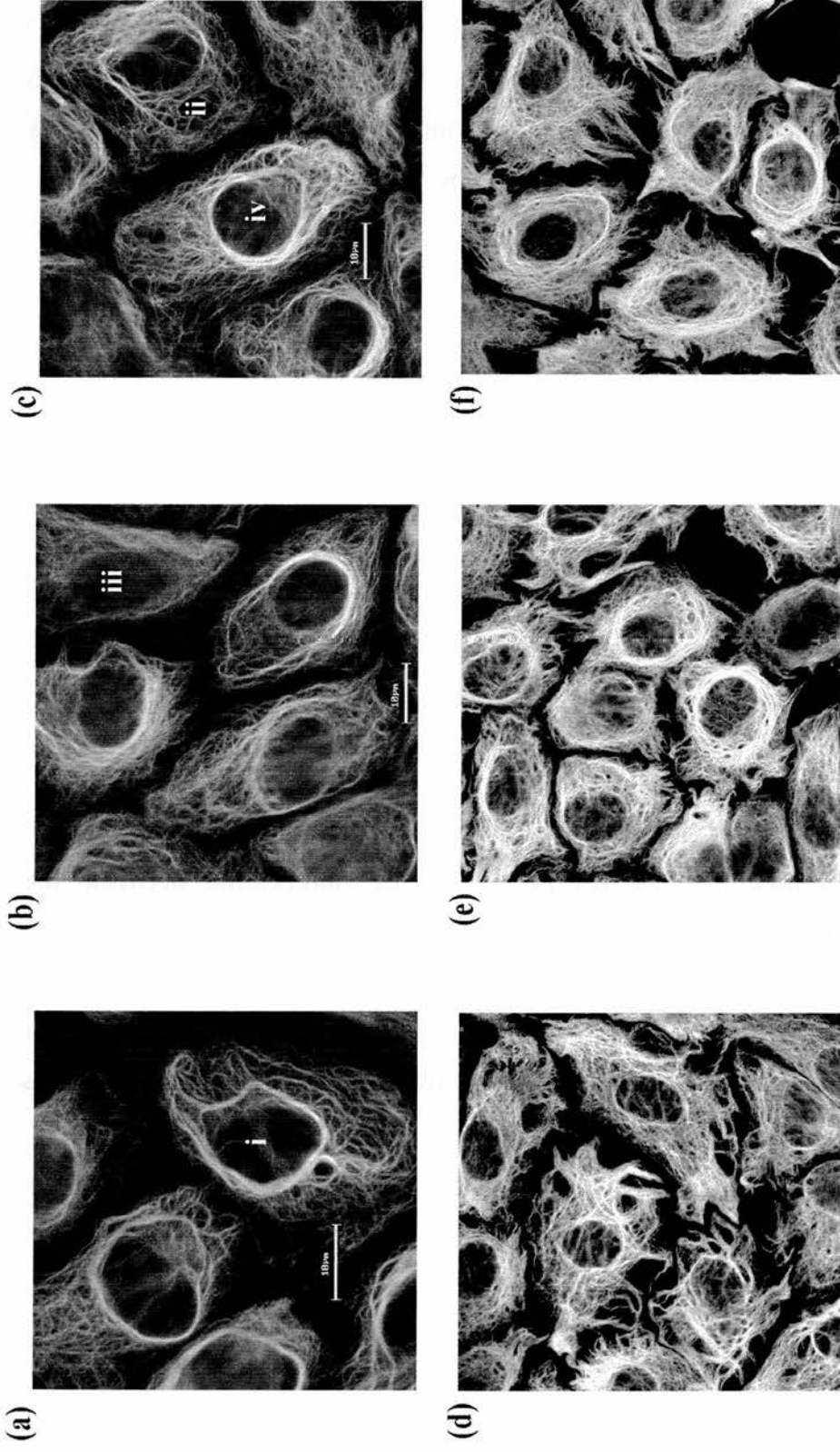
commencing flow (Figure 4.1 a-c). In these, the ring was seen to ‘buckle’ initially and in many instances this was accompanied by ‘fraying’ of the non-adherent segment. In other cells, the effect of flow was more pronounced and the perinuclear ring had dispersed completely by this time, whereas in contrast the perinuclear ring remained more or less intact in some cells after 30 minutes of flow. In monolayers that were exposed to flow for 4 hours, the bundles of intermediate filaments that make up the perinuclear ring became redistributed throughout the cytoplasmic network, often leaving only a small fragment of the adherent portion of the ring attached to the nuclear envelope (Figure 4.1 d-f). At this stage the cells took on a ‘flared’ appearance. After 4 hours the vimentin network appeared to have retracted further from the periphery than in unsheared cells. However, staining with phalloidin confirmed that cell-cell contacts containing actin stress fibres were retained (Figure 4.2). After 4-8 hours the remainder of the perinuclear ring disassembled, the cells became elongated and they began to align with the direction of flow. The elongation and re-alignment of cells was more complete in cells subjected to flow for 16 hours (not shown).

The work of Blose & Meltzer (1981) showed that perinuclear rings are found in endothelial cells *in vivo*: immunofluorescence studies revealed rings of intermediate filaments in endothelial cells of thoracic aortae from guinea-pig, mouse, rabbit and hamster. However, the experiments described above showed that the perinuclear ring rapidly disperses when cells grown under static culture conditions are suddenly subjected to moderate shear stress. This raises the question: *can perinuclear rings in cultured cells reassemble under conditions of sustained (chronic) flow?* The longest time period studied here was 16 hours and there was no evidence that perinuclear rings could reform on this time scale.

The experiments also identified structural connections between intermediate filaments and the nuclear envelope (Figure 4.3). These attachments were not visible in cells in static cultures, but presumably they were present and only became apparent when the intermediate filament network was under strain.

Figure 4.1 Effects of flow on the vimentin cytoskeleton of confluent monolayers of cells containing perinuclear rings.

Indirect immunofluorescence studies using a monoclonal antibody to vimentin illustrated the response of the intermediate filament network in confluent monolayers of cells subjected to 15 dynes.cm^{-2} of shear stress for 30 minutes (a-c) and 4 hours (d-f) respectively. Changes in the perinuclear ring structure were evident after 30 minutes exposure to flow, including buckling (i), fraying of the non-adherent segment (ii) and in some cases the ring had completely disassembled (iii). However, in some cells at this stage the perinuclear ring remained more or less intact (iv). By 4 hours (d-f), cells adopted a 'flared' appearance. In most cases the perinuclear ring had deteriorated further with more bundles of intermediate filaments being distributed throughout the cytoplasm.



Direction of flow

Figure 4.1

Figure 4.2 Actin cell-cell contacts remain after 4 hours of exposure to shear stress.

Indirect immunofluorescence studies using a monoclonal antibody to vimentin and rhodamine labeled phalloidin allowed comparison of the vimentin (a) and actin (b) networks in confluent cells exposed to 4 hours of shear stress. While the vimentin network does not extend to the cell periphery, actin staining of the same area reveals that cell-cell contacts are still present (indicated by *).

Figure 4.3 Exposure to flow reveals structural connections between the intermediate filament network and the nuclear envelope.

Figure 4.3 illustrates intermediate filament bundles associating with the nuclear envelope in a cell which had been subjected to flow for 4 hours. These connections are not visible under static conditions.

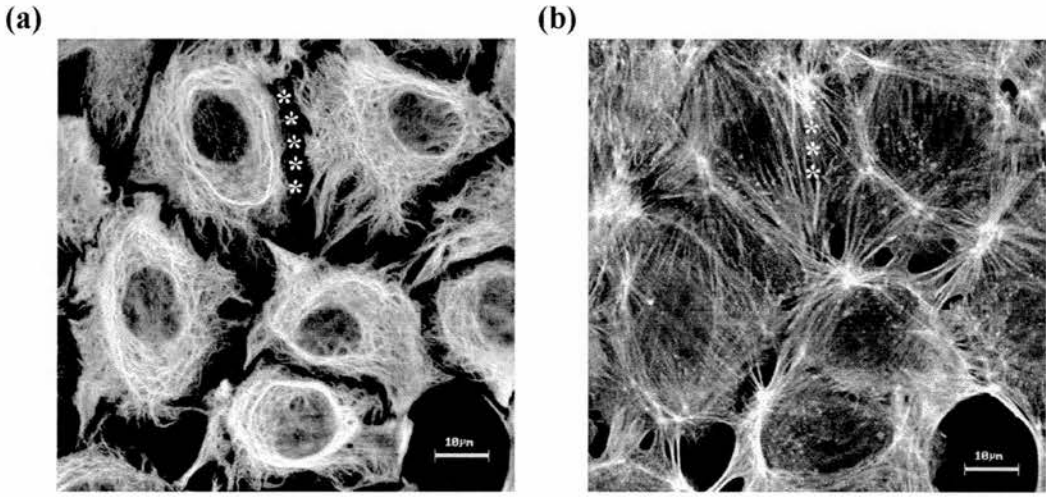


Figure 4.2

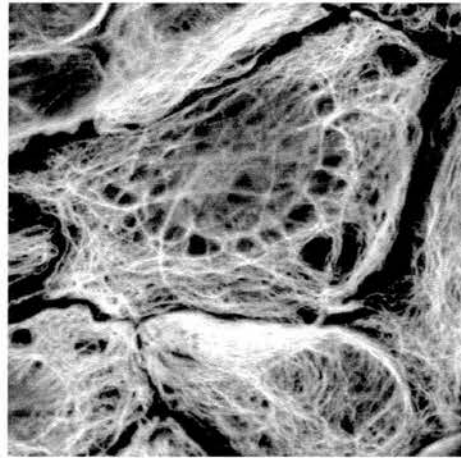
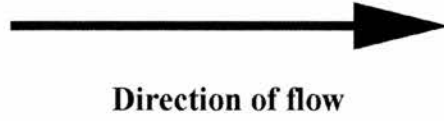


Figure 4.3

The response of the actin-based cytoskeleton to flow has been extensively studied (Wong *et al*, 1984; Franke *et al*, 1984; Levesque & Nerem, 1985; White & Fujiwara, 1986; Masuda & Fujiwara, 1993; Girard & Nerem, 1995; Satcher *et al*, 1997; Fujiwara *et al*, 1998; Kataoka *et al*, 1998). The results obtained here are largely in agreement with these earlier reports. The dense peripheral bands of actin in fully confluent cells disappear under flow and are gradually replaced with dense, parallel arrays of actin stress fibres similar to those seen in freshly plated, spreading cells but are more numerous. Stress fibres progressively align themselves in the direction of flow, a process that appears to commence on the luminal surface and only later affects the basal cell surface (Figure 4.4).

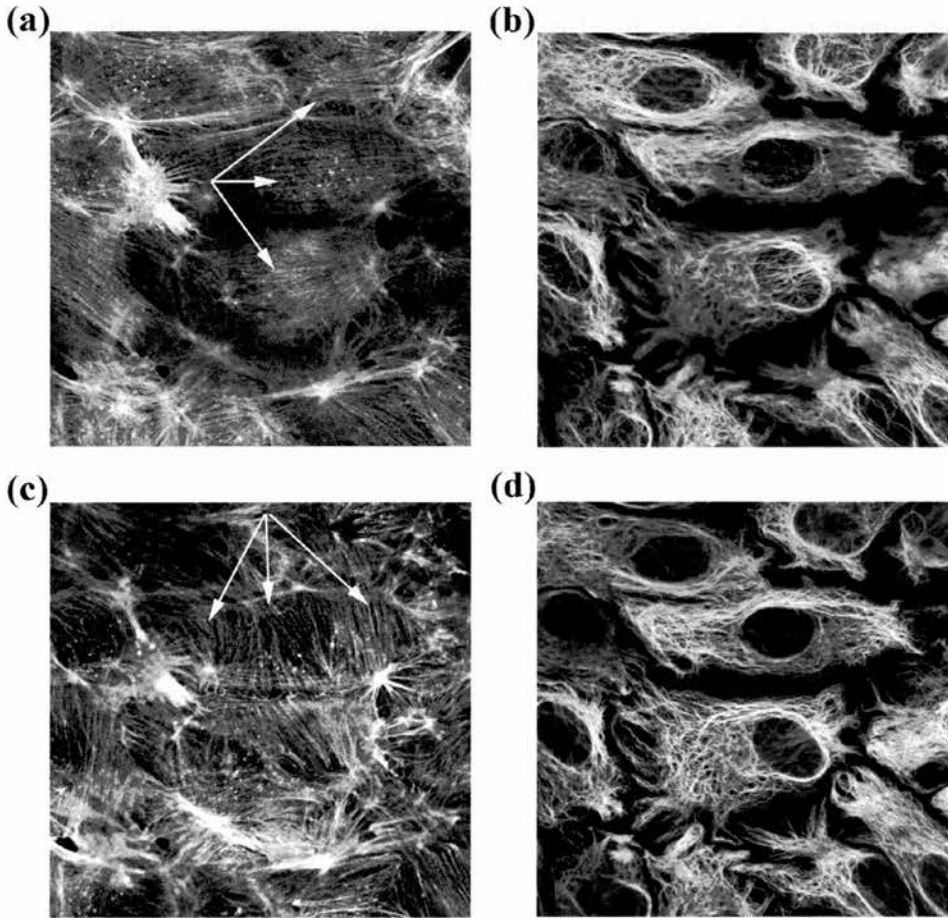
4.2.2. Effects of flow on distribution of intermediate filaments in sub-confluent or newly-confluent cells

The morphological boundary conditions are very different for sub-confluent cells and for cells that have recently become confluent, compared to well-established monolayers, since the former lack cell-cell contacts and they do not contain a perinuclear ring. Instead, fine bundles of intermediate filaments form an extensive 3D network that pervades the cell interior (Figure 3.3 & 4.5), extending from the nuclear envelope to the edge of the cell. Moreover, in some cells, larger bundles of intermediate filaments aggregate to form a multi-stranded band around the periphery, as illustrated earlier (Figure 3.6) and visible in Figure 4.5 a-d. Furthermore, cell-matrix contacts, in the form of discrete focal adhesions, are distributed differently in sub-confluent as compared to confluent monolayers of cells. This can be seen clearly, for example, in cells stained for phosphotyrosine using the PY20 antibody. Figure 3.11 shows that focal adhesions in sub-confluent cells are randomly dispersed over the basal cell surface, coinciding with the tips of actin stress fibres, whereas they become more concentrated around the circumference of the cell in confluent monolayers, corresponding with the position of dense peripheral bands of actin.

Figure 4.4 (a-d) Alignment of actin stress fibres in response to flow.

Figure 4.4 shows confluent monolayers of cells stained using a monoclonal antibody to vimentin and rhodamine labelled phalloidin. Figures 4.4 (a-d) are confocal images of the same region of cells illustrating the actin and vimentin networks near the luminal (a & b) and basal cell surfaces (c & d) after exposure to 4 hours of shear stress. Alignment of actin stress fibres with the direction of flow is seen on the luminal surface of the cell (a) but not at the basal surface (c). Here the stress fibres are aligned at right angles to those at the luminal surface. Figure 4.4b shows an example of the cage of vimentin intermediate filaments which surround the nucleus (*).

Luminal cell surface



Basal cell surface

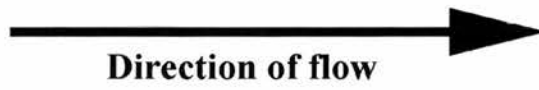


Figure 4.4

Figure 4.5 Effects of flow on the vimentin network of newly confluent cells.

Figure 4.5 (a-l) shows the IF network of newly confluent cells. Unsheared (control) cells (4.5 a-d) are compared to those sheared for 1 hour (4.5 e-h) and 2 hours (4.5 i-l) respectively. Circumferential bundles of IF can be seen in some unsheared cells (4.5 a-d) (arrows). After exposure to 1 hour of flow, these appear to be replaced by 'whorls' of vimentin (4.5 e-h), an effect which is more pronounced after 2 hours exposure to flow (4.5 i-l). Figures 4.5 j & k illustrate some cells beginning to show signs of elongation in the direction of flow after 2 hours of shearing.

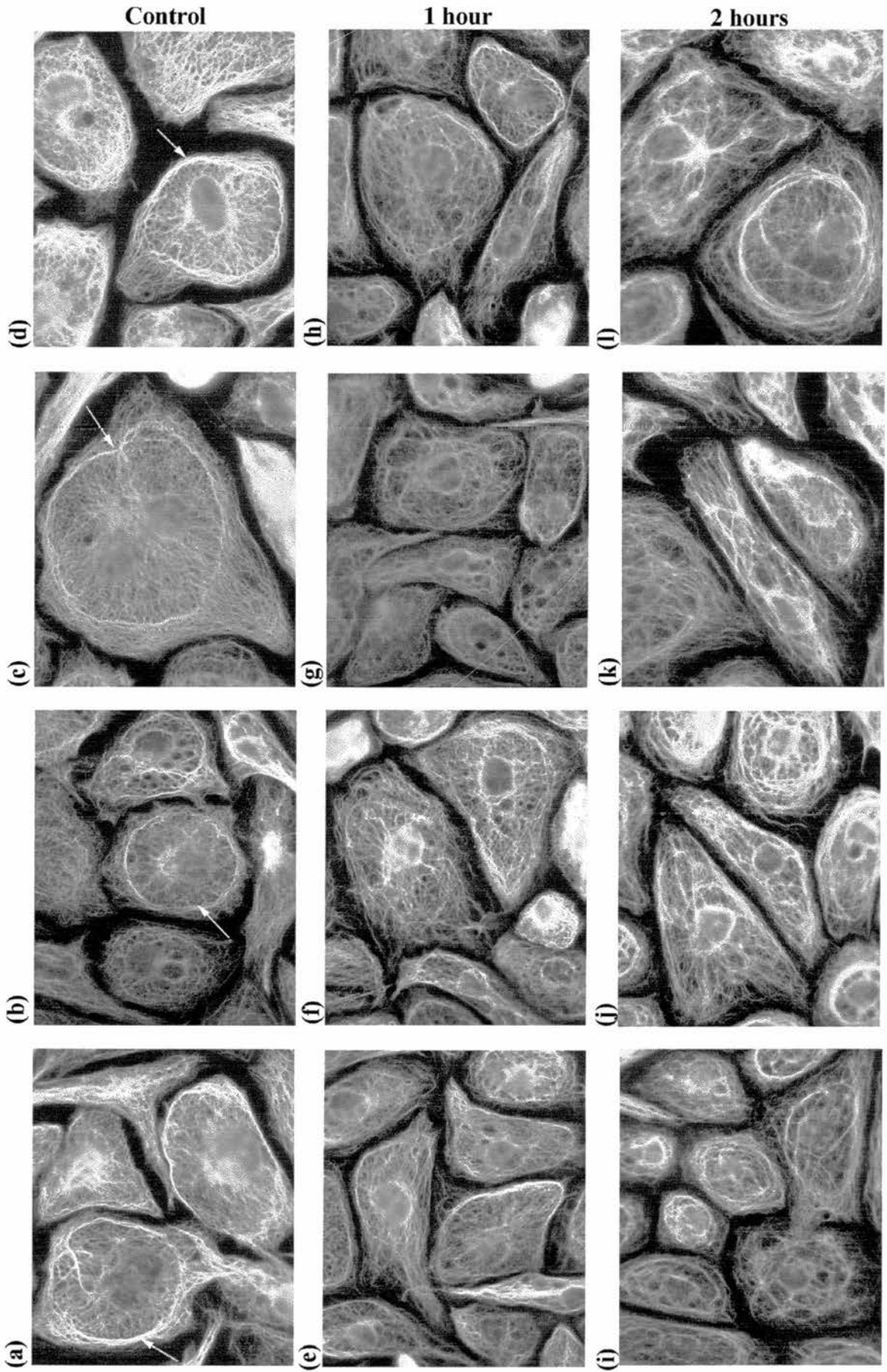


Figure 4.5

These structural differences mean that the mechanical stability of sub-confluent and confluent cells is not the same. It follows that the response to flow will be different from that seen in experiments using cell monolayers, described above.

Figure 4.5 shows a series of images of cells stained for vimentin. Figure 4.5 a-c show cells that were seeded onto glass coverslips and allowed to grow until they started to contact one another, after approximately 3-4 days. This was not sufficient time for perinuclear rings to develop, although cable-like bands of intermediate filaments had formed around the circumference in some cells. It was suggested earlier that these might represent an early stage in the formation of a perinuclear ring.

The distribution of intermediate filaments in newly-confluent monolayers was rapidly affected by flow. The earliest changes occurred within 30-60 minutes (Figure 4.5 e-h). The circumferential bands of intermediate filaments disappeared to be replaced by large ‘whorls’ or ‘loops’ of intermediate filaments which intersected with one another, forming prominent nodes. The formation of increased whorls of intermediate filaments is presumably due to a progressive unravelling of circumferential intermediate filaments. This pattern was more obvious in cells that had been sheared for 2 hours (Figure 4.5 i-l). The mesh size in cells after flow was considerably greater than in non-sheared cells, giving a ‘looser’ appearance to the intermediate filament network. Two hours under flow was sufficient to cause some cells to elongate and begin to align themselves in the direction of flow (Figure 4.5 j & k).

4.3 Effects of flow on the sub-cellular distribution of plectin

Flow also influenced the sub-cellular distribution of plectin. Streaks of plectin staining were scattered randomly over the basal cell surface in non-sheared cells. After shearing cells for 1-2 hours, plectin streaks were preferentially located around the periphery with a tendency to become aligned with the direction of flow (Figure 4.6). It was shown earlier (Chapter 3.6) that plectin co-localises with known components of focal adhesions

Figure 4.6 Effects of flow on the plectin distribution in newly confluent cells.

Figure 4.6 shows a sequence of images depicting changes in the distribution of vimentin (a, c & e) and plectin (b, d & f) under flow in newly confluent cells. Figure 4.6 a&b represents the distribution of vimentin and plectin respectively under static conditions. This is compared to its redistribution in cells exposed to flow for 1 hour (c & d) and 2 hours (e & f) respectively. The staining pattern of plectin becomes increasingly peripheral upon exposure to flow, a pattern resembling that seen with plectin and focal adhesion proteins in sub-confluent cells (Figure 3.10).

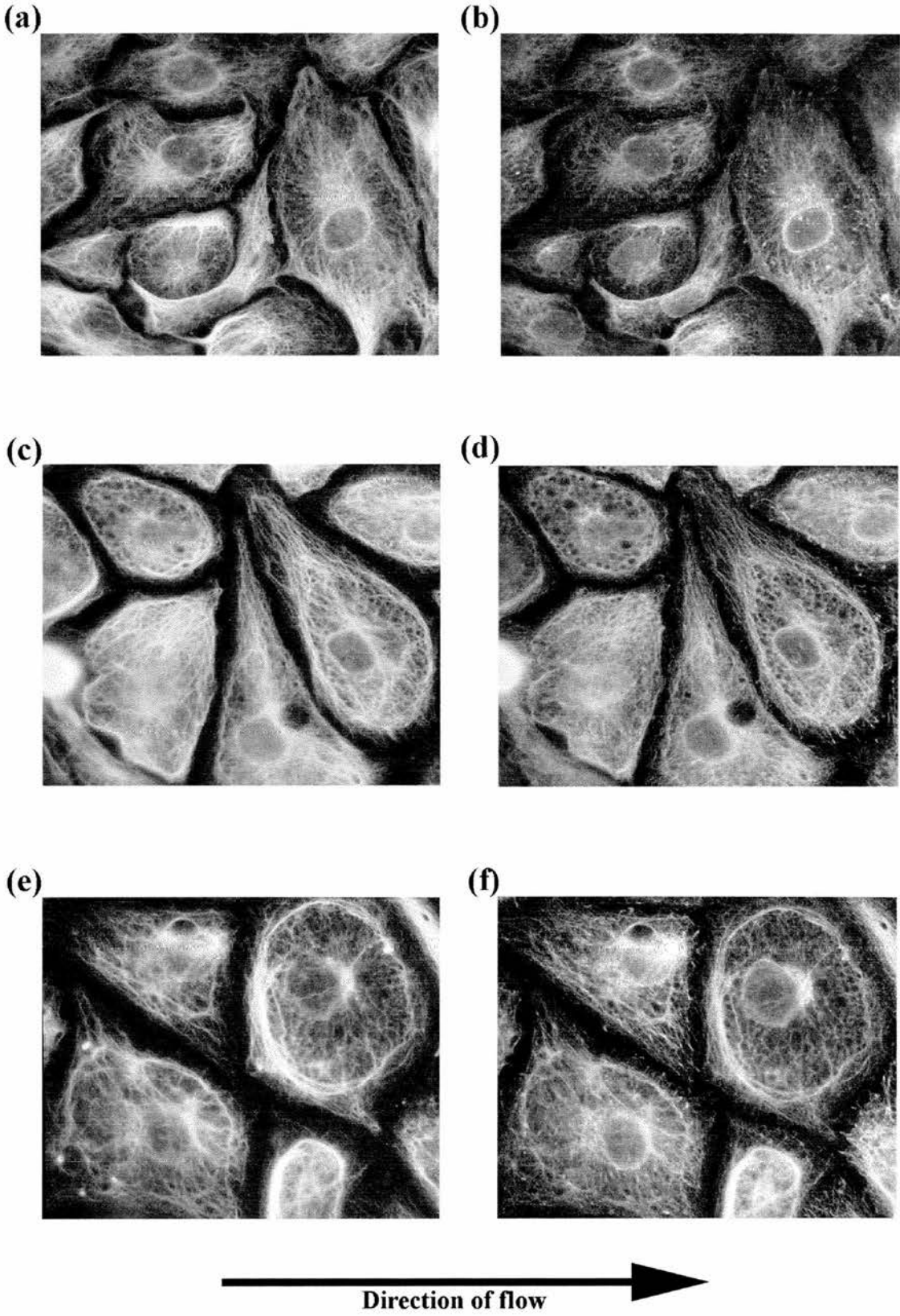


Figure 4.6

such as vinculin, paxillin and PY20. The altered pattern of staining after flow probably reflects changes in the distribution of focal adhesions.

4.4 Effects of flow on cytoskeletal protein expression

Whole cell lysates of sheared cells were prepared for biochemical analysis using semi-quantitative Western blotting (2.4.1 - 2.4.3 & Appendix 3). These experiments were undertaken to determine whether remodelling of the vimentin intermediate filaments and actin networks described above are caused by the redistribution of pre-existing protein, or whether protein expression is affected by flow. The effect of flow on the expression of tubulin was also studied. The relative amount of each protein was expressed as a percentage of the protein present in lysates from unsheared cells.

Examples of immunoblots of cells exposed to flow for between 5 minutes and 16 hours are shown in Figure 4.7. Scans of similar gels (n = 7-8 for each protein) were obtained and the results (mean +/- SEM) are shown graphically in Figure 4.8. Statistical analysis using a one way analysis of variance (ANOVA) showed there was no significant effect of flow on the expression of either of the proteins studied (Appendix 5).

Figure 4.7 Examples of immunoblots used to determine if cytoskeletal protein expression was altered by exposure to shear stress.

Figure 4.7 (a-c) immunoblots of whole cell lysates probed for vimentin actin and tubulin respectively. Protein expression in extracts from unsheared cells (C) were compared to those sheared at 15 dynes.cm^{-2} for up to 16 hours (960 minutes). Graphical results are shown in figure 4.8.

Confluent monolayers of cells at passage numbers 23, 18 and 17 respectively were analysed in figure 4.7 a-c. $1\mu\text{g}$ of protein/well was loaded in figures 4.7 a & b and $3\mu\text{g}$ /well was loaded in figure 4.7c.

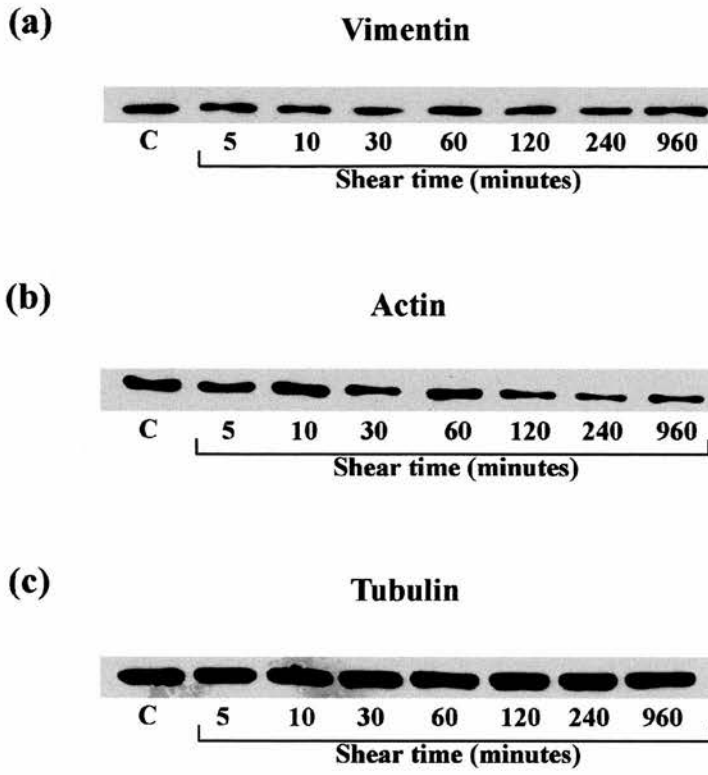


Figure 4.7

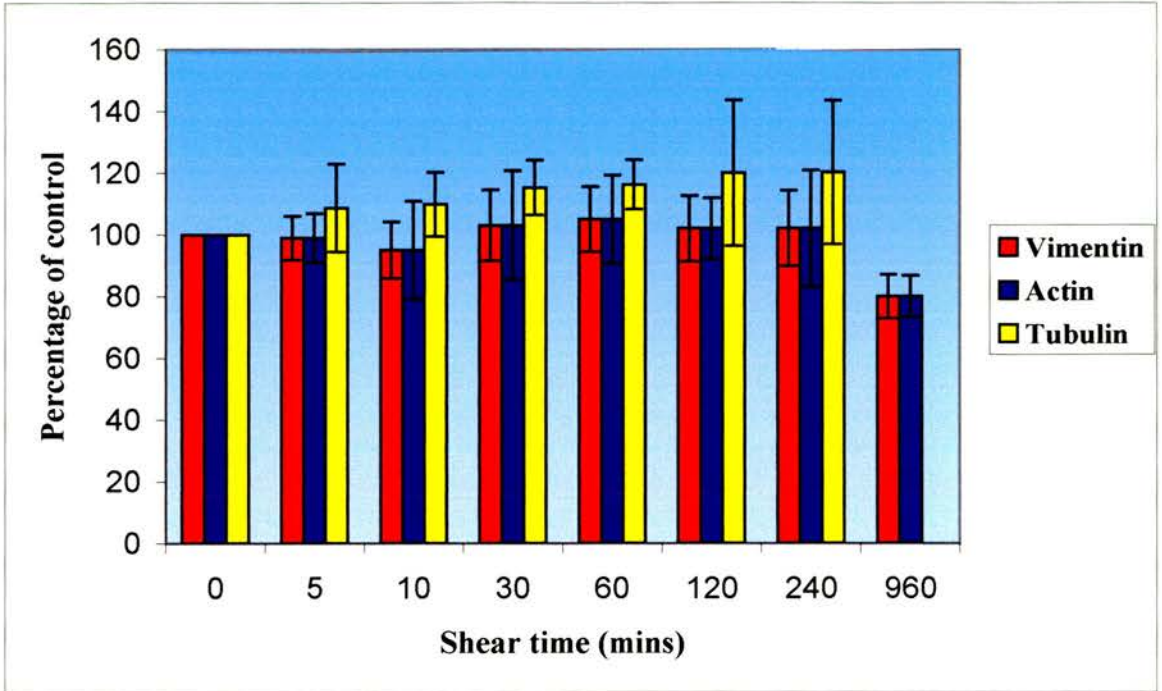


Figure 4.8. Changes in mean (\pm SEM) vimentin, actin and tubulin expression in BAEC upon exposure to 15 dynes.cm² FSS as determined by Western blotting. Results are expressed as a percentage of the control values (0 mins). One way ANOVA analysis (appendix 5) showed that for each protein $p > 0.1$ illustrating that there were no significant changes in cytoskeletal protein expression as a result of exposure to flow.

4.5 Discussion

Endothelial cells are uniquely sensitive to flow although the cellular mechanisms responsible for sensing and responding to shear stress remain uncertain. Some of the morphological changes include extensive remodelling of all three cytoskeletal networks, gross changes in cell shape and realignment of cells in the direction of flow (Davies, 1995).

The experiments described here show that sub-confluent cells respond to flow in a way that differs markedly from cells in tightly packed monolayers. It was argued earlier (Chapter 3) that the development of a perinuclear ring is initiated by the formation of cell-cell contacts, since the proportion of cells containing a perinuclear ring increased significantly only when cells became confluent (Figure 3.8). Endothelial cells lack desmosomes, but adherens-type cell-cell junctions are present in confluent cells and these would materially influence the mechanical properties of the monolayer and affect the way in which individual cells respond to flow. Sub-confluent cells appeared to respond more rapidly than confluent ones but it was difficult to be certain of this, because in both situations the response to flow was highly heterogeneous. This was especially evident when studying the effect of flow on confluent cells. Here, the perinuclear ring in some cells virtually disappeared altogether after only 30 minutes of flow, sometimes leaving just a small remnant of the adherent segment still attached to the nuclear membrane, while in other cells it appeared to be unaffected even after 4 hours (Figure 4.1). Likewise, in sub-confluent cultures the intermediate filament network in a proportion of the cells was dramatically altered after 1 hour, while in others the arrangement of intermediate filaments characteristic of cells in static culture (e.g. peripherally-disposed bands of intermediate filaments) remained largely unchanged.

The response of the actin cytoskeleton to flow was also highly variable. As previously described in the literature, the dense peripheral bands of actin disappear under flow, to be replaced by extensive arrays of linear stress fibres (Wong *et al*, 1984; Franke *et al*, 1984; Levesque & Nerem, 1985; White & Fujiwara, 1986; Masuda & Fujiwara, 1993;

Girard & Nerem, 1995; Satcher *et al*, 1997; Fujiwara *et al*, 1998; Kataoka *et al*, 1998). Phalloidin staining of well-established cell monolayers prior to flow showed what appeared to be a single dense peripheral band, shared between neighbouring cells (Figure 3.11f). After flow, vimentin intermediate filaments had retracted away from the cell periphery, creating the impression that cells were no longer in contact with one another (Figure 4.2a). However, well-defined actin-containing cytoplasmic connections could be seen (Figure 4.2b) between neighbouring cells and numerous fine stress fibres formed on the luminal surface. Interestingly, luminal stress fibres became aligned with the direction of flow more rapidly than those on the basal cell surface. This is evident in Figures 4.4 (a & c), which show the two sets of stress fibres arranged at right angles to one another after 4 hours under flow.

The flow chambers used in this study were carefully tested to ensure that they generated uniform laminar (2-D) shear stresses of known magnitude for a given flow rate. However, these tests were only able to measure the mean shear stress exerted on a uniformly flat surface, and did not take into account localised (i.e. cell-sized) variations in the surface topography of real cell monolayers. In reality, endothelial cells are ‘fried-egg’ shaped in profile, where the height of the cell is greatest above the nucleus. Barbee *et al* (1994; 1995) made atomic force microscopic measurements of living endothelial cells and calculated the spatial gradients of shear stress due to surface undulations. Their analysis showed a $\sim 6 \mu\text{m}$ range in cell surface height with a mean slope of around 11° . The relation between shear stress and cell height under uniform flow is a linear one (Satcher *et al*, 1992) and so gradients of shear stress are created on both uphill (positive) and downhill (negative) slopes. The calculations of Barbee *et al* (1995) showed that for a simulated shear stress of 12 dynes.cm^{-2} the actual shear stress on the steepest region of the cell would change at the rate of $\pm 4.7 \text{ dynes.cm}^{-2}.\mu\text{m}^{-1}$. Thus, if the steepest part of a cell were $2 \mu\text{m}$ long then the real shear stress would vary from $12\text{-}21 \text{ dynes.cm}^{-2}$. This degree of variability might well account for the heterogeneous response of cells to flow seen in the present experiments.

The results of Chapter 3 showed that the MTOC and the Golgi body are located within the non-adherent segment of the perinuclear ring. In static cultures, the area of cytoplasm enclosed by this portion of the ring is not oriented in any preferred direction. However, when sub-confluent cells (bovine carotid endothelial cells) are subjected to high rates of flow for up to 8 hours, generating shear stresses of $\sim 88 \text{ dynes.cm}^{-2}$, both structures migrate to a position upstream of the nucleus (Coan *et al*, 1993). Observations on endothelial cells *in vivo* (Rogers *et al*, 1985) also show that the MTOC and Golgi body are consistently located upstream of the nucleus (i.e. disposed towards the heart) in both arterial and venous endothelial cells. However, Coan *et al* (1993) showed that the localisation of the MTOC/Golgi became randomly orientated in cells exposed to flow for 24 hours. Work in this laboratory, using confluent monolayers and sub-confluent cultures, showed a similar upstream migration of the Golgi and MTOC in cells exposed to 15 or 50 dynes.cm^{-2} for periods of up to 16 hours (McDowell, 1998). Presumably, dispersion of the perinuclear ring under flow may be required for this to happen.

Vimentin interacts indirectly with actin stress fibres (Shah *et al*, 1998) and directly with the IFAP plectin (Goldman *et al*, 1986; Flitney *et al*, 1996; Svitkina *et al*, 1996). Double immunofluorescence shows that antibody to plectin co-localises with the intermediate filament network. However, the staining is clearly punctate, or beaded, rather than smooth and continuous like that of vimentin (Figure 3.10b). Moreover, the intensity of staining varies throughout the intermediate filament network, being greatest in the region closest to the nucleus, relatively weak in the surrounding region and then strong towards the cell periphery, where very intense 'streaks' are found distributed over the basal cell surface (Figure 3.10b). Exposure to flow leads to reorganisation of the intermediate filament network and hence to redistribution of plectin staining. The numbers of plectin 'streaks' and their size both increase, especially towards the cell periphery. These 'streaks' precisely co-localise with tips of actin stress fibres and vinculin, suggesting that they correspond with focal adhesion sites, and are much more prevalent than in monolayers of unsheared cells. Dynamic remodelling of focal adhesions was studied in living cells by Davies *et al* (1993; 1994), who monitored changes in both static cultures and in cells exposed to flow using tandem scanning

confocal microscopy. The remodelling process was essentially random in quiescent cells, but showed directionality under flow, where larger and fewer focal adhesions were ultimately formed, although the total contact area between the basal cell surface and the glass substrate did not change. Realignment of focal adhesions in the direction of flow was described by Girard & Nerem (1993; 1995), who found that vinculin and integrins were more prevalent on the upstream edge of the cell.

Immunoblots of whole cell extracts showed that the ratios of vimentin:actin and vimentin:tubulin increase with time in culture (Figures 3.13 & 3.14), suggesting that vimentin plays an increasingly important role in maintaining the structural integrity of the cell. The results described here show that sub-confluent (i.e. 'younger') cells generally respond to flow more rapidly than confluent ('older') ones, a difference that might be due to increased cell-cell contact in older cultures. However, it is also possible that the greater proportion of vimentin relative to the other two proteins might contribute to the improved stability of older cells. Whatever the reason for the relative increase in vimentin with time in culture, it is clear that exposing confluent cells to flow did not alter the expression of tubulin, actin or vimentin, even though the morphology of all three components changed dramatically. It follows that restructuring of the cytoskeleton under flow is most likely due to the redistribution of existing protein, a process that may involve the disassembly and reassembly of protein polymers by post-translational modification (e.g. phosphorylation and dephosphorylation).

It was reported recently (Gonzales *et al*, 2001) that plectin is an integral component of focal adhesions in endothelial cells and that it may serve to anchor both actin stress fibres and vimentin intermediate filaments to the cytoplasmic face. Electron microscopic studies (Flitney, personal communication) show that individual intermediate filaments are intricately interwoven with actin microfilaments at focal adhesions, confirming a close relationship between the two components. Since remodelling of the actin cytoskeleton occurs on a time scale comparable to that of the vimentin network, and the two proteins appear to be structurally connected at focal adhesions, it is possible that active interaction between actin and myosin may cause contraction of stress fibres and so passively 'pull' intermediate filaments into their new

position (Flitney *et al*, 1995). An hypothesis concerning the possible role of focal adhesions and their association with vimentin intermediate filaments and plectin in the mechanotransduction of flow is considered in the next Chapter.

CHAPTER 5

RESULTS PART I

VIMENTIN-ASSOCIATED MATRIX ADHESIONS AND FLOW-DEPENDENT ENDOTHELIAL GENE TRANSCRIPTION: AN OVERVIEW.

5.1 Introduction

Shear stress is a major determinant of EC phenotype (Davies, 1995; McCormick *et al*, 2001; Garcia-Cardena *et al*, 2001). Flow activates multiple intracellular signalling cascades (Jalali *et al*, 1998; Tseng *et al*, 1995; Berk *et al*, 1995; Ishida *et al*, 1996; Yan *et al*, 1999), whose downstream targets include several inducible nuclear transcription factors (e.g. c-myc, c-fos, c-jun, Egr-1, AP-1, SP-1 and NF- κ B) that are responsible for regulating endothelial gene expression (Resnick *et al*, 1993; Braddock *et al*, 1998; Chien & Shyy, 1998; Bhullar *et al.*, 1998; Khachigian *et al.*, 1995; Lan *et al.*, 1994; Shyy *et al.*, 1995; Nagel *et al*, 1999). There is growing evidence to implicate the NF- κ B/Rel family of transcription factors (May & Ghosh, 1998) in atherosclerosis (de Martin *et al*, 2000). NF- κ B is active in advanced atherosclerotic lesions (Brand *et al*, 1996), where many of the genes that are expressed are NF- κ B-dependent (Collins, 1993), but not in regions of the vasculature that are free of disease yet considered at high risk of developing atheroma in the future. Here, the steady-state levels of some NF- κ B signalling elements (e.g. RelA, I κ B α , I κ B β) are substantially up-regulated (Hajra *et al*, 2000). Endothelial genes that are known to be regulated by NF- κ B include; vascular cell adhesion molecule 1 (VCAM-1), intercellular adhesion molecule 1 (ICAM-1), transforming growth factor- β (TGF- β), E-selectin, several interleukins (IL-1, 6 & 8), tissue factor (TF), plasminogen activator inhibitor-1 (PAI-1), monocyte chemoattractant molecule-1 (MCP-1), inducible and endothelial nitric oxide synthases (iNOS and eNOS) and cyclooxygenase 2 (COX-2).

5.2 Flow-induced activation of NF- κ B

Lan *et al* (1994) showed that unidirectional shear stress rapidly activates NF- κ B in bovine endothelial cells. Resnick *et al* (1993) identified a cis-acting shear stress responsive element (SSRE) in the promoter of the flow-sensitive PDGF-B chain gene and then later (Resnick *et al*, 1997) showed that this acts as a non-consensus binding

site for NF- κ B. The core binding sequence of the SSRE (GAGACC) was discovered in several other genes that were known to be regulated by flow (e.g. tPA, ICAM-1, TGF β , c-fos, c-jun, MCP-1); furthermore, insertion of the SSRE into the promoters of several flow-insensitive genes rendered them inducible by flow (Resnick & Gimbrone, 1995).

5.3 Flow-induced activation of NF- κ B involves the $\alpha_v\beta_3$ integrin

Some elements of the signal pathway involved in the activation of NF- κ B by flow were identified by Bhullar *et al* (1998) using bovine cells. These authors showed that activation of two upstream kinases, called IKK1 and 2, and proteolysis of NF- κ B inhibitor proteins (I κ B), are essential steps in the process. They further demonstrated that induction of NF- κ B-dependent gene transcription by shear stress can be inhibited by pre-treating cells with a blocking antibody (LM609) to the $\alpha_v\beta_3$ integrin. This last observation is of considerable interest since recent experiments with human endothelial cells (Gonzales *et al*, 2001) have shown that this particular integrin plays an essential role in mediating their attachment to the substrate through an unusual type of focal adhesion.

5.4 Vimentin-associated matrix adhesions (VMA)

The prototypical focal adhesion connects actin stress fibres to protein ligands of the extracellular matrix via a large family of integrins. Flitney *et al* (1996) described an unusual type of focal adhesion on bovine aortic endothelial cells that served as a dual anchorage for both actin stress fibres and vimentin intermediate filaments. Furthermore, plectin was found to co-localise with the tips of actin stress fibres, with fine terminals of intermediate filaments and also with known protein components of focal adhesions (including vinculin, talin, paxillin and FAK). The molecular composition of this so-called vimentin-associated matrix adhesion (or VMA) was described in detail some years later (Gonzales *et al*, 2001). VMA were found on

both human microvascular and transformed human bone marrow endothelial cells. The integrin was identified as the $\alpha_v\beta_3$ heterodimer and its extracellular domain was shown to interact with the α_4 G sub- unit of laminin.

This type of cell-matrix interaction has now been identified on HUVEC. Figures 5.1-5.4 show a series of double immunofluorescence images to illustrate its structure, courtesy of Dr F.W. Flitney. These images were taken with the confocal microscope focussed on the basal cell surface, showing the distribution of vimentin intermediate filaments and actin stress fibres in relation to focal adhesion proteins (i.e. talin and vinculin), to plectin and to the β_3 sub-unit of the $\alpha_v\beta_3$ integrin. Figure 5.1 shows the distribution of talin and vinculin with vimentin and actin, respectively. It is clear that actin stress fibres and vimentin intermediate filaments are closely associated with focal adhesions, but the nature of their association is strikingly different. Whereas each end of an actin stress fibres invariably terminates on a *single* focal adhesion (Figure 5.1b and Figure 5.3b), the vimentin filaments appear to ‘wrap’ around focal adhesions and, more importantly, to interconnect neighbouring focal adhesions. This arrangement suggests that intermediate filaments may play an integrative role in the functioning of focal adhesions. Staining for plectin is also concentrated at focal adhesions (Figure 5.4a). Plectin is a highly versatile, cytoskeletal ‘linker’ protein with binding sites for both actin and vimentin (Seifert *et al*, 1992; Svitkina *et al*, 1998; Wiche, 1998), consistent with a role for this protein in attaching stress fibres and intermediate filaments to the cytoplasmic face of focal adhesions, as suggested in Figure 5.5.

The distribution of the β_3 integrin sub-unit in relation to vimentin and actin is shown in Figure 5.3, and in relation to plectin and vinculin in Figure 5.4. Gonzales *et al* (2001) showed that this staining pattern coincided with that obtained using an antibody (2A3) to the α_4 sub-unit of laminin. The $\alpha_v\beta_3$ integrin therefore lies at the core of the VMA. Importantly, over 70% of focal adhesions on bovine and human endothelial cells were of the VMA-type in well-spread cells. It follows that the work of Davies and his colleagues on the dynamics of focal adhesions under flow, referred to in the previous Chapter, most likely refers to restructuring of VMA-type attachments.

Figure 5.1 Comparison of the vimentin intermediate filament and actin stress fibres networks with the distribution of the focal adhesion proteins talin and vinculin.

Figure 5.1a shows double indirect immunofluorescence using antibodies against the focal adhesion protein talin (i) and vimentin (iii). Figure 5.1a (iv) is an overlay of the 2 fluorescent images. Vimentin (green) can be seen to associate with talin (red) at some (arrows) but not all (*) matrix-adhesion sites. A phase contrast image (5.1a(ii)) shows actin stress fibres which associate with talin at adhesion sites. Arrows on images (i-iv) represent regions where talin, vimentin and actin co-localise. Scalebar represents 10 μ m.

Figure 5.1b shows the distribution of vinculin (i) and actin (ii). An overlay of the two images (iii) shows interaction of vinculin with the tips of actin stress fibres. (arrows). The arrows present on each image represent areas of co-localisation. The scale bar represents 10 μ m.

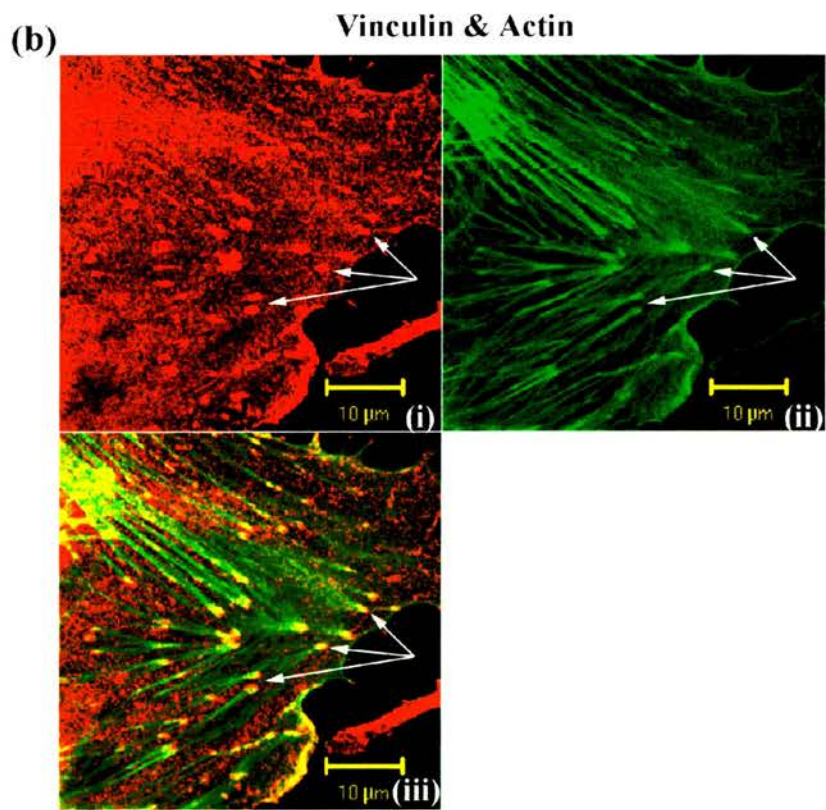
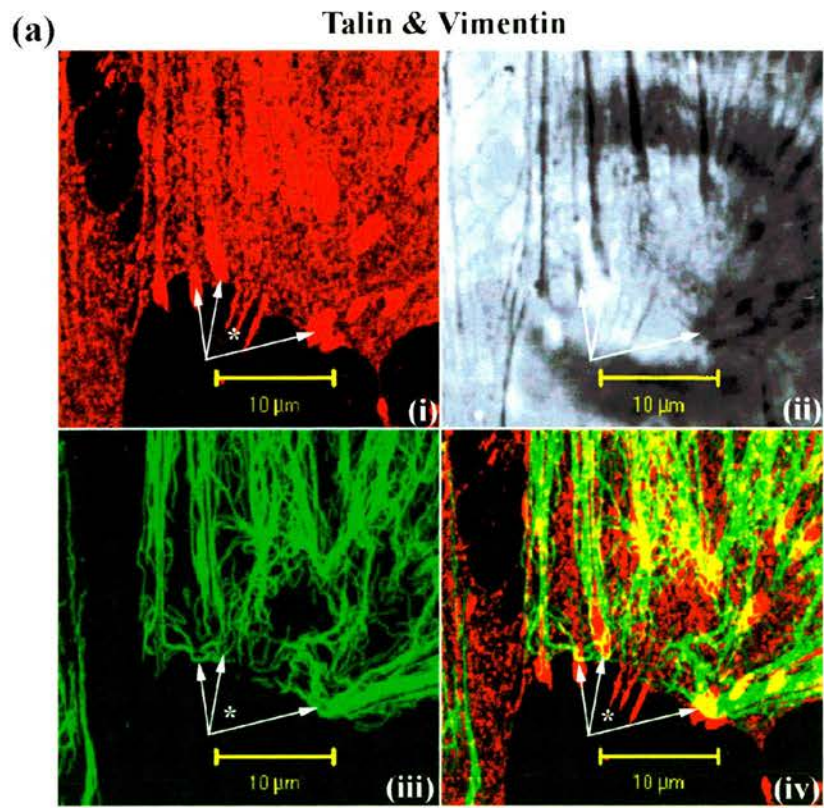


Figure 5.1

Figure 5.2 Comparison of the vimentin IF network with actin SF and plectin distribution.

Figure 5.2a shows the distribution of actin (i) and vimentin (iii). From an overlay image (iv) vimentin appears to have an association with some but not all actin SF. The IF appear to wrap round rather than terminate at the SF. A selection of regions exhibiting actin and vimentin interaction are represented by arrows. The scale bar represents 10 μ m.

Figure 5.2b shows the distribution of plectin (i) and vimentin (iii). From the overlay image (iv), colocalisation of the two networks is visible although plectin (red) extends much further towards the periphery than the vimentin network (green). The scale bar represents 5 μ m.

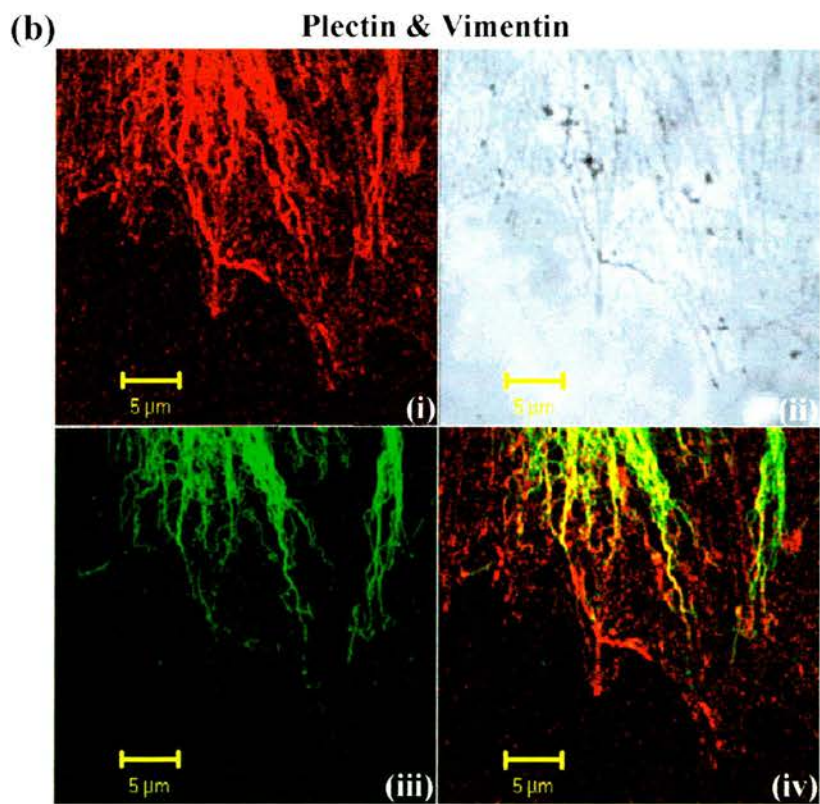
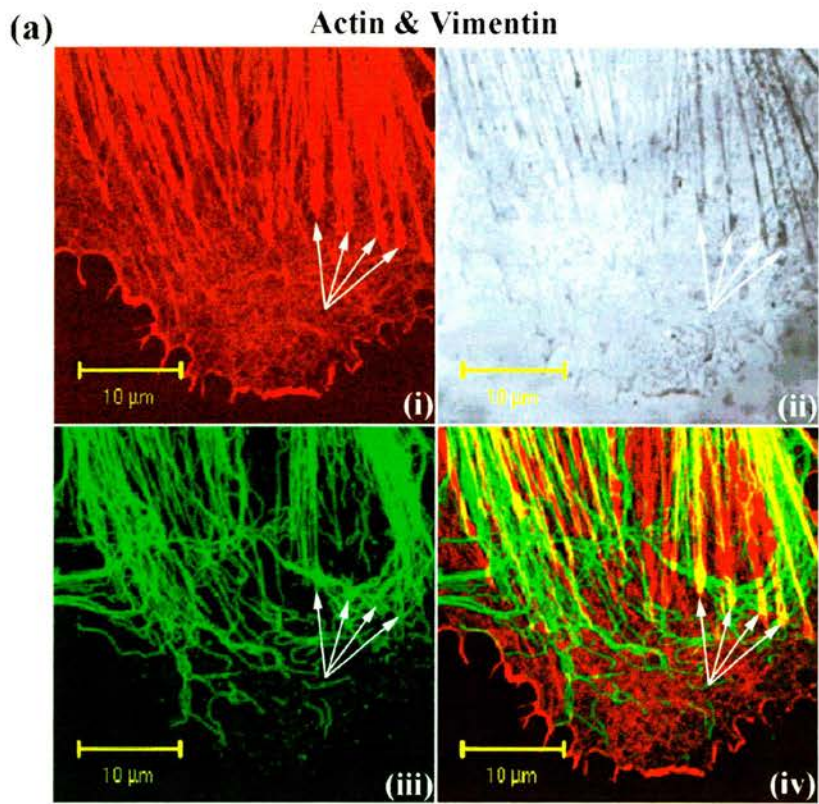


Figure 5.2

Figure 5.3 Comparison of the vimentin IF and actin SF networks with the distribution of β_3 integrin.

Figure 5.3a shows double indirect immunofluorescence using antibodies against β_3 integrin (i) and vimentin (ii). An overlay image (iii) shows that the vimentin IF associate with some of the integrin focal contacts (\leftrightarrow) but not others (*). There is no co-localisation of integrin and vimentin at the edge of the cell as the vimentin network does not appear to extend to the periphery. The scale bar represents 5 μ m.

Figure 5.3b shows the distribution of β_3 integrin (i) and actin (ii). An overlay image (iii) shows that the tips of actin SF colocalise with the majority of integrin clusters (a sample highlighted by \leftrightarrow). Associations between circumferential actin and β_3 integrin is also apparent at the edge of the cell. The scale bar represents 10 μ m.

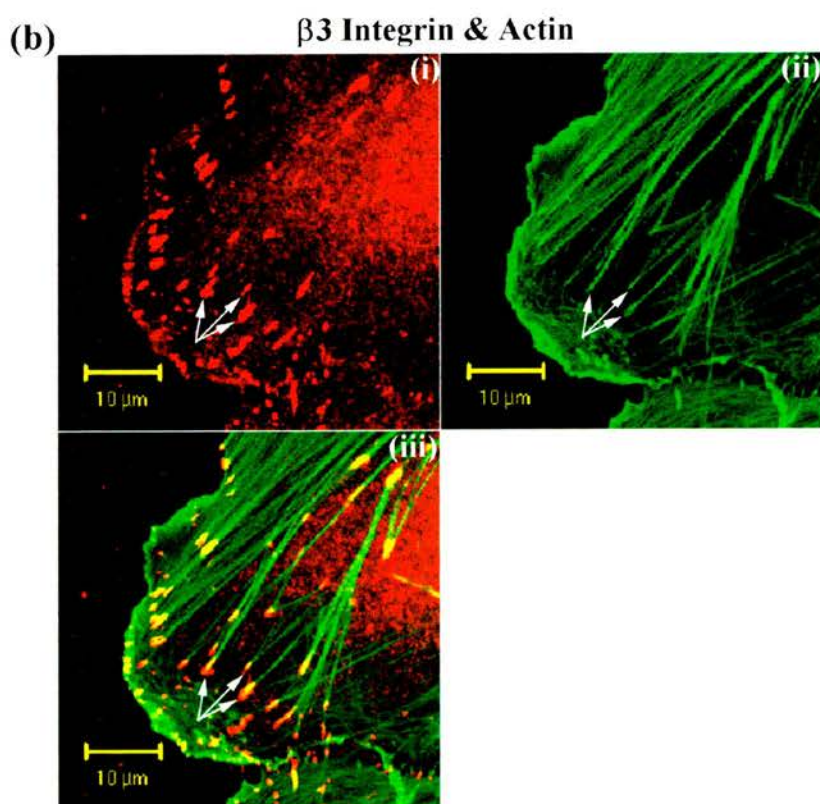
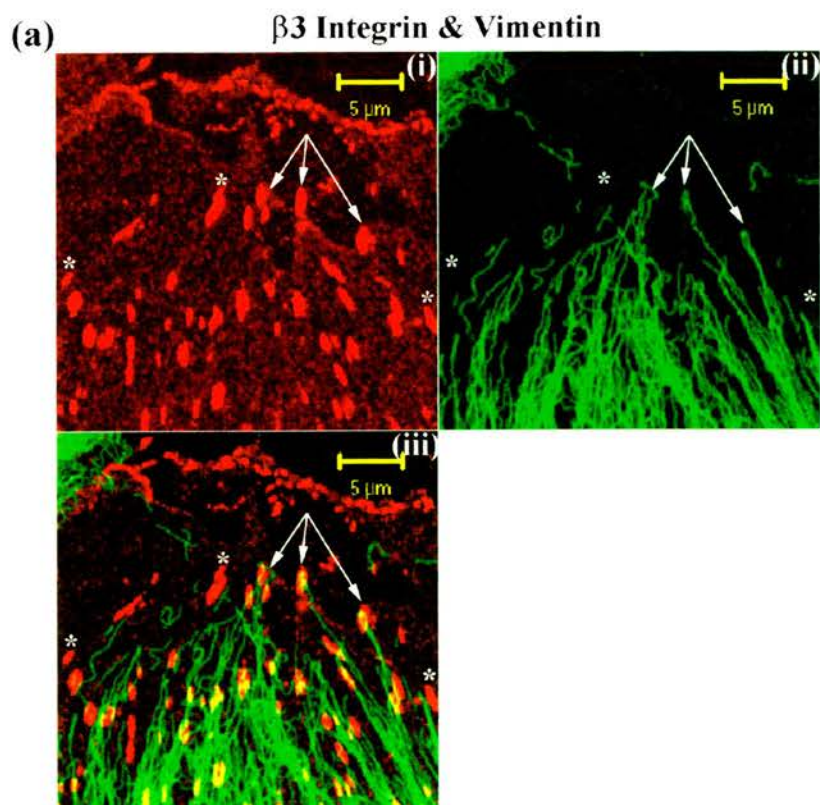


Figure 5.3

Figure 5.4 Comparison of plectin and vinculin distribution with that of the β_3 integrin.

Figure 5.4a shows double indirect immunofluorescence using antibodies against β_3 integrin (i) and plectin (ii). The overlay image (iv) show association of plectin with the sites of concentrated integrin staining (represented by *). The majority of this co-localisation occurs away from the cell periphery. The scalebar represents 5 μ m.

Figure 5.4b illustrated double indirect immunofluorescence using antibodies against β_3 integrin (i) and vinculin (ii). The overlay image (iii) shows almost complete co-localisation of the two proteins at the focal contact sites, predominantly at the cell periphery. The scale bar represents 20 μ m.

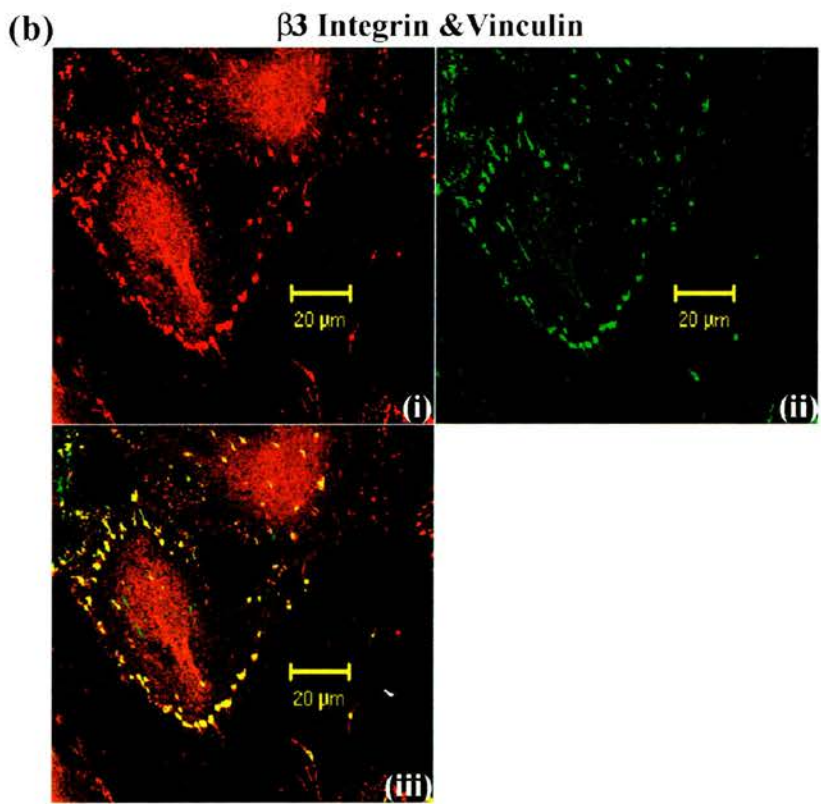
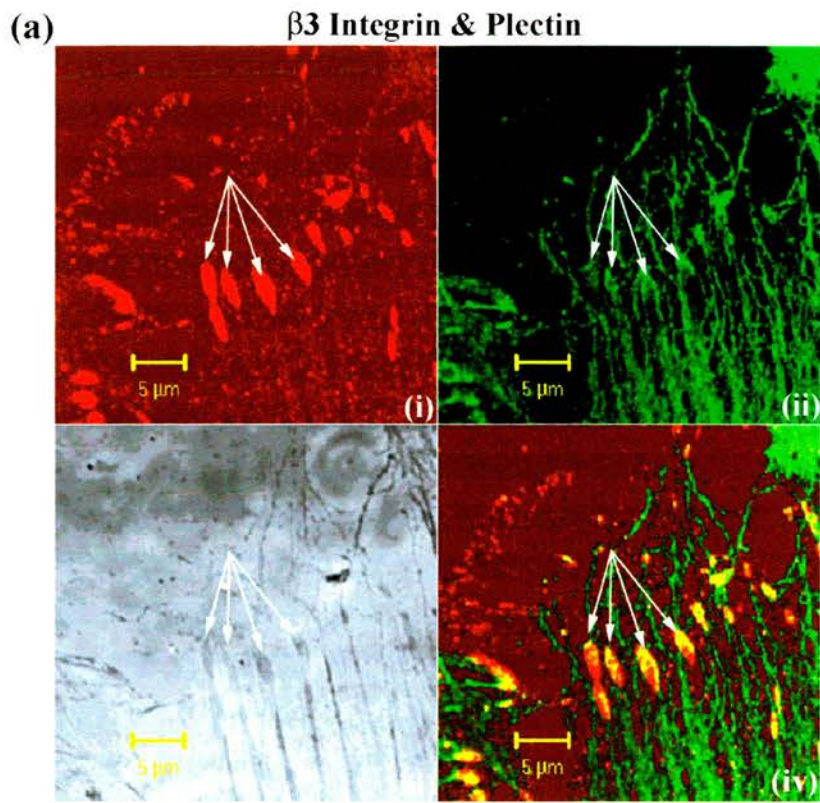


Figure 5.4

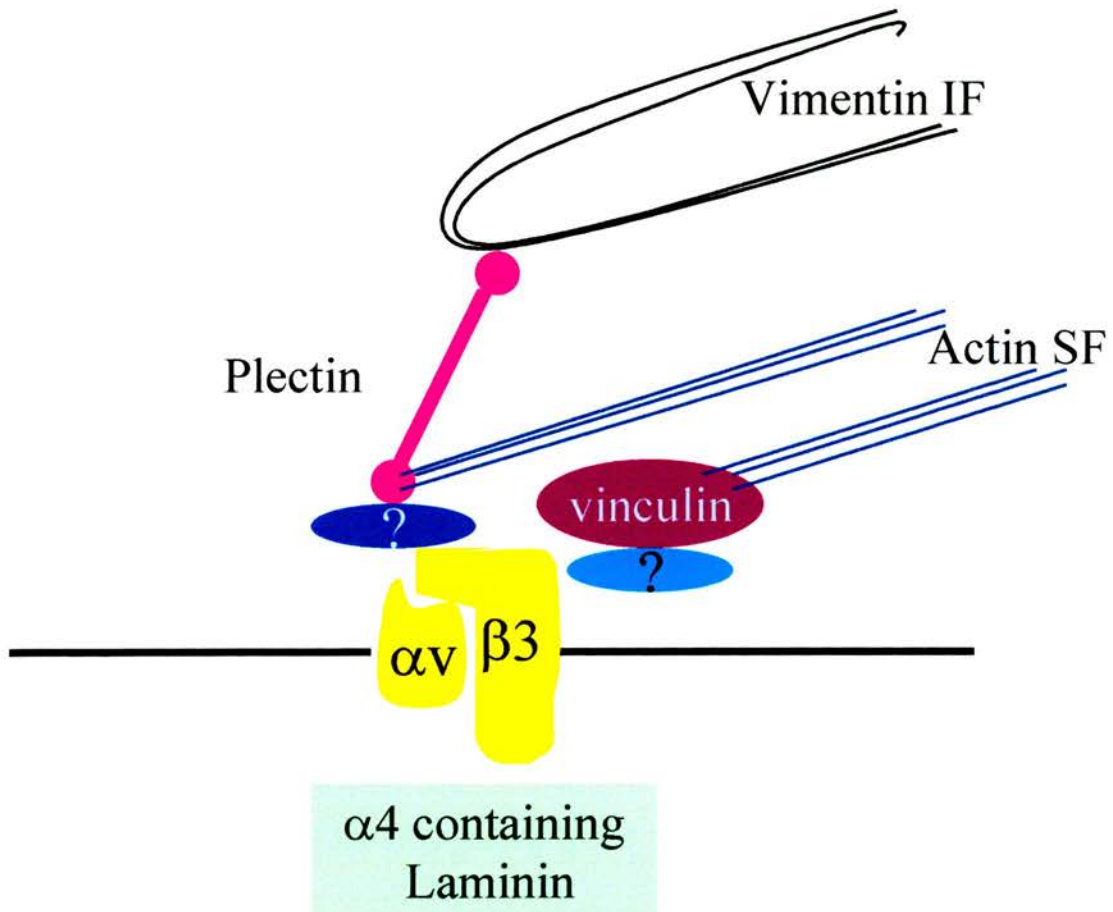


Figure 5.5. Proposed molecular structure of VMA components. The structural core forms as the result of the interaction of $\alpha4$ laminin with the $\alpha v\beta3$ -integrin. Vimentin is thought to associate with the site via plectin. Plectin also contains an actin binding site which is thought to mediate SF association along with the more well known interaction via vinculin. The proteins which are thought to link plectin and vinculin to the $\alpha v\beta3$ -integrin are as yet unidentified but it is speculated that α -actinin may be the vinculin- $\alpha v\beta3$ linker protein. Adapted from Gonzales et al, 2001.

The identification of these VMA suggest that an ' $\alpha_v\beta_3$ integrin-plectin-intermediate filament' mediated pathway may play an important role in endothelial mechanotransduction. Taken together with the findings on flow-induced NF- κ B activation, this raises the question: *Do intermediate filaments play a role in gene transcription activation in response to shear stress?* To date, the nature of the upstream signalling elements involved in flow-dependent activation of NF- κ B in *human* cells has not been investigated, although this is of considerable interest in the light of studies implicating NF- κ B in the pathogenesis of atherosclerosis. This has been investigated, using HUVEC exposed to uniform laminar flow, and the results are presented in the following chapters.

CHAPTER 6

INTRODUCTION- PART II

THE NUCLEAR FACTOR- κ B (NF- κ B) ACTIVATION PATHWAY.

6.1 Introduction

Nuclear factor κ B (NF- κ B) is a dimeric nuclear transcription factor present in an inactive state in most quiescent eukaryotic cells. NF- κ B was first identified as a transcription factor in B-cells where it was found to bind to a specific DNA sequence (5'-GGGACTTCC-3') in the intronic enhancer region of the κ B light chain, hence its name (Sen & Baltimore, 1986a). Upon stimulation, NF- κ B was found to activate transcription in a protein synthesis independent manner (Sen & Baltimore, 1986b).

Subsequent studies have shown NF- κ B to be ubiquitously expressed, serving as a critical regulator of inducible gene expression following activation by a wide variety of stimuli. It is known to be vital in many inflammatory and immune responses, regulating the expression of many genes involved in a wide range of cell functions including cell adhesion, immune stimulation, apoptosis, chemoattraction, differentiation and extra-cellular matrix degradation. It also participates in regulating transcription of the human immunodeficiency virus (HIV) (Hay, 1993). NF- κ B is associated with the initiation and/or progression of a number of disease states e.g. autoimmune arthritis, septic shock, asthma, carcinogenesis, atherosclerosis and AIDS (Baldwin, 1996), and as a result it is currently an area of intensive study.

Inducers of NF- κ B include UV radiation, oxygen free radicals, cytokines (e.g. tumour necrosis factor- α (TNF α) and interleukin-1 (IL-1)) viral and bacterial products (e.g. lipopolysaccharide(LPS)), phorbol esters (e.g. phorbol 12-myristate 13-acetate (PMA)) and fluid shear stress (Lan *et al*, 1994; Baldwin, 1996; Bhullar *et al*, 1998). IL-1, TNF α and PMA were found to potently activate NF- κ B in a time dependent manner, detectable within 5-15 minutes, peaking between 30-60 minutes and remaining elevated for up to 48 hours post stimulation (Bowie *et al*, 1996).

6.1.1 *Rel/NF- κ B transcription proteins*

NF- κ B exists in the cytoplasm of unstimulated cells as homo/heterodimers of a group of structurally related proteins – the Rel/NF- κ B family (May & Ghosh, 1997). To date, 5 mammalian NF- κ B proteins have been identified and subsequently cloned, NF- κ B1 (p50/p105), NF- κ B2 (p52/p100), Rel A (p65), Rel B and c-Rel (Figure 6.1). Each of these Rel/NF- κ B subunits possesses a highly conserved 300 amino acid N-terminal region, referred to as the Rel homology domain (RHD) (Baldwin, 1996). This RHD contains the DNA binding and dimerisation domains thus allowing NF- κ B-DNA binding as well as the formation of Rel/NF κ B homodimers or heterodimers which are pre-requisites for DNA binding. The RHD is also the region where the NF- κ B inhibitory proteins (I κ B) bind (section 6.1.4). A nuclear localising signal (NLS) is also found in the RHD, at the C-terminal end, and this is necessary for transport of activated NF- κ B into the nucleus (section 6.1.6.3).

‘Classic’ NF- κ B exists as a Rel A (p65)/NF- κ B1 (p50) heterodimer although various other dimers occur including p50/p50, p52/p52, Rel A/ Rel A, Rel A/cRel and p50/cRel. Rel B however only forms heterodimers with p50 or p52 and occurs mainly in lymphoid cells where it is believed to be constitutively active in the nuclei (May & Ghosh, 1997).

Rel A (p65), Rel B and c-Rel are produced as transcriptionally active proteins. The importance of their transactivation domain has been illustrated by experiments involving amino acid mutations within the sequence, resulting in a decrease and in some cases, prevention of transcription (May & Ghosh, 1997). In contrast, NF- κ B1 (p50) and NF- κ B2 (p52) are initially synthesised as inactive longer precursor molecules (p105 and p100 respectively) which are subsequently degraded into smaller transcriptionally active forms. Both p50 and p52 lack transactivation domains and as a result can only activate transcription as heterodimers with Rel A and Rel B (May & Ghosh, 1997). It has been shown that combinations of proteins containing p50/p52 can decrease transcription from

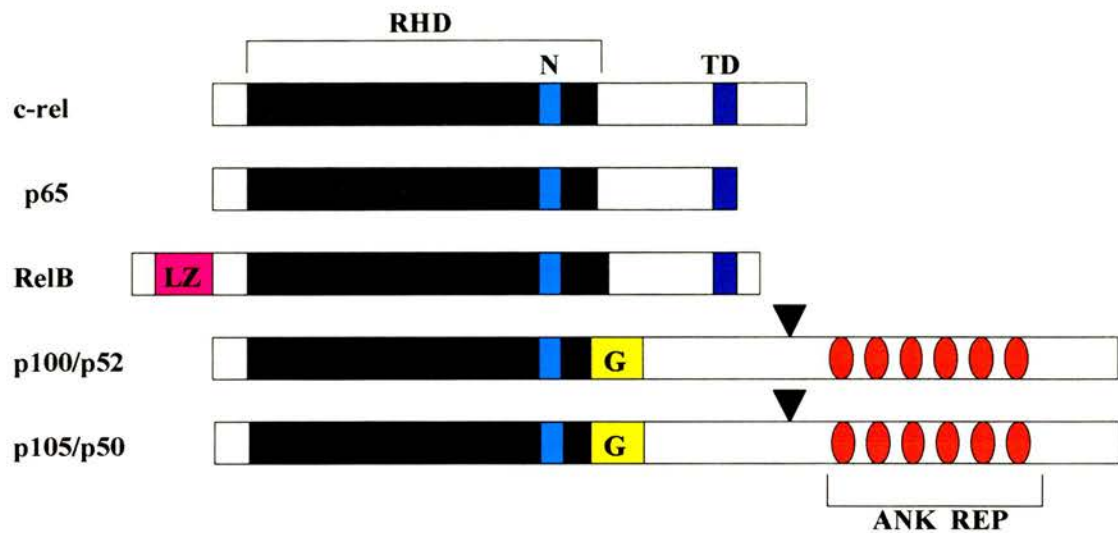


Figure 6.1. Schematic representation of the mammalian Rel/NF- κ B family of proteins. The Rel homology domain is highly conserved between family members while the outer sequences are generally unrelated. Abbreviations: RHD, Rel homology domain; N, nuclear localisation sequence (NLS); TD, transactivation domain; LZ, leucine zipper; G, glycine rich region; ANK REP, ankyrin repeats. The arrow heads denote endoproteolytic cleavage sites in p100/p52 and p105/p50. These proteins are encoded by NF- κ B1 and NF- κ B2 genes respectively and are cleaved to produce p52 and p50 respectively.

κ B sites, which may be related to the absence of transactivation domains. This may be the result of either competition with other active domains for DNA binding or active κ B occupation, which could otherwise have been bound by transactivating Rel/NF- κ B proteins (May & Ghosh, 1997).

In contrast to the C-terminal of p105 and p100 which is phosphorylated, ubiquitinated (see section 6.1.6.2) and degraded, the N-terminal region constitutes the RHD domains of p50 and p52 respectively. The area is located adjacent to a glycine rich region (GRR) followed by the C-terminus which contains ankyrin repeat sequences, which are also found in I κ B proteins. As a result of these ankyrin repeats, both p105 and p100 can mask the NLS of NF- κ B dimers, preventing their activation. The generation of p50 from p105 involves cleavage via ATP and a Mg⁺ dependent protease (Fan & Maniatis, 1991; Belich *et al*, 1999). The latter authors suggest that the release of p50 may occur via phosphorylation of the C-terminus, followed by ubiquitination and degradation of the protein by the proteasome. A similar mechanism has been described for signal induced dissociation of Rel/NF- κ B dimers from their inhibitory proteins. It is important to note that the above mechanism does not explain the pools of p50 in cells in the absence of stimulation. It has been suggested that in unstimulated cells the 23 amino-acid GRR of p105 signals endoproteolytic cleavage resulting in p50 pools, followed by a subsequent degradation of the C-terminus (Lin & Ghosh, 1996).

6.1.2 *Binding of NF- κ B to DNA*

Activated NF- κ B is translocated into the nucleus where it binds to κ B sites on the DNA helix. X-ray crystallography provides a greater understanding of the binding arrangement and hence interaction between Rel/NF- κ B dimers (p50 homodimer) and DNA (Ghosh *et al*, 1995). In contrast to other transcription factors that have small DNA binding domains, the NF- κ B-DNA binding site involves almost all of the RHD, which is composed of two anti-parallel β sheets in a sandwich structure, similar to that of an immunoglobulin fold. When both p50 subunits are bound the structure resembles a

butterfly with a DNA cylinder trapped within its wings. DNA interaction involves 10 loops at the end of each β strand resulting in high affinity between DNA and NF- κ B (Ghosh *et al*, 1995; Muller *et al*, 1995). The advantage that loops have over the more common α -helices and β -sheet arrangement is that they provide increased flexibility, providing a greater variety of DNA sites to which NF- κ B dimers can bind. The amino acids around the NLS allow I κ B interaction. Antibody accessibility experiments (Henkel *et al*, 1992) showed that the NLS of p50 and p65 were masked by I κ B γ and I κ B α respectively.

6.1.3 Inhibitory κ B Proteins – ‘The I κ Bs’

NF- κ B is restricted to the cytoplasm of unstimulated cells by being bound to inhibitory κ B proteins termed I κ Bs. I κ Bs bind to the RHD of NF- κ B dimers, masking its NLS and preventing nuclear import and DNA binding respectively. To date 5 mammalian I κ B proteins have been identified: I κ B α , I κ B β , I κ B γ , I κ B ϵ and Bcl-3 (Figure 6.2), each of which regulates NF- κ B by distinct mechanisms. The first I κ Bs to be described, I κ B α (Baeuerle & Baltimore, 1988) and I κ B β (Zabel & Baeuerle, 1990), had molecular weights of 37 and 43 kDa respectively. It was noted that not only could I κ B α inhibit NF- κ B binding to DNA, both specifically (Baeuerle & Baltimore, 1988) and reversibly, but it could also cause NF- κ B *already* bound to DNA to dissociate (Zabel & Baeuerle, 1990).

Investigations have shown that preferential inhibition of certain NF- κ B dimers occurs within the cytoplasm. I κ B α and β inhibit dimers containing c-Rel and Rel A. Bcl-3 only inhibits p50 or p52 homodimers, while I κ B γ inhibits cRel, p50, p65 and p50 heterodimers. It has been reported that I κ B ϵ (45 kDa) binds only c-Rel, Rel A or their homodimers, while both p100 and p105 have little specificity, forming inhibitory complexes with p50, p52, Rel A and c-Rel (Mercurio *et al*, 1993). To date, I κ B α has been the most extensively studied inhibitor. I κ B α preferentially interacts with c-Rel and

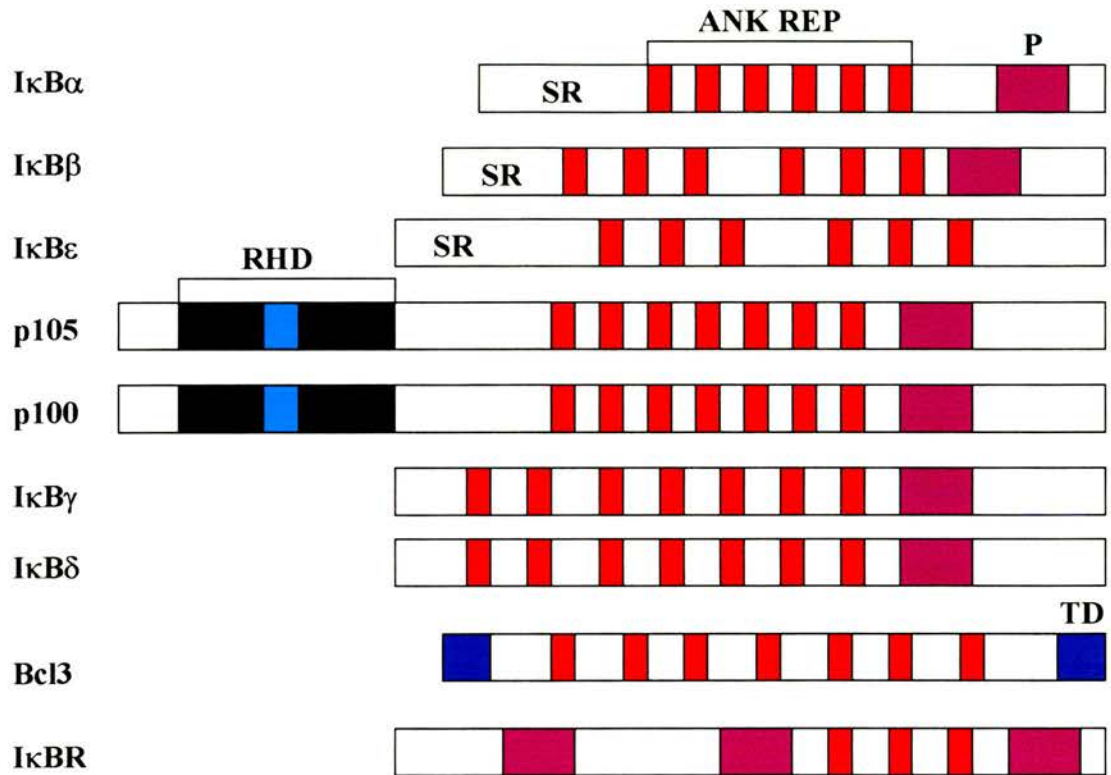


Figure 6.2. Schematic diagram of the IκB family of proteins. SR represents the serine residues responsible for the induction of IκB degradation through their phosphorylation. All IκB proteins contain repeats of approximately 30 amino acids known as ankyrin repeats (ANK REP). The C-terminal of most IκBs possess a high proportion of proline (P), glutamic acid (E), serine (S) and threonine (T) residues referred to as the PEST region (shown in purple). Other abbreviations: RHD, Rel homology domain; TD, transactivation domain.

Rel A, as does I κ B β . Although many similarities exist it has been found that while I κ B α can be targeted by IL-1, LPS, TNF α and PMA pathways, I κ B β is only targeted by IL-1 and LPS in some cells e.g. Jurkat T cells. Also, while I κ B α is rapidly produced in the post-induction repression of NF κ B, I κ B β does not re-accumulate after NF- κ B activation resulting in persistent activity (Baldwin, 1996). Cloning experiments discovered that the C-terminal of p105 and p100 have a similar structure to the I κ B family and thus can be classed as I κ B proteins (Baldwin, 1996).

6.1.4 I κ B structure - Ankyrin repeat domains (ARD) and PEST regions

Jaffray *et al* (1995) showed that I κ B α has a tripartite structure, including a conserved central domain, containing a series of ankyrin repeats, surrounded by a small C-terminal domain and an unstructured N-terminal domain. The N-terminus (~70 amino acids) of I κ B contains the phosphorylation and ubiquitination sites, which are involved in signal induced degradation of the NF- κ B-I κ B complex (section 6.1.6.3).

All I κ Bs possess a common structural motif in the central domain, referred to as the ankyrin repeat domain (ARD), which contains between 5-7 ankyrin repeats, each ranging from 30-35 amino acids in length (Figure 6.2). These sequences obtained their name due to their initial discovery in the erythrocyte protein ankyrin. Ankyrin repeats are known to play an important part in protein-protein interactions between NF- κ B and I κ Bs (Ernst *et al*, 1995) and are thought to mask the NLS (and the region C-terminal to it) of NF- κ B dimers (Phelps *et al*, 2000). Mutations of ARD were shown to block I κ B-NF- κ B interactions (Baeuerle & Henkel, 1994).

The C-terminus of most I κ Bs possess a PEST region (~ 42 amino acids) which contains a high proportion of proline (P), glutamic acid (E), serine (S) and threonine (T) residues. These PEST regions have been found in a range of proteins which are subject to rapid intracellular degradation (Rogers *et al*, 1986, Jaffray *et al*, 1995) and are believed to be

involved in molecule stabilization (Beauparlant *et al*, 1996) and prevention of NF- κ B-DNA binding (Ernst *et al*, 1995). Recent studies (Phelps *et al*, 2000) found that phosphorylation of the PEST region by casein kinase II (CKII) enhanced NF- κ B-I κ B binding. Ernst *et al* (1995) showed that each NF- κ B dimer binds a single I κ B molecule and although the C-terminus is required for inhibition of DNA binding, it has no involvement in masking the NLS or in protein-protein binding. The inhibition of NF- κ B-DNA interaction therefore, is thought to be due either to the direct interaction of the PEST region with the NF- κ B binding site on DNA or with one subunit of the dimer. Work by Beauparlant and co-workers (1996) showed that amino acids 269-287 of the I κ B molecule were responsible for inhibiting formation of the DNA-NF- κ B complex. Deletion of this region prevented TNF α and LPS mediated I κ B breakdown. In contrast, amino acids 288-317, which include most of the PEST region, were found to be dispensable.

The mechanisms which result in NF- κ B inhibition by I κ B are not fully understood, however, it does not seem to be related to the number of ankyrin repeats alone (Inoue *et al*, 1992). Inoue *et al* working on I κ B β showed that although 4 out of 5 ankyrin repeats were necessary for inhibiting DNA binding, they were not sufficient on their own. The C-terminus of I κ B β was also required.

As well as ankyrin repeats and PEST regions, the C and N terminal domains possess structural and functional characteristics. Deletion of either domain does not appear to affect I κ B-NF- κ B binding. However, loss of the C-terminus has been found to prevent I κ B dissociation of DNA bound NF- κ B. I κ B α molecules which lack an N-terminus can still interact with p65 and hence inhibit DNA binding of NF- κ B. However removal of both terminals remove the inhibitory effect of NF- κ B-DNA binding, underlining the importance of the C terminal (Jaffray *et al*, 1995; Ernst *et al*, 1995).

6.1.5 *NF-κB Activation*

The huge diversity of NF-κB inducers highlights the fact that multiple signal transduction pathways, emanating from a diverse array of activators, all converge on a single target – the cytosolic NF-κB-IκB complex to exert their effects. Signals which induce NF-κB activation (Figure 6.3) result in the dissociation followed by degradation of IκB proteins, allowing translocation of NF-κB dimers into the nucleus, where they regulate gene expression.

Much research on the NF-κB-IκB complex has shown that dissociation of the two proteins, and hence NF-κB activation, is a multi-step process. IκB becomes phosphorylated, poly-ubiquitinated and finally degraded by the 26S proteasome, culminating in the translocation of NF-κB from the cytoplasm to the nucleus (Figure 6.4).

6.1.5.1 *Phosphorylation of IκB*

Phosphorylation in effect is the beginning of the end for IκB proteins. Upon phosphorylation, a complex set of protein interactions cause the destruction of IκB. As well as the IκB kinase (IKK) complex (see section 6.1.7), many stimuli which induce NF-κB activation target the IκBα molecule via phosphorylation by casein kinase II (CKII) which then directs the inhibitor proteins to a degradation process via the ubiquitin (Ub) proteasome pathway (Baeuerle & Baltimore, 1996). Degradation of IκB also allows CKII to phosphorylate p65 which increases the transactivation potential of the NF-κB dimer (Wang *et al*, 2000, Pando & Verma, 2000).

Phosphorylation of IκB occurs on serine residues 32 and 36 (DiDonato *et al*, 1996) with the subsequent ubiquitination (i.e. the covalent linking of the 76 amino acid ubiquitin molecule) of lysine residues 21 and 22 (Scherer *et al*, 1995; Rodriguez *et al*, 1995).

Class of gene	NF- κ B dependent gene
<i>Cytokines/growth factors</i>	IL-1 α and β IL-2, -3, -6, -8, -12 TNF α LT α IFN β G-CSF M-CSF c-myc p53
<i>Stress Proteins</i>	SAA
<i>Leukocyte adhesion molecules</i>	ICAM-1 VCAM-1 E-selectin
<i>Immunoregulatory molecules</i>	Ig κ MHC class I and II TCR α & β TAP1 LMP2

Figure 6.3. Table (adapted from May & Ghosh, 1998) of a selection of genes which are activated by NF- κ B predominantly in the immune response. Abbreviations: G-CSF, granulocyte colony-stimulating factor; ICAM-1, intracellular adhesion molecule-1; IFN β , interferon β ; Ig κ , immunoglobulin κ light chain; IL, interleukin; LT α , lymphotoxin α ; M-CSF, macrophage stimulating factor; MHC, major histocompatibility complex; SAA, serum amyloid A protein; TAP1, transporter associated with antigen processing-1; TCR, T-cell receptor; TNF α , tumour necrosis factor α ; VCAM-1, vascular adhesion molecule 1.

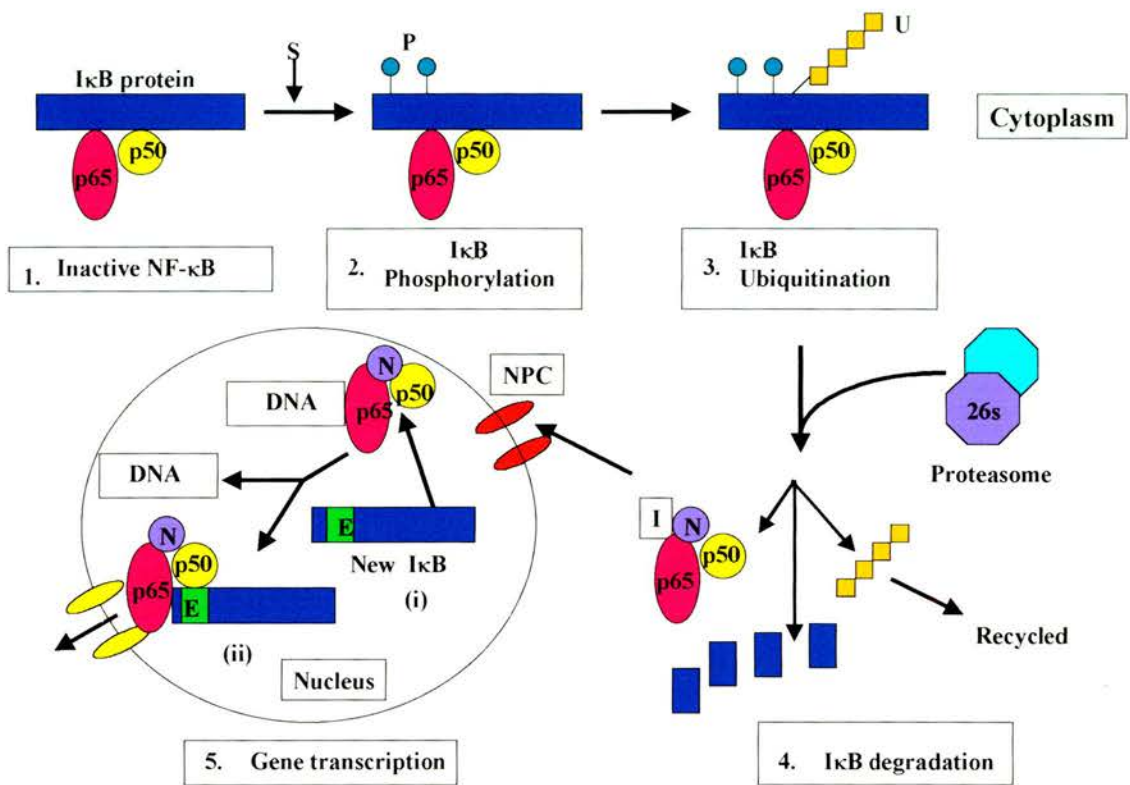


Figure 6.4. Summary of NF- κ B activation. *1.* In unstimulated cells, NF- κ B is sequestered in the cytoplasm due to I κ B proteins masking its Nuclear Localising Sequence (NLS). *2&3.* Upon stimulation (S), I κ B is phosphorylated (P) at serine residues 32 and 36, converting I κ B to a substrate for ubiquitination (U). *4.* I κ B dissociates from NF- κ B and is degraded by the 26S proteasome. This exposes the NLS (N) of NF- κ B and due to binding of importin proteins (I), NF- κ B enters nucleus via a nuclear pore complex (NPC). *5. (i)* In the nucleus it binds DNA and activates its target genes, including that of I κ B. *(ii)* Newly synthesised I κ B enters the nucleus, inhibits DNA-NF- κ B binding via nuclear export sequence (E) and transports the inactivated NF- κ B back into the cytoplasm, thus ending the transcription response of NF- κ B.

Replacement of serine 32 and 36 with threonine blocked inducible I κ B α phosphorylation and hence its degradation, suggesting that phosphorylation represents the rate limiting step in I κ B breakdown. From their results DiDonato *et al* suggested that I κ B α and I κ B β (which is phosphorylated on serines 19 and 23) were either targeted by the same kinase or a similar group of kinases.

6.1.5.2 Ubiquitination of phospho-I κ B

Upon stimulation, phosphorylated I κ B α and I κ B β are then rapidly modified to high molecular weight forms by the addition of ubiquitin (Ub) chains. Using site directed mutagenesis of lysine residues 21, 22, 38 and 47, which surround serines 32 and 36, Scherer *et al* (1995) provided evidence that induced phosphorylation at serine 32 and 36 resulted in the ligation of Ub at lysines 21 and 22 in I κ B α . Since lysine 21 and 22 are located next to serine 32 and 36, presumably phosphorylation of the serine residues as a consequence of cell stimulation induces a conformational change in lysine 21 and 22, allowing the Ub enzymatic processes to continue (Scherer *et al*, 1995).

Treatment of NIH3T3 cells with a proteasome inhibitor e.g. MG132 (Beauparlant *et al*, 1996) was shown to prevent I κ B α degradation but not hyperphosphorylation, illustrating that these events are independent of each other. Hyperphosphorylation of I κ B α does not alter its association with NF- κ B dimers. Instead, it serves to identify the protein as a target for subsequent ubiquitination. This is followed by its dissociation from NF- κ B (DiDonato *et al*, 1995) and proteolytic degradation by the proteasome pathway.

Ubiquitination of I κ B involves a complex set of enzymatic processes (Figure 6.5). It begins with Ub forming a thioester bond with the ubiquitin-activating enzyme, E1 (Adams *et al*, 1992). This process requires ATP and the E1-Ub complex is then referred to as 'activated Ubiquitin'. The activated Ub is subsequently transferred to a second enzyme, E2 – Ub conjugating enzyme (Pickart & Rose, 1985) which can directly

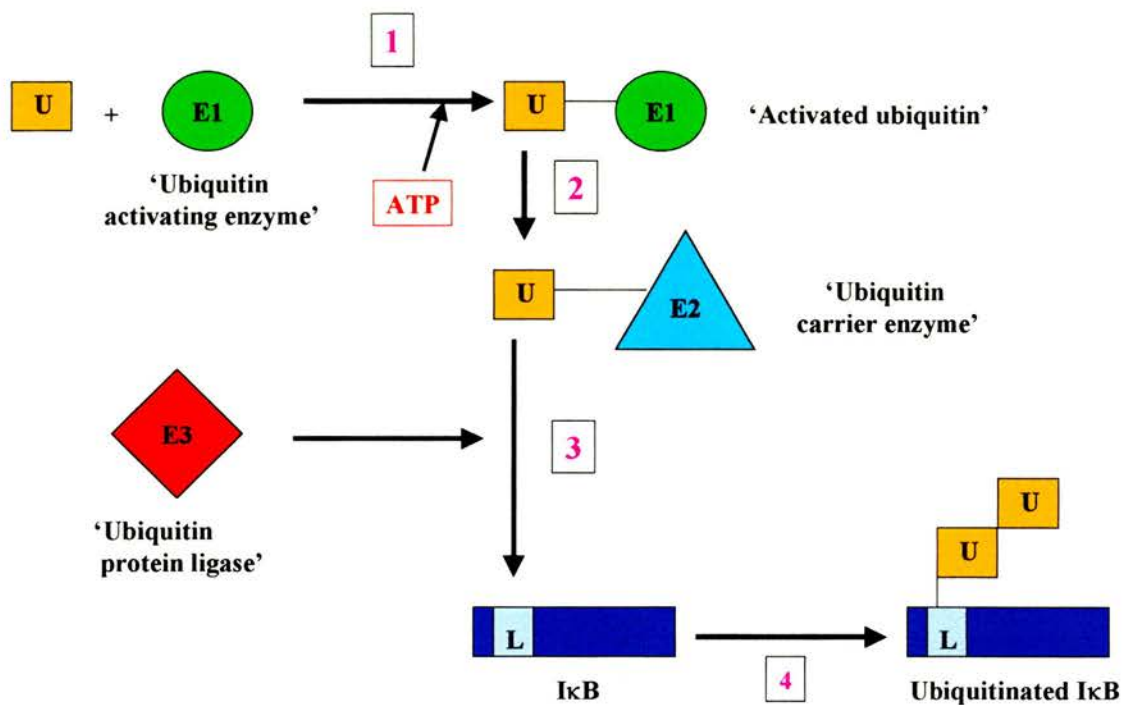


Figure 6.5. Schematic representation of steps involved in the ubiquitination of $I\kappa B$ proteins. Ubiquitin (U) is covalently linked to $I\kappa B$ via a complex series of enzymatic reactions. 1. Ubiquitin, in the presence of ATP, forms a thioester bond with ubiquitin activating enzyme (E1). 2. Activated ubiquitin is transferred to the ubiquitin carrier enzyme (E2). 3. Ubiquitin protein ligase (E3) then transfers ubiquitin from E2 to specific lysine residues (L) on the $I\kappa B$ molecule. In the case of $I\kappa B\alpha$, these residues are lysine 21 and 22. There various E3 enzymes, each one is thought to recognise specific sequences in the target substrate. 4. A ubiquitin chain is formed by repeats of this pathway resulting in consecutively added ubiquitin molecules on $I\kappa B$.

transfer Ub to I κ B. However, in some cases, a Ub protein ligase, E3 is required to catalyse the transfer of Ub from E2 to its target protein (Ciechanover *et al*, 1982).

There are various E3 ligases. For example, in the case of I κ B α , a protein called β -transducin repeat-containing protein (β TRCP) is known to be a specific component of the I κ B α -ubiquitin ligase complex (Hatakeyama *et al*, 1999; Spencer *et al*, 1999) that facilitates ubiquitin transfer to I κ B α . Spencer *et al* (1999) conclude from their investigation that β -TRCP is the specificity determinant for the signal-induced ubiquitination of I κ B α .

It is interesting to note that the Ub system is constitutively active within the cell, however I κ B is only subjected to the above process after phosphorylation. It has been postulated that in unstimulated cells the C-terminus protects I κ B α from proteasome mediated degradation via interaction with p65 (Beauparlant *et al*, 1996). It is thought that serine 32 and 36 regulate I κ B α -E3 ligase interaction during ubiquitination. E3 has distinct substrate specificity and due to the spatial arrangement of the I κ B α N-terminus, E3 interaction with serine 32 and 36 results in Ub attachment to lysine 21 and 22 (Scherer *et al*, 1995). Although the N-terminus is necessary, it is not sufficient for signal induced degradation of I κ B α *in vivo*. The C-terminus is also required (Rodriguez *et al*, 1995).

Research has identified that the Ub-proteasome pathway functions not only in degradation but in the regulation of processing precursors into active proteins as well as protein function (Palombella *et al* 1994; Deshaies, 1995). This discovery coupled with the involvement of NF- κ B in various immune and inflammatory responses suggests that selective inhibition techniques may prove useful in the treatment of various disease states.

6.1.5.3 *IκB degradation, NF-κB Nuclear translocation and IκB feedback mechanism*

Degradation of IκB is carried out by the ATP-dependent 26S proteasome. Evidence of proteasome involvement in this process resulted from experiments using peptide aldehyde inhibitors (Chen *et al* 1995). Pre-treatment of cells with these inhibitors was found to prevent the degradation of IκB, resulting in a build-up of phosphorylated and ubiquitinated IκBα still associated with NF-κB.

Once IκB is degraded by the proteasome and Ub is released for recycling by the cell, NF-κB can translocate to the nucleus (Figure 6.4) and bind to the κB site of the appropriate gene promoter via the RHD, altering gene transcription (Baeuerle & Baltimore, 1996; Baldwin, 1996). Migration from the cytoplasm to the nucleus is an example of NF-κB acting as a second messenger system, transducing activation signals from the cytoplasm to the nucleus (Ghosh & Baltimore, 1990). NF-κB is known to activate over 150 genes including that of its inhibitor IκBα. Nuclear import of NF-κB occurs via a group of proteins known as the importin α family which recognise the NLS. In the cytoplasm, the NLS bound importin α associates with importin β which subsequently guides the complex to the nucleus where it enters via nuclear pores.

NF-κB-dependent gene transcription is self-limiting, because NF-κB activates the gene for IκBα. The newly synthesised IκBα can be detected in the cytoplasm and in the nucleus. Western blot analysis on HeLa S3 cells activated by TNFα and IL-1 showed that newly synthesised IκBα moves from the cytoplasm into the nucleus, where it inhibits binding of NF-κB to DNA (Arenzana-Seisdedos *et al*, 1995). Once IκB has bound to nuclear NF-κB, the complex is exported across the nuclear membrane by means of a nuclear export sequence (NES) present in the C-terminus (amino acids 265-277) of IκBα (Arenzana-Seisdedos *et al*, 1997). The NES is a lysine rich region of IκB which allows the NF-κB-IκBα complex to exit the nucleus via a family of proteins known as the exportins e.g. CRM1 or exportin-1.

The development of I κ B α -specific antibodies provided an insight into what happened to I κ B α during NF- κ B activation. Treatment of cells with NF- κ B inducers resulted in the rapid disappearance of I κ B α less than 10 minutes after activation, followed by its reappearance after approximately 30 minutes. This led to the discovery that the disappearance of I κ B α represented the key step in the activation of NF- κ B and its movement into the nucleus. Furthermore, re-synthesis of I κ B α resulted in the termination of NF- κ B-dependent transcription (Baldwin, 1996). Thus NF- κ B and I κ B α compose a mutual regulatory system where levels of one protein regulate those of the other, ultimately resulting in controlled expression of NF- κ B dependent genes.

6.1.6 *The I κ B kinase (IKK) and the IKK complex*

The NF- κ B activation pathway involving I κ B α dissociation and nuclear translocation for gene transcription is only a small part of a complex signal cascade which results in the transduction of an external stimuli from the plasma membrane to the NF- κ B-I κ B α complex and ultimately the nucleus.

Since most inducers of NF- κ B are thought to act via distinct pathways it seemed likely that at some stage all routes should intersect and sensible that this should be in close proximity to the NF- κ B-I κ B complex. In order for I κ B phosphorylation to occur, a kinase must be present. Many kinases were suggested for this role including PKA, p90-rsk and raf-1 as these had been found to dissociate I κ B α *in vitro* (Ghosh & Baltimore, 1990). However, none of these phosphorylate I κ B α on the critical serine residues 32 and 36 (May & Ghosh, 1998).

Initially, a high molecular weight (700kDa) kinase complex was identified that not only phosphorylated serine 32 and 36 residues on I κ B molecules but also depended on Ub for activity (DiDonato *et al*, 1997; Mercurio *et al*, 1997; Regnier *et al*, 1997; Woronicz *et*

al, 1997; Zandi *et al*, 1997). Further investigation uncovered two catalytic kinases which were components of the 700kDa complex. One of these had been previously reported as the protein CHUK whose function was unknown (Regnier *et al*, 1997). These were subsequently named IKK α /IKK1 and IKK β /IKK2 and were found to have molecular weights of 85 and 87 kDa respectively. These are now known to be directly responsible for phosphorylation of I κ B α , I κ B β and I κ B ϵ with a preference to I κ B α over both I κ B β and I κ B ϵ (Mercurio *et al*, 1997). Experiments with cloned IKK α and IKK β demonstrated rapid induction of kinase activity on exposure to known inducers of NF- κ B (DiDonato *et al*, 1997; Mercurio *et al*, 1997). Although IKK α and IKK β possess distinct roles, they contain common structural motifs, an N-terminal serine/threonine kinase domain, which catalyses phosphorylation of serine residues, a central leucine zipper (LZ) and a C-terminus helix-loop-helix domain (HLH) (Figure 6.6). It is the LZ rather than the HLH domain that mediates dimerisation of IKK α and IKK β , although both components are required for overall activation. IKK α and IKK β can form either homo or heterodimers and purified forms can phosphorylate I κ B α and I κ B β on the appropriate residues (Lee *et al*, 1998). In HeLa cells, IKK α -IKK β heterodimers and IKK β homodimers show different responses to TNF α activation, with the heterodimer exhibiting a more potent response. This indicates that IKK α and its associated proteins are essential for full NF- κ B activation (Mercurio *et al*, 1999). Work carried out on human umbilical vein endothelial cells (HUVEC) identified two I κ B binding sites on each IKK β molecule and that I κ B-IKK complex interactions were mediated by direct enzyme-substrate association (Heilker *et al*, 1999). IKK β was found to be the dominant I κ B-kinase for 4 isoforms of I κ B (α , β 1, β 2 & ϵ), showing higher phosphorylating activity than IKK α when immunoprecipitated. The ability of IKK to form homodimers and heterodimers must enable differential regulation of NF- κ B activation by a variety of mechanisms in different cell lines although as yet details remain unclear (Mercurio *et al*, 1999).

The IKK complex also contains a regulatory subunit that is necessary for the formation of the complex (Yamaoka *et al*, 1998). This protein is known as IKK γ or NF- κ B

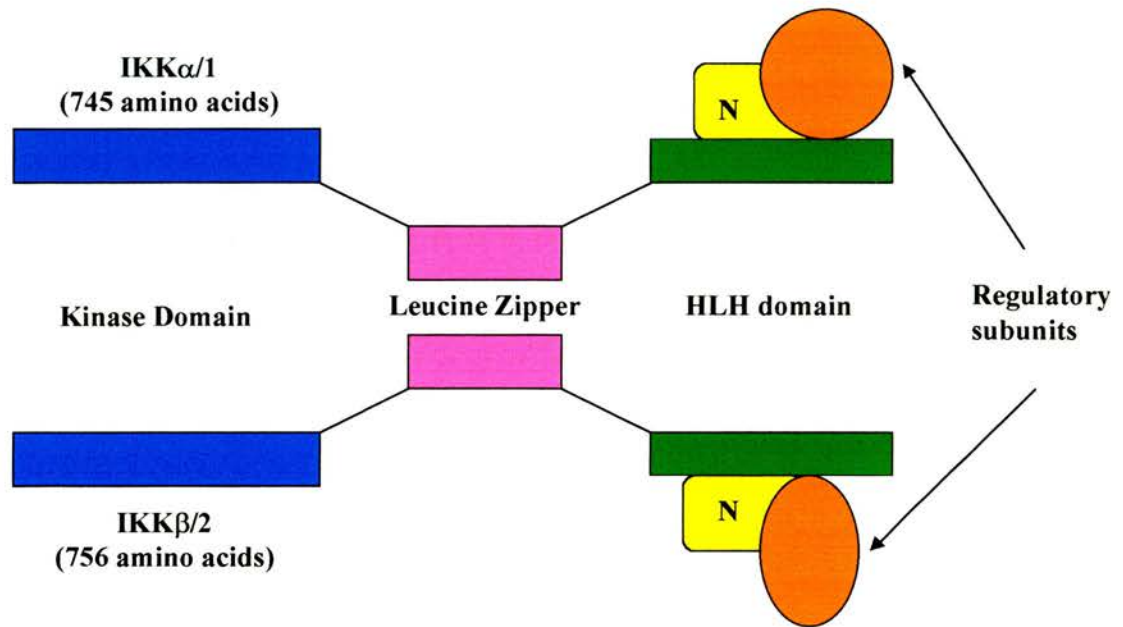


Figure 6.6. Schematic representation of the domain structures of *IKKα* (*IKK1*) and *IKKβ* (*IKK2*). The kinase domain phosphorylates the serine residues of the *IκB* proteins while the leucine zipper region is responsible for formation of homo or heterodimers. The C-terminal helix-loop-helix (HLH) domain is responsible for interaction with the regulatory subunit NEMO (N) and possibly other regulatory subunits e.g. *IKKAP-1*. (Figure adapted from May & Ghosh, 1998).

essential modulating factor (or NEMO), a 419 amino acid, glutamine-rich protein which lacks a catalytic domain but does contain a LZ and several coiled protein motifs. NEMO interacts preferentially with IKK β (Yamaoka *et al*, 1998) and is required for NF- κ B activation. Although a stable interaction occurs between IKK β and NEMO, it is likely that once the activation process is initiated it may also associate with IKK α (Rothwarf *et al*, 1998). Investigations using truncated NEMO showed that although the IKK complex could bind, activation was prevented. This suggested that NEMO is required for IKK activation and may have a specific function in linking the IKK complex to upstream activators (Rothwarf *et al*, 1998).

Recent work by Mercurio *et al* (1999) on the IKK complex yielded a protein common to both IKK α -IKK β heterodimers and IKK β homodimers in HeLa cells. Cloning and purification of this protein I κ B kinase associated protein 1 (IKKAP-1) showed that *in vitro* IKKAP-1 associated with IKK β but not IKK α . Functional analysis showed that IKK β -IKKAP-1 binding required specific residues in the IKKAP-1 N-terminus. Mutations of this region were shown to disrupt NF- κ B signal transduction, suggesting IKKAP-1 plays an essential role in NF- κ B activation, although it is as yet unclear what role this protein might play as it lacks an enzymatic motif. However, possible roles suggested include association with other IKK signalosome components, upstream activators or recruitment of the I κ B substrate. Purification of IKKAP-1 has indicated it to be the human homologue of murine NEMO (Yamaoka *et al*, 1998; Mercurio *et al*, 1999). Thus IKKAP-1 has been postulated to provide a scaffold on which IKK β containing complexes can be localised to the upstream components of the NF- κ B activation pathway.

The IKK complex has also been shown to contain another protein, IKK complex associated protein, or IKAP (Cohen *et al*, 1998). This component was thought to be involved in scaffolding based on its ability to assemble IKK α , IKK β , NF- κ B inducing kinase (NIK) and NF- κ B-I κ B α unit into a complex. However, more recent work (Krappmann *et al*, 2000) has determined that while NEMO is a stoichiometric

component of the IKK complex, essential for NF- κ B signalling, IKAP is not associated with IKK α / β and has no specific role in cytokine-induced NF- κ B activation.

6.1.6.1 Regulation of I κ B-kinase (IKK) activity

Despite the vast amount of research in this area, investigators have yet to elucidate exactly how upstream regulators stimulate IKKs, and hence the pathways from this point on, which ultimately result in NF- κ B activation (Figure 6.7). IKK activation is known to be serine-specific and responsive to a range of NF- κ B activators, most notably TNF α and IL-1 (Ghosh *et al*, 1995). Responses to TNF α are mediated by 2 distinct surface receptors, TNFR1 (p55) and TNFR2 (p75) (Smith *et al*, 1994). TNF receptor associated factors (TRAFs) have been identified as a family of non-kinase, signal-transduction units that can be activated by both TNFR and the interleukin-1 receptor (IL-1R) (Rothe *et al*, 1995; Song & Donner, 1995; Hsu *et al*, 1997). TNFR and IL-1R associate with TRAFs 2 and 6 respectively, in turn activating the appropriate kinases transmitting the stimulus downstream. Recent work suggests that TRAF 2 may couple TNF α and IL-1 receptors in NF- κ B activation (Malinin *et al*, 1997).

Evidence suggests that IKK α and β are phosphorylated on serines 176 & 180 and 177 & 181 respectively (Mercurio & Manning, 1999). One or more of the upstream kinases, likely to be a member of the mitogen-activated-protein kinase-kinase kinase (MAP3K, MAPKKK, or MEKK) family, may mediate this. One of these, NF- κ B-inducing kinase (NIK), was first identified as a TRAF-2 interacting protein, which also associated with IKK α and IKK β (Malinin *et al*, 1997; Woronicz *et al*, 1997). Transfection of an inactive mutant of NIK resulted in inhibition of NF- κ B activation when exposed to TNF α or IL-1, highlighting NIK as a stimulation mediator through each of these pathways (Malinin *et al*, 1997). Work by Nakano *et al* (1998) showed that NIK preferentially phosphorylates IKK α on serine 176 resulting in its activation. Further

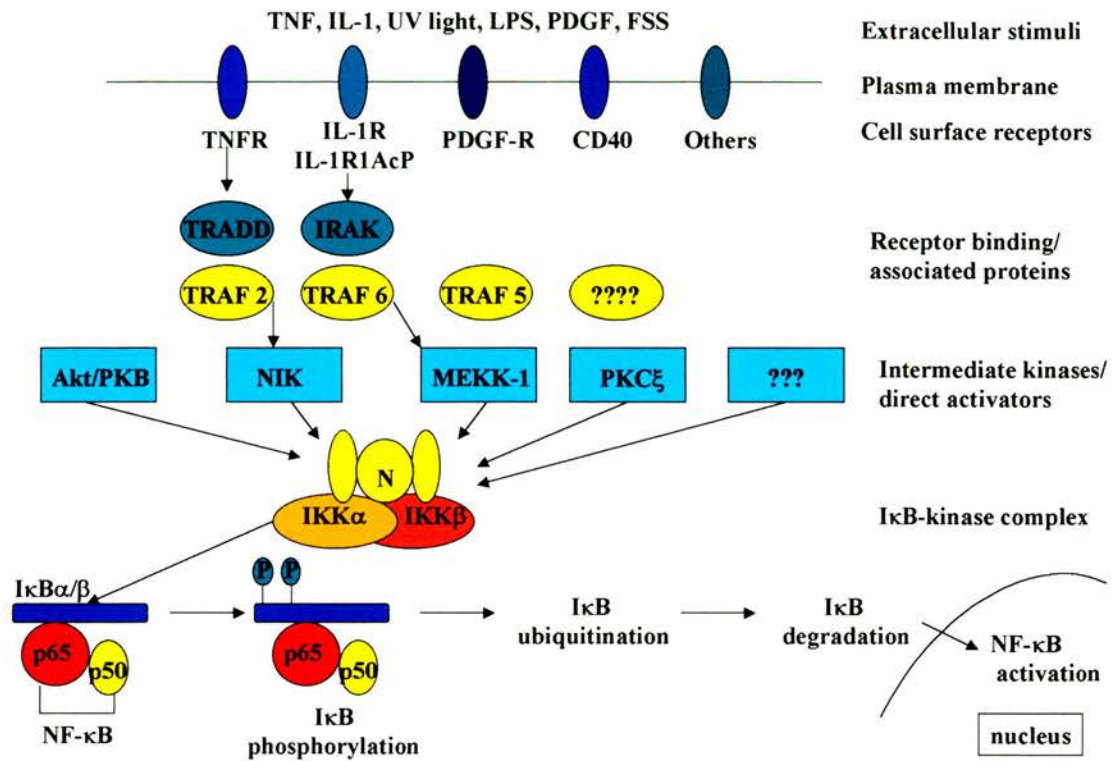


Figure 6.7. Schematic representation of suggested signal transduction pathways which lead to NF- κ B activation. Signals emanating from external stimuli are transduced via membrane receptors. Binding proteins are recruited which do not phosphorylate IKK complex directly but act via various kinases. The precise mechanism for IKK activation remains unknown. The kinase complex then transforms signals into signals responsible for I κ B phosphorylation which ultimately results in NF- κ B activation (figure 6.4). Abbreviations: FSS, fluid shear stress; IL-1, interleukin-1; IL-1R1, IL-1 type 1 receptor; IL-1RacP, IL-1R accessory protein; IRAK, IL-1 receptor-associated protein; LPS, lipopolysaccharide; MEKK-1, mitogen-activated protein kinase/extracellular signal-related kinase kinase-1; N, (NEMO) NF κ B essential modulator; NIK, NF- κ B inducing kinase; TNF, tumour necrosis factor; TNFR, TNF receptor; TRADD, TNFR associated death domain protein; TRAF, TNFR-associated factor.

investigation showed that over-expression of NIK leads to activation of both IKK α and IKK β .

Another MAPKKK, mitogen-activated protein kinase/ERK kinase kinase-1 (MEKK-1) is also thought to be associated with IKK α , IKK β , NEMO and NIK in the signalsome complex (Mercurio *et al*, 1997, Lee *et al*, 1998). Lee *et al* (1998) showed that both IKK α and IKK β could mediate the NF- κ B-inducing activity of MEKK-1. In contrast to NIK, MEKK-1 phosphorylates corresponding serines in the activation loop of IKK β during activation (Nakano *et al*, 1998). Transfection of an inactive mutant of IKK β was found to prevent NF- κ B activation, suggesting that MEKK-1 acts through IKK β alone (Nakano *et al*, 1998).

Although co-expression of NIK and MEKK-1 enhance the ability of IKK to phosphorylate I κ B (Mercurio & Manning, 2000), they appear to be activated by discrete stimuli, providing independent mechanisms for differential activation of IKK α and IKK β and subsequently NF- κ B mediated gene transcription.

Recent findings, however, have questioned the physiological significance of NIK. The importance of NIK as an upstream regulator of the IKK complex was highlighted by studies which determined that IKK α was independently isolated when NIK was used as bait (Regnier *et al*, 1997). In addition, biochemical purification of the IKK complex showed NIK to be present (Woronicz *et al*, 1997). Although in overexpression experiments NIK interacted with IKK α in two mammalian cell lines, there was no interaction detected under physiological conditions. Recent experiments also question the role of NIK as a potent IKK and NF- κ B activator (Malinin *et al*, 1997, Ling, 1998) and cast doubt on its involvement in IKK activation by either TNF α or IL-1 (Hu *et al*, 1999; Takeda *et al*, 1999). In addition, the IKK α subunit which was proposed as the preferential target of NIK is not directly involved in IKK activation and IKK activation depends on the IKK β subunit (Hu *et al*, 1999; Takeda *et al*, 1999).

Research by Romieu-Mourez *et al* (2001) has implicated abnormal IKK and CKII expression and consequent increase in nuclear NF- κ B, and transformation of breast cancer cells. Findings suggest that these kinases play similar roles in intracellular signalling pathways which result in elevated NF- κ B levels in primary mammary tumours. Therefore, these pathways represent potential therapeutic targets in the treatment of breast cancer (Romieu-Mourez *et al*, 2001).

6.2 Fluid Shear Stress and NF- κ B activation

In addition to local and systemic stimuli (e.g. cytokines and bacterial products), it has been recognised that haemodynamic forces also alter endothelial structure, function and most recently, gene expression (Davies & Tripathi, 1993; Davies, 1995; Papadaki & Eskin, 1997; Oluwule *et al*, 1997; Chien *et al*, 1998;).

Resnick *et al* (1993) identified a cis-acting element in the platelet derived growth factor-B (PDGF-B) gene which was involved in fluid shear stress responses and has now been implicated in responses to cyclic strain (Oluwule *et al*, 1997). This shear-stress response element (SSRE) contains a 6 base pair (bp) core binding sequence (GAGACC) which was found to bind transcription factors present in nuclear extracts from sheared BAE cells. Continued studies provided evidence of the effectiveness of the SSRE sequence; thus, insertion of the SSRE into reporter genes was found to make them shear inducible (Resnick & Gimbrone, 1995). It had been initially suggested that shear stress induced changes were dependent either directly or indirectly on gene expression. Resnick *et al* (1993) provided evidence of mechanical force regulated gene expression at the transcription level due to SSRE-transcription factor binding. However, the pathway through which haemodynamic forces were sensed and mediated to the nucleus was still unclear.

Further investigations showed that fluid shear stress caused the activation of NF- κ B and activator protein-1 (AP-1) in BAEC exposed to 12 dynes.cm⁻² (Lan *et al*, 1994), with

NF- κ B being stimulated within 30 minutes and reaching its maximal level by one hour. Khachigian and co-workers (1995) later identified specific binding of NF- κ B p50/p65 heterodimers to the SSRE of PDGF-B in BAEC exposed to a fluid shear stress of 10 dynes.cm⁻², supporting the theory previously put forward by Resnick *et al* (1993). Kachigian's findings implicated direct involvement of NF- κ B in the transactivation of specific endothelial genes in response to flow. NF- κ B translocation in response to shear stress activation was not found to be sufficient to modulate all genes containing NF- κ B recognition sequences (Khachigian *et al*, 1995). Several suggestions have been made as to why this may be the case, including slight differences in the NF- κ B sites of individual genes, fluid shear stress alteration of NF- κ B structure or the interaction of other transcription factors (Kachigian *et al*, 1995; Papadaki & Eskin, 1997), all of which have yet to be proved.

Protein kinases implicated in I κ B phosphorylation, as well as components of the cytoskeleton, have been postulated to play a role in altering gene expression in shear-activated endothelial cells. Fluid shear stress was found to activate the Ras-JNK (Ras, c-jun NH₂-terminal kinase) pathway, stimulating AP-1 preferentially over the extracellular signal related kinase (ERK 1/2) pathway which ultimately activates the early response growth element-1 (Li *et al*, 1996). Fluid shear stress-induced phosphorylation of JNK and ERK pathways via different mechanisms may be significant as ERK is involved in cell growth while JNK has a role in cell death. A balance between these pathways in response to fluid shear stress and other stimuli may be important with regard to cell viability (Chien *et al*, 1998).

6.2.1. Role of the cytoskeleton in gene regulation by flow

Previous research on the effects of cytokines on the cytoskeletal arrangement of HUVEC in static culture (Molony & Armstrong, 1991) showed that addition of cytokines (TNF, IL-1 or PMA) caused actin filaments, microtubules and focal adhesion to reorganise, although there was no significant alteration in protein expression. Allen *et*

al (1991) studied the effects of LPS induced IL-1 and TNF α release in colchicine treated human monocytes. In treated cells, LPS induced a 50% increase in induced IL-1 release and a 50% decrease in induced TNF α release. These results suggest that microtubules contribute to the regulation of endotoxin stimulated cytokine release and that this regulation differs significantly for IL-1 and TNF α .

Cytokines were also found to stimulate NF- κ B activation in static culture (Bowie *et al*, 1996). Work by Rosette & Karin (1995) subsequently showed that HeLa cells exposed to microtubule depolymerising drugs e.g colchicine, induced reversible, NF- κ B activated gene expression. NF- κ B stimulation was found to lag microtubule depolymerisation by 15 minutes, suggesting an ‘unknown’ intermediate step in the activation pathway. The microtubule stabilising drug taxol was found to block these effects. However, other work using taxol (Papadaki & Eskin, 1997) showed that NF- κ B activation in response to TNF α was not inhibited, suggesting that the TNF signalling pathway is not reliant on microtubule reorganisation. Interestingly, microfilament disruption by cytochalasin D did not result in NF- κ B activation, implying that stimulation is due to specific cytoskeletal disruption (Rosette & Karin, 1995). The above data, coupled with experiments on cytoskeletal re-organisation under flow (Chapter 4), provides evidence that the cytoskeleton must play a role in mechanotransduction.

The cytoskeleton provides a structural link between focal adhesions, cell-cell contacts, cell-matrix interactions and the nuclear membrane (Gonzales *et al*, 2001). Much research has focussed on the role of integrins and focal adhesions with respect to fluid shear stress stimulation of NF- κ B (Bhullar *et al*, 1998). Fluid shear stress was found to induce phosphorylation of focal adhesion kinase (FAK) (Girard & Nerem, 1995). This was then discovered to occur via integrin activation, although it was only partially responsible for flow stimulated response in endothelial cells (Ishida *et al*, 1996). Bhullar and co-workers (1998) highlighted the importance of the $\alpha_v\beta_3$ integrin in the activation of IKK, and hence NF- κ B, in BAEC exposed to 12 dynes.cm⁻² fluid shear stress. This

finding is not entirely surprising as previous studies showed increased nuclear binding of NF- κ B (Lan *et al*, 1994; Khachigian *et al*, 1995), as well as increased transcriptional activities of κ B element containing promoters (Shyy *et al*, 1997) in response to fluid shear stress.

In cells exposed to flow, Bhullar *et al* (1998) showed a transient increase in I κ B degradation, coupled with increased nuclear NF- κ B. Both effects were blocked upon transfection with dominant negative mutants of IKK, or by pre-incubation with the $\alpha_v\beta_3$ antibody. These findings suggest that fluid shear stress is detected by the $\alpha_v\beta_3$ integrin, acting as a mechanosensor, which transmits the signal into the cell, ultimately resulting in the phosphorylation of IKK and NF- κ B activation. As yet, the steps upstream of IKK have not been established, although the involvement of MEKK, NIK, TRAFs and TNFR have been suggested (Bhullar *et al*, 1998).

6.2.2 *Fluid shear stress, gene expression and implications for cardiovascular disease states*

It has become increasingly apparent that disrupted fluid shear stress plays an important role in cardiovascular disease. Shear stress has been shown to have profound effects on levels of gene expression *in vitro* (Davies, 1995; Braddock *et al*, 1998) (Figure 6.8). It has been speculated that steady laminar fluid shear stress ($\sim 15\text{-}30$ dynes.cm⁻²) exerts a ‘protective’ effect on the endothelium thus desensitising cells to further stimuli, while low or disturbed fluid shear stress triggers endothelial cell sensitivity (Braddock *et al*, 1998).

Steady laminar shear stress inhibits apoptosis in endothelial cells (Dimmeler *et al*, 1998) which is thought to contribute to the functional integrity of the endothelium. Akt kinase has been found to prevent cell death and research has shown that fluid shear stress stimulates phosphorylation of Akt (protein kinase B or Rac kinase) in a time dependent manner (Dimmeler *et al*, 1998). This signal transduction pathway at present is ill

Gene	Transcription Factor Binding Sites
Endothelin-1	AP-1
VCAM	AP-1, NF- κ B
ACE	SSRE, AP-1, Egr-1
TM	Egr-1
PDGF α	AP-1
PDGF β	SSRE, Egr-1
ICAM-1	SSRE
TGF β	SSRE, AP-1, NF- κ B
Egr-1	SREs
c-fos	SSRE
c-jun	SSRE, AP-1
eNOS	SSRE, AP-1, NF- κ B
MCP-1	SSRE, AP-1, NF- κ B

Figure 6.8. Table listing some genes activated by fluid shear stress in endothelial cells coupled with the transcription factor binding sites. Adapted from figure in Braddock et al (1998). Binding sites abbreviations: AP-1, activator protein-1; Egr-1, early growth response factor; NF- κ B, nuclear factor- κ B; SRE, serum response element; SSRE, shear stress response element. Gene abbreviations: VCAM-1, vascular cell adhesion molecule-1; ACE, angiotensin converting enzyme; TM, thrombomodulin; PDGF, platelet derived growth factor; ICAM-1, intracellular adhesion molecule-1; TGF- β , transforming growth factor β ; eNOS, endothelial nitric oxide synthase; MCP-1, monocyte chemoattractant protein-1.

defined but may contribute to profound changes in endothelial morphology and function in response to changes in haemodynamic forces.

Fluid shear stress regulates the amount of endothelin-1 (ET-1) release via PKC and cGMP in cultured HUVEC (Kuchan & Frangos, 1993). The production of ET-1 was found to be dependent on both the duration and magnitude of fluid shear stress exposure. Constant low fluid shear stress ($1.8 \text{ dynes.cm}^{-2}$) or brief (<1 hour) exposure to high fluid shear stress (10 dynes.cm^{-2}) resulted in sustained release of ET-1. In contrast exposure to $6\text{-}25 \text{ dynes.cm}^{-2}$ for periods of more than 6 hours resulted in a dramatic reduction in the release of ET-1. Kuchan & Frangos concluded that increased ET-1 may be mediated by PKC while the following dramatic decrease was caused by fluid shear stress mediated production of cGMP.

Research by Nagel *et al* (1999) showed that simulation of fluid shear stress using spatial gradients similar to those in atherosclerosis-prone regions, resulted in increased levels of nuclear NF- κ B (using p65 staining) relative to those exposed to laminar fluid shear stress or maintained in static culture. The effect was seen as early as 30 minutes after commencing flow. Interestingly, not all cells contained uniform levels of p65 and it was noted that the greatest population diversity was observed in those cells exposed to disturbed fluid shear stress. Although previous studies (Tardy *et al*, 1997) showed that prolonged exposure to disrupted fluid shear stress resulted in increased cell proliferation and migration, the above investigation provided the first evidence that *gradients* of fluid shear stress, rather than its absolute magnitude, influenced endothelial cell biological responses and expression of individual genes. Disturbed fluid shear stress was found to activate NF- κ B, Egr-1, c-jun and c-fos, despite being regulated via different signal transduction pathways. The different activation pathways that are switched on by flow have characteristic time courses that appear to be related to their functional roles (Chien *et al*, 1998; Davies, 2000). It has been postulated that each pathway activates shear sensitive genes in different ways and that loss of balance in the regulatory control is important in the etiology of CV disease states (Papadaki & Eskin, 1997).

Mohan *et al* (1997) demonstrated that NF- κ B was activated as a result of both prolonged exposure to low fluid shear stress (> 2 hours at 2 dynes.cm^{-2}) and pulsatile low shear ($2 \pm 2 \text{ dynes.cm}^{-2}$) in human aortic endothelial cells (HAEC). In contrast, 30 minutes at a higher level of fluid shear stress (16 dynes.cm^{-2}) produced an early but transient increase in NF- κ B activity relative to that of low fluid shear stress. However, this activity was reversed with continued exposure to high fluid shear stress. These results may be implicated in the increased leukocyte adhesion in atherosclerosis prone sites exposed to chronic low shear patterns *in vivo*.

Akimoto *et al* (2000) showed that laminar shear stress (5 and 30 dynes.cm^{-2}) inhibited cell proliferation in both BAEC and HUVEC. Exposure to disturbed fluid shear stress was found to release cells from this 'cell cycle arrest' and the ensuing increased cell proliferation is thought to be important in atherogenesis. Exposure to laminar shear stresses of $< 1 \text{ dyne.cm}^{-2}$ produced different responses in each cell type. In HUVEC this level of shear stress was sufficient to decrease DNA synthesis, but no significant reduction was observed in BAEC. BAEC must therefore have an inhibition threshold between 1 and 5 dynes.cm^{-2} , which may be due to species differences or to the use of cells from different vessels.

Atherosclerosis, characterised by intimal thickening and plaque formation, has been shown to originate in regions of the vasculature that experience low or complex fluid shear stress patterns e.g. areas of arterial curvature and bifurcation (Braddock *et al*, 1998). Ross (1993) proposed that atherosclerosis develops as a consequence of endothelial cell dysfunction resulting from external stimuli which may act singly or in unison to trigger endothelial responses.

Exercise coupled with a healthy diet has been recommended in an attempt to prevent cardiovascular disease. It has been postulated that the beneficial effect of exercise with regard to atherogenesis may be a result of increasing blood flow to branched or curved regions of blood vessels, thus providing a more favourable haemodynamic environment for modulating gene expression and anti-atherogenic pathways (Chien *et al*, 1998).

Since altered haemodynamics have been linked to the pathogenesis of atherosclerosis, thrombosis and restenosis (Papadaki & Eskin, 1997), the development of atheroprotective gene products could have great therapeutic potential, especially after by-pass surgery where the endothelium is exposed to a sudden increase in fluid shear stress.

The effect of shear stress on the endothelium is evidently an area of considerable scientific interest, with obvious clinical implications as well. Continued research will hopefully provide a greater insight into the role of fluid shear stress in the development and progression of vascular disease. This section of the thesis deals with experiments aimed at identifying some components of the transduction pathway involved in the activation of NF- κ B by shear stress.

CHAPTER 7

MATERIALS AND METHODS PART II – NF-κB.

7.1 Cell Culture

Human Umbilical Vein Endothelial cells (HUVEC) were obtained as a gift from Dr Ailsa Webster (Cell Tech, Slough, UK). Cells prior to passage 10 were used for all experiments and cultured in EBM-2 medium (Clonetics®), a modified MCDB131 medium. This was supplemented with 5% FCS, hEGF, hFGF, VEGF, ascorbic acid, hydrocortisone, long R3-IGF-1, heparin and gentamicin/amphotericin supplied in a ‘bulletkit’ (Clonetics®). Cells were grown in a humidified incubator with 5% CO² and 95% air at 37°C.

For experimentation, cells were seeded at a concentration of 2×10^4 cells.cm⁻². For immunofluorescence experiments, cells were plated onto 22mm² (4.24cm²) (N°.1 thickness) borosilicate glass coverslips (BDH 406/0187/33). For cell lysate, DNA binding assay, kinase assay and luciferase assay experiments, HUVEC were seeded onto 7.6 x 2.6cm (19.76cm²) low iron clear glass microscope slides (1-1.2mm thickness) (BDH 406/0180/04). Details of materials for cell culture can be found in appendix 1.

7.1.1 DNA Plasmids and Transient Transfection – NIK, IKK1 and IKK2

Cells were grown on coverslips until 80% confluent. 5 μ g of pCDNA3 empty vector (Invitrogen) and pcDNA expression plasmids containing cDNAs for NIK (provided by Dr David Wallach, Israel), IKK1 and IKK2 (provided by Dr John Taylor, Pfizer Central Research, Sandwich, Kent, UK) and their catalytically inactive mutants; NIKmut, IKK1mut and IKK2mut, were ectopically expressed in HUVEC via Lipofectamine™ technology (Gibco) transfection method. Following a 4 hour incubation with the lipofectamine and DNA constructs, the newly transfected cells were washed once with EBM-2 medium to remove traces of lipofectamine and maintained in culture until the cells were confluent. In order for transfection to be effective, the shearing experiments and static controls were prepared within 36 hours. Details of the materials used in this technique can be seen in Appendix 6.

Cells on both coverslips and slides were exposed to fluid shear stress using the apparatus described in chapter 2.3.3 for varying periods of time at 15 dynes.cm⁻². As well as the sheared cells, cells not exposed to fluid shear stress were analysed in the same way to provide static controls.

7.2 *Drug treatment of HUVEC*

In this set of experiments cells grown on coverslips were incubated with either 20 μ M of the proteasome inhibitor MG132 (BIOMOL) or 20nM leptomycin B (LMB) (Sigma), an inhibitor of I κ B α nuclear export, 30 minutes prior to shearing. Drug treated static controls were also prepared.

To determine if cellular response to flow was protein kinase C (PKC) dependent, cells were exposed to combinations of 25ng.ml⁻¹ Phorbol 12-myristate 13-acetate (PMA), 1 μ g.ml⁻¹ ionomycin and/or 100nM Bisindolylmaleimide (bisin) for 30 minutes prior to exposure to flow or fixing for immunofluorescence. In the case of PMA, ionomycin and bisin treated cells, cells were pre-treated with bisin for 30 minutes and the culture medium was changed prior to PMA and ionomycin administration.

HUVEC cultured in 6 well plates and slides were treated with 30ng.ml⁻¹ TNF (Insight) for specific time points (0, 5, 10, 20, 30, 60, 120 & 240 minutes) for use in immunoblotting and kinase assay experiments as a comparison to the effects of flow.

7.3 *Immunostaining and Fluorescence Microscopy*

The translocation of NF- κ B in response to fluid shear stress and drug treatment was investigated using immunofluorescence (details of materials can be found in appendix 2). Cells were rinsed (x2) with PBSc before fixing for 10 minutes in 3%

paraformaldehyde/PBS. This was followed by 3 rapid rinses in PBSa before 2 x 10 minute washes in 0.1M Glycine/PBSc to quench the paraformaldehyde. Following 2 rapid washes in PBSa, cells were permeabilised in 0.2% Triton-X100/PBS (Sigma-T8787) for 10 minutes. After rinsing (x3) in PBSa, the cells were blocked in 0.2% BSA/PBS for 5 minutes before adding the primary antibody solution and leaving in the dark for 45 minutes at RT. Monoclonal primary antibodies to hnRNP A1 (gift from Dr G. Dreyfuss, University of Pennsylvania) and p-65 (F-6) (Santa Cruz) were used at working concentrations of 1:200 and 1:100 respectively. Rabbit polyclonal antibodies to NIK (H-248), IKK1 (H-744) and IKK2 (H-470) and p65 (C-20) (all from Santa Cruz) were used at a concentration of 1:100. Following 3 x 5 minute rinses in 0.2% BSA, the following secondary antibodies were used at a concentration of 1:200: Goat anti-mouse FITC (GAMF) and goat anti-rabbit Texas Red (GART)(Southern Biotech Inc.). After 3 further rinses in BSA and one rapid rinse in PBS, the preparations were mounted in hydromount (BDH). The cells were viewed using a Nikon microphot camera at x 100 magnification.

7.4 Immunoblotting

The breakdown of NF- κ B inhibitor proteins (IkB α , IkB β & IkB ϵ) were studied using Western blotting to monitor activation of the transcription factor by flow. In order to investigate the effects of shear stress on IkB α , IkB β & IkB ϵ degradation, cells were sheared for the same time periods as BAEC and lysates were made according to the method detailed in chapter 2.4.1. The western blotting techniques previously described (chapter 2.4.1-2.4.3 & appendix 3) were used to analyse the extracts. Rabbit polyclonal primary antibodies to IkB α (C-21), IkB β (C-20), and IkB ϵ (M-364) (Santa Cruz) were used along with sheep polyclonal affinity purified antibodies to p105 and p50 (Diagnostics Scotland) to detect the appropriate proteins. All primary antibodies were used at a concentration of 1:1000. The secondary antibodies used to detect the immobilised antibody/antigen complexes were anti-sheep HRP (DAKO), goat anti-mouse HRP and goat anti-rabbit HRP (Santa Cruz), used at concentrations of 1:10000.

7.5 *Luciferase assay*

HUVEC were grown on microscope slides and transfected with 10 μ g of the 3enh Con A Luc plasmid which contains 3 binding sites for NF- κ B (Figure 7.1). Other HUVEC were transfected with the negative control Con A Luc plasmid which lacks the NF- κ B binding sites. Both plasmids were the kind gift of Dr F. Arenzana-Seisdedos, Institute Pasteur, Paris. Once cells reached confluence, they were exposed to fluid shear stress for 12 hours and maintained in culture for an additional 24 hours. Cells were lysed and after cell extract standardisation, luciferase activity was assayed. Luciferase activity was measured using the MicroLumat (LB96P) plate reader and expressed in relative light units (RLUs).

7.6 *IKK Immunocomplex kinase activity assay*

HUVEC were exposed to fluid shear stress for the denoted time points and subsequently extracted in 1ml of lysis buffer (appendix 6). The prepared lysate was cleared by high-speed centrifugation at 80,000 RPM at 4^oC for 30 minutes. The supernatant was removed and incubated for 2 hours at 4^oC with 10 μ l of protein A beads conjugated to an antibody raised in sheep and affinity purified against the C-terminus of IKK1 (residues 734-745). The immunoprecipitated material was washed twice with lysis buffer, twice with pulldown buffer and once with kinase assay buffer (see appendix 6). Following washing, the immunocomplex was resuspended in a total volume of 30 μ l containing 20 μ l kinase assay buffer, 3 μ Ci of [γ -³²P] ATP, 10 μ M ATP and 1 μ g of wild type GST-N Terminal I κ B α (amino acids 1-70) or the GST-N Terminal I κ B α 32 S/A and 36 S/A mutant. After 1 hour at 30^oC the reaction was terminated by adding 3x SDS sample. The samples were then boiled for 5 minutes, separated on a 12.5% SDS polyacrylamide

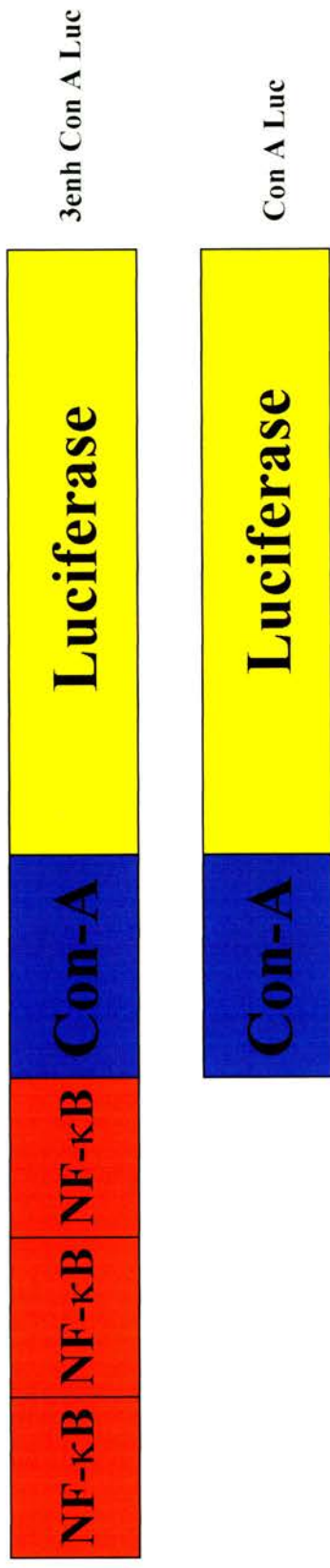


Figure 7.1 Schematic representation of the NF-κB dependent luciferase reporter plasmid insert (3enh Con a Luc), which contains 3 binding sites for NF-κB and the negative control plasmid (Con A Luc), which lacks NF-κB binding sites. These plasmids were transfected into BAEC and HUVEC cell lines to determine the effects of shear stress on NF-κB transcriptional activation (see Chapter 8).

gel. On completion of gel-electrophoresis, the radioactive species was detected using a phosphorimager (Fuji Bas 1500).

N.B. Transfection of cells, luciferase assays and the IKK Immunocomplex kinase activity assays were performed in the BMS building by Dr David Hay and Dr Lesley Thomson respectively.

CHAPTER 8

RESULTS PART II

THE EFFECTS OF FLOW ON I κ B PROTEOLYSIS IN BOVINE AND HUMAN ENDOTHELIAL CELLS.

8.1 Introduction

As previously described (Chapter 6), the NF- κ B/Rel family of inducible transcription factors play a pivotal role in the response of cells to a wide variety of stimuli including cytokines (e.g. TNF α & IL-1), UV radiation and bacterial products (e.g. LPS) (Baldwin, 1996). Lan *et al* (1994) showed that shear stress also rapidly activates the transcription factor NF- κ B in cultured bovine endothelial cells. In the experiments described here, the kinetics of I κ B isoform (I κ B α , I κ B β and I κ B ϵ) degradation in response to uniform laminar flow were investigated in BAEC and HUVEC.

8.2 Fluid shear stress enhances NF- κ B dependent gene transcription

To determine the functional consequences of shear stress on NF- κ B transcriptional activation, BAEC and HUVEC were transfected with either a NF- κ B dependent luciferase reporter (3enh Con A Luc) or a plasmid lacking the κ B consensus binding sites (Con A Luc) which acted as a negative control. Once transfected, cells were exposed to 15 dynes.cm⁻² for 12 hours and were then cultured for a further 12 hours before determining luciferase reporter activity. The 3enh Con A Luc transfected cells exhibited a 19-fold increase in reporter activity (Figure 8.1). This assay was also performed on BAEC sheared for up to 16 hours (not shown) where a similar result was obtained, indicating that in both cell lines NF- κ B is specifically activated under these conditions.

8.3 Fluid shear stress-induced degradation of I κ B isoforms in BAEC

Monolayers of BAEC were exposed to 15 dynes.cm⁻² for time periods ranging from 5 minutes to 16 hours. Whole cell extracts were prepared (Section 2.4.1) and I κ B levels in sheared and unsheared (control) cells were estimated by Western blotting using rabbit

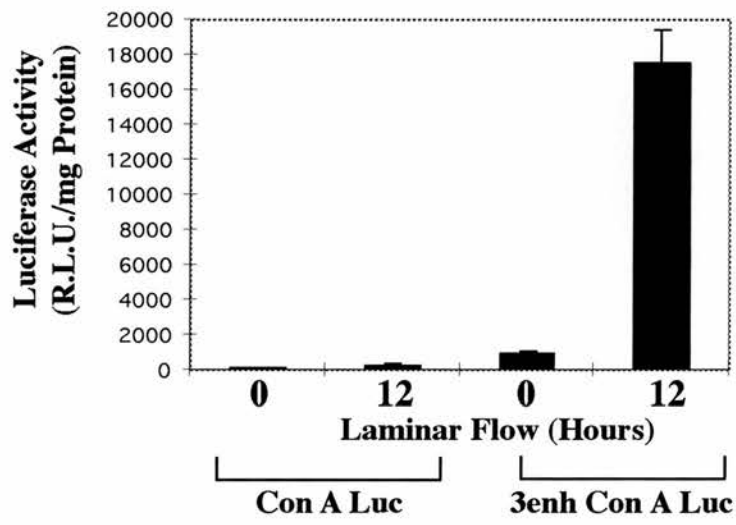


Figure 8.1

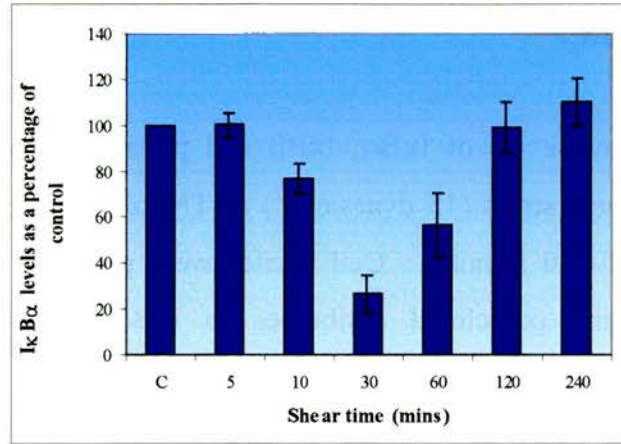
polyclonal antibodies to IκBα, IκBβ and IκBε. The levels of each IκB-isoform present in sheared cells were expressed as a percentage of the 'static' controls. Results showed that flow induced a detectable reduction in the levels of IκBα, IκBβ and IκBε (Figure 8.2 a-c) within 10 minutes. Levels of IκB were found to decrease to 20% of their control levels within 30 minutes (IκBα), 60 minutes (IκBβ) and 60-120 minutes (IκBε) respectively. IκBα and IκBβ levels recovered fully by 120 minutes exposure while IκBε remained depressed at ~40-60% of its 'unsheared' level even after 16 hours. Increasing the magnitude of shear stress from 15 to 50 dynes.cm⁻² (not shown) resulted in little change in the kinetics of IκB degradation, except for a transient overshoot in IκBα recovery to 1.5 times the control levels after 240 minutes under flow.

8.4 Fluid shear stress-induced degradation of IκB isoforms in HUVEC

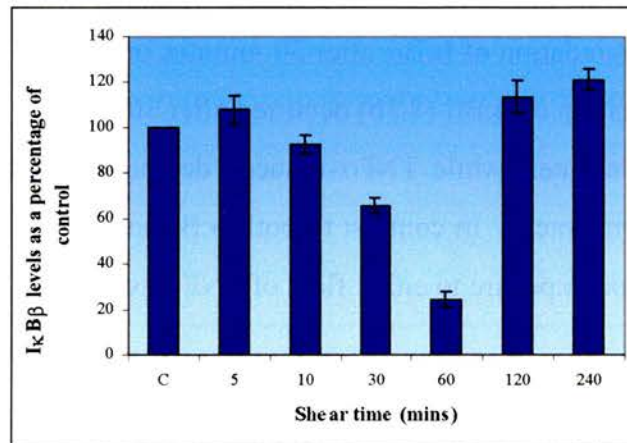
HUVEC were subjected to 15 dynes.cm⁻² of shear stress for up to 16 hours and whole cell extracts were prepared. Samples were then analysed by Western blotting using rabbit polyclonal antibodies to IκBα, IκBβ and IκBε and densitometry readings of immunoblots were standardised to actin controls.

The findings showed that IκBα was maximally degraded after 30 minutes exposure to shear stress (Figure 8.3a) with resynthesised IκBα detectable after 60 and 120 minutes of flow. However, after 240 minutes, IκBα levels were found to decrease once again, suggestive of a biphasic pattern of breakdown. Densitometric analysis showed that IκBα levels were reduced to 32% and 35% of the static control values after 30 and 240 minutes respectively. The trend observed for IκBβ contrasted with that of IκBα. IκBβ was found to be maximally degraded after 30 and 60 minutes exposure to flow but had fully recovered by 120 minutes, with no further evidence of degradation at any of the longer time points (Figure 8.3b). Densitometric analysis for IκBβ showed IκBβ levels were reduced to 6% and 7% of the static control values at 30 and 60 minutes, respectively.

(a)



(b)



(c)

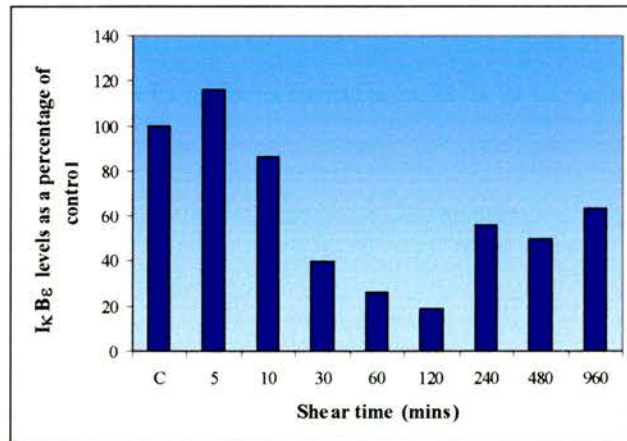
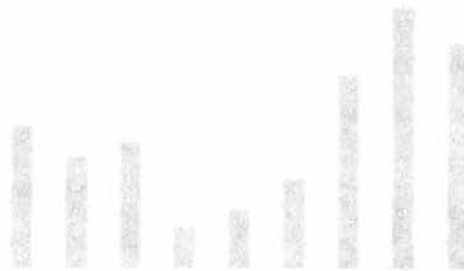


Figure 8.2 (a-c) A graphical representation of levels of IκBα (a), IκBβ (b) and IκBε (c) respectively in BAEC exposed to 15 dynes.cm⁻² for time periods ranging from 0-960 minutes. Cell lysates were prepared and analysed by Western blotting. The mean levels (+/- SEM; n= 5, 3 & 1 respectively) of each isoform are expressed as a percentage of levels present in 'static' controls. The pattern of flow-induced degradation was different for each isoform. IκBα and IκBβ degradation was maximal after 30 and 60 minutes respectively and recovered to that of control cells by 120 minutes. IκBε showed maximal degradation between 60 and 120 minutes and recovery was not complete, even after 960 minutes.

Figure 8.3 Shear stress induces degradation of I κ B α and I κ B β but not p105 degradation in HUVEC.

Figures 8.3 (a-c) show levels of I κ B α , I κ B β and p105 respectively in HUVEC subjected to either shear stress (15 dynes.cm⁻²) or TNF α treatment (30ng.ml⁻¹) for times ranging from 0-240 minutes. Cell lysates were prepared and analysed by Western blotting using polyclonal antibodies to I κ B α , I κ B β and p105 and densitometry readings were standardised to immunoblots of actin expression. The patterns of degradation was found to be different for different I κ B isomers.

Figure 8.3a shows degradation of I κ B α after 30 minutes of flow or TNF α treatment. Flow-induced degradation of I κ B β (8.3b) occurred after 30 minutes, and remained at this level until 120 minutes, while TNF α -induced degradation did not occur until after 120 minutes of treatment. In contrast to both I κ B α and I κ B β , p105 showed no signs of degradation on exposure to either flow or TNF α even after 4 hours.



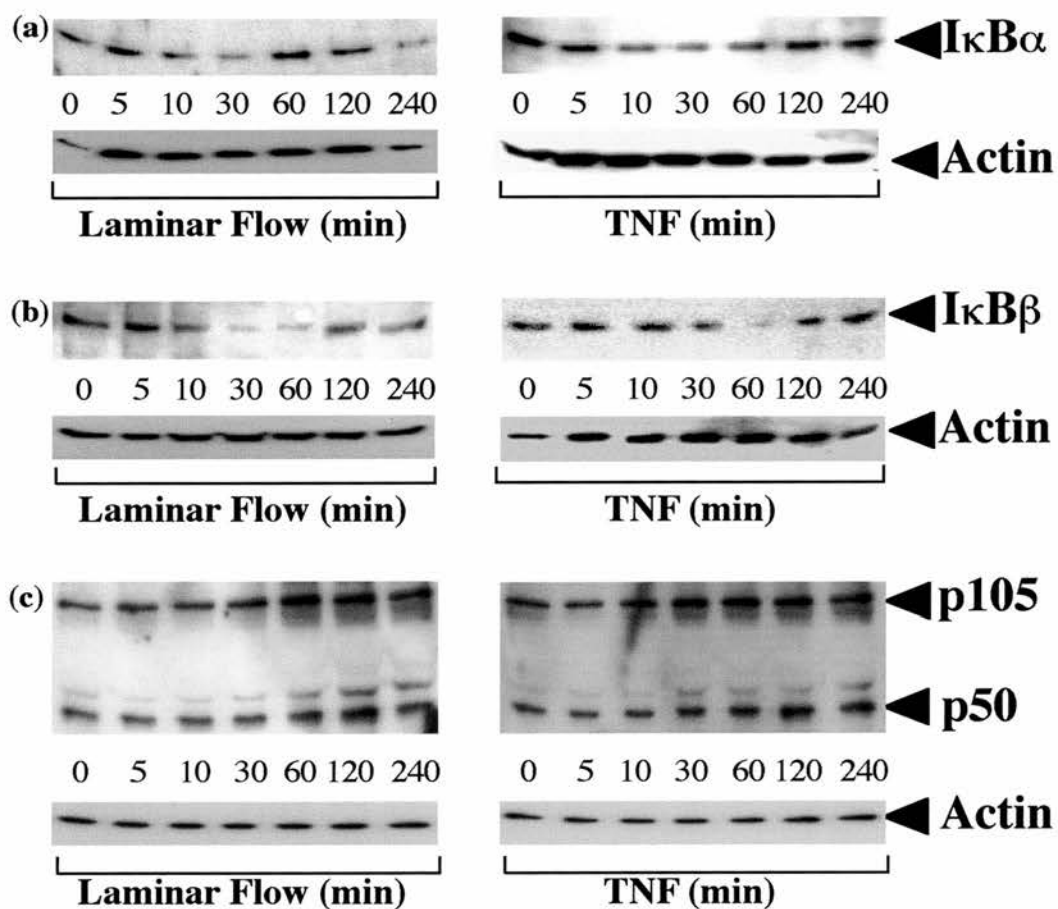


Figure 8.3

8.5 Time course of IκB degradation in response to TNFα stimulation

Shear stress-induced IκB degradation was compared to that resulting from TNFα stimulation (30ng.ml⁻¹). TNFα induced a transient decrease in IκBα levels. Maximum degradation was obtained after 30 minutes treatment (Figure 8.3a), with levels of ~ 48% of the untreated (control) cells. IκBα rose to control levels after ~120 minutes of treatment (Figure 8.3a). TNFα treatment resulted in maximum degradation of IκBβ after 60 minutes, to ~ 11% of the untreated control.

Whole cell extracts were also analysed by Western blotting using affinity-purified sheep polyclonal antibody to p105/p50 (Figure 8.3c). In contrast to the IκB isoforms, levels of p105 did not decrease in response to either shear stress or TNFα.

8.6 Discussion

Measurements of gene transcription using the NF-κB-dependent luciferase reporter (3 enhancer Con A-Luc) are consistent with previously described bovine models showing that shear stress is an activator of NF-κB (Resnick *et al*, 1993; Lan *et al*, 1994, Khachigian *et al*, 1995; Bhullar *et al*, 1998). In separate experiments, conducted with Dr David Hay, a DNA binding assay using a ³²P-labelled oligonucleotide containing a known SSRE was performed on nuclear extracts from HUVEC exposed to varying periods of shear stress. Binding of this oligonucleotide to the SSRE was measured by an electrophoretic mobility shift assay (EMSA). Results showed a transient peak in DNA binding after 30 minutes of shearing which decreased to ~ 50% of its maximum value when cells were sheared for 60-240 minutes. Pre-treatment of nuclear extracts with anti-p65/anti-p50 produced a super shift of labelled oligonucleotide confirming that shear stress activates the p65/p50 heterodimer.

The results presented in this chapter show that flow induces degradation of IκBα, β and ε isoforms in both BAEC and HUVEC cell lines. IκBα is degraded first, followed by IκBβ and then IκBε. IκBα and IκBβ recover rapidly, however IκBε shows little recovery even after 16 hours. The recovery of IκBα levels at longer shear times (>60 minutes) is consistent with the fact that NF-κB is known to activate transcription of the IκBα gene. Newly-synthesised IκBα attaches to NF-κB, reducing its binding to DNA and terminating its transcriptional activity (Arenzana-Seisdedos *et al*, 1995). The fact that IκBβ and IκBε also recovered under flow, at least in part, suggests that NF-κB might also regulate IκBβ and IκBε transcription in a similar manner.

Previous work on bovine endothelial cells (Bhullar *et al*, 1998) identified some elements of the signalling pathway involved in flow-induced activation of NF-κB. Their findings showed that proteolysis of IκB and activation of IKK1, IKK2 were essential in this process. The experiments described here confirm flow-induced degradation of the IκB

isoforms in human as well as bovine endothelial cells. The following chapter investigates further the NF- κ B activation pathway in cultured HUVEC exposed to uniform laminar flow.

CHAPTER 9

RESULTS PART II

ROLE OF IKK1, IKK2 & NIK IN FLOW -INDUCED NF- κ B ACTIVATION.

9.1 Introduction

To date, the nature of the upstream signalling elements involved in flow-dependent activation of NF-κB in human cells has not been investigated, although this is of considerable interest in the light of studies implicating the involvement of NF-κB in the pathogenesis of atherosclerosis (Collins, 1993; Brand *et al*, 1996; Nagel *et al*, 1999; Hajra *et al*, 2000). Based on these studies it was decided to discontinue working with bovine cells and concentrate on human endothelial cells only.

The aim of the experiments described here was to determine whether IKK1, IKK2 and NIK play a part in shear stress-induced NF-κB activation in HUVEC. Cells grown on glass microscope slides and coverslips were exposed to uniform laminar flow (15 dynes.cm⁻²) for various periods ranging from 5-240 minutes. They were then analysed biochemically and by immunofluorescence to assess the degree of NF-κB activation.

9.2 Fluid shear stress induces IKK activation in cultured endothelial cells

In order to establish whether shear stress-induced degradation of IκB isomers was IKK1 and IKK2 dependent, the endogenous activity of IKK was measured in HUVEC extracts. Cells were either stimulated by flow (15 dynes.cm⁻²) or by treatment with TNFα (30ng.ml⁻¹) prior to performing a kinase assay (Chapter 7.6). Cell extracts were prepared and the IKK complex was immunoprecipitated with a polyclonal antibody against the C-terminal of IKK1. This antibody also recognises IKK2. Kinase activity was assessed by measuring the amount of ³²P incorporated into a GST-IκBα 1-70 wild type (WT) fusion protein. A negative control was employed in the form of GST-IκBα 1-70 S32E/S36E (S/E) substrate, in which the critical phosphoacceptor serine residues (S) 32 and 36 had been replaced by glutamic acids (E). IKK recovery was recorded by immunoblotting for IKK1.

Figure 9.1 (a-d) illustrates the results of the HUVEC kinase assay. Shear stress caused a rapid activation of IKK, with maximum kinase activity detected after 5 minutes and then again after 120 minutes exposure to flow (Figure 9.1 a & b). In contrast, TNF α treated cells exhibited peak kinase activity after 10 minutes of TNF α treatment, decreasing thereafter to control levels between 30 and 240 minutes (Figure 9.1 c & d). The mutant substrate (GST-I κ B α 1-70 E) showed no signs of phosphorylation upon exposure to either shear stress or TNF α (Figure 9.1 a & c), confirming the specificity of the kinase assay. Levels of IKK recovered after immunoprecipitation following exposure to flow or TNF α were detected via immunoblotting (Figure 9.1 a & c) and were found to remain constant.

9.3 Immunofluorescence analysis of flow-induced NF- κ B activation

NF- κ B activation was detected in single cells by monitoring the nuclear translocation of the p65 subunit via indirect immunofluorescence. Untransfected (control) cells and HUVEC transfected with empty plasmid (pCDNA3) were exposed to shear stress (15 dynes.cm⁻²) for 0, 30 and 120 minutes (Figure 9.2). Immunostaining with a mouse monoclonal p65 antibody (F6) monitored p65 translocation into the nucleus (Figure 9.2 a & b). The number of cells exhibiting nuclear p65 staining was measured using photographic enlargements of randomly selected areas of coverslip and expressed as a percentage of the total number of cells examined.

NF- κ B nuclear translocation was found to be maximal after 30 minutes of flow. A similar percentage of untransfected (42% +/- 12%) and pCDNA transfected (45% +/- 3%) cells were activated (Figure 9.2 a & b). These results are in agreement with the previous findings showing maximum degradation of I κ B α and I κ B β after 30 minutes exposure to flow (Figure 8.2). Nuclear p65 was slightly reduced after 120 minutes exposure to flow, with 33% +/- 5.5% and 39% +/- 7.8% of untransfected and pCDNA transfected cells, respectively, displaying NF- κ B nuclear translocation (Figure 9.2 a & b).

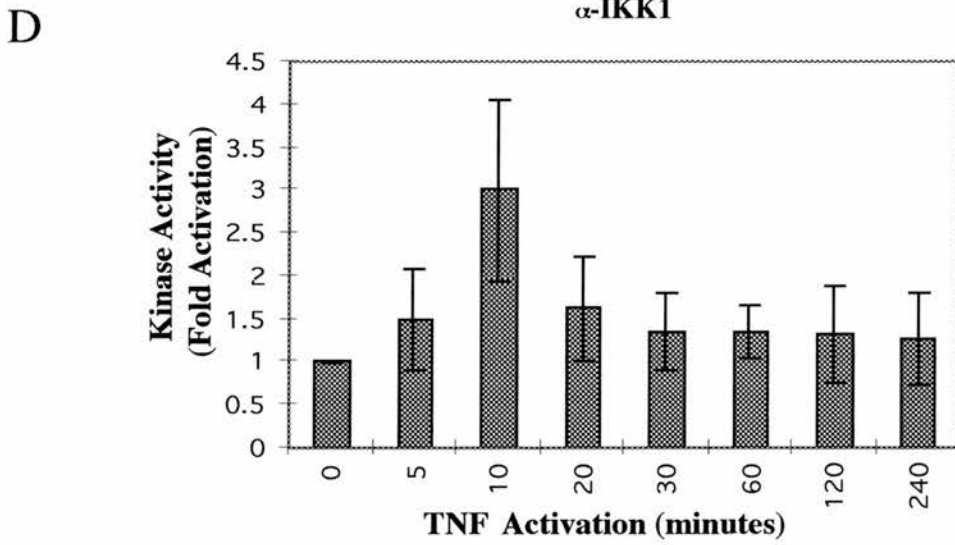
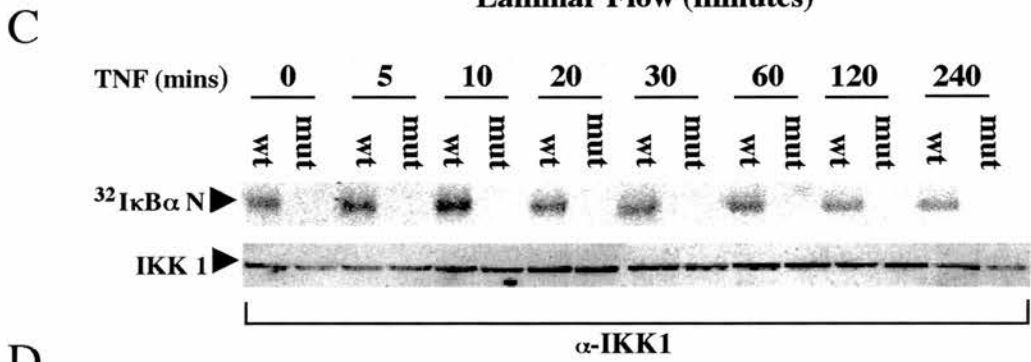
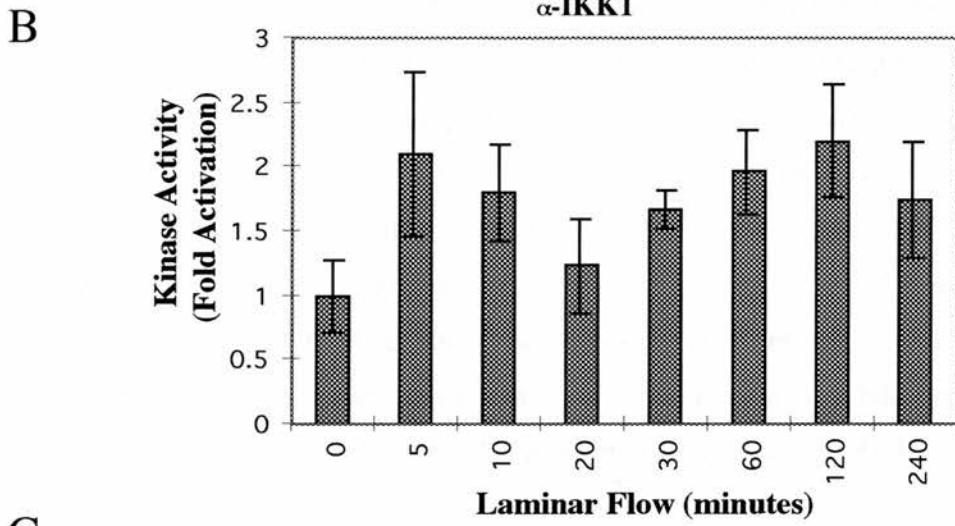
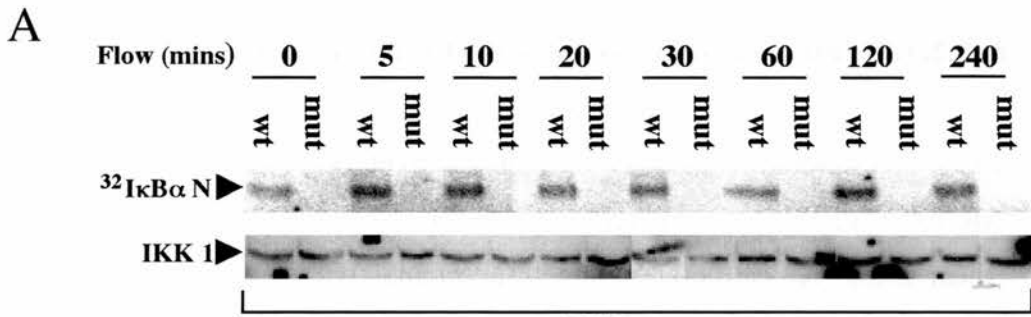


Figure 9.1

Figure 9.2. (a-e) Fluid shear stress induces NF- κ B nuclear translocation.

HUVEC which were untreated (a), transfected with pCDNA (b) and those pre-treated with MG132 (c) and LMB (d) were exposed to 0, 30 and 120 minutes of 15 dynes cm^{-2} shear stress. All cells were then immunostained with a monoclonal antibody to the p65 subunit of NF- κ B (except figure (e) where a monoclonal antibody to hnRNP was used). Figure 9.2(a) shows p65 redistribution in untransfected (control) cells. NF- κ B-p65 undergoes translocation from cytoplasm to nucleus within 30 depicting NF- κ B activation, an effect which was reversed by 120 minutes as a result of activation of nuclear export pathways. Figure 9.2b illustrates the effect of FSS on HUVEC transfected with pCDNA. As with control cells (a), nuclear translocation was evident by 30 minutes exposure and was reduced by 120 minutes. Thus, transfection did not appear to inhibit the shear stress response. Treatment of HUVEC with the proteasome inhibitor MG132 for 30 minutes prior to shearing (c) was found to inhibit nuclear translocation of NF- κ B-p65. In contrast, pre-treatment of cells with LMB (d) allowed nuclear translocation of p65, but prevented nuclear export. Untreated HUVEC were also immunostained with a monoclonal antibody to hnRNP-A1 before and after exposure to FSS. The distribution of hnRNP-A1 was not affected by flow.

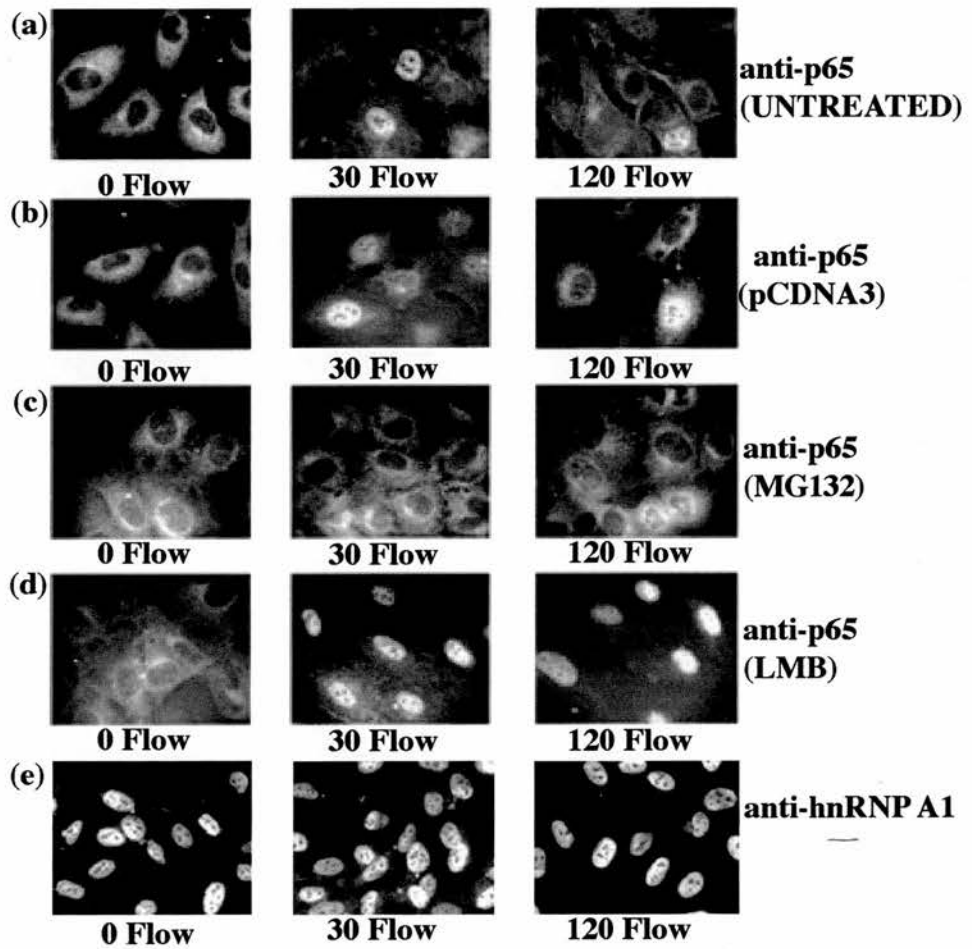


Figure 9.2

HUVEC were also treated with MG132 and leptomycin B (LMB). MG132 specifically inhibits proteasome activity and therefore prevents NF- κ B activation. This results in cytoplasmic accumulation of polyubiquitinated I κ Bs (Chen *et al*, 1995) and blocks p65 nuclear translocation. In contrast, LMB targets CRM1/exportin-1, inhibiting nuclear export of I κ B α , leading to an accumulation of NF- κ B-I κ B complexes in the nucleus (Forenerod *et al*, 1997; Ossareh-Nazari *et al*, 1997).

MG132 or LMB were administered 30 minutes prior to exposure to flow. After shearing, immunostaining revealed nuclear translocation of p65 in those cells treated with LMB but not MG132 (Figure 9.2 c & d). HUVEC incubated with MG132 showed that only a small fraction of cells exhibited p65 nuclear staining (9% +/- 1.9%) and (6% +/- 1.7%) after 30 minutes and 120 minutes respectively (Figure 9.2c). In contrast, 97% +/- 0.9% and 98% +/- 1.7% of LMB treated cells exhibited nuclear staining after the same time periods (Figure 9.2d).

9.4 Catalytically inactive mutants of IKK1 and IKK2 inhibit NF- κ B nuclear translocation

HUVEC were transfected with plasmids encoding either the wild type IKK1 and IKK2 proteins (IKK1 and IKK2) or their catalytically inactive mutants (IKK1mut and IKK2mut) to determine what role, if any, IKK1/2 play in flow-induced NF- κ B activation. Cells were exposed to flow for 30 and 120 minutes, while unsheared cells were used as static controls. Double indirect immunofluorescence using a monoclonal p65 antibody was used to detect NF- κ B nuclear translocation in cells transfected with IKK wild type and IKKmut plasmids (Figures 9.3 (a-d) and 9.4 (a-d)). Individual cells that were transfected with IKK1/2 were identified using polyclonal antibodies. The threshold of antibody detection was again too high to detect endogenous IKKs (Figures 9.3 (b & d) and 9.4 (b & d)).

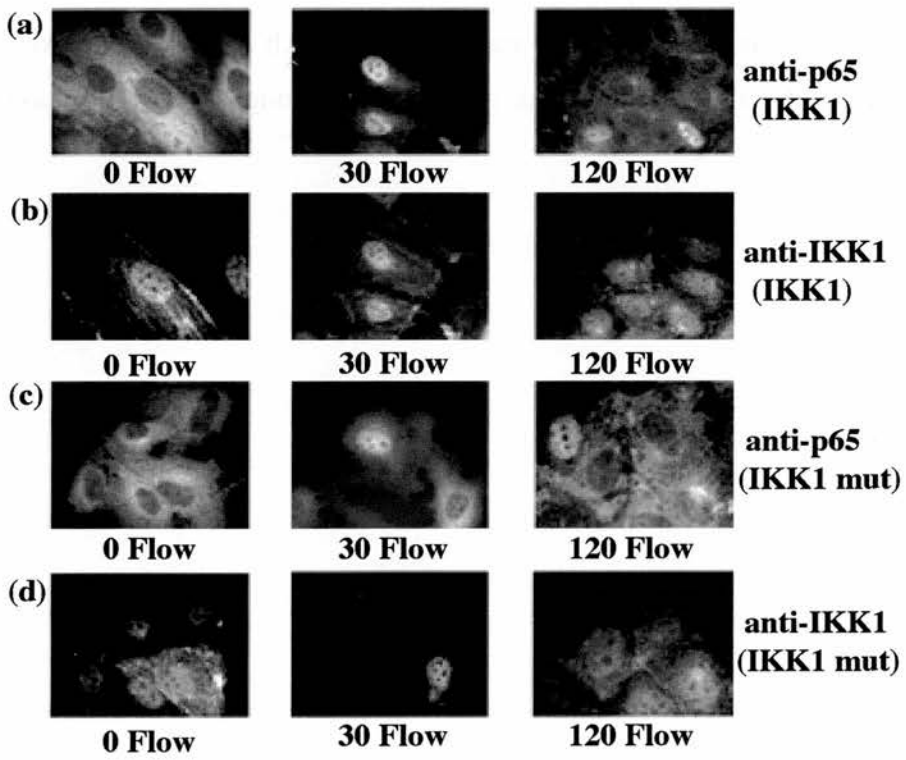


Figure 9.3

Figure 9.4 (a-d). Transfection of HUVEC with IKK2 and IKK2mut plasmids.

HUVEC transfected with IKK2 and IKK2mut plasmids were exposed to 15 dynes.cm⁻² FSS for 0, 30 and 120 minutes respectively. Immunostaining with monoclonal p65 detected nuclear translocation of NF-κB-p65 (a & c). p65 was present in the nucleus after 30 minutes in IKK2 transfected cells (a). By 120 minutes these cells had reduced levels of nuclear p65 due to the auto-regulatory NF-κB feedback mechanism. In contrast to IKK2, transfection of the catalytically inactive mutant IKK2mut was found to inhibit nuclear translocation of NF-κB (c). An antibody to IKK2 was used to detect transfected cells (b & d). Only exogenous IKK2 was detected, as the method was not sensitive enough to reveal endogenous levels.

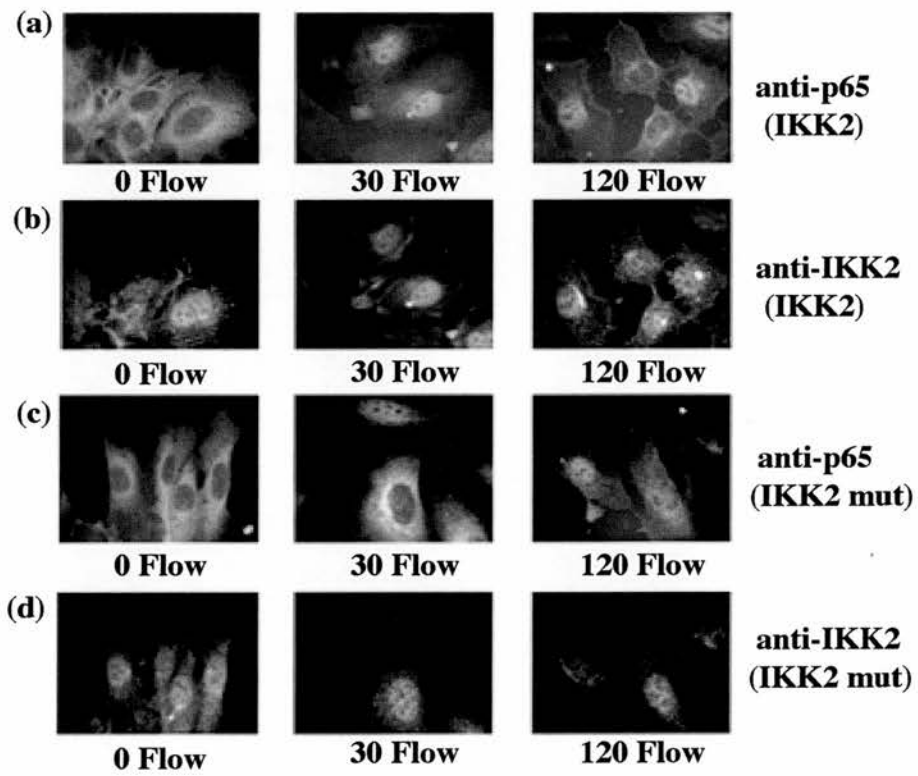


Figure 9.4

The results (Figures 9.3 (a & c) and 9.4 (a & c)) show that p65 was present in the nuclei of cells over-expressing IKK1 and IKK2 after flow, but not in cells that had been transfected with IKK1mut or IKK2mut.

9.5 *The catalytically inactive mutant of NIK inhibits NF- κ B nuclear translocation*

HUVEC were also transfected with plasmids coding for wild-type NF- κ B inducing kinase (NIK) or its catalytically inactive mutant (NIKmut) to establish whether NIK is involved in the shear stress-induced NF- κ B activation pathway. Cells were exposed to shear stress for 30 minutes and 120 minutes and unsheared cells were used as static controls (Figure 9.5 a & c). Nuclear translocation of NF- κ B was monitored using the p65 antibody and cells that were transfected with NIK or with NIKmut were identified using a rabbit polyclonal antibody to NIK. As above, only transfected cells were detected under these experimental conditions (Figure 9.5 b & d), as the levels of endogenous NIK were below the level of antibody detection.

Shear stress induced nuclear translocation of NF- κ B-p65 in cells transfected with wild type NIK but not in NIKmut cells (Figure 9.5). In NIK transfected cells, p65 nuclear translocation was optimal after 30 minutes and had decreased by 120 minutes, implying nuclear clearing via the NF- κ B negative feedback loop.

9.6 *Activation of NF- κ B by flow is not dependent upon protein kinase C*

Protein kinase C (PKC) is known to activate NF- κ B in response to treatment with phorbol 12-myristate 13-acetate (PMA; 25ng.ml⁻¹) and ionomycin (1 μ g.ml⁻¹; Brockman *et al*, 1995; May & Ghosh, 1998). Bisindolylmaleimide –1 (bisin) is a selective inhibitor of the ATP-binding site of PKC (Toullec *et al*, 1991). The following experiment was performed to determine if flow-induced activation of NF- κ B is also dependent upon PKC. First, control cells were treated for 30 min with PMA and ionomycin only.

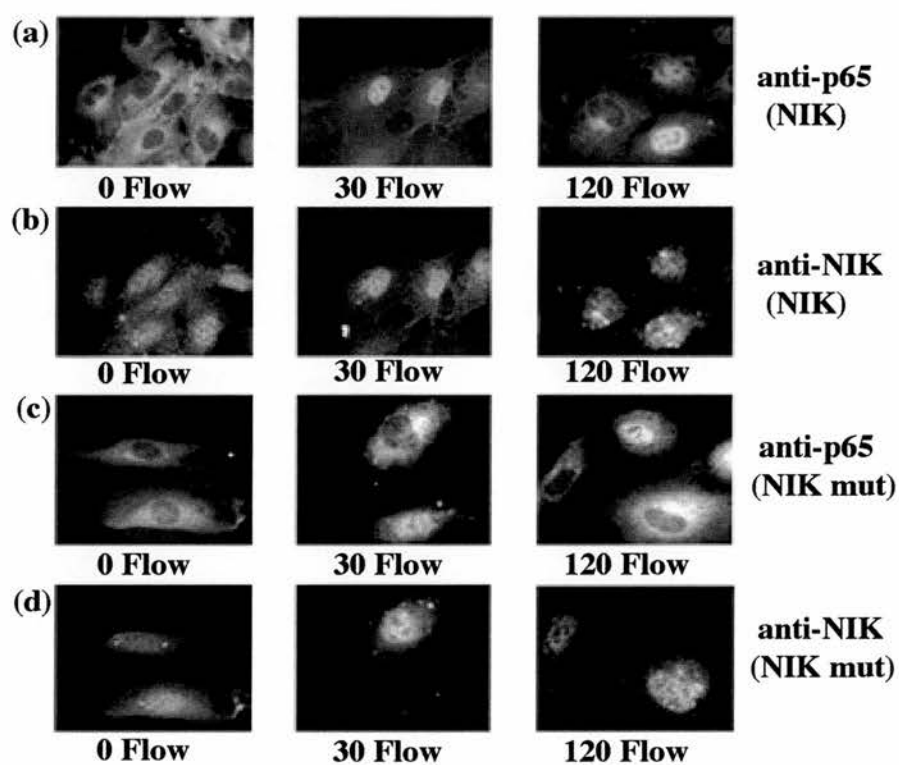


Figure 9.5

Nuclear translocation of p65 occurred in virtually 100% of the cells. Under static conditions, only minimal evidence of NF- κ B-p65 translocation was observed in untreated (2%), bisin treated (3%; 100nM) and a combination of bisin + PMA + ionomycin treated (4%) cells respectively. However, nuclear translocation was normal in cells that were pre-treated with bisin and then subjected to flow (Figure 9.6). Nuclear translocation was optimal after 30 minutes. These results show that PKC is not involved in the activation of NF- κ B by shear stress.

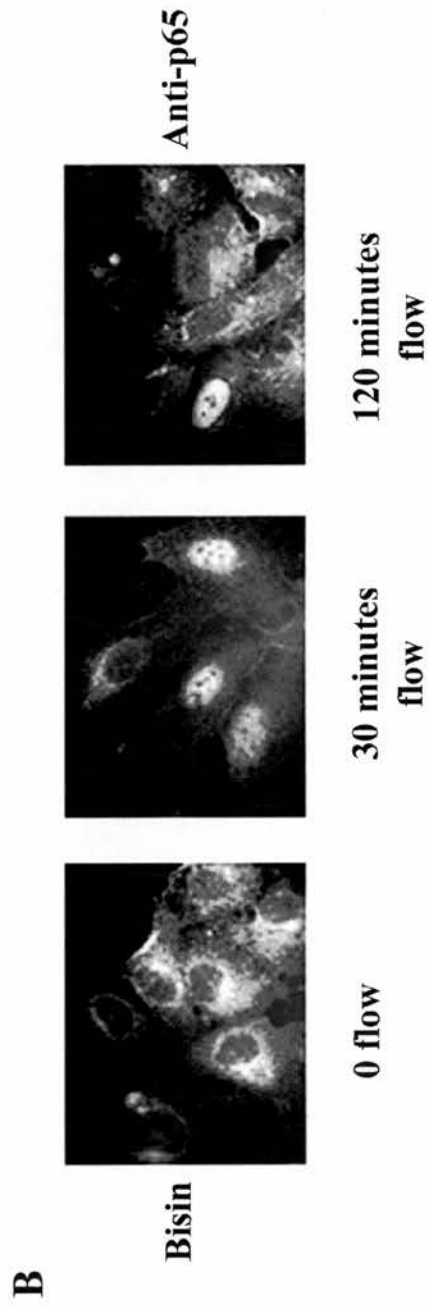
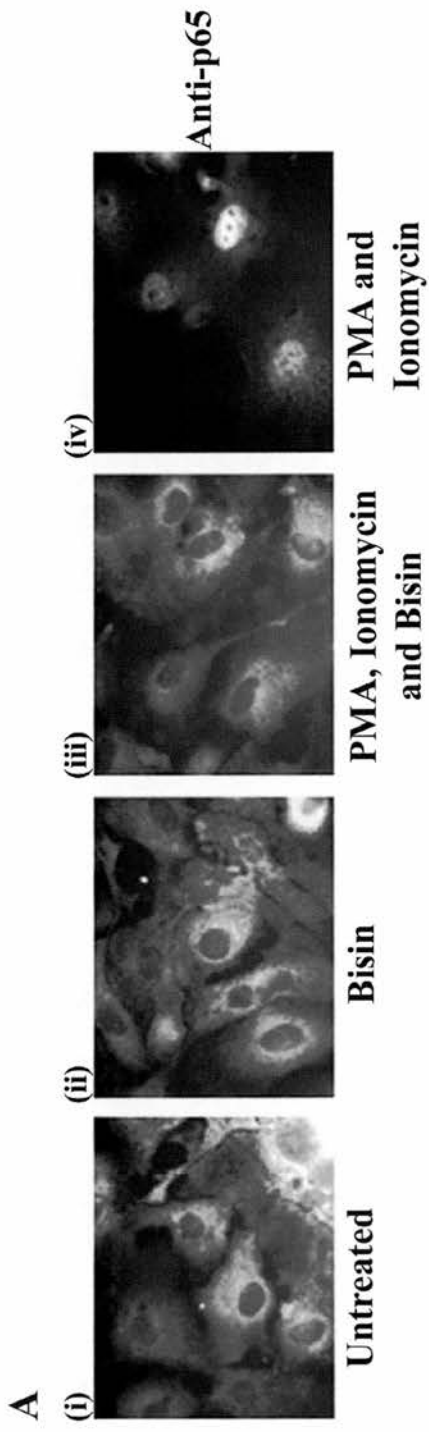


Figure 9.6

9.7 Discussion

Shear stress increases the transcriptional activity of NF- κ B (Resnick *et al*, 1993; Lan *et al*, 1994; Khachigian *et al*, 1995; Shyy *et al*, 1995; Bhullar *et al*, 1998). Bhullar *et al* (1998) studied flow-dependent activation of IKK1 and 2 in bovine cells over-expressing haemagglutinin (HA) epitope-tagged IKK1 and IKK2. Their results showed that HA-IKK1/2 activity was enhanced by shear stress (12 dynes.cm⁻²). Increased activity was detectable after 5 minutes of flow and reached a maximum of ~ 3.3 x control levels after 30 minutes. The time course of IKK activation under flow was considerably different in the present experiments. Here, wild type HUVEC were used and *endogenous* kinase activity was measured. The results obtained suggest a more complex pattern of activation. An early increase, rising to ~ 2 x control levels was seen after only 5 minutes, then a decline to control levels after 20 minutes, followed by a secondary peak, comparable in size to the first, after 120 minutes of flow. This is suggestive of a *biphasic* pattern of activation, or possibly even of a *cyclical* pattern, although more experiments with time points >240 minutes would be required to confirm or refute this hypothesis.

Nuclear translocation of p65 sub-unit was blocked in cells transfected with catalytically inactive mutant forms of IKK1 or IKK2, but not in cells transfected with wild type IKK1 or IKK2. These results are in agreement with those of Bhullar *et al* (1998) and show that activation of NF- κ B by flow requires both kinases. IKK1 and 2 are themselves downstream targets for members of the MAP kinase kinase kinase (MAPKKK) family of enzymes, one of which, called NF- κ B-inducing kinase (NIK) activates IKK1 and 2 by phosphorylating serine residues. The experiments described here demonstrate that cells transfected with the catalytically inactive mutant of NIK failed to show nuclear translocation of p65 in response to flow. It follows from this that NIK, as well as IKK1 and 2, is required for flow activated NF- κ B-dependent gene transcription. In contrast to this result, unpublished experiments from this laboratory (Hay, Cameron & Flitney, personal communication) found that treating cells with an inactive mutant of a related kinase, called TPL2 (tumour progression locus 2) kinase, did not prevent nuclear

translocation, showing that this enzyme is not an upstream component of the flow-activated pathway. Similarly, the inability to prevent nuclear translocation of p65 with bisin shows that PKC is not involved in the pathway.

Activation of the NIK-IKK1/2 pathway by flow was followed by a transient reduction in I κ B α and I κ B β levels. Western blotting showed that I κ B α and I κ B β degradation was maximal after 30 and 30-60 minutes, respectively. Pre-flow levels of both inhibitors were re-established after 60-120 minutes of flow. These results are comparable to those obtained using bovine cells, reported in an earlier Chapter, and with the results of Bhullar *et al* (1998). NF- κ B is known to initiate transcription of the I κ B α gene, leading to the synthesis of new protein in the cytoplasm. Newly synthesised I κ B α then enters the nucleus, binds to NF- κ B and inhibits its transcriptional activity. The NF- κ B-I κ B α complex is then transported out of the nucleus back into the cytoplasm. The existence of this autoregulatory feedback loop means that the activation of NF- κ B is transient, as reflected in the results of the 3 κ B-conA-luciferase reporter assay, described earlier.

MG132 is a selective inhibitor of the 26S proteasome pathway. Pre-treating cells with MG132 prevented nuclear translocation of p65, showing that proteasome-mediated degradation of I κ B is an essential step in the activation of NF- κ B by flow. The operation of a nuclear export mechanism, transporting NF- κ B-I κ B complexes back into the cytoplasm, was confirmed by treating cells with LMB. These experiments showed that p65 was retained in the nucleus at the longer flow times (~120 minutes), when p65 had re-appeared in the cytoplasm of cells that had not been treated with LMB.

Bhullar *et al* (1998) showed that IKK1/2 activation by flow could be prevented by treating cells with blocking antibody (LM609) to the $\alpha_v\beta_3$ integrin, as noted previously (Chapter 5). These authors therefore suggested that this heterodimer might function as a flow mechanosensor. In addition, they were able to show that treatment of cells with genistein, a tyrosine kinase inhibitor, could also prevent activation of HA-tagged IKK1/2, again suggesting an important role for $\alpha_v\beta_3$ in the mechanotransduction of flow. The involvement of the $\alpha_v\beta_3$ integrin is clearly of special interest, given that it

constitutes a key structural element of the VMA-type cell-matrix junction described earlier, forming an essential link in the chain of proteins that connects the vimentin and actin cytoskeletons to the extracellular matrix.

In conclusion, the results show that the activation of NF- κ B by shear stress requires NIK as well as IKK1 and 2 and that it involves proteasome-dependent degradation of I κ B α and I κ B β . These events facilitate nuclear translocation of the p50/p65 heterodimer, binding to DNA and NF- κ B-dependent gene transactivation. The process does not appear to involve TPL2 kinase and it is also independent of PKC.

CHAPTER 10

DISCUSSION AND SCOPE FOR FURTHER STUDY.

Endothelial dysfunction underpins many cardiovascular disorders, including atherosclerosis, a progressive disease that can ultimately lead to myocardial infarction, stroke, aneurysms and peripheral vascular disease. The 'response to injury' hypothesis postulates that local haemodynamic forces combined with systemic risk factors activate endothelial cells and initiate chronic inflammatory and immune responses that can lead to atheroma formation. The crucial importance of haemodynamic factors in atherogenesis is highlighted by the focal nature of the disease. A better understanding of the cellular mechanisms involved in the response of endothelial cells to flow is therefore of considerable clinical relevance.

10.1. Morphological studies

Endothelial cells are exquisitely responsive to fluid shear stress. In his 1995 review, Davies documented over 60 morphological, biochemical and physiological responses to flow and the list has grown substantially since then. These responses may be very rapid, on the msec-sec time scale, or they may require sustained flow over several days. Although their sensitivity to flow is well established, it is much less clear how endothelial cells can sense and then respond to altered flow. Davies' (1995) decentralised model of mechanotransduction envisages an important role for the cytoskeleton. The idea is that primary mechanosensors in the surface membrane respond to flow initially and the effect is then transmitted to other sites within the cell via the cytoskeleton acting as an intracellular force transmission pathway. Important sites of signal transduction within the cell include cell-cell junctions, cell-matrix attachments, the nuclear envelope and the cortical cytoskeleton.

Much emphasis has been placed on the possible role of the actin cytoskeleton in the mechanotransduction process, since this was the first component that was shown to change under flow (Wong *et al*, 1984; Franke *et al*, 1984; Levesque & Nerem, 1985; White & Fujiwara, 1986; Masuda & Fujiwara, 1993; Girard & Nerem, 1995; Satcher *et al*, 1997; Fujiwara *et al*, 1998; Kataoka *et al*, 1998). In comparison, the possible involvement of intermediate filaments has received much less attention. The present study looked at changes to the intermediate filament cytoskeleton on time scales

ranging from 30 minutes to 16 hours. The nature of the response was shown to depend upon cell density, as this was found to have a profound influence on the morphology of the intermediate filament network. The most important structural feature of cells in fully-developed monolayers was the presence of the perinuclear ring of intermediate filaments, since this configuration most closely approximates to the *in vivo* situation, as reported some years ago (Blose & Meltzer, 1981). The fact that the ring of intermediate filaments lies in a plane parallel to the substrate suggested to us that it might serve as a sensor, perhaps by tilting in response to altered flow. It is easy to see how a tilting motion could convey information on both the magnitude and direction of flow, since the upstream edge of the ring would be displaced upwards, and *vice versa* for the downstream edge, by amounts that relate to the change in shear stress. However, the ring structure rapidly disappeared when cells grown in static cultures were subjected to flow, and it did not re-appear when cells were sheared for much longer periods, up to 24 hours. This observation is difficult to reconcile with a role for the perinuclear ring as a flow sensor, although it is possible that longer periods of shearing (i.e. >24 hours) might be required for the ring to reform and this possibility should be investigated in any future studies. There is another explanation that needs to be considered. It is known that the shape of cells in intact arteries can be either fusiform and aligned with the direction of flow, as in regions of vessel experiencing laminar shear stress, or polygonal and not aligned, typical of regions where the pattern of flow is disturbed and wall shear stress is very low. The gross morphology of the latter type of cell resembles that of cells grown in static culture, exhibiting the 'cobblestone' morphology, and it is quite possible that they may therefore possess a perinuclear ring-type configuration. Unfortunately, the region of aorta studied by Blose and co-workers is not stated in their publications and so this idea cannot be evaluated at present. This matter could be resolved in the future by examining different regions of aorta by immunofluorescence using antibody to vimentin.

The results presented here show that the non-adherent segment of the perinuclear ring encloses both the Golgi apparatus and the MTOC. It was pointed out earlier (Chapter 3) that the G58K protein, now identified as the enzyme formiminotransferase cyclodeaminase (or FTCD), associates with vimentin intermediate filaments. Gao & Sztul (2001) showed that FTCD binds to vimentin

sub-units and to polymerised vimentin intermediate filaments *in vitro* and *in vivo*. FTCD-containing fibres emanate from the Golgi region. This process is coupled to the assembly of vimentin filaments and is not seen in vimentin knockout mice. Gao & Sztul suggest that FTCD functions as a Golgi-intermediate filament linker protein and therefore be considered a new IFAP.

Although the function of the perinuclear ring remains unclear, recent evidence suggests that intermediate filaments may be involved in sensing flow. The studies by Helmke *et al* (2000, 2001), using living endothelial cells expressing GFP-tagged vimentin, showed that peripheral intermediate filaments undergo a rapid displacement shortly after the onset of flow (~ 3 minutes). Interestingly, intermediate filaments located upstream and above the nucleus, the thickest part of the cell and the region likely to experience the highest shear forces, showed the greatest displacement. In addition, peripheral intermediate filaments showed co-ordinated movements between neighbouring cells, suggesting that some kind of mechanical continuity may exist. The fact that rapid displacements of this nature can be detected may well be the outward sign that the intermediate filament network transmits force from the apical surface to other sites within the cell, consistent with Davies (1995) 'decentralised' model. More direct evidence for a role for intermediate filaments in sensing flow comes from work using transgenic mice lacking one or both alleles for the vimentin gene (Henrion *et al*, 1997). These experiments employed isolated mesenteric resistance arteries and studied the well-known vasodilator response to increased flow. Arteries taken from control animals (vim^{+/+} mice) responded normally, with an increase in diameter of 19 +/- 3µm upon stepping the flow rate from 0-150 µl.min⁻¹. Animals deficient in only one allele (vim^{+/-} mice) showed a similar response to flow, but the dilation of arteries from double negative mutants (vim^{-/-} mice) was reduced to 13 +/- 2µm, or only two thirds that of control arteries. This is a crucial observation because it is well known that vasodilation in response to altered flow is mediated by increased nitric oxide (NO) release. Since NO is not stored but produced on demand from L-arginine, this shows that intermediate filaments are most likely involved in the mechanism by which flow increases endothelial NO synthase activity.

The restructuring of vimentin intermediate filaments under flow is accompanied by substantial changes in the distribution of actin. The question is: *are these co-ordinated in any way?* In cells from confluent monolayers, actin is present as a dense band at the periphery of the cell, the dense peripheral band. The dense peripheral band disappears in cells exposed to flow and is replaced by numerous, parallel arrays of actin stress fibres. Recent evidence has shown that focal adhesions on endothelial cells serve to anchor both the actin and vimentin components of the cytoskeleton to the cytoplasmic face of the basal cell surface (Flitney *et al*, 1996; Gonzales *et al*, 2001). This type of vimentin-associated matrix attachment (VMA) is found on several kinds of endothelial cells, including BAEC and HUVEC, and it accounts for more than 70% of the total number of focal adhesions. Interestingly, actin stress fibres typically only interact with two focal adhesions, each located at either end of the fibre, while vimentin intermediate filaments were found to interconnect numerous neighbouring focal adhesions. Clearly, the existence of dual anchorage points for actin and vimentin could be important in co-ordinating the restructuring of both components during flow.

The model of the VMA proposed by Flitney *et al* (1996) and Gonzales *et al* (2001) envisages a key role for plectin in binding different components of the matrix attachment together. Plectin is an extraordinarily versatile linker protein that establishes structural connections between all three components of the cytoskeleton: between neighbouring intermediate filaments, between intermediate filaments and microtubules, intermediate filaments and actin microfilaments and intermediate filaments and myosin II minifilaments (Svitkina *et al*, 1996). Plectin also cross-links adjacent actin microfilaments and mediates the attachment of intermediate filaments to desmosomes and hemidesmosomes (Foisner & Wiche, 1991; Skalli *et al*, 1994; Jones *et al*, 1998). The critical importance of plectin as a mechanical integrator of the cytoskeleton is illustrated by the finding that the skin blistering disease epidermolysis bullosa simplex associated with muscular dystrophy (EBS-MD) is the result of a defective plectin gene (McLean *et al*, 1996).

The molecular structure of plectin is very well-suited to function as a cytoskeletal linker protein. The molecule (>500 kDa) is dumbbell-shaped, consisting of a central α -helical, coiled-coil rod, approximately 200nm long, flanked by large globular

amino and carboxy terminal domains. The C terminus contains a sequence of 50 amino acids that can interact with a variety of intermediate filament proteins, including vimentin, glial fibrillary acidic protein (GFAP), some keratins, neurofilament proteins, desmin and lamin B. The N terminus has a conserved actin-binding domain (ABD), similar to that of fodrin, dystrophin and neuronal dystonin (Wiche, 1998), and a region that interacts directly with the cytoplasmic domain of the β_4 integrin sub-unit found in hemidesmosomal cell-matrix attachments (Geerts *et al*, 1999).

Focal adhesions are labile structures that undergo continual restructuring and in the case of endothelial cells the process shows directionality in response to flow (Davies *et al*, 1994). The fact that focal adhesions become reoriented under flow, and that most focal adhesions on endothelial cells are of the VMA-type, implies that the nature of the interaction between plectin and the various components of the matrix attachment must be continually changing. Plectin is a target for several protein kinases (CaMII, PKA, PKC, p34^{cdc2}) that together regulate its interaction with intermediate filament proteins (Foisner *et al*, 1991). The possibility that its state of phosphorylation is altered by flow should be considered in future studies.

Plectin also interacts with microtubules (Svitkina *et al*, 1996). Malek & Izumo (1996) reported that the change of shape and up-regulation of actin stress fibres produced by flow can be prevented by treating cells with nocodazole, a microtubule depolymerising agent. They also showed that treatment with acrylamide had no effect on the shape change, implying that intermediate filaments are not involved in the process. However, because of the extensive structural integration between all three elements of the cytoskeleton, it is impossible to disrupt one without affecting the others. Nevertheless, future work should aim to re-investigate the role of microtubules since this was not included in the present study.

10.2. Biochemical studies

The second part of this study is concerned with the signalling pathway involved in the activation of NF- κ B by flow. Shear stress activates multiple intracellular

signalling cascades in the cell (Jalali *et al*, 1998; Tseng *et al*, 1995; Berk *et al*, 1995; Ishida *et al*, 1996; Yan *et al*, 1999), whose downstream targets include several inducible nuclear transcription factors (e.g. c-myc, c-fos, c-jun, Egr-1, AP-1, SP-1 and NF- κ B) that are responsible for regulating endothelial gene expression (Hsieh *et al*, 1993; Resnick *et al*, 1993; Braddock *et al*, 1998; Chien & Shyy, 1998; Bhullar *et al*, 1998; Khachigian *et al*, 1995; Lan *et al*, 1994; Shyy *et al*, 1995; Nagel *et al*, 1999). Lan *et al* (1994) showed that unidirectional shear stress rapidly activates NF- κ B in bovine endothelial cells. Resnick *et al* (1993) identified a cis-acting shear stress responsive element (SSRE) in the promoter of the flow-sensitive PDGF-B chain gene and then later (Resnick *et al*, 1997) showed that this acts as a non-consensus binding site for NF- κ B. The core binding sequence of the SSRE (GAGACC) was discovered in several other genes that were known to be regulated by flow (e.g. ICAM-1, TGF β , c-fos, c-jun, MCP-1); furthermore, insertion of the SSRE into the promoters of several flow-insensitive genes rendered them inducible by flow (Resnick & Gimbrone, 1995).

NF- κ B regulates over 50 genes that encode various cytokines, growth factors, acute phase response proteins, adhesion molecules, immunoregulatory proteins and some viruses (May & Ghosh, 1998). There is growing evidence to implicate NF- κ B in atherosclerosis (de Martin *et al*, 2000). NF- κ B is active in advanced atherosclerotic lesions (Brand *et al*, 1996), where many of the genes that are expressed are NF- κ B-dependent (Collins, 1993), but not in regions of the vasculature that are free of disease but considered at high risk of developing atheroma in the future. Here the steady-state levels of some NF- κ B signalling elements are substantially elevated (Hajra *et al*, 2000). The latter authors showed that in control mice levels of p65, I κ B α and I κ B β were 5-18 fold greater in 'high risk' regions although little NF- κ B was activated, suggesting that the NF- κ B signal transduction pathway is 'primed' in such regions to respond later to systemic risk factors.

Understanding the nature of the signalling pathway activated by flow is clearly of considerable interest. The experiments described in Chapters 8 and 9 were undertaken to determine whether flow activates the same pathway as that used when NF- κ B is stimulated by TNF α . The results show that the process requires NIK as

well as IKK1 and 2 and that it involves proteasome-dependent degradation of I κ B α and I κ B β . These events facilitate nuclear translocation of p50/p65 heterodimer and NF- κ B-dependent gene transactivation. The process does not appear to involve PKC isoforms. Thus, it appears from data obtained so far that there are close similarities in the way NF- κ B is activated by flow and by TNF α . The role of several other upstream kinases (e.g. MEKK1, TPL-2) in the response to flow remains to be determined by future work.

10.3. Imaging living cells

The present studies were of necessity undertaken using fixed material, comparing different cell populations before and after flow. Many of the uncertainties of this approach can be avoided by using living cells expressing one or more cytoskeletal elements (e.g. vimentin, vinculin, actin, tubulin) tagged with fluorescent protein markers (e.g. GFP, YFP, CFP). This would allow greater spatio-temporal resolution of the structural changes induced by flow. Similarly, nuclear translocation of p65 tagged with fluorescent protein could be monitored as an indicator of NF- κ B activation.

- Abercrombie, M., Heaysman, J.E. & Pegrum, S.M. (1971) The locomotion of fibroblasts in culture. *Exp. Cell. Res.* 67: 359-367.
- Adams, M.D., Dubnick, M., Kerlavage, A.R., Moreno, R., Kelley, J.M., Utterback, T.R., Nagle, J.W., Fields, C. & Venter, J.C. (1992) Sequence identification of 2375 human brain genes. *Nature* 355: 632-634.
- Akimoto, S., Mitsumata, M., Sasaguri, T. & Yoshida, Y. (2000) Laminar shear stress inhibits vascular endothelial cell proliferation by inducing cyclin-dependent kinase inhibitor p21^{Sdi1/Cip1/Waf1}. *Circ. Res.* 86: 185-190.
- Alberts, B., Bray, D., Lewis, J., Raff, M., Roberts, K. & Watson, J.D. (1994) *Molecular Biology of the Cell*. 3rd Edition. Garland publishing, New York.
- Allen, J. N., Herzyk, D.J. & Wewers, M.D. (1991) Colchicine has opposite effects on interleukin-1 β and tumour necrosis factor- α production. *Am. J. Physiol.* 261: L315-L321.
- Allen, P.G. & Shah, J.V. (1999) Brains and brawn: plectin as regulator and reinforcer of the cytoskeleton. *BioEssays* 21: 451-454.
- Ando, S., Tanabe, K., Gonda, Y., Sato, C. & Inagaki, M. (1989) Domain-and sequence – specific phosphorylation of vimentin induces disassembly of the filament structure. *Biochemistry* 28 (7): 2974-2479.
- Ando, S., Tokui, T., Yamauchi, T., Sugiura, H., Tanabe, K. & Inagaki, M. (1991) Evidence that ser-82 is a unique phosphorylation site on vimentin for Ca²⁺-calmodulin-dependent protein kinase II. *Biochem. Biophys. Res. Commun.* 175 (3): 955-962.
- Ando, S., Tsujimura, K., Matsuoka, Y., Tokui, T., Hisanaga, S., Okumura, E., Uchiyama, M., Kishimoto, T., Yasuda, H. & Inagaki, M. (1993) Phosphorylation of synthetic vimentin peptides by cdc2 kinase. *Biochem. Biophys. Res. Commun.* 195 (2): 837-843.

- Andra, K., Nikolic, B., Stocher, M., Drenckhahn, D. & Wiche, G. (1998) Not just scaffolding: plectin regulates actin dynamics in cultured cells. *Genes. Dev.* 12: 3442-3451.
- Anrather, J., Csizmadia, V., Soares, M.P. & Winkler, H. (1999) Regulation of NF- κ B Rel A phosphorylation and transcriptional activity by p21^{ras} and protein kinase C ζ in primary endothelial cells. *J. Biol. Chem.* 271 (19): 13594-13603.
- Arenzana-Seisdedos, F., Thompson, J., Rodriguez, M.S., Bachelierie, F., Thomas, D. & Hay, R.T. (1995) Inducible nuclear expression of newly synthesised I κ B α negatively regulates DNA-binding and transcriptional activities of NF- κ B. *Mol. Cell. Biol.* 15 (5): 2689-2696.
- Arenzana-Seisdedos, F., Turpin, F., Rodriguez, M., Thomas, D., Hay, R.T. & Dargemont, C. (1997) Nuclear localisation of I kappa B alpha promotes active translocation of NF-kappa B from nucleus to the cytoplasm. *J. Cell. Sci.* 110 (3): 369-378.
- Baeuerle, P.A. & Baltimore, D. (1988) I κ B: A specific inhibitor of the NF- κ B transcription factor. *Science* 242: 540-546.
- Baeuerle, P.A. & Henkel, T. (1994) Function and activation of NF- κ B in the immune system. *Ann. Rev. Immunol.* 12: 141-179.
- Baeuerle, P.A. & Baltimore, D. (1996) NF- κ B: Ten years after. *Cell* 87: 13-20.
- Baldwin, A.S. (1996) The NF- κ B and I κ B proteins: New discoveries and insights. *Annu. Rev. Immunol.* 14: 649-681.
- Ballerman, J., Dardik, A., Eng, E. & Liu, A. (1998) Shear stress and the endothelium. *Kid. Intl.* 54 (67): S100-108.

- Barbee, K.A., Davies, P.F. & Lal, R. (1994) Shear stress induced re-organisation of surface topography of living endothelial cells imaged by atomic force microscopy. *Circ. Res.* 74: 163-171.
- Barbee, K.A., Mundel, T., Lal, R. & Davies, P.F. (1995) Subcellular distribution of shear stress at the surface of flow-aligned and non-aligned endothelial monolayers. *Am. J. Physiol.* 268: H1765-H1772.
- Beauparlant, P., Lin, R. & Hiscott, J. (1996) The role of the C-terminal domain of I κ B α in protein degradation and stabilization. *J. Biol. Chem.* 271 (18): 10690-10696.
- Beckerle, M.C. & Yeh, R.K. (1990) Talin: Role at sites of cell-substratum adhesion. *Cell. Motil. Cyto.* 16: 7-13.
- Belich, M.P., Salmeron, A., Johnston, L.H. & Ley, S.C. (1999) TPL-2 kinase regulates the proteolysis of the NF- κ B inhibitory protein NF- κ B1 p105. *Nature* 397 (6717): 363-368.
- Berk, B.C., Corson, M.A., Peterson, T.E. & Tseng, H. (1995) Protein kinases as mediators of fluid shear stress stimulated signal transduction in endothelial cells: A hypothesis for calcium dependent and calcium independent events activated by flow. *J. Biomech.* 28 (12): 1439-1450.
- Bevan, J.A. (1997) Shear stress, the endothelium and the balance between flow-induced contraction and dilation in animals and man. *Int. J. Microcirc.* 17: 248-256.
- Bhullar, I.S., Li, Y.-S., Miao, H., Zandi, E., Kim, M. & Shyy, J.Y.-J. (1998) Fluid shear stress activation of I κ B kinase is integrin dependent. *J. Biol. Chem.* 273 (46): 30544-30549.
- Blose, S.H. & Chacko, S. (1976) Rings of intermediate (100A) filament bundles in the perinuclear region of vascular endothelial cells. *J. Cell. Biol.* 70: 459-466.

- Blose, S.H. (1979) Ten-nanometer filaments and mitosis: Maintenance of structural continuity in dividing endothelial cells. *Proc. Natl. Acad. Sci.* 76 (7): 3372-3376.
- Blose, S.H. (1981) The distribution of 10nm filaments and microtubules in endothelial cells during mitosis: Double-label immunofluorescence study. *Cell Motility 1*: 417-431.
- Blose, S.H. & Meltzer, D.I. (1981) Visualization of the 10nm filament vimentin rings in vascular endothelial cells in situ. *Exp. Cell. Res.* 135: 299-309.
- Blose, S.H., Meltzer, D.I. & Feramisco, J.R. (1984) 10-nm filaments are induced to collapse in living cells microinjected with monoclonal and polyclonal antibodies against tubulin. *J. Cell. Biol.* 98: 847-858.
- Booyse, F.M., Sedlak, B.J. & Rafelson, M.E. (1975) Culture of arterial endothelial cells. *Thrombos. Diathes. Haemorrh.* 34: 825-839.
- Bowie, A., Moynagh, P.N. & O'Neill, L.A.J. (1996) Mechanism of NF- κ B activation by interleukin-1 and tumour necrosis factor in endothelial cells. *Biochem. Soc. Trans.* 24:2s.
- Braddock, M., Schwachtgen, J-L., Houston, P., Dickson, M.C., Lee, M.J. & Campbell C.J. (1998) Fluid shear stress and modulation of gene expression in endothelial cells. *News Physiol. Sci.* 13:241-246.
- Brand, K., Page, S., Rogler, G., Bartsch, A., Brandl, R., Knuechei, R., Page, M., Kaltschmidt, C., Baeuerle, P.A. & Neumeier, D. (1996) Activated transcription factor nuclear factor-kappa B is present in the atherosclerotic lesion. *J. Clin. Invest.* 97 (7): 1715-1722.

- Brockman, J.A., Scherer, D.C., McKinsey, T.A., Hall, S.M., Qi, X., Young Lee, W. & Ballard, D.W. (1995) Coupling of a signal response domain in I κ B α to multiple pathways of NF- κ B activation. *Mol. Cell. Biol.* 15 (5): 2809-2818.
- Burrige, K., Chrzanowska-Wodnicka, M. & Zhong, C. (1997) Focal adhesion assembly. *Trends. Cell Biol.* 7: 342-347.
- Burrige, K., Fath, K., Kelly, T., Nuckolls, G. & Turner, C. (1988) Focal Adhesions: between the extracellular matrix and the cytoskeleton. *Ann. Rev. Cell. Biol.* 4: 487-525.
- Burrige, K. & Fath, K. (1989) Focal contacts: Transmembrane links between the extracellular matrix and the cytoskeleton. *BioEss.* 10 (4): 104-108.
- Campbell, G.R., Chamley-Campbell, J., Groschel-Stewart, U., Small, J.V. & Anderson, P. (1979) Antibody staining of 10-nm (100-A) filaments in smooth, cardiac and skeletal muscle cells. *J. Cell Sci.* 37: 303-22.
- Cary, R.B., Klymkowsky, M.W., Evans, R.M., Domingo, A., Dent, J.A. & Backhus, L.E. (1994) Vimentin's tail interacts with actin containing structures in vivo. *J. Cell. Sci.* 107: 1609-1622.
- Casella, J.F., Flanagan, M.D. & Lin, S. (1981) Cytochalasin D inhibits actin polymerisation and induces depolymerisation of actin filaments formed during platelet shape change. *Nature* 293: 303-305.
- Chalfie, M., Tu, Y., Euskirchen, G., Ward, W.W. & Prasher, D.C. (1994) Green fluorescent protein as a marker for gene expression. *Science* 263: 802-805.
- Chamley-Campbell, J., Campbell, G.R. & Ross, R. (1979) The smooth muscle cell in culture. *Physiol. Rev.* 59 (1): 1-61.

- Chen, K-D., Li, Y-S., Kim, M., Li, S., Yuan, S., Chien, S. & Shyy, J.Y.-J. (1999) mechanotransduction in response to shear stress. *J. Biol. Chem.* 274 (26): 18393-18400.
- Chen, Z., Hagler, J., Palombelli, V.J., Melandri, F., Scherer, D., Ballard, D. & Maniatis, T. (1995) Signal-induced site-specific phosphorylation targets I kappa B alpha to the ubiquitin-proteasome pathway. *Gen. Dev.* 9 (13): 1586-1597.
- Chien, S., Li, S. & Shyy, J.Y.J. (1998) Effects of mechanical forces on signal transduction and gene expression in endothelial cells. *Hypertension* 31 (2): 162-169.
- Chien, S. & Shyy, J.Y.J. (1998) Effects of Haemodynamic forces on gene expression and signal transduction in endothelial cells. *Biol. Bull.* 194: 390-393.
- Chou, Y.-H., Rosevar, E. & Goldman, R.D. (1989) Phosphorylation and disassembly of intermediate filaments in mitotic cells. *Proc. Natl. Acad. Sci.* 86: 1885-1889.
- Chou, Y.-H., Bischoff, J.R., Beach, D. & Goldman, R.D. (1990) Intermediate filament reorganisation during mitosis is mediated by p34^{cdc2} phosphorylation of vimentin. *Cell* 62: 1063-1071.
- Chou, Y.-H., Ngai, K.L. & Goldman, R.D. (1991) The regulation of intermediate filament reorganisation in mitosis. p34^{cdc2} phosphorylates vimentin at a unique N-terminal site. *J. Biol. Chem.* 266 (12): 7325-7328.
- Chou, Y.-H., Opal, P., Quinlan, R.A. & Goldman, R.D. (1996) The relative roles of specific N- and C-terminal phosphorylation sites in the disassembly of intermediate filament in mitotic BHK-21 cells. *J. Cell. Sci.* 109: 817-826.
- Chou, Y.-H. & Goldman, R.D. (2000) Intermediate filaments on the move. *J. Cell. Biol.* 150 (3): F101-F105.

- Chou, Y.-H., Helfand, B.T. & Goldman, R.D. (2001) New horizons in cytoskeletal dynamics: transport of intermediate filaments along microtubule tracks. *Curr. Opin. Cell. Biol.* 13: 106-109.
- Ciechanover, A., Elias, S., Heller, H. & Hersko, A. (1982) 'Covalent affinity' purification of ubiquitin-activating enzyme. *J. Biol. Chem.* 257 (5): 2537-2542.
- Clubb, B., Chou, Y.-H., Herrmann, H., Svitkina, T.M., Borisy, G.G. & Goldman, R.D. (2000) The 300-kDa intermediate filament-associated protein (IFAP300) is a hamster plectin ortholog. *Biochem. Biophys. Res. Commun.* 273.(1): 183-187.
- Coan, D.E., Wechezak, A.R., Viggers, R.F. & Sauvage, L.R. (1993) Effects of shear stress upon localization of the Golgi apparatus and microtubule organizing center in isolated cultured endothelial cells. *J. Cell. Sci.* 104: 1145-1153.
- Cohen, L., Henzel, W.J. & Baeuerle, P.A. (1998) IKAP is a scaffold protein of the I κ B kinase complex. *Nature* 395: 292-296.
- Collins, T. (1993) Endothelial nuclear factor-kappa B and the initiation of the atherosclerotic lesion. *Lab. Invest.* 68 (5): 499-508.
- Correia, I., Chu, D., Chou, Y.-H., Goldman, R.D. & Matsudaira, P. (1999) Integrating the actin and vimentin cytoskeletons: Adhesion-dependent formation of fibrin-vimentin complexes in macrophages. *J. Cell Biol.* 146 (4): 831-842.
- Coulombe, P.A., Bousquet, O., Ma, L., Yamada, S. & Wirtz, D. (2000) The 'ins' and 'outs' of intermediate filament organisation. *Trends in Cell Biol.* 10: 420-428.
- Cowin, P. & Burke, B. (1996) Cytoskeleton-membrane interactions. *Curr. Opin. Cell. Biol.* 8: 56-65.
- Craig, S.W. & Johnson, R.P. (1996) Assembly of focal adhesions: progress, paradigms and portents. *Curr. Opin. Cell. Biol.* 8: 74-85.

- Davies, P.F., Remuzzi, A., Gordon, E.J., Dewey, C.F. & Gimbrone, M.A. (1986) Turbulent fluid shear stress induces vascular endothelial turnover *in vitro*. *Proc. Natl. Acad. Sci.* 83: 2114-2117.
- Davies, P.F. (1989) How do vascular endothelial cells respond to flow? *NIPS* 4: 22-25.
- Davies, P.F. & Tripathi, S.C. (1993) Mechanical stress mechanisms and the cell. *Circ. Res.* 72: 239-245.
- Davies, P.F., Robotewskyj, A. & Griem, M.L. (1993) Endothelial cell adhesion in real time. *J. Clin. Invest.* 91: 2640-2652.
- Davies, P.F., Robotewskyj, A. & Griem, M.L. (1994) Quantitative studies of endothelial cell adhesion. *J. Clin. Invest.* 93: 2031-2038.
- Davies, P.F. (1995) Flow-mediated endothelial mechanotransduction. *Physiol. Rev.* 75 (3): 519-560.
- Davies, P.F., Barbee, K.A., Volin, M.V., Robotewskyj, A., Chen, J., Joesph, L., Griem, M.L., Wernick, M.N., Jacobs, E., Polacek, D.C., DePaola, N. & Barakat, A.I. (1997) Spatial relationships in early signalling events of flow mediated endothelial mechanotransduction. *Annu. Rev. Physiol.* 59: 527-49.
- Davies, P.F. (2000) Spatial haemodynamics, the endothelium and focal atherogenesis – a cell cycle link? *Circ. Res.* 86: 114-116.
- De Martin, R., Hoeth, M., Hofer-Warbinek, R. & Schmid, J.A. (2000) The transcription factor NF- κ B and the regulation of cell function. *Arterio. Thromb. Vasc. Biol.* 20 (11): E83-E88.
- Demeester, S.L., Cobb, J.P., Hotchkiss, R.S., Osborne, D.F., Karl, I.E., Tinsley, K.W. & Buchman, T.G. (1998) Stress-induced fractal rearrangement of the endothelial cell cytoskeleton causes apoptosis. *Surgery* 124: 362-371.

DePaola, N., Gimbrone, M.A., Davies, P.F. & Dewey, C.F. (1992) Vascular endothelium responds to fluid shear stress gradients. *Arterioscler. Thromb. Vasc. 12*: 1254-1257. [published erratum *Arterioscler. Thromb. 1993 13 (3)*: 465].

Deshaies, R.J. (1995) Make it or break it: the role of ubiquitin-dependent proteolysis in cellular regulation. *Trends In Cell. Biol. 5*: 428-434.

Dewey, C.F. Jr., Bussolari, S.R., Gimbrone, M.A. Jr. & Davies, P.F. (1981) The dynamic response of vascular endothelial cells to fluid shear stress. *J. Biomech. Eng. 103 (3)*: 177-185.

Dewey, C.F. Jr. (1984) Effects of fluid flow on living vascular cells. *J. Biomech. Eng. 106*: 31-35.

DiDonato, J.A., Mercurio, F. & Karin, M. (1995) Phosphorylation of I κ B α precedes but is not sufficient for its dissociation from NF- κ B. *Mol. Cell. Biol. 15 (3)*: 1302-1311.

DiDonato, J.A., Mercurio, F., Rosette, C., Wu-Li, J., Suyang, H., Ghosh, S. & Karin, M. (1996) Mapping of the Inducible I κ B phosphorylation sites that signal its ubiquitination and degradation. *Mol. Cell. Biol. 16 (4)*: 1295-1304.

DiDonato, J.A., Hayakawa, M., Rothwarf, D.M., Zandi, E. & Karin, M. (1997) A cytokine-responsive I κ B kinase that activates the transcription factor NF- κ B. *Nature 388*: 548-554.

Dimmeler, S., Haendeler, J., Rippmann, V., Nehls, M. & Zeiher, A.M. (1996) Shear stress inhibits apoptosis in human endothelial cells. *FEBS. Lett. 399 (1-2)*: 71-74.

Dimmeler, S., Hermann, C. & Zeiher, A.M. (1998a) Apoptosis of endothelial cells. Contribution to the pathophysiology of Arteriosclerosis? *Eur. Cytokine Netw. 9 (4)*: 697-698.

- Dimmeler, S., Assmus, B., Hermann, C., Haendeler, J. & Zeiher, A.M. (1998b) Fluid shear stress stimulates phosphorylation of Akt in human endothelial cells. *Circ. Res.* 83: 334-341.
- Eckes, B., Dogic, D., Colucci-Guyon, E., Wang, N., Maniotis, A., Ingber, D., Merckling, A., Langa, F., Aumailley, M., Delouvee, A., Koteliensky, V., Babinet, C. & Krieg, T. (1998) Impaired mechanical stability, migration and contractile capacity in vimentin deficient fibroblasts. *J. Cell. Sci.* 111: 1897-1907.
- Eriksson, J.E., Brautigan, D.L., Vallee, R., Olmsted, J. & Fujiki, H. (1992) Cytoskeletal integrity in interphase cells requires protein phosphatase activity. *Proc. Natl. Acad. Sci.* 89: 11093-11097.
- Ernst, M.K., Dunn, L.L., & Rice, N.R. (1995) The PEST-like sequence of I κ B α is responsible for inhibition of DNA binding but not for cytoplasmic retention of c-Rel or RelA homodimers. *Mol. Cell. Biol.* 15 (2): 872-882.
- Fan, C.-M. & Maniatis, T. (1991) generation of p50 subunit of NF- κ B by processing of p105 through an ATP-dependent pathway. *Nature* 354: 395-398.
- Ferrari, S., Battini, R., Kaczmarek, L., Rittling, S., Calabretta, B., De Riel, K.J., Philiponis, V., Wei, J.-F. & Baserga, R. (1986) Coding sequence and growth regulation of the human vimentin gene. *Mol. & Cell. Biol.* 6 (11): 3614-3620.
- Flitney, F.W., Goldman, R.D., Skalli, O., Mercurius, K.O. & Davies, P.F. (1995) Dynamic properties of intermediate filaments in cultured endothelial cells: The effects of controlled fluid shear stress. *Biol. Nitric Oxide* 5: 251-253. S. Moncada, J. Stamler, S.Gross & E.A. Higgs Ed. Portland Press, London 251.
- Flitney, F.W., Melville, J.M., Khoun, S. & Goldman, R.D. (1996) The co-localisation of an intermediate filament associated protein (IFAP-300) and vimentin with focal adhesion proteins in cultured bovine endothelial cells. *Mol. Biol. Cell.* 10: 397.

- Flitney, F.W., Beers, C., Cameron, V., Jones, J., Khuon, S. & Goldman, R.D. (2001a) Fluid shear stress-dependent remodelling of the intermediate filament (IF) cytoskeleton in cultured endothelial cells. *In Vasc. Endo.- Source & target of inflammatory mediators 1 (330): 356-357. J.D. Catravas et al Editors.*
- Flitney, F.W., Hay, D.C., Cameron, V., Beers, C. & Hay, R.T. (2001b) Flow-induced degradation of I κ B and NF- κ B-dependent gene transcription in cultured endothelial cells. *In Vasc. Endo.- Source & target of inflammatory mediators. J.D. Catravas et al Editors 1 (330): 288-289.*
- Fornerod, M., Ohno, M., Yoshida, M. & Mattaj, I.W. (1997) CRM1 is an export receptor for leucine-rich nuclear export signals. *Cell 90: 1051-1060.*
- Franke, R.-P., Grafe, M., Schnittler, H., Seiffge, D. & Mittermayer, C. (1984) Induction of human vascular endothelial stress fibres by fluid shear stress. *Nature 307: 648-649.*
- Franke, W.W., Schmid, E., Osborn, M. & Weber, K. (1978) Different intermediate-sized filaments distinguished by immunofluorescence microscopy. *Proc. Natl. Acad. Sci. 75 (10): 5034-5038.*
- Franke, W.W., Schmid, E., Osborn, M. & Weber, K. (1979a) Intermediate sized filaments of human endothelial cells. *J. Cell. Biol. 81 (3): 570-580.*
- Franke, W.W., Schmid, E., Winter, S., Osborn, M. & Weber, K. (1979b) Widespread occurrence of intermediate sized filaments of the vimentin type in cultured cells from diverse vertebrates. *Exp. Cell Res. 123 (1): 25-46.*
- Fujiwara, K., Masuda, M., Osawa, M., Katoh, K., Kano, Y., Harada, N. & Lopes, R.B. (1998) Response of vascular endothelial cells to fluid flow. *Biol. Bull. 194: 384-386.*

- Fuchs, E. & Weber, K. (1994) Intermediate filaments: structure, dynamics, function and disease. *Ann. Rev. Biochem.* 63: 345-382.
- Fuchs, E. & Cleveland, D.W. (1998) A structural scaffolding of intermediate filaments in health and disease. *Science* 279 (5350): 514-519.
- Fuchs, E. & Yang, Y. (1999) Crossroads on the cytoskeletal highways. *Cell* 98: 547-550.
- Fuchs, E. & Karakesisoglou, I. (2001) Bridging cytoskeletal intersections. *Gene Dev.* 15: 1-14.
- Gabbiani, G., Gabbiani, F., Lombardi, D. & Schwartz, S.M. (1983) Organisation of actin cytoskeleton in normal and regenerating arterial endothelial cells. *Proc. Natl. Acad. Sci.* 80: 2361-2364.
- Geerts, D., Fontao, L., Nievers, M.G., Schaapveld, R.Q.J., Purkis, P.E., Wheeler, G.N., Lane, E.B., Leigh, I.M. & Sonnenberg, A. (1999) Binding of integrin $\alpha_6\beta_4$ to plectin prevents plectin association with F-actin but does not interfere with intermediate filament binding. *J. Cell Biol.* 147 (2): 417-434.
- Gao, Y.-S. & Sztul, E. (2001) A novel interaction of the Golgi complex with the vimentin intermediate filament cytoskeleton. *J. Cell Biol.* 152 (5): 877-893.
- Garcia-Cardena, G., Comander, J., Anderson, K.R., Blackman, B.R. & Gimbrone, M.A. (2001) Biomechanical activation of vascular endothelium as a determinant of its functional phenotype. *Proc. Natl. Acad. Sci.* 98 (8): 4478-4485.
- Garrod, D.R. (1993) Desmosomes and hemidesmosomes. *Curr. Opin. Cell. Biol.* 5: 30-40.
- Geiger, B., Volk, T., Volberg, T. & Bendori, R. (1987) Molecular interactions in adherens type contacts. *J. Cell. Sci. Suppl* 8: 251-272.

Georgatos, S.D. & Marchesi, V.T. (1985a) The binding of vimentin to human erythrocyte membranes: A model system for the study of intermediate filament-membrane interactions. *J. Cell Biol.* 100: 1955-1961.

Georgatos, S.D., Weaver, D.C. & Marchesi, V.Y. (1985b) Site specificity in vimentin-membrane interactions: Intermediate filament subunits associate with the plasma membrane via their head domains. *J. Cell Biol.* 100: 1962-1967.

Georgatos, S.D. & Blobel, G. (1987a) Lamin B constitutes an intermediate filament attachment site at the nuclear envelope. *J. Cell Biol.* 105: 117-125.

Georgatos, S.D. & Blobel, G. (1987b) Two attachment sites for vimentin along the plasma membrane and nuclear envelope in avian erythrocytes; a basis for vectorial assembly of intermediate filaments. *J. Cell Biol.* 105: 105-115.

Ghosh, G., Van Duyne, G., Ghosh, S. & Sigler, P.B. (1995) Structure of NF- κ B p50 homodimer bound to a κ B site. *Nature* 373: 303-310.

Ghosh, S. & Baltimore, D. (1990) Activation *in vitro* of NF- κ B by phosphorylation of its inhibitor I κ B. *Nature* 344: 678-682.

Ghosh, S., May, M.J. & Kopp, E.B. (1998) NF- κ B and rel proteins: evolutionary conserved mediators of immune responses. *Ann. Rev. Immunol.* 16: 225-260.

Gimbrone, M.A. (1976) Culture of vascular endothelium. *Prog. Hemost. Thromb.* 3: 1-28.

Gimbrone, M.A. Jr., Nagel, T. & Topper, J.N. (1997) Biomechanical activation: An emerging paradigm in endothelial adhesion biology. *J. Clin. Invest.* 99 (8): 1809-1813

Girard, P.R. & Nerem, R.M. (1993) Endothelial cell signalling and cytoskeletal changes in response to shear stress. *Front. Med. Biol. Eng.* 5: 31-36.

Girard, P.R. & Nerem, R.M. (1995) Shear stress modulates endothelial cell morphology and F-actin organisation through the regulation of focal adhesion-associated proteins. *J. Cell. Physiol.* 163: 179-193.

Goldman, R.D., Goldman, A.E., Green, K.J., Jones, J.C.R., Jones, S.M., Lieska, N. & Yang, H.-Y. (1985) Intermediate filaments: Possible functions as cytoskeletal connecting linkers between nucleus and cell surface. *Ann. NY. Acad. Sci.* 455: 1-17.

Goldman, R.D., Goldman, A.E., Green, K.J., Jones, J.C.R., Jones, S.M. & Yang, H.-S. (1986) Intermediate filaments networks: Organisation and possible functions of a diverse group of cytoskeletal elements. *J. Cell Sci. Suppl.* 5: 69-97.

Goldman, R.D., Chou, Y.-H., Dessev, C., Eriksson, J., Goldman, A., Khuon, S., Kohnken, R., Lowy, M., Miller, R., Murphy, K., Opal, P., Skalli, O. & Straube, K. (1991) Dynamic aspects of cytoskeletal and karyoskeletal intermediate filament systems during the cell cycle. *The Cell Cycle. CSHSQB. Vol. LVI:* 692-642.

Goldman, R.D., Khoun, S., Chou, Y.-H., Opal, P. & Steinert, P.M. (1996) The function of intermediate filaments in cell shape and cytoskeletal integrity. *J. Cell Biol.* 134 (4): 971-983.

Goldman, R.D., Clement, S., Khuon, S., Moir, R., Trejo-Skalli, A., Spann, T. & Yoon, M. (1998) Intermediate filament cytoskeletal system: Dynamic and mechanical properties. *Biol. Bull.* 194: 361-363.

Gonzales, M., Weksler, B., Tsuruta, D., Goldman, R.D., Yoon, K.J., Hopkinson, S.B., Flitney, F.W. & Jones, J.C.R. (2001) Structure and function of a vimentin-associated matrix adhesion in endothelial cells. *Mol. Biol. Cell.* 12: 85-100.

Goto, H., Kosako, H., Tanabe, K., Yanagida, M., Sakurai, M., Amano, M., Kaibuch, K. & Inagaki, M. (1998) Phosphorylation of vimentin by Rho-associated kinase at a unique amino-terminal site that is specifically phosphorylated during cytokinesis. *J. Biol. Chem.* 273 (19): 11728-11736.

Granger, B.L. & Lazarides, E. (1982) Structural associations of synemin and vimentin filaments in avian erythrocytes revealed by immunoelectron microscopy. *Cell* 30: 263-257.

Green, K.J., Talian, J.C. & Goldman, R.D. (1986) Relationship between intermediate filaments and microfilaments in cultured fibroblasts: Evidence for common foci during cell spreading. *Cell Motil. Cyto.* 6: 406-418.

Green, K.J. & Jones, J.C. (1996) Desmosomes and hemidesmosomes: Structure and function of molecular components. *FASEB. J.* 8: 871-81.

Gyoeva, F.K. & Gelfand, V.I. (1991) Coalignment of vimentin intermediate filaments with microtubules depends on kinesin. *Nature* 353: 445-448.

Hajra, L., Evans, A. I., Chen, M., Hyduk, S.J., Collins, T. & Cybulsky, M.I. (2000) The NF- κ B signal transduction pathway in aortic endothelial cells is primed for activation in regions predisposed to atherosclerotic lesion formation. *Proc. Natl. Acad. Sci.* 97 (16): 9052-9057.

Hanazawa, S., Takeshita, A., Amano, S., Semba, T., Nirazuka, T., Katoh, H. & Kitano, S. (1993) Tumour necrosis factor-alpha induces expression of monocyte chemoattractant JE via fos and jun genes in clonal osteoblastic MC3T3-E1 cells. *J. Biol. Chem.* 268 (13): 9526-9532.

Harada, N., Masuda, M. & Fujiwara, K. (1995) Fluid flow and osmotic stress induce tyrosine phosphorylation of an endothelial cell 128kDa surface glycoprotein. *Biochem. Biophys. Res. Commun.* 214 (1): 69-74.

Hatakeyama, S., Kitagawa, M., Nakayama, K., Shirane, M., Matsumoto, M., Hattori, K., Higasi, H., Nakano, H., Okumura, K., Onue, K., Good, R.A. & Nakayama, K.-I. (1999) Ubiquitin-dependent degradation of I κ B α is mediated by a ubiquitin ligase skp1/cull1/f-box protein FWD1. *Proc. Natl. Acad. Sci.* 96: 3859-3863.

- Hay, R.T. (1993) Control of nuclear factor-kappa B DNA-binding activity by inhibitory proteins containing ankyrin repeats. *Biochem. Soc. Trans.* 21 (4): 926-930.
- Hay, D.C., Kemp, G.D., Dargemont, C. & Hay, R.T. (2001) Interaction between hnRNPA1 and I κ B α is required for maximal activation of NF- κ B dependent transcription. *Mol. Cell. Biol.* 21 (10): 3482-3490.
- Hay, D.C., Beers, C., Cameron, V., Thomson, L., Flitney, F.W. & Hay, R.T. (submitted) Activation of NF- κ B nuclear transcription factor in cultured human endothelial cells under uniform laminar flow.
- Hazel, A.L. & Pedley, T.J. (2000) Vascular endothelial cells minimize the total force on their nuclei. *Biophys. J.* 78: 47-54.
- Hegland, D.D., Sullivan, D.M., Rovira, I.I., Li, A., Kovesdi, I., Bruder, J.T. & Finkel, T. (1999) Regulation of endothelial cell adherens junctions by a Ras-dependent signal transduction pathway. *Biochem. Biophys. Res. Commun.* 260: 371-376.
- Heidermann, S. R. (1993) A new twist on integrins and the cytoskeleton. *Science* 260: 1080-1081.
- Heilker, R., Freuler, F., Pulfer, R., Di Padova, F. & Eder, J. (1999) All three I κ B isoforms and most Rel family members are stably associated with the I κ B kinase 1 /2 complex. *Eur. J. Biochem.* 259: 253-261.
- Helmke, B.P., Goldman, R.D. & Davies, P.F. (2000) Rapid displacement of vimentin intermediate filaments in living endothelial cells exposed to flow. *Circ. Res.* 86: 745-752.

- Helmke, B.P., Thakker, D.B., Goldman, R.D. & Davies, P.F. (2001) Spatiotemporal analysis of flow-induced intermediate filament displacement in living endothelial cells. *Biophys. J.* 80: 184-194.
- Henkel, T., Zabel, U., Van Zee, K., Muller, J.M., Fanning, E. & Baeuerle, P.A. (1992) Intramolecular masking of the nuclear location signal and dimerisation domain in the precursor for the p50 NF- κ B subunit. *Cell* 68: 1121-1133.
- Henrion, D., Terzi, F., Matrougui, K., Duriez, M., Boulanger, C., Colucci-Guyon, E., Babinet, C., Briand, P., Friedlander, G., Polyevin, P. & Levy, B.I. (1997) Impaired flow-induced dilation in mesenteric resistance arteries from mice lacking vimentin. *J. Clin. Invest.* 100 (11): 2909-2914.
- Hermann, H. & Aebi, U. (2000) Intermediate filaments and their associates: Multi-talented structural elements specifying cytoarchitecture and cytodynamics. *Curr. Opin. Cell Biol.* 12: 79-90.
- Ho, C.-L., Martys, J.L., Mikhailov, A., Gundersen, G.G. & Liem, R.K.H. (1998) Novel features of intermediate filament dynamics revealed by green fluorescent protein chimeras. *J. Cell Sci.* 111: 1767-1778.
- Ho, C.-L., Mikhailov, A.V., Gundersen, G.G. & Liem, R.K.H. (1996) Use of GFP-Vimentin construct to examine intermediate filament dynamics in living cells. *Mol. Biol. Cell.* 10: 384.
- Ho, C.-L., Martys, J.L., Mikhailov, A.V., Gundersen, G.G. & Liem, R.K.H. (1998) Novel features of intermediate filaments dynamics revealed by green fluorescent protein chimeras. *J. Cell Sci.* 111: 1767-1778.
- Houseweart, M.K. & Cleveland, D.W. (1998) Intermediate filaments and their associated proteins: Multiple dynamic personalities. *Curr. Opin. Cell Biol.* 10: 93-101.

- Hsu, H., Solovyev, I., Colombero, A., Elliot, R., Kelley, M. & Boyle, W.J. (1997) ATAR, a novel tumor necrosis factor receptor family member, signals through TRAF2 and TRAF5. *J. Biol. Chem.* 272 (21): 13471-13474.
- Hu, Y., Hochleitner, B., Wick, G. & Xu, Q. (1998) Decline of shear stress-induced activation of extracellular signal-regulated kinases, but not stress-activated protein kinases, in *in vitro* propagated endothelial cells. *Exp. Gerontology* 33 (6): 601-613.
- Hu, Y., Baud, V., Delhase, M., Zhang, P., Deernick, T., Ellisman, M., Johnson, R. & Karin, M. (1999) Abnormal morphogenesis but intact IKK activation in mice lacking the IKK α subunit of I κ B kinase. *Science* 284: 316-320.
- Hynes, R.O. (1992) Integrins: Versatility, modulation and signalling in cell adhesion. *Cell* 69: 11-25.
- Inada, H., Togashi, H., Nakamura, Y., Kaibuchi, K. & Nagata, K.-I. (1999) Balance between activities of Rho kinase and type 1 protein phosphatase modulates turnover of phosphorylation and dynamics of desmin/vimentin filaments. *J. Biol. Chem.* 274 (49): 34932-34939.
- Inagaki, M., Matsuoka, Y., Tsujimura, K., Ando, S., Tokui, T., Takahashi, T. & Inagaki, N. (1996) Dynamic property of intermediate filaments: regulation by phosphorylation. *BioEss.* 18 (6): 481-487.
- Inagaki, N., Goto, H., Ogawara, M., Nishi, Y., Ando, S. & Inagaki, M. (1997) Spatial patterns of Ca²⁺ signals define intracellular distribution of a signalling by Ca²⁺/calmodulin-dependent protein kinase II. *J. Biol. Chem.* 272 (40): 25195-25199.
- Inoue, J.-I., Kerr, L.D., Rashid, D., Davis, N., Bose, H.R. & Verma, I.M. (1992) Direct association of pp40/I κ B β with rel/NF- κ B transcription factors: Role of ankyrin repeats in the inhibition of DNA binding activity. *Proc. Natl. Acad. Sci.* 89: 4333-4337.

- Irvine, A.D., Rugg, E.L., Lane, E.B., Hoare, S., Peret, C., Hughes, A.E. & Heagerty, A.H. (2001) Molecular confirmation of the unique phenotype of epidermolysis bullosa simplex with mottled pigmentation. *Brit. J. Derm.* 144 (1): 40-49.
- Ishida, T., Peterson, T.E., Kovach, N.L. & Berk, B.C. (1996) MAP kinase activation by flow of endothelial cells. Role of beta 1 integrins and tyrosine kinases. *Circ. Res.* 79 (2): 310-316.
- Ives, C.L., Eskin, S.G. & McIntire, L.V. (1986) Mechanical effects on endothelial cell morphology: *in vitro* assessment. *In Vitro Cell. Dev. Biol.* 22 (9): 500-507.
- Jaffray, E., Wood, K.M. & Hay, R.T. (1995) Domain organisation of I κ B α and sites of interaction with NF- κ B p65. *Mol. Cell. Biol.* 15 (4): 2166-2172.
- Jalali, S., Angel del Pozo, M., Chen, K.-D., Miao, H., Li, Y.-S., Schwartz, M.A. & Shyy, J. Y.-J. (2001) Integrin-mediated mechanotransduction requires its dynamic interaction with specific extracellular matrix (ECM) ligands. *Proc. Natl. Acad. Sci.* 98 (3): 1042-1046.
- Janmey, P.A., Euteneuer, U., Traub, P. & Schliwa, M. (1991) Viscoelastic properties of vimentin compared with other filamentous bipolymer networks. *J. Cell Biol.* 113 (1): 155-60.
- Jones, J.C.R. & Goldman, R.D. (1985) Intermediate filaments and the initiation of desmosome assembly. *J. Cell Biol.* 101: 506-517.
- Jones, J.C. & Green, K.J. (1991) Intermediate filament – plasma membrane interactions. *Curr. Opin. Cell. Biol.* 3: 127-132.
- Kataoka, N., Ujita, S. & Sato, M. (1998) Effect of flow direction on the morphological responses of cultured bovine aortic endothelial cells. *Med. Biol. Eng. Comp.* 36: 122-128.

- Khachigian, L.M., Resnick, N., Gimbrone, M.A. & Collins, T. (1995) Nuclear factor- κ B interacts functionally with the platelet-derived growth factor B-chain shear-stress response element in vascular endothelial cells exposed to fluid shear stress. *J. Clin. Invest.* 96: 1169-1175.
- Kiosses, W.B., McKee, N.H. & Kalnins, V.I. (1997) Relationship between the distribution of stress fibers and centrosomes in endothelial cells of the rat aorta. *Cell. Motil. Cyto.* 36: 228-235.
- Kirkpatrick, C.J., Wagner, M., Hermanns, I., Klein, C.L., Kohler, H., Otto, M., van Kooten, T.G. & Bittinger, F. (1997) Physiology and cell biology of the endothelium: A dynamic interface for cell communication. *Int. J. Microcirc.* 17: 231-240.
- Kosako, H., Goto, H., Yanagida, M., Matsuzawa, K., Fujita, M., Tomono, Y., Okigaki, T., Odai, H., Kaibuchi, K. & Inagaki, M. (1999) Specific accumulation of Rho-associated kinase at the cleavage furrow during cytokinesis: cleavage furrow-specific phosphorylation of intermediate filaments. *Oncogene* 18 (17): 2783-2788.
- Krappmann, D., Hatada, E.N., Tegethoff, S., Li, J., Klippel, A., Giese, K., Baeuerle, P.A. & Scheidereit, C. (2000) The I κ B Kinase (IKK) complex is tripartite and contains IKK γ but not IKAP as a regular component. *J. Biol. Chem.* 275 (38): 29779-29787.
- Kuchan, M.J. & Frangos, J.A. (1993) Shear stress regulates endothelin-1 release via protein kinase C and cGMP in cultured endothelial cells. *Am. J. Physio.* 264: H150-H156.
- Lampugnani, M.G., Resnati, M., Dejana, E. & Marchisio, P.C. (1991) The role of integrins in the maintenance of endothelial monolayer integrity. *J. Cell Biol.* 112 (3): 479-490.

- Lan, Q., Mercurius, K.O. & Davies, P.F. (1994) Stimulation of transcription factors NF- κ B and AP1 in endothelial cells subjected to shear stress. *Biochem. Biophys. Res. Commun.* 201 (2): 950-956.
- Lane, E.B. (1994) Keratin diseases. *Curr. Opin. Gen Dev.* 4: 412-418.
- Lazarides, E. (1980) Intermediate filaments as mechanical integrators of cellular space. *Nature* 283: 249-255.
- Lazarides, E. (1982) Intermediate filaments: A chemically heterogeneous, developmentally regulated class of proteins. *Ann. Rev. Biochem.* 51: 219-250.
- Lee, F.S., Peters, R.T., Dang, L.C. & Maniatis, T. (1998) MEKK1 activates both I κ B kinase α and I κ B kinase β . *Proc. Natl. Acad. Sci.* 95: 9319-9324.
- Levesque, M.J. & Nerem, R.M. (1985) The elongation and orientation of cultured endothelial cells in response to shear stress. *J. Biomech. Eng.* 107: 341-347.
- Li, Q., Van Antwerp, D., Mercurio, F., Lee, K.-F. & Verma, I.M. (1999a) Severe liver degeneration in mice lacking the I κ B kinase 2 gene. *Science* 284: 321-325.
- Li, Q., Lu, Q., Hwang, J.Y., Buscher, D., Lee, K.F., Izpisua-Belmonte, J.C. & Verma, I. (1999b) IKK1-deficient mice exhibit abnormal development of skin and skeleton. *Gene. Dev.* 13: 1322-1328.
- Li, S., Chen, B.P.C., Azuma, N., Hu, Y.-L., Wu, S.Z., Sumpio, B.E., Shyy, J., Y.-J. & Chien, S. (1999) Distinct roles for the small GTPases Cdc42 and Rho in endothelial responses to shear stress. *J. Clin. Invest.* 103 (8): 1141-1150.
- Li, Y.-S., Shyy, J. Y.-J., Li, S., Lee, J., Su, B., Karin, M. Chien, S. (1996) The Ras-JNK pathway is involved in shear-induced gene expression. *Mol. Cell. Biol.* 16 (11): 5947-5954.

- Li, Z.W., Chu, W., Hu, Y., Delhase, M., Deerinck, T., Ellisman, M., Johnson, R. & Karin, M. (1999c) The IKK β subunit of the I κ B kinase (IKK) is essential for NF- κ B activation and prevention of apoptosis. *J. Exp. Med.* 189: 1839-1845.
- Liao, G. & Gundersen, G.G. (1998) Kinesin is a candidate for cross-bridging microtubules and intermediate filaments. *J. Biol. Chem.* 273 (16): 9797-9803.
- Lieska, N., Yang, H.-Y. & Goldman, R.D. (1985) Purification of the 300K intermediate filament-associated protein and its in vitro recombination with intermediate filaments. *J. Cell. Biol.* 101: 802-813.
- Lin, L. & Ghosh, S. (1996) A glycine-rich region in NF- κ B p105 functions as a processing signal for the generation of the p50 subunit. *Mol. Cell. Biol.* 16 (5): 2248-2254.
- Ling, L., Cao, Z. & Goeddel, D.V. (1998) NF-kappa B-inducing kinase activates IKK-alpha by phosphorylation of Ser-176. *Proc. Natl. Acad. Sci.* 95 (7): 3792-3797.
- Ludin, B. & Matus, A. (1998) GFP illuminates the cytoskeleton. *Trends Cell. Biol.* 8: 72-77.
- McCormick, S.M., Eskin, S.G., McIntire, L.V., Teng, C.L., Lu, C.-H., Russell, C.G. & Chittur, K.K. (2001) DNA microarray reveals changes in gene expression of shear stressed human umbilical vein endothelial cells. *Proc. Natl. Acad. Sci.* 98 (16): 8955-8960.
- McDowell, K. (1998) Effects of flow on the tubulin cytoskeleton of endothelial cells. *University of St Andrews Honours Project Thesis.*
- McIntire, L.V., Wagner, J.E., Papadaki, M., Whitson, P.A. & Eskin, S.G. (1998) Effect of flow on gene regulation in smooth muscle cells and macromolecular transport across endothelial cell monolayers. *Biol. Bull.* 194: 394-399.

McLean, W.H.I. & Lane, E.B. (1995) Intermediate filaments in disease. *Curr. Opin. Cell Biol.* 7: 118-125.

McLean, W.H.I., Pulkkinen, L., Smith, F.J.D., Rugg, E.L., Lane, E.B., Bullrich, F., Burgeson, R.E., Amano, S., Hudson, D.L., Owaribe, K., McGrath, J.A., McMillan, J.R., Eady, R.A.J., Leigh, I.M., Christiano, A.M. & Uitto, J. (1996) Loss of plectin causes epidermolysis bullosa with muscular dystrophy: cDNA cloning and genomic organisation. *Gen. Dev.* 10: 1724-1735.

McNeil, P.L. (1993) Cellular and molecular adaptations to injurious mechanical stress. *Trends. Cell Biol.* 3: 302-307.

Malek, A.M., Zhang, J. & Izumo, S. (1994) Cytoskeletal involvement and cell shape contribution to the regulation of Endothelin-1 gene expression by fluid shear stress. *Circulation* 90 (4): 1570.

Malek, A.M. & Izumo, S. (1996) Mechanism of endothelial cell shape change and response to fluid shear stress. *J. Cell Sci.* 1089: 713-726.

Malinin, N.L., Boldin, M.P., Kovalenko, A.V. & Wallach, D. (1997) MAP3K-related kinase involved in NF- κ B induction by TNF, CD95 and IL-1. *Nature* 385: 540-544.

Maniatis, T. (1997) Catalysis by a multiprotein I κ B kinase complex. *Science* 278: 818-819.

Maniotis, A.J., Chen, C.S. & Ingber, D.E. (1997) Demonstration of mechanical connections between integrins, cytoskeletal filaments and nucleoplasm that stabilize nuclear structure. *Proc. Natl. Acad. Sci.* 94: 849-854.

Masuda, M. & Fujiwara, K. (1993a) Morphological responses of single endothelial cells exposed to physiological levels of fluid shear stress. *Front. Med. Biol. Engng.* 5 (2): 79-87.

- Masuda, M. & Fujiwara, K. (1993b) The biased lamellipodium development and microtubule organization center position in vascular endothelial cells migrating under the influence of fluid flow. *Biol. Cell* 77: 237-245.
- Mathur, A.B., Truskey, G.A. & Reichert, W.M. (2000) Atomic force and total internal reflection fluorescence microscopy for the study of force transmission in endothelial cells. *Biophys. J.* 78: 1725-1735.
- Matsushima, A., Kaisho, T., Rennert, P.D., Nakano, H., Kurosawa, K., Uchida, D., Takeda, K., Akira, S. & Matsumoto, M. (2001) Essential role of nuclear factor (NF)- κ B-inducing kinase and inhibitor of κ B (I κ B) kinase α in NF- κ B activation through lymphotoxin β receptor, but not through tumour necrosis factor receptor I. *J. Exp. Med.* 193 (5): 631-636.
- Matthews, J.R. & Hay R.T. (1995) Regulation of DNA Binding Activity of NF- κ B. *Int. J. Biochem. Cell. Biol.* 27 (9): 865-879.
- May, M. J. & Ghosh, S. (1997) Rel/NF- κ B and I κ B proteins: an overview. *Cancer Biology* 8: 63-73.
- May, M. J. & Ghosh, S. (1998) Signal transduction through NF- κ B. *Immunol. Today* 19 (2): 80-88.
- Mercurio, F., DiDonato, J.A., Rosette, C. & Karin, M. (1993) p105 and p98 precursor proteins play an active role in NF-kappa B-mediated signal transduction. *Gen. Dev.* 7 (4): 705-718.
- Mercurio, F., Zhu, H., Murray, B.W., Shevchenko, A., Bennett, B.L., Li, J., Young, D.B., Barbosa, M., Mann, M., Manning, A. & Rao, A. (1997) IKK-1 and IKK-2: cytokine activated I κ B kinase essential for NF- κ B activation. *Science* 278: 860-866.
- Mercurio, F. & Manning, A.M. (1999a) Multiple signals converging on NF- κ B. *Curr. Opin. Cell Biol.* 11: 226-232.

Mercurio, F., Murray, B.W., Shevchenko, A., Bennett, B.L., Young, D.B., Li, J.W., Pascual, G., Motiwala, A., Zhu, A., Mann, M. & Manning, A.M. (1999b) I κ B Kinase (IKK)-associated protein 1, a common component of the heterogeneous IKK complex. *Mol. Cell. Biol.* 19 (2): 1526-1538.

Mercurio, F. & Manning, A.M (2000) Regulation of NF- κ B function – Novel molecular targets for pharmacological intervention. *Signalling networks and cell cycle control: The molecular basis of cancer and other diseases* 429-438. Ed. J.S. Gutkind, Humana Press Inc, Totowa, NJ.

Michael, W.M., Choi, M. & Dreyfuss, G. (1995) A nuclear export signal in hnRNP A1: A signal mediated, temperature dependent nuclear protein export pathway. *Cell* 83 (3): 415-422.

Mohan, S., Mohan, N., & Sprague, E.A. (1997) Differential activation of NF- κ B in human aortic endothelial cells conditioned to specific flow environments. *Am. J. Physiol.* 273: C572-C578.

Molony, L. & Armstrong, L. (1991) Cytoskeletal reorganisations in human umbilical vein endothelial cells as a result of cytokine exposure. *Exp. Cell. Res.* 196: 40-48.

Muller, C.W. & Harrison, S.C. (1995) The structure of the NF-kappa B p50:DNA-complex: a start to analyzing the Rel family. *FEBS Lett* 369 (1): 113-117.

Muller, C.W., Rey, F.A., Sodeoka, M., Verdien, G.L. & Harrison, S.C. (1995) Structure of the NF- κ B p50 homodimer bound to DNA. *Nature* 373: 311-317.

Nagel, T., Resnick, N., Dewey, F. & Gimbrone, M.A. (1999) Vascular endothelial cells respond to spatial gradients in fluid shear stress by enhanced activation of transcription factors. *Arterioscler. Thromb. Vasc. Biol.* 19: 1825-1834.

- Nakano, H., Shindo, M., Sakon, S., Nishinaka, S., Mihara, M., Yagita, H. & Okumura, K. (1998) Differential regulation of the I κ B kinase α and β by two upstream kinases, NF- κ B-inducing kinase and mitogen-activated protein kinase/ERK kinase, kinase-1. *Proc. Natl. Acad. Sci.* 95: 3537-3542.
- Nerem, R.M., Levesque, M.J. & Cornhill, J.F. (1981) Vascular endothelial morphology as an indicator of the pattern of blood flow. *J. Biomech. Eng.* 103 (3): 172-176.
- Nerem, R.M., Alexander, R.W., Chappell, D.C., Medford, R.M., Varner, S.E. & Taylor, R.T. (1998) The study of the influence of flow on vascular endothelial biology. *Am. J. Med. Sci.* 316 (3): 169-175.
- Nishizawa, K., Yano, T., Shibata, M., Ando, S., Saga, S., Takahashi, T. & Inagaki, M. (1991) Specific localisation of phosphointermediate filament protein in the constricted area of dividing cells. *J. Biol. Chem.* 266 (5): 3074-3079.
- Noll, G., Tschudi, M., Nava, E. & Luscher, T.F. (1997) Endothelium and high blood pressure. *Int. J. Microcirc. Clin. Exp.* 17 (5): 273-279.
- Oakley, C. & Brunette, D. M. (1993) The sequence of alignment of microtubules, focal contacts and actin filaments in fibroblasts spreading on smooth and grooved titanium substrata. *J. Cell. Sci.* 106: 343-354.
- Ogawara, M., Inagaki, N., Tsujimura, K., Takai, Y., Sekimata, M., Ha, M.H., Imajoh-Ohmi, S., Hirai, S., Sugiura, H., Yamauchi, T. & Inagaki, M. (1995) Differential targeting of protein kinase C and CAM kinase II signalling to vimentin. *J. Cell Biol.* 131 (4): 1055-1066.
- Olivier, L.A., Yen, J., Reichert, W.M. & Truskey, G.A. (1999) Short-term cell/substrate contact dynamics of subconfluent endothelial cells following exposure to laminar flow. *Biotechnol. Prog.* 15: 33-42.

Oluwole, B.O., Du, W., Mills, I. & Sumpio, B.E. (1997) Gene regulation by mechanical forces. *Endothelium* 5: 85-93.

Ossareh-Nazari, B., Bachelerie, F. & Dargemont, C. (1997) Evidence for a role of CRM1 in signal mediated nuclear protein export. *Science* 278: 141-144.

Otto, J.J. (1990) Vinculin. *Cell. Motil. Cyto.* 16: 1-6.

Palmer, R.M.J., Ferrige, A.G. & Moncada, S. (1987) Nitric oxide release accounts for biological activity of endothelium-derived relaxing factor. *Nature* 327: 524-526.

Palombella, V.J., Rando, O.J., Goldberg, A.L. & Maniatis, T. (1994) The ubiquitin-proteasome pathway is required for processing the NF- κ B1 precursor protein and the activation of NF- κ B. *Cell* 78: 773-785.

Pando, M.P. & Verma, I.M. (2000) Signal-dependent and -independent degradation of free and NF- κ B-bound I κ B α . *J. Biol. Chem.* 275 (28): 21278-21286.

Papadaki, M & Eskin, S.G. (1997) Effects of fluid shear stress on gene regulation of vascular cells. *Biotechnol. Prog.* 13: 209-221.

Phelps, C.B., Sengchanthalangsy, L.L., Huxford, T. & Ghosh, G. (2000) Mechanism of I κ B α binding to NF- κ B dimers. *J. Biol. Chem.* 275 (38): 29840-29846.

Pickart, C.M. & Rose, I.A. (1985) Ubiquitin carboxyl-terminal hydrolase acts on ubiquitin carboxyl-terminal amides. *J. Biol. Chem.* 260 (13): 7903-7910.

Pinol-Roma, S. & Dreyfuss, G. (1992) Shuttling of pre-mRNA binding proteins between the nucleus and cytoplasm. *Nature* 355 (6362): 730-732.

Prahlad, V., Yoon, M., Moir, R., Vale, R.D. & Goldman, R.D. (1998) Rapid movements of vimentin on microtubule tracks: Kinesin-dependent assembly of intermediate filament networks. *J. Cell Biol.* 143 (1): 159-170.

- Regnier, C.H., Song, H. Y., Gao, X., Goeddel, D.V., Cao, Z. & Rothe, M. (1997) Identification and characterisation of an I κ B kinase. *Cell* 90: 373-383.
- Resnick, N., Collins, T., Atkinson, W., Bonthorn, D.T., Dewey, C.F. & Gimbrone, M.A. (1993) Platelet-derived growth factor B chain promoter contains a cis-acting fluid shear-stress responsive element. *Proc. Natl. Acad. Sci.* 90: 4591-4595.
- Resnick, N. & Gimbrone, M.A. (1995) Haemodynamic forces are complex regulators of endothelial gene expression. *FASEB J.* 9: 874-882.
- Riveline, D., Zamir, E., Balaban, N.Q., Schwarz, U.S., Ishizaki, T., Narumiya, S., Kam, Z., Geiger, B. & Bershadsky, A.D. (2001) Focal contacts as mechanosensors: Externally applied local mechanical forces induces growth of focal contacts by an mDia1-dependent and ROCK-independent mechanism. *J. Cell Biol.* 153 (6): 1175-1185.
- Robotewskyi, A., McKibben, S., Dull, R., Griem, M.L. & Davies, P.F. (1991) Dynamics of focal adhesion site remodelling in living endothelial cells in response to shear stress forces using confocal image analysis. *FASEB J.* 5: A527.
- Rodriguez, M.S., Michalopoulos, I., Arenzana-Seisdedos, F. & Hay, R.T. (1995) Inducible degradation of I κ B α in vitro and in vivo requires the acidic C-terminal domain of the protein. *Mol. Cell. Biol.* 15 (5): 2413-2419.
- Rodriguez, M.S., Thompson, J., Hay, R.T. & Dargemont, C. (1999) Nuclear retention of I κ B α protects it from signal-induced degradation and inhibited nuclear factor κ B transcriptional activation. *J. Biol. Chem.* 274 (13): 9108-9115.
- Rogers, S., Wells, R. & Rechsteiner, M. (1986) Amino acid sequences common to rapidly degraded proteins: The PEST hypothesis. *Science* 234: 364-369.

- Romieu-Mourez, R., Landesman-Bollag, E., Seldin, D.C., Traish, A.M., Mercurio, F. & Sonenshein, G.E. (2001) Roles of IKK kinases and protein kinase CK2 in activation of nuclear factor- κ B in breast cancer. *Cancer Res.* 61: 3810-3818.
- Rosette, C. & Karin, M. (1995) Cytoskeletal control of gene expression: depolymerisation of microtubules activated NF- κ B. *J. Cell Biol.* 128 (6): 1111-1119.
- Ross, R. (1993) The pathogenesis of atherosclerosis: a perspective for the 1990's. *Nature* 362: 801-808.
- Rothe, M., Sarma, V., Dixit, V.M. & Goeddel, D.V. (1995) TRAF2-mediated activation of NF- κ B by TNF receptor 2 and CD40. *Science* 269: 1424-1426.
- Rothwarf, D.M., Zandi, E., Natoli, G. & Karin, M. (1998) IKK- γ is an essential regulatory subunit of the I κ B kinase complex. *Nature* 395: 297-300.
- Satcher, R.L., Bussolari, S.R., Gimbrone, M.A. & Dewey, C.F. (1992) The distribution of fluid forces on model arterial endothelium using computational fluid dynamics. *Biomech. Eng.* 114: 309-316.
- Satcher, R., Dewey, C.F. & Hartwig, J.H. (1997) Mechanical remodelling of the endothelial surface and actin cytoskeleton induced by fluid flow. *Microcirc.* 4 (4): 439-453.
- Savion, N., Vlodavsky, I., Greenburg, G. & Gospodarowicz, D. (1982) Synthesis and distribution of cytoskeletal elements in endothelial cells as a function of cell growth and organisation. *J. Cell Physiol.* 110: 129-141.
- Scherer, D.C., Brockman, J.A., Chen, Z., Maniatis, T. & Ballard, D.W. (1995) Signal-induced degradation of I κ B α requires site-specific ubiquitination. *Proc. Natl. Acad. Sci.* 92: 11259-11263.

Schnittler, H., Schmandra, T. & Drenckhahn, D. (1998) Correlation of endothelial vimentin content with hemodynamic parameters. *Histochem. Cell. Biol.* 110: 161-167.

Schoenwaelder, S.M. & Burridge, K. (1999) Bidirectional signalling between the cytoskeleton and integrins. *Curr. Opin. Cell Biol.* 11: 274-286.

Schwartz, E.A., Bizios, R., Medow, M.S. & Gerritsen, M.E. (1999) Exposure of human vascular endothelial cells to sustained hydrostatic pressure stimulates proliferation. *Circ. Res.* 84: 315-322.

Schwartz, M.A. (1992) Transmembrane signalling by integrins. *Trends Cell. Biol.* 2: 304-307.

Seifert, G.J., Lawson, D. & Wiche, G. (1992) Immunolocalisation of the intermediate filament-associated protein plectin at focal contacts and actin stress fibres. *Eur. J. Cell Biol.* 59: 138-147.

Sen, R. & Baltimore, D. (1986a) Multiple nuclear factors interact with the immunoglobulin enhancer sequences. *Cell* 46: 705-716.

Sen, R. & Baltimore, D. (1986b) Inducibility of κ immunoglobulin enhancer-binding protein NF- κ B by a post-translational mechanism. *Cell* 47: 921-928.

Shah, J.V., Wang, L.Z., Traub, P. & Janmey, P.A. (1998) Interaction of vimentin with actin and phospholipids. *Biol. Bull.* 194: 402-405.

Shyy, J.Y., Li, Y.S., Lin, M.C., Chen, W., Yuan, S., Usami, S. & Chien, S. (1995) Multiple cis-elements mediate shear stress-induced gene expression. *J. Biomech.* 28 (12): 1451-1457.

Shyy, J.Y.-J. & Chien, S. (1997) Role of integrins in cellular responses to mechanical stress and adhesion. *Curr. Opin. Cell Biol.* 9: 707-713.

Silkworth, J.B. & Stehbens, W.E. (1975) The shape of endothelial cells in *en face* preparations of rabbit blood vessels. *Angiology* 26: 474-487.

Sin, W.C., Chen, X.Q., Leung, T. & Lim, L. (1998) Rho-A binding kinase alpha translocation is facilitated by the collapse of the vimentin intermediate filament network. *Mol. Cell. Biol.* 18 (11): 6325-6339.

Sirois, E., Charara, J., Ruel, J., Dussault, J.C., Gagnon, P. & Doillon, C.J. (1998) Endothelial cells exposed to erythrocytes under shear stress: An *in vitro* study. *Biomaterials* 19: 1925-1934.

Skalli, O. & Goldman, R.D. (1991) Recent insights into the assembly, dynamics and function of intermediate filament networks. *Cell. Motil. Cyto.* 19: 67-79.

Skalli, O., Chou, Y.H. & Goldman, R.D. (1992a) Cell cycle-dependent changes in the organisation of an intermediate filament associated protein: Correlation with phosphorylation by p34^{cdc2}. *Proc. Natl. Acad. Sci.* 89: 11959-11963.

Skalli, O., Chou, Y.-H. & Goldman, R.D. (1992b) Intermediate filaments: not so tough after all. *Trends Cell Biol.* 2: 308-312.

Skalli, O., Jones, J.C.R., Gagescu, R. & Goldman, R.D. (1994) IFAP 300 is common to desmosomes and hemidesmosomes and is a possible linker of intermediate filaments to these junctions. *J. Cell Biol.* 125 (1): 159-170.

Smith, C.A., Farrah, T. & Goodwin, R.G. (1994) The TNF receptor superfamily of cellular and viral proteins; activation, costimulation and death. *Cell* 76: 959-962.

Smith, F.J.D., Eady, R.A.J., Leigh, I.M., McMillan, J.R., Rugg, E.L., Kelsell, D.P., Bryant, S.P., Spurr, N.K., Geddes, J.F., Kirtschig, G., Milana, G., de Bono, A.G., Owaribe, K., Wiche, G., Pulkkinen, L., Uitto, J., McLean, W.H.I. & Lane, E.B. (1996) Plectin deficiency results in muscular dystrophy with epidermolysis bullosa. *Nature Gen.* 13: 450-457.

- Song, H.Y. & Donner, D.B (1995) Association of a RING finger protein with the cytoplasmic domain of the human type-2 tumour necrosis factor receptor. *Biochem. J.* 309: 825-829.
- Spencer, E., Jiang, J. & Chen, Z.J. (1999) Signal-induced ubiquitination of I κ B α by the F-box protein slimb/ β -TrCP. *Gene. Dev.* 13: 284-294.
- Stancovski, I. & Baltimore, D. (1997) NF- κ B activation: The I κ B kinase revealed? *Cell* 91: 299-302.
- Starger, J.M., Brown, W.E., Goldman, A.E. & Goldman, R.D. (1978) Biochemical and immunological analysis of rapidly purified 10nm filaments from the baby hamster kidney (BHK-21) cells. *J. Cell Biol.* 78: 93-109.
- Steinbock, F.A. & Wiche, G. (1999) Plectin: a cytolinker by design. *Biol. Chem.* 380 (2): 151-158.
- Steinert, P.M., Jones, J.C.R. & Goldman, R.D. (1984) Intermediate Filaments. *J. Cell. Biol.* 99 (1): 22s-27s.
- Steinert, P.M. & Roop, D.R. (1988) Molecular and cellular biology of intermediate filaments. *Ann. Rev. Biochem.* 57: 593-625.
- Steinert, P.M. & Liem, R.K.H. (1990) Intermediate filament dynamics. *Cell* 60: 521-523.
- Steinert, P.M., Chou, Y., Prahlad, V., Parry, D.A.D., Marekov, L.N., Wu, K.C., Jang, S. & Goldman, R.D. (1999) A high molecular weight intermediate filament associated protein in BHK-21 cells is Nestin, a type IV intermediate filament protein: Limited co-assembly in vitro to form heteropolymers with type III vimentin and type IV α -internexin. *J Biol. Chem.* 274 (14): 9881-9890.

- Sun, D., Huang, A., Sharma, S., Koller, A. & Keley, G. (2001) Endothelial microtubule disruption blocks flow-dependent dilation of arterioles. *Am. J. Heart. Circ. Physiol.* 280: H2087- H2093.
- Svitkina, T.M., Verkhovsky, A.B. & Borisy, G.B. (1998) Plectin sidearms mediate interactions of intermediate filaments with microtubules and other components of the cytoskeleton. *J. Cell Sci.* 135 (4): 991-1007.
- Takahashi, M. & Berk, B.C. (1996) Mitogen-activated Protein Kinase (ERK1/2) activation by shear stress and adhesion in endothelial cells. *J. Clin. Invest.* 98 (11): 2623-2631.
- Takai, Y., Ogawara, M., Tomono, Y., Moritoh, C., Imajoh-Ohmi, S., Tsutsumi, O., Taketani, Y. & Inagaki, M. (1996) Mitosis-specific phosphorylation of vimentin by protein kinase C coupled with reorganisation of intracellular membranes. *J. Cell Biol.* 133 (1): 141-149.
- Takeda, K., Takeuchi, O., Tsujimura, T., Itami, S., Adachi, O., Kawai, T., Sanjo, H., Yoshikawa, K., Terada, N. & Akira, S. (1999) Limb and skin abnormalities in mice lacking IKK α . *Science* 284: 313-316.
- Tanaka, M., Fuentes, M.E., Yamaguchi, K., Durnin, M.H., Dalrymple, S.A., Hardy, K.L. & Goeddel, D.V. (1999) Embryonic lethality, liver degeneration and impaired NF- κ B activation in IKK β -deficient mice. *Immunity* 10: 421-429.
- Tardy, Y., Resnick, N., Gimbrone, M.A. & Dewey, C.F. (1997) Shear stress gradients remodel endothelial monolayers in vitro via a cell proliferation-migration-loss cycle. *Arterioscler. Thromb.* 17: 3120-3106.
- Thoumine, O., Ziegler, T., Girard, P.G. & Nerem, R.M. (1995) Elongation of confluent endothelial cells in culture: the importance of fields of force in the associated alterations of their cytoskeletal structure. *Exp. Cell Res.* 219: 427-441.

- Tint, I.S., Hollenbeck, P.J., Verkhovsky, A.B., Surgucheva, I.G. & Bershadsky, A.D. (1991) Evidence that intermediate filament reorganisation is induced by ATP-dependent contraction of the actomyosin cortex in permeabilized fibroblasts. *J. Cell Sci.* 98: 375-384.
- Topper, J.N. & Gimbrone, M.A. (1999) Blood flow and vascular gene expression: fluid shear stress as a modulator of endothelial phenotype. *Mol. Med. Today.* 5 (1): 40-46.
- Touellec, D., Pianetti, P., Coste, H., Bellevergue, P., Grand-Perret, T., Ajakane, M., Baudet, V., Boissin, P., Boursier, E. & Loriolle, F. (1991) The bisindolylmaleimide GF 109203X is a potent and selective inhibitor of protein kinase C. *J. Biol. Chem.* 266 (24): 15771-15781.
- Traub, O. & Berk, B.C. (1998) Laminar Shear Stress: Mechanisms by which endothelial cells transduce an atheroprotective force. *Arterioscler. Thromb. Vasc. Biol.* 18: 677-685.
- Tsujimura, K., Ogawara, M., Takeuchi, Y., Imajoh-Ohmi, S., Ha, M.H. & Inagaki, M. (1994) Visualisation and function of vimentin phosphorylation by cdc2 kinase during mitosis. *J. Biol. Chem.* 269 (49): 31097-31106.
- Turner, C.E., Glenny, J.R. & BurrIDGE, K. (1990) Paxillin: A new vinculin binding protein present in focal adhesions. *J. Cell Biol.* 111: 1059-1068.
- Tzima, E., Angel del Pozo, M., Shattil, S.J., Chien, S. & Schwartz, M.A. (2001) Activation of integrins in endothelial cells by fluid shear stress mediates Rho-dependent cytoskeletal alignment. *EMBO J.* 20 (17): 4639-4647.
- Viggers, R.F., Wechezak, A.R. & Sauvage, L.R. (1986) An apparatus to study the response of cultured endothelium to shear stress. *Trans. ASME* 108: 332-337.
- Vikstrom, K.L., Borisy, G.G. & Goldman, R.D. (1989) Dynamic aspects of intermediate filament networks in BHK-21 cells. *Proc. Nat. Acad. Sci.* 86: 549-533.

- Vikstrom, K.L., Lim, S.-S., Goldman, R.D. & Borisy, G.G. (1992) Steady state dynamics of intermediate filament networks. *J. Cell Biol.* 118 (1): 121-129.
- Vilcek, J. & Lee, T.H. (1991) Tumour necrosis factor: The new insights into the molecular mechanisms of its multiple actions. *J. Biol. Chem.* 266 (12): 7313-7316.
- Wang, D., Westerheide, S.D., Hanson, J.L. & Baldwin, A.S. (2000) Tumour necrosis factor α -induced phosphorylation of RelA/p65 on ser⁵²⁹ is controlled by casein kinase II. *J. Biol. Chem.* 275 (42): 32592-32597.
- Wang, N., Butler, J.P. & Ingber, D.E. (1993) Mechanotransduction across the cell surface and through the cytoskeleton. *Science* 260: 1124-1127.
- Wang, N. (1998) Mechanical interactions among cytoskeletal filaments. *Hypertension* 32: 162-165.
- Wang, W. & Passaniti, A. (1999) Extracellular matrix inhibits apoptosis and enhances endothelial cell differentiation by an NF- κ B-dependent mechanism. *J. Cell. Biochem.* 73: 321-331.
- Wechezak, A.R., Wight, T.N., Viggers, R.F. & Sauvage, L.R. (1989) Endothelial adherence under shear stress is dependent upon microfilament reorganisation. *J. Cell Physiol.* 139 (1): 136-146.
- White, G.E., Gimbrone, M.A. & Fujiwara, K. (1983) Factors influencing the expression of stress fibers in vascular endothelial cells in situ. *J. Cell Biol.* 97: 416-424.
- White, G.E. & Fujiwara, K. (1986) Expression and intracellular distribution of stress fibres in aortic endothelium. *J. Cell Biol.* 103: 63-70.
- Wiche, G. (1989) Plectin: general overview and appraisal of its potential role as a subunit protein of the cytomatrix. *Crit. Rev. Biochem. Mol. Biol.* 24 (1): 41-63.

- Wiche, G. (1998) Role of plectin in cytoskeleton organisation and dynamics. *J. Cell. Sci.* 111: 2477-2486.
- Wong, A.J. & Pollard, T.D. (1983) Actin filament stress fibres in endothelial cells in vivo. *Science* 219: 867-869.
- Woronicz, J.D., Goa, X., Cao, Z., Rothe, M. & Goeddel, D.V. (1997) NF- κ B kinase- β : NF- κ B activation and complex formation with I κ B kinase- α and NIK. *Science* 278: 866-869.
- Xiao, G., Harhaj, E.W. & Sun S.C. (2001) NF-kappa B-inducing kinase regulates the processing of NF-kappaB2 p100. *Mol. Cell.* 7 (2): 401-409.
- Yamada, K.M. & Geiger, B. (1997) Molecular interaction in cell adhesion complexes. *Curr. Opin. Cell Biol.* 9: 76-85.
- Yamaguchi, T. Hishiai, K., Okino, H., Kakurai, A., Hanai, S., Masuda, M. & Fujiwara, K. (1993) Shear stress distribution over confluent cultured endothelial cells studied by computational fluid dynamics. *Adv. Bioeng.* 20: 167-170.
- Yamaoka, S., Courtois, G., Bessia, C., Whiteside, S.T., Weil, R., Agou, F., Kirk, H.E., Kay, R.J. & Israel, A. (1998) Complementation cloning of NEMO, a component of the I κ B kinase complex essential for NF- κ B activation. *Cell* 93: 1231-1240.
- Yang, F., Moss, L.G. & Phillips, G.N. (1996a) The molecular structure of Green Fluorescent Protein. *Nat. Biotechnol.* 10: 1246-1251.
- Yang, H.-Y., Lieska, N., Goldman, A.E. & Goldman, R.D. (1985) A 300,000-mol-wt intermediate filament associated protein in baby hamster kidney (BHK-21) cells. *J. Cell Biol.* 100: 620-631.

- Yang, H.-Y., Lieska, N., Goldman, A.E. & Goldman, R.D. (1992) Colchicine-sensitive and colchicine-insensitive intermediate filament systems distinguished by a new intermediate filament associated protein, IFAP-70/280kD. *Cell. Motil. & Cyto.* 22: 185-199.
- Yang, Y., Dowling, J., Yu, Q.-C., Koulis, P., Cleveland, D.W. & Fuchs, E. (1996b) An essential cytoskeletal linker protein connecting actin microfilaments to intermediate filaments. *Cell* 86: 655-665.
- Yin, L., Wu, L., Wesche, H., Arthur, C.D., White, J.M., Goeddel, D.V. & Schreiber, R.D. (2001) Defective lymphotoxin-beta receptor-induced NF-kappa B transcriptional activity in NIK-deficient mice. *Science* 291 (5511): 2162-2165.
- Yin, M.-J., Christerson, L.B., Yamamoto, Y., Kwak, T.-T., Xu, S., Mercurio, F., Barbosa, M., Cobb, M.H. & Gaynor, R.B. (1998) HTLV-1 tax protein binds to MEKK1 to stimulate I κ B kinase activity and NF- κ B activation. *Cell* 93: 875-884.
- Yoon, M., Moir, R.D., Prahlad, V. & Goldman, R.D. (1998) Motile properties of vimentin intermediate filament networks in living cells. *J. Cell Biol.* 143 (1): 147-157.
- Zabel, U. & Baeuerle, P.A. (1990) Purified human I κ B can rapidly dissociate the complex of the NF- κ B transcription factor with its cognate DNA. *Cell* 61: 255-265.
- Zackroff, R.V. & Goldman, R.D. (1979) In vitro assembly of intermediate filaments from baby hamster kidney (BHK-21) cells. *Proc. Natl. Acad. Sci.* 76 (12): 6226-6230.
- Zandi, E., Rothwarf, D.M., Delhase, M., Hayakawa, M. & Karin, M. (1997) The I κ B kinase complex (IKK) contains two kinase subunits, IKK α and IKK β , necessary for I κ B phosphorylation and NF- κ B activation. *Cell* 91: 243-252.

Ziegler, T., Silacci, P., Harrison, V.J. & Hayoz, D. (1998) Nitric Oxide Synthase expression in endothelial cells exposed to mechanical forces. *Hypertension* 32: 351-355.

Zigmond, S.H. (1996) Signal transduction and actin filament organisation. *Curr. Opin. Cell Biol.* 8: 6-73.

APPENDIX 1

CELL CULTURE MATERIALS.

*N.B. Clonetics® products are distributed in the UK by Biowhittaker.
Suppliers and catalogue numbers are provided for all materials.*

1. Cells

Bovine Aortic Endothelial Cells (BAEC) were obtained from European Collection of Animal Cell Cultures (ECACC) (Centre for Applied Microbiology and Research, Salisbury, Wiltshire).

Human Coronary Artery Endothelial Cells (HCAEC) were obtained from Clonetics® (BW 2535).

Human Umbilical Vein Endothelial Cells (HUVEC) were obtained from Ailsa Webster (Cell Tech, Slough, UK).

2. Growth medium

BAEC

Dulbeccos MEM, High Glucose w/o Glutamine (Gibco 10938-025) supplemented with 10% Foetal Calf Serum (Globepharm – Lot 18974) or 10% Donor Calf Serum (TCS Biologicals - Lot 81980).

50iu/ml Penicillin, 50ug/ml Streptomycin (Sigma P3539)

2mM (which is 29.4mg/100ml MW = 147.1g) L-Glutamine (ICN 15-801-15).

HCAEC and HUVEC

“EGM2 – Bullet kit” – modified MCDB131 (Biowhittaker BW 3162) containing:

- 500ml Basal Medium – EGM-2

- Supplements:

25ml foetal calf serum (FCS),

0.5ml human recombinant epidermal growth factor (hEGF),

2.0ml human fibroblast growth factor – basic with heparin (hFGF),

0.5ml vascular endothelial growth factor (VEGF),

0.5ml Ascorbic acid,

0.2ml Hydrocortisone,
0.5ml Long R3-IGF-1,
0.5ml Heparin ,
0.5ml Gentamicin/amphotercin.

N.B. Concentrations of the above supplements are not supplied by Clonetics®.

3. *Trypsin*

BAEC

0.05% Trypsin (Gibco 25090-028) and 0.01% EDTA (Sigma E5134) made up in sterile PBSa. EDTA is stored as a 1% stock in sterile PBSa at 4°C.

HCAEC and HUVEC

Clonetics® trypsinisation reagents pack (Biowhittaker BW 5034) containing:

100ml hepes buffered saline solution (HBSS) (BW 5022)
100ml trypsin (0.025%)/EDTA (0.01%) (BW 5012)
100ml trypsin neutralising solution (TNS) (BW 5002).

3. *Slides, coverslips & Petri dishes*

Coverslips: 22mm² (No1 thickness) borosilicate glass (BDH 406/0187/33).

Microscope Slides: 7.6cm x 2.6cm (19.76cm²) low iron clear glass slides, 1.0-1.2mm thickness (BDH 406/0180/04).

Petri dishes: 30mm non tissue culture grade (Bibby Sterilin 121V).

90mm non tissue culture grade (Bibby Sterilin 101VR20).

APPENDIX 2

MATERIALS FOR IMMUNOFLUORESCENCE.

(A) Solutions

1. Phosphate buffered saline

Phosphate Buffered saline (x1) (PBSa) in DH₂O made from x10 concentrate (Gibco 14200): 1.71M NaCl, 0.03M KCl, 0.018M KH₂PO₄, 0.042M Na₂HPO₄.2H₂O.

PBSc (complete), dilute as above add 1ml 1M CaCl₂ (BDH 190464K) and 0.5ml 1M MgCl₂ (BDH 22093) per litre.

2. Fixatives

16% EM Grade Formaldehyde (TAAB F017) working dilution 1% in PBSc.

37% Formaldehyde (Sigma F1635) working dilution 3.7% in PBSc.

3% Paraformaldehyde (Sigma P6148) in PBSc. Quenched by 0.1M Glycine/PBSc (Sigma G8898) – 750mg in 100ml PBSc.

Sodium Azide, (Sigma, S8032) used at concentration of 0.1% sodium azide/PBSc. 20µl of 10% sodium azide/DH₂O in 2 ml PBSc. Prevents contamination of preparation before staining process.

3. Detergents

Nonidet P40 (Sigma N2368) used at 1% in PBSc.

Triton X-100 (Sigma, T8787) used at 0.2% in PBSc.

4. Blocking Agents

- *Goat Serum* (Diagnostics Scotland T-028) used at 5% to block non-specific sites.
- *Donkey Serum* (Diagnostics Scotland T-027).

- *Sheep Serum* (Diagnostics Scotland T-031).
- *Bovine Serum Albumin* (BDH AnalR 441555J) used at a concentration of 0.2% in PBSc.

5. *Mountants*

Gelvatol (Airvol 205) polyvinyl alcohol resin. 25g in 100ml 0.14M NaCl, 0.01M KH_2HPO_4 (BDH) and 0.01M Na_2HPO_4 (BDH)(pH 7.2).

100mg/ml of 1, 4, Diazabicyclo [2,2,2] octane (DABCO) (Sigma D2522), anti-fade agent was added before use.

Hydromount (BDH 362452L) ready to use, contains anti-fade agent. .

(B) *Antibodies*

(i) *Primary Antibodies*

The following primary antibodies were used in various combinations to study the cytoskeletal structure and focal adhesion sites. Generally, monoclonal antibodies were raised in mice and polyclonal antibodies raised in rabbits.

(Monoclonal = mono, Polyclonal = poly)

ANTIBODY	RAISED IN	SUPPLIER	WORKING DILUTION
<i>Monoclonal antibodies</i>			
Mono α Tubulin	Mouse	Sigma (T5168)	1:50
Mono IFAP ₃₀₀ 471	Mouse	Gift from Dr R.D.Goldman, Northwestern University, Chicago	1:5
Mono Paxillin	Mouse	Transduction Lab. (P13520)	1:100

Appendix 2 – Materials for Immunofluorescence.

Mono Phospho-tyrosine-20(PY-20)	Mouse	Transduction Lab.	1:100
Mono Plectin (#417D)	Mouse	Gift from Ying Hao-Chou, Northwestern University, Chicago	1:100
Mono Vimentin (V9)	Mouse	Boehringer Mannheim (814318)	1+3 from stock
Mono Vimentin (V9)	Mouse	Sigma (V3660)	1:50
Mono Vinculin	Mouse (ascites)	Sigma (V4505)	1:100
MonoG58K(Golgi)	Mouse	Sigma (G2404)	1:50
<i>Polyclonal antibodies</i>			
Poly β_3 integrin	Rabbit	Chemicon (AB1932)	1:50
Poly IFAP ₃₀₀ 268, 291	Rabbit	Gift from Dr. R.D. Goldman, Northwestern University, Chicago	1:10
Poly Vimentin	Rabbit	ICN (691272)	1:50

NF κ B: Primary Antibodies used in Immunofluorescence

ANTIBODY	RAISED IN	SUPPLIER	WORKING DILUTION
Mono hnRNP	Mouse	Gift from DR G Dreyfuss, University of Pennsylvania.	1:200
Mono p65 (F-6)	Mouse	Santa Cruz (sc-8008)	1:100
Poly IKK α /1 (H-744)	Rabbit	Santa Cruz (sc-7218)	1:100
Poly IKK β /2 (H-470)	Rabbit	Santa Cruz (sc-7607)	1:100
Poly NIK (H-248)	Rabbit	Santa Cruz (sc-7211)	1:100
Poly p65 (C20)	Rabbit	Santa Cruz (sc-372)	1:100

(ii) Secondary Antibodies

The components labeled by primary antibodies were then stained using secondary antibodies, most of which were used at the same concentration. These antibodies were labeled either; green Fluorescein Isothiocyanate (FITC/Fluorescein), red Tetramethylrhodamine Isothiocyanate (TRITC/Rhodamine) or Texas Red[®]. Mouse and rabbit secondary antibodies are used against monoclonal and polyclonal primary antibodies respectively.

ANTIBODY	ABBREVIATION	SUPPLIER AND CAT #	WORKING DILUTION
Donkey anti Rabbit Fluorescein	DARF	Diagnostics Scotland (T-076)	1:50
Donkey anti Goat Fluorescein	DAGF	Diagnostics Scotland (T-078)	1:20
Goat anti Mouse Alexa 488 (green)	GAMA	Molecular Probes (A11001)	1:200
Goat anti Mouse Fluorescein	GAMF	Jackson (115-095-003)	1:20
Goat anti Mouse Rhodamine	GAMR	Sigma (T5393)	1:20
Goat anti Rabbit Alexa 568 (red)	GARA	Molecular Probes (A-11011)	1:200
Goat anti Rabbit Fluorescein	GARF	Sigma (F6005)	1:20
Goat anti Rabbit Rhodamine	GARR	Sigma (T5268)	1:20
Goat anti Rat Fluorescein	GARaF	Santa Cruz (sc-2011)	1:100-1:400
Sheep anti Mouse Fluorescein	SAMF	Diagnostics Scotland (T-075)	1:20
Sheep anti Mouse Fluorescein	SAMF	Boehringer Mannheim (821462)	1:40

NFκB Secondary Antibodies used in Immunofluorescence

ANTIBODY	ABBREVIATION	SUPPLIER AND CAT #	WORKING DILUTION
Goat anti-mouse Fluorescein	GAMF	Southern Biotech Inc, Alabama (1010-02)	1:200

Goat anti-Rabbit Texas Red	GART	Southern Biotech Inc, Alabama (4010-07)	1:200
-------------------------------	------	--	-------

(c) *Phalloidin*

The actin component of the cells was stained using TRITC or FITC labeled phalloidin (Fluka 77418, 77415) used at concentration 1:250 from 50 μ M stock solution. This was less than the recommended dilutions as there was too much 'bleed-through' on the slides.

APPENDIX 3

**METHOD OVERVIEW & MATERIALS REQUIRED FOR
LYSATE PREPARATION, PROTEIN ESTIMATIONS, SDS
PAGE, WESTERN BLOTTING AND ECL™.**

(a) Method Overview

1. SDS PAGE Preparation

Gel plates were prepared via a series of washes, Decon 90, DH₂O, 70% Alcohol, DH₂O and assembled. Combs were inserted and a mark was made 1cm below the level of the teeth indicating maximum running gel height.

The running and stacking gel mixes were made up in universals. Just prior to pouring, 1ml of running gel was transferred to a separate container and 40µl 10% ammonium persulphate (APS) (Sigma) and 4µl N', N', N', N'- tetramethylethylenediamine (TEMED) (Anachem) were added. This acts as a sealing layer and must be added to the rig quickly to prevent gel polymerisation before forming a layer at the base of the rig. The appropriate volumes of APS and TEMED were added to the running and stacking gels just prior to pouring.

The running gel (8%) was added to the rig first and any air bubbles were removed. A thin layer of 10% water saturated n- butanol (Sigma) was added to prevent oxygen inhibiting acrylamide polymerisation and the gel was left to set for 20 minutes.

Once set, the n-butanol was poured off, the surface was rinsed with DH₂O and dried. The stacking gel was activated and pipetted on top. A 24-tooth comb was inserted to form the loading wells and the gel was left to set for 15 minutes.

Once the gel was set, the plates were inserted in the MV2-DC rig (Anachem) which was then filled with Tris-glycine electrophoresis buffer (EB). The combs were removed and each well rinsed using a needle and syringe to remove air bubbles and any unpolymerised gel.

2. Sample Loading and SDS PAGE

Appropriate amounts of lysates were added to the wells. In the case of sheared lysates, equal amounts of protein from control, 5, 10, 30, 60, 120, 240, 480 and 960 minutes

shear runs were loaded. 2 μ l Cruz-markers (Santa Cruz) whose proteins range from 23-132 kDa molecular weight (MW) were added to a well. Cruz Markers have compatible secondary antibodies which show the MW lane at the ECL™ stage of the process (see later). The rig was connected to the cold tap to prevent overheating of the gel. The power pack (Anachem, Psu 400/200) set to 70V and increased to 110-120V once the dye front was through the stacking gel.

3. *Western Blot (Protein Transfer)*

On removal from the rig, plates were prized apart and the stacking gel was removed. The remaining gel was measured and had the bottom left hand corner and dye front nicked. At this stage the gel was immersed in Tris/Glycine/SDS semi-dry transfer buffer (TB) for 20 minutes along with 2 thick filter papers (BIO-RAD 170-3958) and a piece of nitrocellulose membrane (Protran®). One filter pad was then placed on the anode of a transfer unit (Bio-Rad Trans-Blot® S.D.) and rolled with a wet glass rod to expel air bubbles. The nitrocellulose membrane was gently placed on top and rolled followed by the gel and finally the second filter pad. The unit was set to 15V and run for 1 hour. This was increased to 90 minutes if two gels were being transferred.

Once complete, any excess membrane was trimmed and the bottom left corner was marked along with the gel front. The membrane was placed in Ponceau Red, a non-permanent stain for 3 minutes on the agitator as a check of protein transfer. The membrane was then rinsed in distilled H₂O until the background was clear. The gel was placed in Coomassie blue stain overnight at 4°C, then rinsed with agitation in Coomassie de-stain until the background is clear to highlight 'un-transferred' protein; ideally the gel should be clear.

4. Protein Detection –Antibody staining

In order to block non-specific protein binding sites, the membrane was placed in 15% Marvel™ (dried skimmed milk) made up in PBSa/0.05%Tween 20 (PBST) for 1 hour at RT (or 4°C overnight), then rinsed (x2) with PBST and placed in a plastic pocket. The primary antibody solution (0.1ml antibody mix.cm⁻²), made up in 15% marvel/PBST was added and the pocket was sealed using a vacuum bag sealer (Salton, #1101) and placed on a Matburn mixer (Surgical Equipment Ltd – SCM-2168) for 1 hour at RT (or 4°C overnight). After incubation, the membrane was rinsed (x2) in PBST for 5 minutes followed by a 15 minute rinse and finally (x2) for 5 minutes. All rinsing was carried out with on an agitator (Heidolph Rotamax 120). The secondary antibody was added to the membrane in the same way as the primary and incubated for 30 minutes. Once complete the membrane was rinsed as above in preparation for the final step in the process.

5. Protein Visualization – Enhanced Chemiluminescence (ECL™) Method.

Proteins present on the membrane are visualised using the ECL™ western blotting analysis system (Amersham). ECL™ Western Blotting is a light emitting, non-radioactive method for the detection of immobilised specific antigens conjugated directly or indirectly with horseradish peroxidase labelled antibodies. This technique is extremely sensitive and requires optimisation of primary and secondary antibody concentrations for best results. Generally antibodies are used at much lower concentrations than in other conventional systems.

The membrane was drained and placed protein side up on a flat piece of cling-film. In a dark room the required quantities of solutions A+B are mixed ((0.5 x 0.125 x membrane surface area (cm²)/2 of A+B), pipetted onto membrane surface and left for exactly 1 minute. The membrane was then drained and placed protein side down in a translucent plastic envelope. This parcel (protein side up) was then placed in a developing case with a piece of detection film (Hyperfilm, Amersham) on top. The film had the bottom left

corner and the margins of the membrane marked. The cassette was sealed for three minutes before developing. The membrane was then soaked in developer (Kodak) for 3 minutes (this time can be altered depending on intensity of the protein band) before being placed in fixative (Kodak) for 3 minutes.

To re-probe a membrane following ECL™ to confirm results or using a different antibody, it was rinsed 3 times (15, 5 & 5 minutes) in PBST before repeating the above procedure from the blocking step onwards.

(A) Materials

1. Lysate preparation

Lysis buffer – ‘Laemmli Buffer’ (for 10ml x1 buffer): 1ml Glycerol, 600µl Tris 1.0M pH 6.8, 2.0ml 10% sodium dodecylsulphate (SDS) (Sigma L3771), 1ml 10mM sodium pervanadate (Sodium Orthovanadate Na₃VO₄) (Sigma S6508) and 5.4ml mQ H₂O.

2. Protein estimation

Protein estimation kit (BIO-RAD 500-0112)

Bromophenol blue dye (Sigma 3269) made up in DH₂O

β-mercaptoethanol (Sigma M7154)

3. SDS PAGE

Running Gel (8%): 8.0ml of pure (mQ) H₂O, 3ml 40% acrylamide/bis (Anachem SL-9223), 3.8ml 1.5M Tris (Tris (hydroxymethyl) methylamine) (BDH AnalR 103156x) (pH 8.8) and 150µl 10% SDS/DH₂O, 150µl 10% Ammonium Persulphate (APS) (Sigma A3678) and 9µl N, N, N, N tetramethylethylenediamine (TEMED) (Anachem 20-3000-01).

Stacking Gel (4%): 3.6ml mQ H₂O, 623µl 40% acrylamide, 630µl 1M Tris (pH 6.8) and 50µl 10% SDS. 150µl 10% APS and 12µl TEMED.

N-Butanol – H₂O saturated (1:1 ratio) isobutanol (Sigma BT-105).

Electrophoresis Buffer Running Buffer (pH 8.3): 10g SDS [0.1%], 30g Tris (BDH 103156X) [0.025M], 144g Glycine (Sigma G8898) [0.24M]. Made up to 2 litres with DH₂O and diluted 1:5 for use. ([] denotes final concentration in solution).

Cytoskeletal protein standards:

- *Vimentin:* recombinant human vimentin, gift from Ying Hao Chung (Goldman Lab, North Western University, Chicago).
- *Actin:* Chicken gizzard (Sigma A4785).
- *Tubulin:* Bovine Brain (ICN 771121).

MOLECULAR WEIGHT MARKERS

COMPONENT	MW	Log ₁₀ MW
Boehringer-Combitek (1317 474)		
α ₂ -marcoglobulin	170,000	5.230
β-Galactosidase	116,353	5.066
Fructose-6-phosphate	85,204	4.930
Glutamate dehydrogenase	56,000	4.745
Aldose	39,000	4.593

Triose phosphate isomerase	27,000	4.425
Santa-Cruz-Cruz Marker™ molecular Weight Standrds (sc2035)		
	132,000	5.12
	90,000	4.95
	55,000	4.74
	43,000	4.63
	34,000	4.53
	23,000	4.36

N.B. **Cruz Markers™** must be used in conjunction with Cruz Marker™ compatible secondary antibodies for Western blotting.

4. Western Blot

Nirtocellulose transfer membrane – Protran BA 85 (Scheicher & Schuell, Germany, 10401196).

Blotting Filter papers (BIO-RAD 170-3958)

Semi-dry Transfer Buffer: 15g [0.025M] Tris, 72g [0.192M] Glycine. 20% Methanol (1litre), 18.75ml 10% SDS [0.375%]. Make up to 5 litres with DH₂O

Ponceau Red stain: 0.2g Ponceau Red Stain (Sigma P3504), 3g trichloroacetic acid (BDH AnalR 30490), 3g sulphosalicylic acid (Sigma S2130) in 100ml DH₂O.

Coomassie Blue stain: 1.5g Coomassie brilliant blue (Sigma B0149), 900ml ethanol, 200ml glacial acetic acid, 900ml DH₂O.

De-stain: As above minus the brilliant blue dye.

5. Protein detection – antibody staining

PBST: 0.05% Tween 20 detergent (Sigma P9416)/DH₂O or *PBST* tablets (BDH 18902-015) - 2 tablets per litre DH₂O.

Combined with Marvel™ (dried skimmed milk) to produce 15% blocking solution and also for antibody solutions. .

6. Antibodies

N.B. For both primary and secondary antibodies, incubation time is one hour at room temperature or 4°C overnight unless otherwise stated.

Primary Antibodies

Antibody	Supplier and Cat. #	Optimal Working Dilution
<i>BAEC</i>		
Mono vimentin (V9)	Boehringer Mannheim (814318)	1:5000
Mono vimentin (V9)	Sigma (V6630)	1:30,000
Rabbit poly IκBβ (c-20)	Santa Cruz (sc-945)	1:500
Rabbit poly IκBα (c-21)	Santa Cruz (sc-371)	1:750
Rabbit poly IκBε (M121)	Santa Cruz (sc-7156)	1:750

Appendix 3 – Lysate Preparation and Western Blotting Materials.

HUVEC		
Rabbit poly IκBα (c-21)	Santa Cruz (sc-371)	1:1000
Rabbit poly IκBβ (c-20)	Santa Cruz (sc-945)	1:1000
Rabbit poly IκBε (M-364)	Santa Cruz (sc-7155)	1:1000
Sheep poly p105	Diagnostics Scotland	1:1000
Sheep poly p50	Diagnostics Scotland	1:1000

Secondary Antibodies

Antibody	Abbreviation	Supplier and Cat #	Optimal Working Dilution
BAEC			
Donkey anti-goat HRP	DAGP	Santa Cruz (sc-2033)	1:1000-1:2000
Goat anti-mouse HRP	GAMP	Santa Cruz (sc-2031)	1:1000-1:2000 (1:5000 for vimentin)
Goat anti-rabbit HRP	GARP	Santa Cruz (sc-2030)	1:1000-1:2000
HUVEC			
Goat anti-mouse HRP	GAMP	Santa Cruz (sc-2031)	1:10000

Goat anti-rabbit HRP	GARP	Santa Cruz (sc-2030)	1:10000
Rabbit anti-sheep HRP	RASP	DAKO (PO163)	1:10000

7. Enhanced Chemiluminescence – ‘ECL™’

ECL™ Western blotting detection reagents (Amersham, RPN 2209).

Hypercassette (Amersham RPN 1642).

X-Ray film: ‘Hyperfilm’ ECL™ (Amersham RPN 2103).

Developer: (Kodak LX24 507 0933).

Fixative: (Kodak Unifix 973 2526).

APPENDIX 4

FLOW CHAMBER DIMENSIONS, CHARACTERISATION AND DETERMINATION OF FLUID SHEAR STRESS.

Appendix 4 – Flow chamber dimensions, characterisation and determination of fluid shear stress.

1. Calculations of medium density and viscosity

Thanks to Ms Kirsty McDowell and Dr. J Armitage for their assistance in calculating these properties.

1.1 Density

Calculated using 25cm³ density bottle.

Density of water and medium was measured at 36°C.

Balance was calibrated to ensure accurate measurements.

Actual mass (g)	Balance Reading i.e Measured mass (g)
10	10.05
20	20.05
30	30.10
50	50.10
60	60.10
70	70.10
100	100.10

Plotting Actual vs Measured $y = 1.001x + 0.058$. All masses were converted according to this equation.

For Water @ 36°C

Empty Bottle	20.82g
Bottle with Water	44.997g
Mass of water	24.177g
Volume of Bottle	25cm ³

Density = Mass/ volume $24.177 / 25 = \underline{0.96708\text{g/cm}^3}$

For Medium @ 36°C

Empty Bottle	20.82g
Bottle with medium	45.25g
Mass of medium	24.43g
Volume of Bottle	25cm ³

Density = Mass/volume $24.43 / 25 = 0.9772 \text{ g.cm}^{-3}$

Actual density of H₂O @36°C = 0.9937g.cm⁻³

Appendix 4 – Flow chamber dimensions, characterisation and determination of fluid shear stress.

$$\text{Therefore density of medium} = \frac{\text{Measured medium density} * \text{Real H}_2\text{O density}}{\text{Measured H}_2\text{O density}}$$

=

$$\frac{0.9772 / 0.9937}{0.967}$$

$$\text{Medium Density} = 1.004 \text{g.cm}^{-3}$$

(N.B. The actual density of H₂O at 36°C (0.9937g.cm⁻³) was obtained from Kaye & Laby, 1986)

1.2 Viscosity measurements

Fluids possess a definite resistance to changes of form. This ‘internal friction’ is termed viscosity (Kaye & Laby, 1986)

Viscosity was measured using a Canon Fenske viscometer (BDH 338/0050/01).

The table of viscosity measurements was taken from Kaye, 1986. Viscosity is measured in Poise (p) – the unit of absolute viscosity = g / (seconds x cm). Poise can also be expressed as dyne.s .cm²

Temperature (°C)	Viscosity (cp)
32	0.7647
33	0.7491
34	0.7340
35	0.7194
36	0.7052
37	0.6915

The viscosity of both water and medium was determined at 35°C and then converted to what it would be at 37°C.

Water

Viscosity @ 35°C (η) = 0.7194cp
 Time for chamber to empty = 63, 64, 62, 63, 62
 Mean = 62.8s

Medium

Time for chamber to empty 66, 68, 67, 68, 68
 Mean = 67.4s

Viscosity @ 35°C =
 (67.4 / 62.8) * 0.7194
 η = 0.7698cp

Appendix 4 – Flow chamber dimensions, characterisation and determination of fluid shear stress.

At 37°C

Assuming same ratio.

From tables η of H₂O at 37°C = 0.6915cp

$$\begin{aligned} \text{Therefore for medium } \eta &= (67.4 / 62.8) * 0.6915 \\ &= 0.7399\text{cp} \\ &= 7.399 \times 10^{-3} \text{ p} \end{aligned}$$

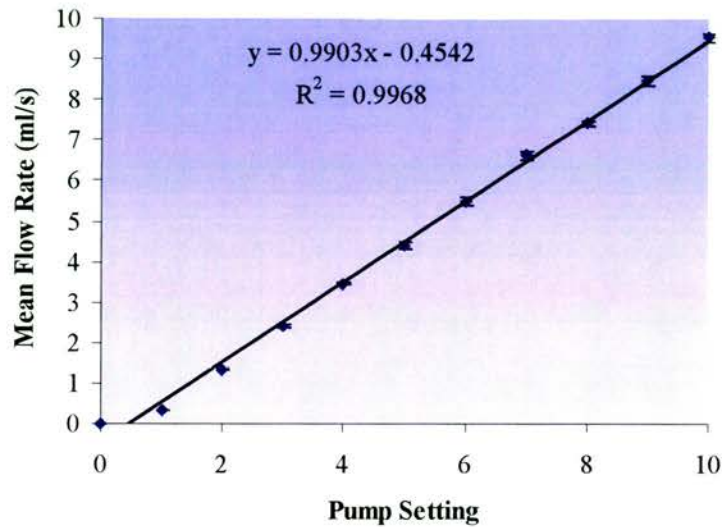
2. Chamber dimensions

Chamber number	Average channel height	SEM channel height	Channel height 'a'	1/2 Channel width 'w'	Channel width	Distance between pressure points 'l'	Width: height ratio.
2 (Slide)	347 μ m	14.26 μ m	0.0174cm	2.3cm	8.0cm	66.28	
3 (coverslip)	568 μ m	3.48 μ m	0.0284cm	2.0cm	2.9cm	35.21	
4 (coverslip)	392 μ m	4.26 μ m	0.0196cm	2.0 cm	2.85cm	51.02	

3. Flow rate (FR) through apparatus

The following flow rates (ml/s⁻¹) were used to determine fluid shear stress (FSS) in absence of flow chamber as the amount of medium delivered is directly related to the pump output.

Setting	(FR) (i)	FR (ii)	FR (iii)	FR (iv)	FR (v)	FR (vi)	Mean FR	SEM (n=6)
1	0.3	0.3	0.35	0.34	0.34	0.325	0.326	0.0088
2	1.31	1.29	1.45	1.32	1.35	1.33	1.342	0.0231
3	2.39	2.31	2.47	2.4	2.38	2.55	2.417	0.0338
4	3.29	3.36	3.59	3.44	3.65	3.43	3.46	0.0357
5	4.18	4.28	4.76	4.26	4.48	4.33	4.382	0.0859
6	5.38	5.22	5.65	5.38	5.47	5.87	5.495	0.0944
7	6.5	6.52	7.0	6.52	6.38	6.88	6.633	0.1005
8	7.5	7.33	8.07*	7.26	7.59	7.38	7.41	0.0593
9	8.22	8.14	8.87	8.31	8.64	8.64	8.47	0.118
10	9.25	9.28	9.62	9.68	9.95	9.44	9.537	0.109



Graph 1 shows the relationship found between the mean flow rate ($\text{ml}\cdot\text{s}^{-1}$) and the pump setting using PharMed tubing (size 16). SEM were calculated (see table) are contained within the symbol.

4. Pressure differences (PD)

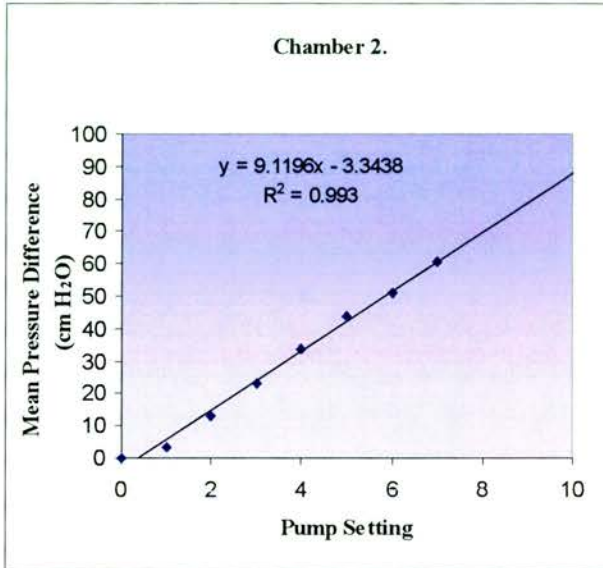
Pressure difference is proportional to internal chamber dimensions, therefore PD were recorded along the length of each chamber.

Pump setting	Mean chamber 2	PD	SEM	Mean chamber 3	PD	SEM	Mean chamber 4	PD	SEM
1	3.3		0.05	0.25		0.019	0.975		0.025
2	13.1		0.2	1.10		0.025	3.925		0.225
3	22.9		0.15	1.97		0.038	7.225		0.425
4	33.88		0.125	2.87		0.029	11.1		0.7
5	43.73		0.125	3.80		0.099	14.1		1.25
6	51.10		0.5	4.42		0.040	18.075		1.275
7	60.60		0.0	5.22		0.08	23.475		1.375
8				6.0		0.096			

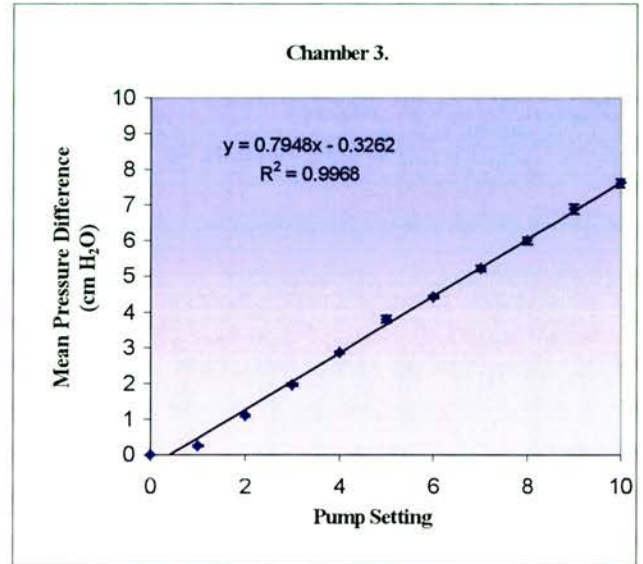
Appendix 4 – Flow chamber dimensions, characterisation and determination of fluid shear stress.

9			6.90	0.132		
10			7.61	0.119		

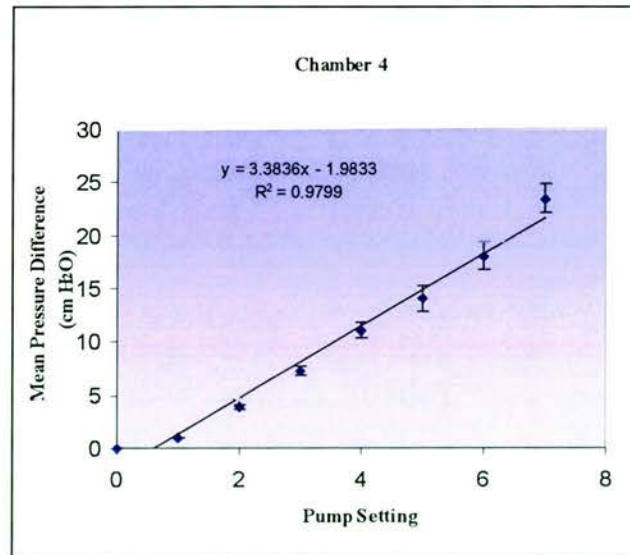
a



b



c



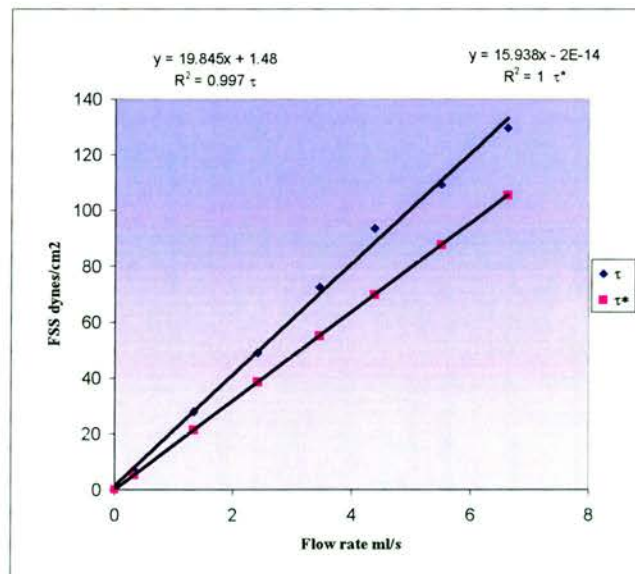
Graphs 2(a-c) illustrate the relationship between the mean pressure difference across the chambers with pump setting. The data used to produce the graphs can be viewed in the table above. Error bars are contained within the symbols.

4. Calculation and comparisons of measured (τ) and theoretical (τ^*) fluid shear stress (FSS).

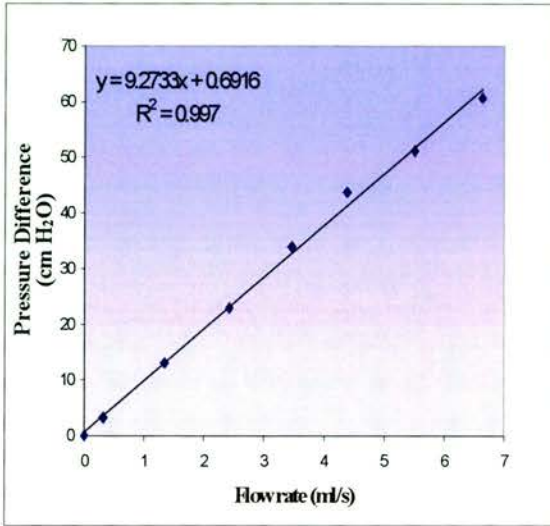
Chamber 2

Pump setting	Mean FR (ml.s ⁻¹)	Mean PD (cm H ₂ O)	τ	τ^*
0	0	0	0	0
1	0.326	3.3	7.06	5.19
2	1.34	13.1	28.03	21.36
3	2.42	22.9	49.0	38.57
4	3.46	33.88	72.5	55.15
5	4.38	43.73	93.5	69.81
6	5.5	51.1	109.36	87.65
7	6.63	60.6	129.67	105.67

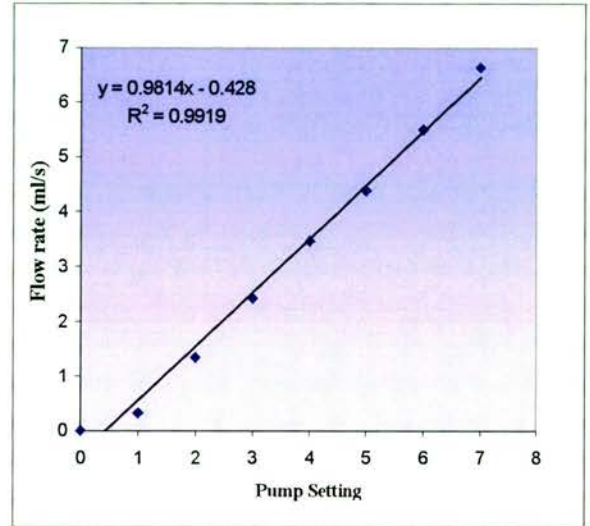
a



b



c

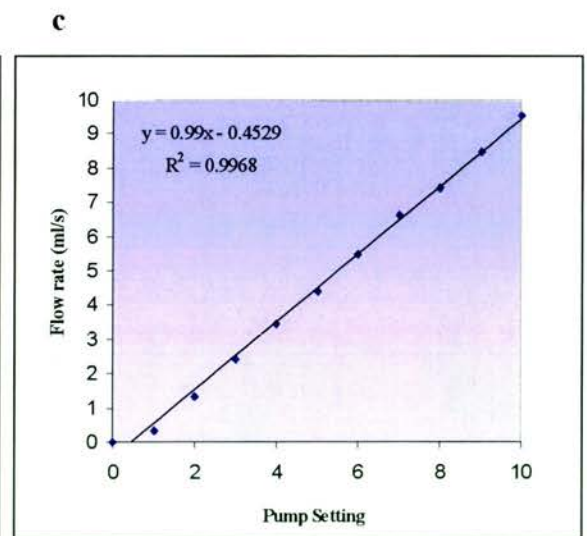
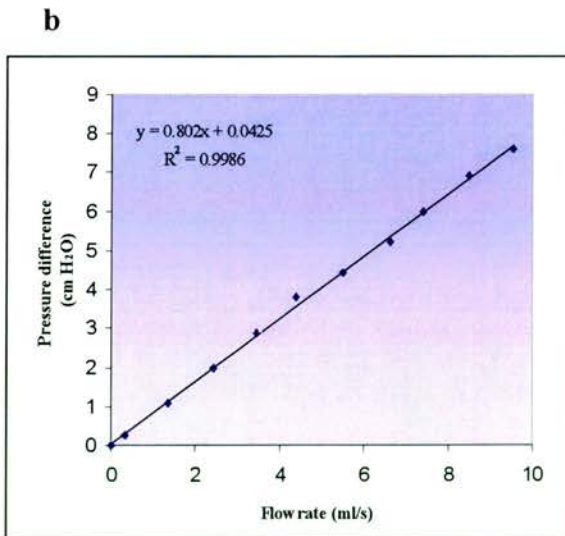
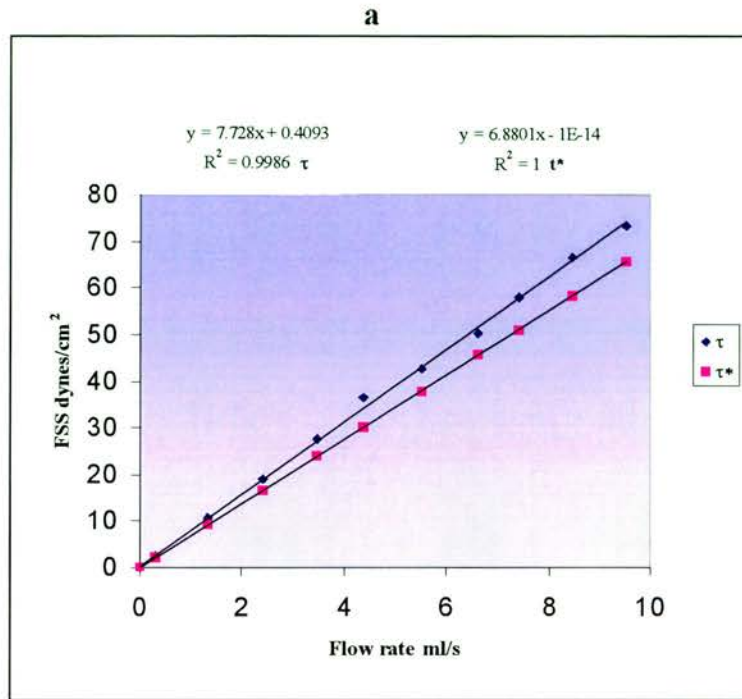


Graphs 3 (a-c) illustrate the calibration curves for chamber 2. Graph 3a illustrates the relationship between both τ and τ^* for chamber 2 with flow rate. Graphs 3 b & c show the relationships in chamber 2 between pressure difference and flow rate and flow rate and pump setting respectively. From these results the pump setting for a given fluid shear stress value was determined.

Chamber 3

Pump setting	Mean FR (ml.s ⁻¹)	Mean PD (cm H ₂ O)	τ	τ^*
0	0	0	0	0
1	0.326	0.25	2.41	2.24
2	1.34	1.1	10.60	9.22
3	2.42	1.97	18.98	16.65
4	3.46	2.87	27.65	23.80
5	4.38	3.8	36.62	30.14
6	5.5	4.42	42.59	37.84
7	6.63	5.22	50.30	45.61
8	7.41	6.0	57.81	50.98
9	8.47	6.9	66.49	58.27
10	9.53	7.61	73.33	65.57

Appendix 4 – Flow chamber dimensions, characterisation and determination of fluid shear stress.

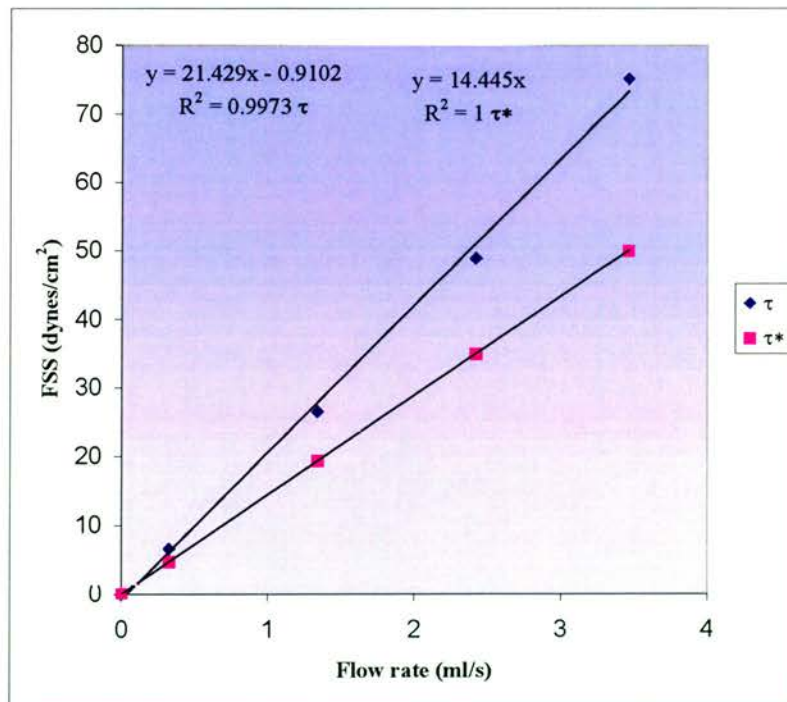


Graphs 4 (a-c) illustrate the calibration curves for chamber 3. Graph 4a illustrates the relationship between both τ and τ^* for chamber 3 with flow rate. Graphs 4 b & c show the relationships in chamber 3 between pressure difference and flow rate and flow rate and pump setting respectively. From these results the pump setting for a given fluid shear stress value was determined.

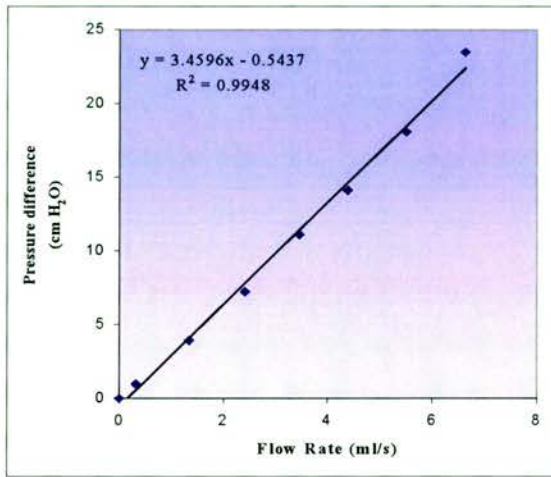
Chamber 4

Pump setting	Mean FR (ml.s ⁻¹)	Mean PD (cm H ₂ O)	τ	τ^*
0	0	0	0	0
1	0.326	1.0	6.77	4.91
2	1.34	3.7	25.04	19.36
3	2.42	6.8	46.01	34.52
4	3.46	10.4	70.37	51.28
5	4.38	12.85	86.95	63.13
6	5.5	16.8	113.68	78.29
7	6.63	22.1	149.54	93.17

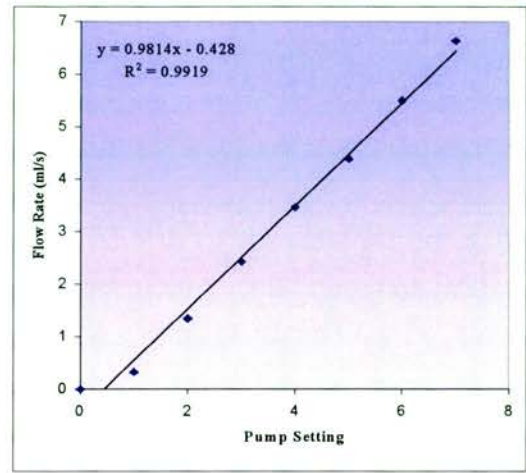
a



b



c



Graphs 5 (a-c) illustrate the calibration curves for chamber 4. Graph 5a illustrates the relationship between both τ and τ^* for chamber 4 with flow rate. Graphs 5 b & c show the relationships in chamber 4 between pressure difference and flow rate and flow rate and pump setting respectively. From these results the pump setting for a given fluid shear stress value was determined.

APPENDIX 5

PERINUCLEAR RING FORMATION AND CYTOSKELETAL PROTEIN DISTRIBUTION AND EXPRESSION WITH TIME IN CULTURE AND UPON EXPOSURE TO FLUID SHEAR STRESS.

Appendix 5- Perinuclear ring formation, cytoskeletal protein distribution & expression with time in culture and upon exposure to fluid shear stress.

1. Cell Density data

Mean cell density counts recorded for passage 20-22 BAE cells are shown in the table below. An average of 5 random low power (x40) pictures were taken for various times in culture.

Based on the knowledge that the scale bar (x40) represents 25 μ m, the area of each photograph was found to be 69519.5 μ m². From these figures the cell density per cm² could be estimated (i.e. by multiplying by 1x10⁸).

The data in the table below is combined from passage 20-22 cells.

Day	Total cells	Areas counted (n)	Mean Density.cm⁻²	SE
1	140	5	40277	2652
2	892	15	85540	8619
3	455	5	130899	6352
5	1090	10	156791	8330
7	2282	23	181744	7176
10	2384	19	180487	6196
14	2202	19	166708	5255
17	1818	18	145283	2697
21	1760	19	133246	3117

Appendix 5- Perinuclear ring formation, cytoskeletal protein distribution & expression with time in culture and upon exposure to fluid shear stress.

2. Whole cell area and shape index (SI)

Combined data of passage 20-22 and adjusted accordingly.

Day	Sample number (n)	Total Area (μm^2)	Mean Area (μm^2)	SE (μm)	Total Peri-meter (μm)	Mean Peri-meter (μm)	SE (μm)	Shape Index
2	364	301248	827.6	44.76	44836	121.2	3.35	0.685
5	500	155852	311.7	9.6	35212	70.5	1.18	0.790
7	725	200189	276.1	8.71	49298	67.9	1.07	0.751
10	825	201550	244.3	6.13	48919	59.3	0.8	0.873
14	758	222826	294.0	7.54	50108	66.1	0.94	0.845
17	678	198849	293.3	8.53	44063	65	0.98	0.872
21	465	141260	303.8	8.14	30806	66.25	0.93	0.870

3. Perinuclear ring (PNR) development

Combined data of passage 20-22 cells.

Day	Total Cells	Areas counted (n)	% cells with PNR	SE (%)
1	140	5	6.82	2.07
2	892	15	4.47	0.61
3	455	5	9.45	0.61
5	1090	10	65.34	2.62
7	2282	23	76.92	4.24
10	2384	19	92.5	3.99
14	2202	19	93.3	8.32
17	1818	18	94.51	6.2
21	1760	19	94.51	5.12

Appendix 5- Perinuclear ring formation, cytoskeletal protein distribution & expression with time in culture and upon exposure to fluid shear stress.

4. Ring area and shape index

Combined data from passage 20-22 BAE cells.

Day	Sample (n)	Total Area (μm^2)	Mean Area (μm^2)	SE (μm^2)	Total Perimeter (μm)	Mean Perimeter (μm)	SE (μm)	SI
7	100	13662	136.62	4.74	4288	42.88	0.8	0.934
10	249	33636	135.09	4.13	10607	42.60	0.67	0.936
14	405	48752	120.37	3.24	16319	40.29	0.61	0.932
17	365	48160	131.95	4.69	15425	42.26	0.76	0.927
21	186	25621	137.75	5.08	7968	42.84	0.86	0.943

5. Changes in cytoskeletal protein expression with time in culture.

5.1 Vimentin

Day	Vimentin $\mu\text{g}/\text{mg}$ total protein	SEM	Vimentin expression as a % of day 3.	SEM	n
3	61.67	5.32	100	0	9
5	75.44	6.3	120.4	3.34	9
7	80.33	4.09	134.3	14.08	9
10	89.33	4.65	148.8	17.85	9
14	97.22	7.29	156.7	14.73	9

A single one-way analysis of variance (anova) was performed on values standardized as a percentage of day 3 to determine whether the trend in vimentin expression with time

Appendix 5- Perinuclear ring formation, cytoskeletal protein distribution & expression with time in culture and upon exposure to fluid shear stress.

was significant. $p=0.01647$ i.e. $p < 0.05$ therefore the increased vimentin expression with time in culture was found to be significant.

5.2 Actin

Day	μg Actin/mg total protein	SEM	Actin expression as % of day 3	SEM	n
3	264.5	14.2	100	0	14
5	241.29	13.2	90.93	2.82	14
7	231.79	14.2	86036	1.93	14
10	225.29	17.4	86036	3.63	14
14	198.21	16.2	73	3.96	14

A single one-way analysis of variance (anova) was performed on values standardized as a percentage of day 3 to determine whether the trend in actin expression with time was significant. $p=1.96 \times 10^{-7}$ i.e. $p < 0.0001$ therefore the increased actin expression with time in culture was found to be very significant.

5.3 Tubulin

Day	μg Tubulin/mg total protein	SEM	Tubulin expression as % of day 3	SEM	n
3	34.71	1.6	100	0	7
5	28.28	2.19	81.29	4.49	7
7	20.57	1.8	59.71	3.13	7
10	20.29	3.37	59.0	7.93	7
14	16.86	1.68	49.29	3.46	7

Appendix 5- Perinuclear ring formation, cytoskeletal protein distribution & expression with time in culture and upon exposure to fluid shear stress.

A single one-way analysis of variance (anova) was performed on values standardized as a percentage of day 3 to determine whether the trend in tubulin expression with time was significant. $p=3.92 \times 10^{-8}$ i.e. $p < 0.001$ therefore the increased tubulin expression with time in culture was found to be significant.

6. Changes in cytoskeletal protein expression upon exposure to fluid shear stress.

6.1 Vimentin

Shear Time	(n)	Vimentin expression as a % of control	SEM
0 (control)	5	100	0
5	5	99	7.03
10	5	95	9.15
30	5	103	11.5
60	5	105	10.5
120	5	102	10.65
240	5	102	12.25
960	5	80	6.99

A single one way analysis of variance (anova) was performed on values standardised as a percentage of the control (0 minutes) samples. $p = 0.63$ i.e. $p > 0.05$ therefore no significant change in vimentin expression occurred as a result of exposure to fluid shear stress.

Appendix 5- Perinuclear ring formation, cytoskeletal protein distribution & expression with time in culture and upon exposure to fluid shear stress.

6.2 Actin

Shear Time	(n)	Actin expression as a % of control	SEM
0 (control)	3	100	0
5	3	96	7.98
10	3	91	15.85
30	3	120	17.62
60	3	108	14.24
120	3	105	9.98
240	3	117	18.84
960	3	89	6.65

A single one way analysis of variance (anova) was performed on values standardised as a percentage of the control (0 minutes) samples. $p = 0.615$ i.e. $p > 0.05$ therefore no significant change in actin expression occurred as a result of exposure to fluid shear stress.

6.3 Tubulin

Shear Time	(n)	Tubulin expression as a % of control	SEM
0 (control)	3	100	0
5	3	109	14.23
10	3	110	10.4
30	3	115	8.86
60	3	116	8.04
120	3	120	23.66
240	3	120	23.28

A single one way analysis of variance (anova) was performed on values standardised as a percentage of the control (0 minutes) samples. $p = 0.958$ i.e. $p > 0.05$ therefore no

Appendix 5- Perinuclear ring formation, cytoskeletal protein distribution & expression with time in culture and upon exposure to fluid shear stress.

significant change in tubulin expression occurred as a result of exposure to fluid shear stress.

APPENDIX 6

NF- κ B MATERIALS, I κ B DEGRADATION AND IKK TRANSFECTION STUDIES.

1. Transfections

LipofectAMINE (Invitrogen, 18324-111).

Plasmids

PCDNA3 empty vector (Invitrogen V385-20).

IKK1, IKK1mut, IKK2 & IKK2 mut – (gift from Dr John Taylor, Pfizer Central Research, Sandwich, Kent, UK).

NIK & NIK mut - (gift from Dr David Wallach, Israel).

2. Drug Treatment

MG132 (BIOMOL PI-202) 20 μ M in culture medium.

Leptomycin B (Sigma L2913) 20nM in culture medium.

Phorbol 12-myristate 13-acetate (PMA) (Sigma P8139) 25ng.ml⁻¹ in culture medium.

Ionomycin (IONO) (Sigma I0634) 1 μ g.ml⁻¹ in culture medium.

Bisindolylmaleimide (BISIN) (Calbiochem 203290) 100nM in culture medium.

TNF α (Insight Biotechnology IB-1034) 30ng/ml in culture medium.

3. Immunostaining - For details see Appendix 2.

4. Immunoblotting – For details see Appendix 3.

5. Luciferase Assay

Plasmids – 3Enh Con A Luc, Con A Luc (Gift from Dr. F Arenzana-Seisdedos, Institut Pasteur, Paris).

Lysis Buffer- 25mM tris phosphate, 8mM MgCl₂, 1mM DTT, 1% Triton X-100 and 15% glycerol.

Luciferase Buffer (made up in lysis buffer)- 25mM luciferin, 1mM ATP, 1% BSA.

6. Kinase Assay

Lysis Buffer: 20mM Tris-HCL, pH 8.0, 500mM NaCl, 1mM EDTA, 1mM EGTA, 0.25% NP-40, 1mM DTT, 10mM β -glycerophosphate, 300 μ M sodium orthovanadate, 2SF, 2 μ M phenylmethylsulfonylfluoride (PMSF), 10mM sodium fluoride and a protease inhibitor cocktail tablet (Boehringer Mannheim) or 10 μ g.ml⁻¹ aprotinin, 1 μ g.ml⁻¹ leupeptin & 1 μ g.ml⁻¹ pepstatin.

Protein A beads conjugated with sheep affinity purified primary antibody to C-terminal of IKK (Diagnostics Scotland).

Pulldown Buffer: 40mM Tris-HCL, pH 8.0, 500mM NaCl, 6mM EDTA, 6mM MEGTA, 0.1% NP-40, 1mM DTT, 10mM β -glycerophosphate, 300 μ M sodium orthovanadate, 2 μ M PMSF, 10mM sodium fluoride and a protease inhibitor cocktail tablet (Boehringer Mannheim).

Kinase Assay Buffer: 20mM HEPES, pH 7.7, 2mM MgCl₂, 1mM DTT, 10mM β -glycerophosphate, 300 μ M sodium orthovanadate, 10mM sodium fluoride and a protease inhibitor cocktail tablet (Boehringer Mannheim).

Additives: 3 μ Ci [γ -³²P] ATP. 1 μ g wildtype GST-N terminal I κ B α (amino acids 1-70) or GST-N I κ B α 32 S/A.

APPENDIX 7

FIGURE KEY.

Figure N ^o	Reference
Chapter 3	
3.3a	70bvimd
3.3b	
3.3c	#08-35a
3.3d	#08-20a
3.4a	#13-12
3.4b	#13-13
3.4c	Colour #08-21
3.4d	Ef2cr
3.4e	#46-23
3.4f	#46-24
3.5a	#10-12
3.5b	#10-11
3.5c	#34-25
3.5d	#34-26
3.6a	#10-26 (115-02cr)
3.6b	#10-25 (15-02)
3.6c	#07-25 (1415cv)
3.7a	#12-05a
3.7b	#12-30a
3.7c	#12-26a
3.7d	#07-25
3.10a	#7/14 ch
3.10b	#7/15 ch
3.10c	#18-36a
3.10d	#18-35a
3.10e	Colour #12-07
3.10f	Colour #34-13a
3.11a	#71-35
3.11b	#71-36
3.11c	#77-03
3.11d	#77-04
3.11e	#71-31
3.11f	#71-33
3.12a	#08-21

3.12b	#08-22
3.12c	#13-08
3.12d	#13-09
3.12e	#06-06
3.12f	#06-07
3.12g	#08-26
3.12h	#08-25

Chapter 4

4.1a	8211vy12
4.1b	8211vy06
4.1c	8211vy10
4.1d	8727ve03
4.1e	8727vd04
4.1f	8727ve04
4.2a	8727va04
4.2b	8727aa04
4.3	8727vk05
4.4a	8727ac00
4.4b	8727vc03
4.4c	8727ac06
4.4d	8727vc06
4.5a	ch19-02
4.5b	ch12-16
4.5c	ch19-05
4.5d	ch19-15
4.5e	ch19-21
4.5f	ch19-22
4.5g	ch19-20
4.5h	ch19-19
4.5i	ch19-30
4.5j	ch19-25
4.5k	ch12-25
4.5l	ch12-32
4.6a	ch23-19
4.6b	ch23-20
4.6c	ch20-32
4.6d	ch20-31
4.6e	ch11-23
4.6f	ch11-22

Chapter 5

5.1a	170801-23	(bobpower slide-2)
5.1b	070801b-01	(bobpower slide 19)
5.2a	170801-14	(bobpower slide 5)
5.2b	170801-10	(bobpower slide 21)
5.3a	080801-32	(bobpower slide 8)
5.3b	080801-02	(bobpower slide 20)
5.4a	250801-11	(bobpower slide 45)
5.4b	080801-05	(bobpower slide 27)